

**MIDDLE DISTILLATE HYDROTREATMENT ZEOLITE CATALYSTS
CONTAINING Pt/Pd OR Ni**

A Dissertation

by

CELIA MARIN-ROSAS

Submitted to the Office of Graduate Studies of
Texas A&M University
in partial fulfillment of the requirements for the degree of

DOCTOR OF PHILOSOPHY

December 2006

Major Subject: Chemical Engineering

MIDDLE DISTILLATE HYDROTREATMENT ZEOLITE CATALYSTS
CONTAINING Pt/Pd OR Ni

A Dissertation

by

CELIA MARIN-ROSAS

Submitted to the Office of Graduate Studies of
Texas A&M University
in partial fulfillment of the requirements for the degree of

DOCTOR OF PHILOSOPHY

Approved by:

Co-Chairs of Committee,	Gilbert F. Froment Rayford G. Anthony
Committee Members,	Kenneth R. Hall Abraham Clearfield
Head of Department,	N.K. Anand

December 2006

Major Subject: Chemical Engineering

ABSTRACT

Middle Distillate Hydrotreatment Zeolite Catalysts Containing Pt/Pd or Ni.

(December 2006)

Celia Marin-Rosas, B.S., Universidad Nacional Autonoma de Mexico, Mexico;

M.S., Instituto Politecnico Nacional, Mexico

Co-Chairs of Advisory Committee: Dr. Gilbert F. Froment

Dr. Rayford G. Anthony

A study on middle distillate hydrotreatment zeolite catalysts containing Pt/Pd and/or Ni was performed. The effect of the addition of the corresponding CoMo, CoMoPd, CoMoPtPd and CoMoNi in PdNiPt-zeolite, Pt-zeolite, Ni-zeolite, and PdPt-zeolite was studied. The catalysts were characterized physically and chemically by methods and techniques such as Brunauer-Emmett-Teller (BET), Barret-Joyner-Hallenda (BJH), and neutron activation analysis. The structures of the Ni and Pt containing zeolite were studied by X-ray Photoelectron Spectroscopy (XPS).

An experimental apparatus was constructed to investigate the activity of the experimental catalysts. The catalysts activity measured in terms of conversion of dibenzothiophene (DBT), substituted dibenzothiophenes (sDBT) and phenanthrene as well as molar-averaged conversion was evaluated in a continuous flow Robinson Mahoney reactor with stationary basket in the hydrodesulfurization and hydrogenation of heavy gas oil which contains sulphur refractory compounds such as 4-methyldibenzothiophene (4-MDBT) and 4,6-dimethyldibenzothiophene (4,6-DMDBT).

DBT, 4-MDBT, 3-MDBT, 1-EDBT, 3-EDBT, 4,6-DMDBT, 3,6-DMDBT, 2,8-DMDBT and 4-methylnaphtho[2,1-b]thiophene were selected to calculate the molar-averaged conversion.

The conversions of the sulfur containing compounds and phenanthrene were determined as a function of the operating variables: space time (W/F_{DBT}^0), temperature, H_2/HC mol ratio and pressure. The Conversions of DBT and 4,6-DMDBT into their

reaction products such as Biphenyl (BPH), Cyclohexylbenzene (CHB), Bicyclohexyl (BCH) and 3,4-Dimethylbiyphenyl (3,4-DMBPH) were determined only as a function of space time in the interval of 4000-6000 $\text{kg}_{\text{cat}}\text{h}/\text{kmol}$.

The results of this work showed that Pt-HY and PdPt-HY are good noble metals catalysts for the hydrodesulfurization of heavy gas oil. Moreover, this study showed that CoMoPd/Pt-HY and CoMoNi/PdPt-HY catalysts are good candidates for deep HDS and hydrogenation of heavy gas oil. It was found that the conversions of sulfur compounds were higher than the conversions provided by the conventional CoMo/Al₂O₃ catalyst. Also higher hydrogenation of phenanthrene was observed. Deactivation of the catalysts was not observed during the operation.

Finally, the study not only contributed to define the technical bases for the preparation of the noble metal catalysts for hydrodesulfurization of heavy gas oil at pilot scale, but also provided technical information for developing the kinetic modeling of the hydrodesulfurization of heavy gas oil with the noble metal catalysts.

DEDICATION

This dissertation is dedicated to my husband, Luis Carlos, for his unending support and love during these difficult years. His patience and many sacrifices were essential to my study and research.

Also this dissertation is dedicated to everyone in my family, especially my parents, brothers, sisters, nephews and nieces whose love and encouragement have enabled me to succeed and achieve my dream.

Furthermore, this dissertation is dedicated to the memories of my brother, Ricardo, grandmothers, Sabas and Micaela, my grandfather Pedro and my in-laws, Maria and Esteban. They all will be remembered in our hearts.

ACKNOWLEDGMENTS

I would like to express my gratitude to my research advisor, Dr. Gilbert F. Froment, for his guidance, support and patience throughout the course of this research at Texas A&M University. I would also like to thank Dr. Rayford G. Anthony, Dr. Kenneth R. Hall, Dr. Abraham Clearfield for their advice, suggestions, and service as my committee members. I thank Dr. Perla B. Balbuena from the Department of Chemical Engineering, who kindly served as a committee member substitute. I am grateful to Mr. Charles Isdale for his advice, suggestions and analytical instrumentation for use in the setup. Without this equipment the setup would have not been possible.

I would like to thank Dr. William D. James from Elemental Analysis Laboratory for his suggestions and analysis of metal contents of the catalysts and Dr. Jose Sericano for your valuable advice and suggestions for the GC-MS analysis. I am thankful to Linh Dinh, Dr. Abraham Clearfield, Dr. Sharath Kirumakki and Yulia Vasilyeva for their help in the characterization of the metal-zeolite catalyts by XPS. A special thanks goes to Dr. Xianchun Wu, Dr. Sung-Hyun Kim and Dr. C.V. Phillip for their help and suggestions in the laboratory. I am grateful to our chemical engineering shop technician, Mr. Randy Marek for his help in fixing many things.

I also thank my former and current fellow graduate students in my group; Dr. Ammar Alkhaldeh, Dr. Saeed Al-Wahabi, Dr. Jagannathan, Govindhakannan, Dr. Bo. Wang, Dr. Won Jae Lee, Dr. Rogelio Sotelo, Dr. Hans Kumar Gupta, Nicolas Rouckout, Luis Carlos Castaneda, Bradley Atkinson, Pedro Rojas and also Dr. Bedri Bozkurt, TEES Research Engineer, and Dr. Swades K. Chaudhuri, TEES Asst. Research Scientist, for their help and company that made my life in the lab and office more enjoyable.

For this degree, mostly, I was financially supported by Instituto Mexicano del Petroleo, Mexico. As a scholarship student, I would like to thank all managers for their help and services. The support provided by Dr. Kenneth Hall in the final step of my research when he was the department head is greatly acknowledged.

I am thankful to the Artie McFerrin Department of Chemical Engineering at Texas A&M University and its staff for offering me the opportunity to pursue my PhD.

I would like to thank all my friends in College Station for their friendship and support that made my life in College Station enjoyable and relaxing. They are Benny, Sam, Isdale, Francis, Utermark, Patricia, Bruno, Miguel, Monse, Alberto, Zully and Luis Carlos V.

The almost 20 year-friendship and encouragement from my friends Tere Cortez, Florentino Murrieta, Jose Manuel Dominguez, Jorge Munoz and Amalia Tobon is appreciated and will always be remembered.

Finally, I am thankful to my husband, Luis Carlos, and everyone in my family: my parents, Pablo and Celia; my sisters and brothers, Hortencia, Rosa, Patricia, Maria de los Angeles, Maria Elena, Leticia, Lourdes, Veronica, Pablo, Jorge and Luis Alberto; my nephews, Pablo and Miguel; and my nieces Deyanira, Karina and Vanessa. Everything good in my life would not possibly have happened without them.

TABLE OF CONTENTS

	Page
ABSTRACT.....	iii
DEDICATION.....	v
ACKNOWLEDGMENTS.....	vi
TABLE OF CONTENTS.....	viii
LIST OF FIGURES.....	xiv
LIST OF TABLES.....	xxxii
 CHAPTER	
I INTRODUCTION.....	1
1.1 Motivation and Significance of Research.....	2
1.2 Scope of Research	3
II LITERATURE REVIEW.....	6
2.1 Hydrotreating Processes.....	6
2.1.1 Process Chemistry.....	6
2.1.2 Sulfur Compounds in Raw Oil Materials.....	9
2.1.3 Compositional Features of Distillate Fuel Oil.....	10
2.2 Hydrodesulfurization Process.....	12
2.2.1 Chemical Concepts	14
2.2.2 Hydrodesulfurization Network of Dibenzothiophene	16
2.2.3 Hydrodesulfurization Network of 4-Methyldibenzothiophene and 4,6-Dimethyldibenzothiophene.....	17
2.2.4 Thermodynamics	20
2.2.5 Reactivities	21
2.2.5.1 Reactivities Based on the Strength of C-S Bonds.....	21

CHAPTER	Page
2.2.5.2 Reactivities Based on the Steric Hindrance.....	23
2.3 Effect of H ₂ S on Hydroprocessing Reactions.....	24
2.4 Poisons of the Hydrodesulfurization Catalyst.....	26
2.4.1 Effect of Sodium on Catalyst Performance.....	26
2.4.2 Effect of Arsenic on Catalyst Performance.....	28
2.5 Catalyst Formulations.....	30
2.6 Structure of Active Phase.....	32
2.6.1 Monolayer Model.....	33
2.6.2 Intercalation Model.....	33
2.7. Zeolites.....	34
2.7.1 Introduction.....	34
2.7.2 Shape-selectivity.....	36
2.7.3 “Y” Zeolite (Faujasite) as Support of HDS Catalysts.....	36
III SYNTHESIS AND CHARACTERIZATION OF THE CATALYSTS.....	 39
3.1 Raw Chemicals.....	39
3.1.1 Ultrastable Y Faujasite.....	39
3.1.2 Chemicals.....	40
3.2 Synthesis of the Catalysts.....	41
3.2.1 Synthesis of Catalysts Containing USY-12.....	41
3.2.1.1 CoMoPtPd/HY (HDS-1).....	41
3.2.2 Synthesis of Catalysts Containing Ni-USY.....	43
3.2.2.1 Synthesis of CoMoPtPd/Ni-HY (HDS-3) Catalyst.....	44
3.2.3 Synthesis of Catalysts Containing Pt-USY.....	47
3.2.3.1 Synthesis of CoMoPd/Pt-HY (HDS-5) Catalyst.....	48
3.2.3.2 Synthesis of CoMo/PdNiPt-HY (HDS-8) Catalyst.....	50
3.2.3.3 Synthesis of CoMoNi/PdPt-HY (HDS-10) Catalyst.....	52
3.3 Characterization of the Catalysts.....	54
3.3.1 Analytical Techniques.....	55
3.3.1.1 Neutron Activation Analysis.....	55
3.3.1.2 Adsorption-Desorption Isotherms of Nitrogen.....	56
3.3.1.3 X-ray Photoelectron Spectroscopy Technique (XPS).....	58
3.4 Results and Discussion.....	60
3.4.1 Characterization of Ni-HY and Pt-HY.....	61
3.4.1.1 Metal Contents.....	61
3.4.1.2 Textures.....	61
3.4.1.3 X-ray Photoelectron Spectroscopy (XPS).....	64

CHAPTER	Page
3.4.2 Characterization of CoMoPtPd/HY (HDS-1), CoMoPtPd/Ni-HY(HDS-3) and CoMoPd/Pt-HY (HDS-5) Catalysts.....	67
3.4.2.1 Metal Contents.....	68
3.4.2.2 Textures.....	69
3.4.3 Characterization of CoMo/PdNiPt-HY (HDS-8) and CoMoNi/PdPt-HY (HDS-10) Catalysts.....	74
3.4.3.1 Metal Contents.....	74
3.4.3.2 Textures.....	75
3.5 Concluding Remarks	79
 IV EXPERIMENTAL SET UP AND METHODS FOR THE ACTIVITY TEST OF THE CATALYSTS.....	 81
4.1 Description of the Setup	81
4.2 Analysis of Product.....	84
4.2.1 Gaseous Product.....	84
4.2.2 Liquid Product.....	86
4.3 GC-MS Data Processing.....	87
4.4 Catalysts Activation.....	94
4.4.1 Description of the Sulphiding Procedure	96
4.5 Catalysts Testing for HDS of Real Feedstock.....	96
 V CHARACTERIZATION OF FEEDSTOCK AND REACTION PRODUCTS.....	 99
5.1 Characterization of Heavy Gas Oil and Light Cycle Oil by GC-MS....	99
5.2 Characterization of HDS Reaction Products.....	111
 VI TEST OF THE CATALYSTS.....	 115
6.1 Sulphiding.....	116
6.2 Activity test of CoMo/Al ₂ O ₃ and the Zeolite Catalysts in the HDS of Heavy Gas oil.....	119
6.2.1 CoMo/Al ₂ O ₃ Catalyst (HDS-0).....	119
6.2.1.1 Effect of Space Time at Molar H ₂ /HC Ratio of 2.8.....	120
6.2.1.2 Effect of Space Time at Molar H ₂ /HC Ratio of 7.2.....	122
6.2.1.3 Effect of Space Time and Molar Hydrogen/Hydrocarbon Ratio at 330 °C.....	126

CHAPTER	Page
6.2.2 CoMoPtPd/HY Catalyst (HDS-1)	129
6.2.2.1 Effect of Space Time and Temperature.....	129
6.2.2.2 Effect of the Molar Hydrogen/Hydrocarbon Ratio for the CoMoPtPd/HY Catalyst at 65 and 75 Bar.....	132
6.2.3 CoMo/PdNiPt-HY (HDS-8) Catalyst.....	136
6.2.3.1 Effect of the Space Time at 330 and 310 °C under Molar H ₂ /HC Ratio of 7.2.....	137
6.2.3.2 Effect of the Space Time at 310 °C and Molar H ₂ /HC Ratio of 11.2.....	140
6.2.3.3 Effect of the Molar Hydrogen/Hydrocarbon Ratio at 310 °C and 65-75 bar	142
6.2.4 CoMoNi/PdPt-HY (HDS-10) Catalyst	144
6.2.4.1 Effect of the Space Time at 330 °C and 310 °C under Molar H ₂ /HC Ratio of 7.2.....	145
6.2.4.2 Effect of the Space Time at 310 °C under Molar H ₂ /HC Ratio of 11.2.....	147
6.2.4.3 Effect of the Molar Hydrogen/Hydrocarbon Ratio at 310 °C under 65-75 Bar	149
6.2.5 CoMoPtPd/Ni-HY (HDS-3) Catalyst.....	152
6.2.5.1 Effect of the Space Time at 310 °C under Molar H ₂ /HC Ratio of 7.2.....	152
6.2.5.2 Effect of the Molar Hydrogen/Hydrocarbon Ratio at 310 °C under 65 Bar	154
6.2.6 CoMoPd/Pt-HY (HDS-5) Catalyst	156
6.2.6.1 Effect of the Space Time at 310 °C under Molar H ₂ /HC Ratio of 7.2.....	157
6.2.6.2 Effect of the Molar Hydrogen/Hydrocarbon Ratio at 310 °C and 65 Bar.....	159
6.3 Concluding Remarks.....	160
 VII COMPARISON OF THE ACTIVITY IN TERMS OF CONVERSION OF DBT AND REFRACTORY SULFUR SPECIES.....	 161
7.1 Effect of Space Time at Molar H ₂ /HC Ratio of 7.2.....	161
7.1.1 HDS of Heavy Gas Oil over Conventional CoMo/Al ₂ O ₃ Catalyst, CoMoPtPd/HY and CoMoPd/Pt-HY Catalysts.....	161
7.1.2 HDS of Heavy Gas Oil over CoMoPtPd/HY, CoMoPtPd/Ni-HY and CoMoPd/Pt-HY Catalysts.....	165
7.1.3 HDS of Heavy Gas Oil over CoMo/PdNiPt-HY, CoMoNi/PdPt- HY, and CoMoPtPd/Ni-HY Catalysts.....	169

. CHAPTER	Page
7.1.4 HDS of Heavy Gas Oil over CoMo/PdNiPt-HY, CoMoNi/PdPt-HY, and CoMoPd/Pt-HY Catalysts.....	173
7.2 Effect of the Molar H ₂ /HC Ratio at Space Time of 6000 kg _{cat} /kmol.....	177
7.2.1 HDS of Heavy Gas Oil over CoMoPtPd/HY, CoMoPtPd/Ni-HY, and CoMoPd/Pt-HY Catalysts.....	178
7.2.2 HDS of Heavy Gas Oil over CoMo/PdNiPt-HY, CoMoNi/PdPt-HY, and CoMoPtPd/Ni-HY Catalysts.....	182
7.2.3 HDS of Heavy Gas Oil over CoMo/PdNiPt-HY, CoMoNi/PdPt-HY, and CoMoPd/Pt-HY Catalysts.....	186
7.3 Concluding Remarks.....	190
VIII COMPARISON OF ACTIVITY IN TERMS OF CONVERSION OF DBT AND 4,6-DMDBT INTO THEIR REACTION PRODUCTS.....	191
8.1 Effect of Space Time at 310 °C and Molar H ₂ /HC Ratio of 7.2.....	191
8.1.1 Commercial CoMo/Al ₂ O ₃ (HDS-0) Catalyst.....	191
8.1.1.1 Conversion of DBT in HDS of Heavy Gas Oil.....	191
8.1.1.2 Conversion of 4,6-DMDBT in HDS of Heavy Gas Oil...	193
8.1.2 CoMoPtPd/HY (HDS-1) Catalyst.....	194
8.1.2.1 Conversion of DBT in HDS of Heavy Gas Oil.....	195
8.1.2.2 Conversion of 4,6-DMDBT in HDS of Heavy Gas Oil	196
8.1.3 CoMoPd/Pt-HY (HDS-5) Catalyst.....	197
8.1.3.1 Conversion of DBT in HDS of Heavy Gas Oil.....	197
8.1.3.2 Conversion of 4,6-DMDBT in HDS of Heavy Gas Oil...	199
8.1.4 CoMoPtPd/Ni-HY (HDS-3) Catalyst.....	201
8.1.4.1 Conversion of DBT in HDS of Heavy Gas Oil.....	201
8.1.4.2 Conversion of 4,6-DMDBT in HDS of Heavy Gas Oil...	202
8.1.5 CoMo/PdNiPt-HY (HDS-8) Catalyst.....	204
8.1.5.1 Conversion of DBT in HDS of Heavy Gas Oil.....	204
8.1.5.2 Conversion of 4,6-DMDBT in HDS of Heavy Gas Oil...	205
8.1.6 CoMoNi/PdPt-HY (HDS-10) Catalyst.....	207
8.1.6.1 Conversion of DBT in HDS of Heavy Gas Oil.....	207
8.1.6.2 Conversion of 4,6-DMDBT in HDS of Heavy Gas Oil...	209
8.2 Concluding Remarks	211
IX CONCLUSIONS.....	212

	Page
LITERATURE CITED.....	214
APPENDIX A TEXTURES OF HY AND BOUND ZEOLITE.....	221
VITA.....	226

LIST OF FIGURES

FIGURE	Page
2.1 Some examples of hydrotreating reactions.....	7
2.2 Scheme of a typical desulfurizer unit.....	13
2.3 Proposed reaction network for the HDS of DBT by Houalla et al. (1978).....	17
2.4 Reaction scheme for the HDS of 4-MeDBT.....	18
2.5 Reaction scheme for the HDS of 4,6-DMDBT.....	18
2.6 Reaction pathway of 4,6-DMDBT over zeolite containing CoMo/Al ₂ O ₃ catalyst.....	19
2.7 Multiphase reaction network proposed for the HDS of 4,6-dimethyldibenzothiophene.....	20
2.8 Effect of recycle gas H ₂ S content on the temperature.....	26
2.9 Effect of the sodium content on catalysts on the activity relative to fresh catalyst.	27
2.10 Effect of arsenic on relative volumetric activity.....	29
2.11 HDS activities as a function of the calculated metal-sulfur bond energies.....	31
2.12 Schematic representation of the monolayer model.....	33
2.13 Locations of the promoter atoms in the MoS ₂ structure proposed by the intercalation and psudo-intercalation models.....	34

FIGURE	Page
2.14 The structure of Y-type zeolite or Faujasite (USY).....	38
3.1 Preparation of CoMoPtPd/HY (HDS-1) catalyst. Introduction of PtPd and CoMo into USY zeolite.....	42
3.2 Schematic presentation of the preparation of CoMoPtPd/HY (HDS-1) catalyst. Introduction of Pt, Pd, Co and Mo into zeolite...	43
3.3 Schematic presentation of ion exchange procedure with an aqueous nickel solution.....	45
3.4 Preparation of CoMoPtPd/Ni-HY (HDS-3) catalyst. Introduction of PtPd and CoMo into Ni-USY zeolite.....	46
3.5 Schematic presentation of the preparation of (CoMoPtPd/Ni-HY (HDS-3) catalyst. Introduction of Pt, Pd, Co, and Mo into zeolite...	46
3.6 Schematic procedure of platinum containing zeolite.....	47
3.7 Preparation of CoMoPd/Pt-HY (HDS-5) catalyst. Introduction of Pd and CoMo into Pt-USY zeolite.....	48
3.8 Schematic presentation of the preparation of CoMoPd/Pt-HY (HDS-5) catalyst. Introduction of Pd and CoMo into zeolite.....	49
3.9 Preparation of CoMo/PdNiPt-HY (HDS-8) catalyst. Introduction of Pd, Ni and CoMo into Pt-USY zeolite.....	50
3.10 Schematic presentation of the preparation of CoMo/PdNiPt-HY (HDS-8) catalyst. Introduction of Ni, Pd, Pt and CoMo into zeolite.	51
3.11 Preparation of CoMoNi/PdPt-HY (HDS-10) catalyst. Introduction of Pd, NiMo and CoMo into Pt-USY zeolite.....	52

FIGURE	Page
3.12 Schematic presentation of the preparation of CoMoNi/PtPd-HY (HDS-10) catalyst. Introduction of Pd, Ni and CoMo into zeolite...	53
3.13 Micromeritics BET machine Model ASAP 2010	57
3.14 X-ray photoelectron spectroscopy machine model Kratos AxisIHIs.....	59
3.15 Texture of HY, Ni-loaded zeolite, and Pt-loaded zeolite pressed at 3 and 4.5 Ton/cm ² . (a) Surface area (BET), (b) Total pore volume (BJH desorption).....	63
3.16 Textures of HY, Ni loaded zeolite and Pt-loaded zeolite pressed at 3 and 4.5 Ton/cm ² . (a) Micropore area, (b) Micropore volume.....	63
3.17 Pore size distribution of HY, Ni-loaded zeolite and Pt-loaded zeolite pressed at 3 and 4.5 Ton/cm ²	64
3.18 XPS spectrum of Pt 4d of the sample Pt-HY with 0.73 wt% of Pt...	65
3.19 Ni 2p core level XPS spectrum of calcined Ni-HY zeolite.....	66
3.20 Surface area of HY, CoMoPtPd/HY (HDS-1), CoMoPdPt/Ni-HY (HDS-3) and CoMoPd/Pt-HY (HDS-5) pressed at 3 and 4.5 Ton/cm ²	71
3.21 Micropore area of HY, CoMoPtPd/HY (HDS-1), CoMoPdPt/Ni-HY (HDS-3) and CoMoPd/Pt-HY (HDS-5) pressed at 3 and 4.5 Ton/cm ²	71
3.22 Total pore volumes (BJH desorption) of HY, CoMoPtPd/HY (HDS-1), CoMoPdPt/Ni-HY (HDS-3) and CoMoPd/Pt-HY (HDS-5) pressed at 3 and 4.5 Ton/cm ²	72

FIGURE	Page
3.23 Micropore volume of HY, CoMoPtPd/HY (HDS-1), CoMoPdPt/Ni-HY (HDS-3) and CoMoPd/Pt-HY (HDS-5) pressed at 3 and 4.5 Ton/cm ²	72
3.24 Pore size distribution of HY, CoMoPtPd/HY (HDS-1), CoMoPdPt/Ni-HY (HDS-3) and CoMoPd/Pt-HY (HDS-5) pressed at 3 and 4.5 Ton/cm ²	73
3.25 Surface area of HY, CoMoPtPd/HY (HDS-1), CoMo/PdNiPt-HY (HDS-8) and CoMoNi/PdPt-HY (HDS-10) catalysts pressed at 3 and 4.5 Ton/cm ²	77
3.26 Total pore volumes (BJH desorption) of HY, CoMoPtPd/HY (HDS-1), CoMo/PdNiPt-HY (HDS-8) and CoMoNi/PdPt-HY (HDS-10) catalysts pressed at 3 and 4.5 Ton/cm ²	77
3.27 Micropore area of HY, CoMoPtPd/HY (HDS-1), CoMo/PdNiPt-HY (HDS-8) and CoMoNi/PdPt-HY (HDS-10) catalysts pressed at 3 and 4.5 Ton/cm ²	78
3.28 Micropore volume of HY, CoMoPtPd/HY (HDS-1), CoMo/PdNiPt-HY (HDS-8) and CoMoNi/PdPt-HY (HDS-10) catalysts pressed at 3 and 4.5 Ton/cm ²	78
3.29 Pore distribution of HY, CoMoPtPd/HY (HDS-1), CoMo/PdNiPt-HY (HDS-8) and CoMoNi/PdPt-HY (HDS-10) catalysts pressed at 3 and 4.5 Ton/cm ²	79
4.1 Schematic representation of the Robinson-Mahoney catalyst testing reactor.....	81
4.2 Schematic of high pressure experimental setup for the hydrodesulfurization of heavy gas oil.....	82
4.3 Stainless steel Catalyst Basket modified by the Chemical Engineering workshop at A&M University.....	83

FIGURE	Page
4.4 Schematic representation of the configuration on Shimadzu 17A GC-TCD in load position (loading sample and backflush).....	85
4.5 Schematic representation of the configuration on Shimadzu 17A GC-TCD in inject position (analysis online and manual injection).....	85
4.6 Total ion chromatogram of heavy gas oil.....	88
4.7 Total ion chromatogram of one product obtained in the hydrodesulfurization of heavy gas oil.....	88
4.8 Molecular structures of the sulfur compounds present in heavy gas oil.....	89
4.9 Molecular structures of 2,8-dimethyldibenzothiophene and 3,6-dimethyldibenzothiophene present in heavy gas oil.....	90
4.10 Molecular structures of the aromatic compounds present in heavy gas oil.	90
4.11 Molecular structures of the reactions products of DBT and 4,6-DMDBT.....	91
4.12 Diagram of the procedure carried out for activating the experimental zeolite containing catalysts, reaction-activity test and shut down.	97
5.1 Typical total chromatogram of light cycle oil (LCO) using GC-MS.....	101
5.2 Typical total chromatogram of heavy gas oil (HGO) using GC-MS.....	102

FIGURE	Page
5.3 Part of the total ion chromatogram of the HGO and the LCO showing part of the peaks with retention times in the interval of 12-26 min.....	103
5.4 Part of the total ion chromatogram of the HGO and the LCO showing part of the peaks with retention times in the interval of 25-38 min.....	104
5.5 Part of the total ion chromatogram of the HGO and the LCO showing part of the peaks with retention times in the interval of 44-60 min.	105
5.6 Part of the total ion chromatogram of the HGO and the LCO showing part of the peaks with retention times in the interval of 60-67 min.	106
5.7 Part of the total ion chromatogram of the HGO and the LCO showing part of the peaks with retention times in the interval of 79-83.5 min.	107
5.8 Part of the total ion chromatogram of the HGO and the LCO showing part of the peaks with retention times in the interval of 99-104.5 min.	108
5.9 Part of the total ion chromatogram of the HGO and the LCO showing part of the peaks with retention times in the interval of 106-114 min.	109
5.10 Part of the total ion chromatogram of the HGO and the LCO showing part of the peaks with retention times in the interval of 114-121 min.	110
5.11 Fluorene hydrogenation network (From Lapinas et al., (1991)).	112

FIGURE	Page
5.12 Part of the total ion chromatogram of a typical HDS product and the HGO showing the peaks of the reaction products of HDS of DBT.....	113
5.13 Part of the total ion chromatogram of a typical HDS product and the HGO showing the peaks of fluorene and reaction products of HDS of 4,6-DMDBT.	114
6.1 Evolution of temperature with time obtained during the activation of the CoMoPtPd/HY (HDS-1) catalyst.....	116
6.2 Evolution of temperature with time obtained during the activation of the CoMo/Al ₂ O ₃ (HDS-0) catalyst.....	117
6.3 Concentration of H ₂ S in the gas phase during the activation of the CoMo/Al ₂ O ₃ (HDS-0) catalyst. P= 1 atm, T=330°C.....	118
6.4 Concentration of H ₂ S in the gas phase during the activation of the CoMoPtPd/HY (HDS-1) catalyst. P= 1 atm, T=330°C.....	118
6.5 Conversions of DBT, MDBT's and phenanthrene as a function of space time (W/F_{DBT}^0) for the commercial CoMo/Al ₂ O ₃ (HDS-0) catalyst. Reaction conditions were 65 bar, 330 °C and 2.8 molar H ₂ /HGO ratio. Feed: Heavy Gas Oil.....	121
6.6 Molar-averaged conversions as a function of space time (W/F_{DBT}^0) and temperature for the commercial CoMo/Al ₂ O ₃ (HDS-0) catalyst. Reaction conditions were 65 bar, and 2.8 molar H ₂ /HGO ratio. Feed: Heavy Gas Oil.....	121
6.7 Conversions of DBT, MDBT's and phenanthrene as a function of space time (W/F_{DBT}^0) for the commercial CoMo/Al ₂ O ₃ (HDS-0) catalyst. Reaction conditions were 65 bar, 330 °C and 7.2 molar H ₂ /HGO ratio. Feed: Heavy Gas Oil.....	123

FIGURE	Page
6.8 Conversions of DBT, MDBT's and phenanthrene as a function of space time (W/F_{DBT}^0) for the commercial CoMo/Al ₂ O ₃ (HDS-0) catalyst. Reaction conditions were 65 bar, 310 °C and 7.2 molar H ₂ /HGO ratio. Feed: Heavy Gas Oil.....	124
6.9 Conversions of DBT, MDBT's and phenanthrene as a function of space time (W/F_{DBT}^0) for the commercial CoMo/Al ₂ O ₃ (HDS-0) catalyst. Reaction conditions were 65 bar, 290 °C and 7.2 molar H ₂ /HGO ratio. Feed: Heavy Gas Oil.....	125
6.10 Molar-averaged conversions as a function of space time (W/F_{DBT}^0) and temperature for the commercial CoMo/Al ₂ O ₃ (HDS-0) catalyst. Reaction conditions were 65 bar, and 7.2 molar H ₂ /HGO ratio. Feed: Heavy Gas Oil.....	126
6.11 Conversions of DBT as a function of space time (W/F_{DBT}^0) and H ₂ /HGO mol ratio for the commercial CoMo/Al ₂ O ₃ (HDS-0) catalyst. Reaction conditions were 65 bar, 330 °C. Feed: Heavy Gas Oil.	127
6.12 Conversion of phenanthrene as a function of space time (W/F_{DBT}^0) and H ₂ /HGO mol ratio for the commercial CoMo/Al ₂ O ₃ (HDS-0) catalyst. Reaction conditions were 65 bar, 330 °C. Feed: Heavy Gas Oil.	128
6.13 Molar averaged-conversions as a function of space time (W/F_{DBT}^0) and molar H ₂ /HGO ratio for the commercial CoMo/Al ₂ O ₃ (HDS-0) catalyst. Reaction conditions were 65 bar, 330 °C. Feed: Heavy Gas Oil.....	129
6.14 Conversion of DBT, MDBT's and phenanthrene as a function of space time (W/F_{DBT}^0) for the CoMoPtPd/HY (HDS-1) catalyst. Reaction conditions were 65 bar, 330 °C and 7.2 molar H ₂ /HGO ratio. Feed: Heavy Gas Oil.....	130
6.15 Conversions of DBT, MDBT's and phenanthrene as a function of space time (W/F_{DBT}^0) for the CoMoPtPd/HY (HDS-1) catalyst.....	131

FIGURE	Page
6.16 Molar-averaged conversion as a function of space time (W/F_{DBT}^0) and temperature for the CoMoPtPd/HY (HDS-1) catalyst. Reaction conditions were 65 bar and 7.2 molar H_2 /HGO ratio. Feed: Heavy Gas Oil.....	132
6.17 Conversion of DBT, MDBT's and phenanthrene as a function of H_2 /HGO mol ratio for the CoMoPtPd/HY (HDS-1) catalyst. Reaction conditions were 65 bar, 310 °C, 6000 kg _{cat} h/kmol. Feed: Heavy Gas Oil.....	133
6.18 Conversion of DBT, MDBT's and phenanthrene as a function of H_2 /HGO mol ratio for the CoMoPtPd/HY (HDS-1) catalyst. Reaction conditions were 75 bar, 310 °C, 6000 kg _{cat} h/kmol. Feed: Heavy Gas Oil.....	134
6.19 Molar-averaged conversion as a function of the molar H_2 /HGO ratio and pressure for the CoMoPtPd/HY (HDS-1) catalyst. Reaction conditions were 310 °C, 6000 kg _{cat} h/kmol. Feed: Heavy Gas Oil.	135
6.20 Typical chromatogram of a gaseous reaction product (E16T4 experiment) showing the retention time for H_2 and CH_4 . Reaction conditions were 310 °C, 6000 kg _{cat} h/kmol, 65 bar, 9.2 molar H_2 /HGO ratio and CoMoPtPd/HY (HDS-1) catalyst.....	136
6.21 Conversion of DBT, MDBT's and phenanthrene as a function of space time (W/F_{DBT}^0) for CoMo/PdNiPt-HY (HDS-8) catalyst. Reaction conditions were 330 °C, 65 bar, and 7.2 molar H_2 /HGO ratio. Feed: Heavy Gas Oil.....	138
6.22 Conversion of DBT, MDBT's and phenanthrene as a function of space time (W/F_{DBT}^0) for CoMo/PdNiPt-HY (HDS-8) catalyst. Reaction conditions were 310 °C, 65 bar, and 7.2 molar H_2 /HGO ratio. Feed: Heavy Gas Oil.	139
6.23 Molar-averaged conversion as a function of space time (W/F_{DBT}^0) and temperature for CoMo/PdNiPt-HY (HDS-8) catalyst. Reaction conditions were 65 bar and 7.2 molar H_2 /HGO ratio.....	140

FIGURE	Page
6.24 Conversion of DBT, MDBT's and phenanthrene as a function of space time (W/F_{DBT}^0) for CoMo/PdNiPt-HY (HDS-8) catalyst. Reaction conditions were 310 °C, 65 bar, and 11.2 molar H ₂ /HGO ratio. Feed: Heavy Gas Oil.	141
6.25 Molar-averaged conversion as a function of space time (W/F_{DBT}^0) and H ₂ /HGO mol ratio for CoMo/PdNiPt-HY (HDS-8) catalyst. Reaction conditions were 310 °C, 65 bar, and 7.2 and 11.2 molar H ₂ /HGO ratio. Feed: Heavy Gas Oil.....	141
6.26 Conversion of DBT, sDBT and phenanthrene as a function of molar H ₂ /HGO ratio for CoMo/PdNiPt-HY (HDS-8) catalyst. Reaction conditions were 310 °C, 65 bar and 6000 kg _{cat} /h/kmol. Feed: Heavy Gas Oil.	142
6.27 Conversion of DBT, sDBT and phenanthrene as a function of molar H ₂ /HGO ratio for CoMo/PdNiPt-HY (HDS-8) catalyst. Reaction conditions were 310 °C , 75 bar and 6000 kg _{cat} /h/kmol. Feed: Heavy Gas Oil.	143
6.28 Molar-averaged conversion as a function of H ₂ /HGO mol ratio and pressure for CoMo/PdNiPt-HY (HDS-8) catalyst. Reaction conditions were 310 °C, 6000 kg _{cat} /h/kmol. Feed: Heavy Gas Oil...	143
6.29 Conversion of DBT, MDBT's and phenanthrene as a function of space time (W/F_{DBT}^0) for CoMoNi/PdPt-HY (HDS-10) catalyst. Reaction conditions were 330 °C , 65 bar, and 7.2 molar H ₂ /HGO ratio. Feed: Heavy Gas Oil.....	146
6.30 Conversion of DBT, MDBT's and phenanthrene as a function of space time (W/F_{DBT}^0) for CoMoNi/PdPt-HY (HDS-10) catalyst. Reaction conditions were 310 °C , 65 bar, and 7.2 molar H ₂ /HGO ratio. Feed: Heavy Gas Oil.....	146

FIGURE	Page
6.31 Molar-averaged conversion as a function of space time (W/F_{DBT}^0) and temperature for CoMoNi/PdPt-HY (HDS-10) catalyst. Reaction conditions were 65 bar and 7.2 molar H_2/HGO ratio. Feed: Heavy Gas Oil.	147
6.32 Conversion of DBT, MDBT's and phenanthrene as a function of space time (W/F_{DBT}^0) for CoMoNi/PdPt-HY (HDS-10) catalyst. Reaction conditions were 310 °C , 65 bar, and 11.2 molar H_2/HGO ratio. Feed: Heavy Gas Oil.....	148
6.33 Molar-averaged conversion, as a function of space time (W/F_{DBT}^0) and H_2/HGO mol ratio CoMoNi/PdPt-HY (HDS-10) catalyst. Reaction conditions were 310 °C, 65 bar, and 7.2 and 11.2 molar H_2/HGO ratio. Feed: Heavy Gas Oil.....	149
6.34 Conversion of DBT, sDBT and phenanthrene as a function of molar H_2/HGO ratio for CoMoNi/PdPt-HY (HDS-10) catalyst. Reaction conditions were 310 °C , 65 bar and 6000 $kg_{cat}h/kmol$. Feed: Heavy Gas Oil.....	150
6.35 Conversion of DBT, sDBT and phenanthrene as a function of molar H_2/HGO ratio for CoMoNi/PdPt-HY (HDS-10) catalyst. Reaction conditions were 310 °C , 75 bar and 6000 $kg_{cat}h/kmol$. Feed: Heavy Gas Oil.....	151
6.36 Molar-averaged conversion as a function of H_2/HGO mol ratio and pressure for CoMoNi/PdPt-HY (HDS-10) catalyst. Reaction conditions were 310 °C, 6000 $kg_{cat}h/kmol$. Feed: Heavy Gas Oil...	151
6.37 Conversion of DBT, MDBT's and phenanthrene as a function of space time (W/F_{DBT}^0) for CoMoPt Pd/Ni-HY (HDS-3) catalyst. Reaction conditions were 310 °C , 65 bar, and 7.2 molar H_2/HGO ratio. Feed: Heavy Gas Oil.....	153
6.38 Molar-averaged conversion as a function of space time (W/F_{DBT}^0) for CoMoPt Pd/Ni-HY (HDS-3) catalyst. Reaction conditions were 310 °C, 65 bar and 7.2 molar H_2/HGO ratio.....	154

FIGURE	Page
6.39 Conversion of DBT, sDBT and phenanthrene as a function of molar H ₂ /HGO ratio for CoMoPt Pd/Ni-HY (HDS-3) catalyst. Reaction conditions were 310 °C , 65 bar and 6000 kg _{cat} /kmol. Feed: Heavy Gas Oil.....	155
6.40 Molar-averaged conversion as a function of H ₂ /HGO mol ratio for CoMoPt Pd/Ni-HY (HDS-3) catalyst. Reaction conditions were 310 °C, 65 bar, 6000 kg _{cat} /kmol. Feed: Heavy Gas Oil.....	156
6.41 Conversion of DBT, sDBT and phenanthrene as a function of space time (W/F ⁰ _{DBT}) for CoMoPd/Pt-HY (HDS-5) catalyst. Reaction conditions were 310 °C , 65 bar, and 7.2 molar H ₂ /HGO ratio. Feed: Heavy Gas Oil.....	158
6.42 Molar-averaged conversion as a function of space time (W/F ⁰ _{DBT}) for CoMoPd/Pt-HY (HDS-5) catalyst. Reaction conditions were 310 °C, 65 bar and 7.2 molar H ₂ /HGO ratio. Feed: Heavy Gas Oil..	158
6.43 Conversion of DBT, sDBT and phenanthrene as a function of molar H ₂ /HGO ratio for CoMoPd/Pt-HY (HDS-5) catalyst. Reaction conditions were 310 °C , 65 bar and 6000 kg _{cat} /kmol. Feed: Heavy Gas Oil.....	159
6.44 Molar-averaged conversion as a function of H ₂ /HGO mol ratio for CoMoPd/Pt-HY (HDS-5) catalyst. Reaction conditions were 310 °C, 65 bar, 6000 kg _{cat} /kmol.....	160
7.1 Hydrodesulfurization conversions of dibenzothiophene (DBT) in heavy gas oil over CoMo/Al ₂ O ₃ , CoMoPtPd/HY, and CoMoPd/Pt-HY catalysts. (65 bar, 310 °C, 7.2 molar H ₂ /HGO ratio).....	163
7.2 Hydrodesulfurization conversions of 4-methyldibenzothiophene (4-MDBT) in heavy gas oil over CoMo/Al ₂ O ₃ , CoMoPtPd/HY, and CoMoPd/Pt-HY catalysts. (65 bar, 310 °C, 7.2 molar H ₂ /HGO ratio).....	163

FIGURE	Page
7.3 Hydrodesulfurization conversions of 4,6-dimethyldibenzothiophene (4,6-DMDBT) in heavy gas oil over CoMo/Al ₂ O ₃ , CoMoPtPd/HY, and CoMoPd/Pt-HY catalysts. (65 bar, 310 °C, 7.2 molar H ₂ /HGO ratio).....	164
7.4 Hydrogenation conversions of phenanthrene in heavy gas oil over CoMo/Al ₂ O ₃ , CoMoPtPd/HY, and CoMoPd/Pt-HY catalysts. (65 bar, 310 °C, 7.2 molar H ₂ /HGO ratio).....	164
7.5 Molar-averaged conversions in heavy gas oil over CoMo/Al ₂ O ₃ , CoMoPtPd/HY, and CoMoPd/Pt-HY catalysts. (65 bar, 310 °C, 7.2 molar H ₂ /HGO ratio).....	165
7.6 Hydrodesulfurization conversions of dibenzothiophene (DBT) in heavy gas oil over CoMoPtPd/HY, CoMoPtPd/Ni-HY and CoMoPd/Pt-HY catalysts. (65 bar, 310 °C, 7.2 molar H ₂ /HGO ratio).	167
7.7 Hydrodesulfurization conversions of 4-methyldibenzothiophene (4-MDBT) in heavy gas oil over CoMoPtPd/HY, CoMoPtPd/Ni-HY and CoMoPd/Pt-HY catalysts. (65 bar, 310 °C, 7.2 molar H ₂ /HGO ratio).....	167
7.8 Hydrodesulfurization conversions of 4,6-dimethyldibenzothiophene (4,6-DMDBT) in heavy gas oil over CoMoPtPd/HY, CoMoPtPd/Ni-HY and CoMoPd/Pt-HY catalysts. (65 bar, 310 °C, 7.2 molar H ₂ /HGO ratio).....	168
7.9 Hydrodesulfurization conversions of phenanthrene in heavy gas oil over CoMoPtPd/HY, CoMoPtPd/Ni-HY and CoMoPd/Pt-HY catalysts. (65 bar, 310 °C, 7.2 molar H ₂ /HGO ratio).....	168
7.10 Molar-averaged conversions in heavy gas oil over CoMoPtPd/HY, CoMoPtPd/Ni-HY and CoMoPd/Pt-HY catalysts. (65 bar, 310 °C, 7.2 molar H ₂ /HGO ratio).....	169

FIGURE	Page
7.11 Hydrodesulfurization conversions of dibenzothiophene (DBT) in heavy gas oil over CoMo/PdNiPt-HY, CoMoNi/PdPt-HY and CoMoPtPd/Ni-HY catalysts. (65 bar, 310 °C, 7.2 molar H ₂ /HGO ratio).	171
7.12 Hydrodesulfurization conversions of 4-methyldibenzothiophene (4-MDBT) in heavy gas oil over CoMo/PdNiPt-HY, CoMoNi/PdPt-HY and CoMoPtPd/Ni-HY catalysts. (65 bar, 310 °C, 7.2 molar H ₂ /HGO ratio).....	171
7.13 Hydrodesulfurization conversions of 4,6-dimethyldibenzothiophene (4,6-DMDBT) in heavy gas oil over CoMo/PdNiPt-HY, CoMoNi/PdPt-HY and CoMoPtPd/Ni-HY catalysts. (65 bar, 310 °C, 7.2 molar H ₂ /HGO ratio).....	172
7.14 Hydrogenation conversions of phenanthrene in heavy gas oil over CoMo/PdNiPt-HY, CoMoNi/PdPt-HY and CoMoPtPd/Ni-HY catalysts. (65 bar, 310 °C, 7.2 molar H ₂ /HGO ratio).....	172
7.15 Molar-averaged conversions in heavy gas oil over CoMo/PdNiPt-HY, CoMoNi/PdPt-HY and CoMoPtPd/Ni-HY catalysts. (65 bar, 310 °C, 7.2 molar H ₂ /HGO ratio).....	173
7.16 Hydrodesulfurization conversions of dibenzothiophene (DBT) in heavy gas oil over CoMo/PdNiPt-HY, CoMoNi/PdPt-HY and CoMoPd/Pt-HY catalysts. (65 bar, 310 °C, 7.2 molar H ₂ /HGO ratio)..	175
7.17 Hydrodesulfurization conversions of 4-methyldibenzothiophene (4-MDBT) in heavy gas oil over CoMo/PdNiPt-HY, CoMoNi/PdPt-HY and CoMoPd/Pt-HY catalysts. (65 bar, 310 °C, 7.2 molar H ₂ /HGO ratio).....	175
7.18 Hydrodesulfurization conversions of 4,6-dimethyldibenzothiophene (4,6-DMDBT) in heavy gas oil over CoMo/PdNiPt-HY, CoMoNi/PdPt-HY and CoMoPd/Pt-HY catalysts. (65 bar, 310 °C, 7.2 molar H ₂ /HGO ratio).....	176

FIGURE	Page
7.19 Hydrodesulfurization conversions of phenanthrene in heavy gas oil over CoMo/PdNiPt-HY, CoMoNi/PdPt-HY and CoMoPd/Pt-HY catalysts. (65 bar, 310 °C, 7.2 molar H ₂ /HGO ratio).....	176
7.20 Molar-averaged conversions in heavy gas oil over CoMo/PdNiPt-HY, CoMoNi/PdPt-HY and CoMoPd/Pt-HY catalysts. (65 bar, 310 °C, 7.2 molar H ₂ /HGO ratio).....	177
7.21 Hydrodesulfurization conversions of dibenzothiophene (DBT) in heavy gas oil over CoMoPtPd/HY, CoMoPtPd/Ni-HY and CoMoPd/Pt-HY catalysts. (65 bar, 310 °C, and space time of 6000 kg _{cat} h/kmol).	179
7.22 Hydrodesulfurization conversions of 4-methyldibenzothiophene (4-MDBT) in heavy gas oil over CoMoPtPd/HY, CoMoPtPd/Ni-HY and CoMoPd/Pt-HY catalysts. (65 bar, 310 °C, and space time of 6000 kg _{cat} h/kmol).....	180
7.23 Hydrodesulfurization conversions of 4,6-dimethyldibenzothiophene (4,6-DMDBT) in heavy gas oil over CoMoPtPd/HY, CoMoPtPd/Ni-HY and CoMoPd/Pt-HY catalysts. (65 bar, 310 °C, and space time of 6000 kg _{cat} h/kmol).....	180
7.24 Hydrodesulfurization conversions of phenanthrene in heavy gas oil over CoMoPtPd/HY, CoMoPtPd/Ni-HY and CoMoPd/Pt-HY catalysts. (65 bar, 310 °C, and space time of 6000 kg _{cat} h/kmol).....	181
7.25 Molar-averaged conversions in heavy gas oil over CoMoPtPd/HY, CoMoPtPd/Ni-HY and CoMoPd/Pt-HY catalysts. (65 bar, 310 °C, and space time of 6000 kg _{cat} h/kmol).....	181
7.26 Hydrodesulfurization conversions of dibenzothiophene (DBT) in heavy gas oil over CoMo/PdNiPt-HY, CoMoNi/PdPt-HY and CoMoPtPd/Ni-HY catalysts. (65 bar, 310 °C, and space time of 6000 kg _{cat} h/kmol).....	183

FIGURE	Page
7.27 Hydrodesulfurization conversions of 4-methyldibenzothiophene (4-MDBT) in heavy gas oil over CoMo/PdNiPt-HY, CoMoNi/PdPt-HY and CoMoPtPd/Ni-HY catalysts. (65 bar, 310 °C, and space time of 6000 kg _{cat} /kmol).....	184
7.28 Hydrodesulfurization conversions of 4,6-dimethyldibenzothiophene (4,6-DMDBT) in heavy gas oil over CoMo/PdNiPt-HY, CoMoNi/PdPt-HY and CoMoPtPd/Ni-HY catalysts. (65 bar, 310 °C, and space time of 6000 kg _{cat} /kmol).....	184
7.29 Hydrogenation conversions of phenanthrene in heavy gas oil over CoMo/PdNiPt-HY, CoMoNi/PdPt-HY and CoMoPtPd/Ni-HY catalysts. (65 bar, 310 °C, and space time of 6000 kg _{cat} /kmol).....	185
7.30 Molar-averaged conversions in heavy gas oil over CoMo/PdNiPt-HY, CoMoNi/PdPt-HY and CoMoPtPd/Ni-HY catalysts. (65 bar, 310 °C, and space time of 6000 kg _{cat} /kmol).....	185
7.31 Hydrodesulfurization conversions of dibenzothiophene (DBT) in heavy gas oil over CoMo/PdNiPt-HY, CoMoNi/PdPt-HY and CoMoPd/Pt-HY catalysts. (65 bar, 310 °C, and space time of 6000 kg _{cat} /kmol).	187
7.32 Hydrodesulfurization conversions of 4-methyldibenzothiophene (4-MDBT) in heavy gas oil over CoMo/PdNiPt-HY, CoMoNi/PdPt-HY and CoMoPd/Pt-HY catalysts. (65 bar, 310 °C, and space time of 6000 kg _{cat} /kmol).....	187
7.33 Hydrodesulfurization conversions of 4,6-dimethyldibenzothiophene (4,6-DMDBT) in heavy gas oil over CoMo/PdNiPt-HY, CoMoNi/PdPt-HY and CoMoPd/Pt-HY catalysts. (65 bar, 310 °C, and space time of 6000 kg _{cat} /kmol).....	188
7.34 Hydrodesulfurization conversions of phenanthrene in heavy gas oil over CoMo/PdNiPt-HY, CoMoNi/PdPt-HY and CoMoPd/Pt-HY catalysts. (65 bar, 310 °C, and space time of 6000 kg _{cat} /kmol).....	189

FIGURE	Page
7.35 Molar-averaged conversions in heavy gas oil over CoMo/PdNiPt-HY, CoMoNi/PdPt-HY and CoMoPd/Pt-HY catalysts. (65 bar, 310 °C, and space time of 6000 kg _{cat} h/kmol).....	189
8.1 Conversions as a function of W/F°_{DBT} over CoMo/Al ₂ O ₃ catalyst. (X_{DBT}) total conversion of DBT, (X_{BPH}) conversion of DBT into BPH, (X_{CHB}) conversion of DBT into CHB, (X_{BCH}) conversion of DBT into BCH. Experimental conditions: $T= 310\text{ }^{\circ}\text{C}$, $p_t = 65\text{ bar}$, $H_2/HGO=7.2$, Feed: Heavy Gas Oil.....	192
8.2 Conversions as a function of W/F°_{DBT} over CoMo/Al ₂ O ₃ catalyst. ($X_{4,6\text{-DMDBT}}$) total conversion of 4,6-DMDBT, ($X_{3,4\text{-DMBPH}}$) conversion of 4,6-DMDBT into 3,4-DMBPH. Experimental conditions: $T= 310\text{ }^{\circ}\text{C}$, $p_t = 65\text{ bar}$, $H_2/HGO=7.2$, Feed: Heavy Gas Oil.....	194
8.3 Conversions as a function of W/F°_{DBT} over CoMoPtPd/HY catalyst. (X_{DBT}) total conversion of DBT, (X_{BPH}) conversion of DBT into BPH, (X_{CHB}) conversion of DBT into CHB, (X_{BCH}) conversion of DBT into BCH. Experimental conditions: $T= 310\text{ }^{\circ}\text{C}$, $p_t = 65\text{ bar}$, $H_2/HGO=7.2$. Feed: Heavy Gas Oil.....	196
8.4 Conversions as a function of W/F°_{DBT} over CoMoPtPd/HY catalyst. ($X_{4,6\text{-DMDBT}}$) total conversion of 4,6-DMDBT, ($X_{3,4\text{-DMBPH}}$) conversion of 4,6-DMDBT into 3,4-DMBPH. Experimental conditions: $T= 310\text{ }^{\circ}\text{C}$, $p_t = 65\text{ bar}$, $H_2/HGO=7.2$. Feed: Heavy Gas Oil.....	197
8.5 Conversions as a function of W/F°_{DBT} over CoMoPd/Pt-HY catalyst. (X_{DBT}) total conversion of DBT, (X_{BPH}) conversion of DBT into BPH, (X_{CHB}) conversion of DBT into CHB, (X_{BCH}) conversion of DBT into BCH. Experimental conditions: $T= 310\text{ }^{\circ}\text{C}$, $p_t = 65\text{ bar}$, $H_2/HGO=7.2$. Feed: Heavy Gas Oil.....	199
8.6 Conversions as a function of W/F°_{DBT} over CoMoPd/Pt-HY catalyst. ($X_{4,6\text{-DMDBT}}$) total conversion of 4,6-DMDBT, ($X_{3,4\text{-DMBPH}}$) conversion of 4,6-DMDBT into 3,4-DMBPH.	200

FIGURE	Page
8.7 Conversions as a function of W/F_{DBT}^0 over CoMoPtPd/Ni-HY catalyst. (X_{DBT}) total conversion of DBT, (X_{BPH}) conversion of DBT into BPH, (X_{CHB}) conversion of DBT into CHB, (X_{BCH}) conversion of DBT into BCH. Experimental conditions: $T= 310$ °C, $p_t = 65$ bar, $H_2/HGO=7.2$. Feed: Heavy Gas Oil.....	202
8.8 Conversions as a function of W/F_{DBT}^0 over CoMoPtPd/Ni-HY catalyst. ($X_{4,6-DMDBT}$) total conversion of 4,6-DMDBT, ($X_{3,4-DMBPH}$) conversion of 4,6-DMDBT into 3,4-DMBPH. Experimental conditions: $T= 310$ °C, $p_t = 65$ bar, $H_2/HGO=7.2$. Feed: Heavy Gas Oil.....	203
8.9 Conversions as a function of W/F_{DBT}^0 CoMo/PdNiPt-HY catalyst. (X_{DBT}) total conversion of DBT, (X_{BPH}) conversion of DBT into BPH, (X_{CHB}) conversion of DBT into CHB, (X_{BCH}) conversion of DBT into BCH. Experimental conditions: $T= 310$ °C, $p_t = 65$ bar, $H_2/HGO=7.2$. Feed: Heavy Gas Oil.....	205
8.10 Conversions as a function of W/F_{DBT}^0 over CoMo/PdNiPt-HY catalyst. ($X_{4,6-DMDBT}$) total conversion of 4,6-DMDBT, ($X_{3,4-DMBPH}$) conversion of 4,6-DMDBT into 3,4-DMBPH. Experimental conditions: $T= 310$ °C, $p_t = 65$ bar, $H_2/HGO=7.2$. Feed: Heavy Gas Oil.	207
8.11 Conversions as a function of W/F_{DBT}^0 over CoMoNi/PdPt-HY catalyst. (X_{DBT}) total conversion of DBT, (X_{BPH}) conversion of DBT into BPH, (X_{CHB}) conversion of DBT into CHB, (X_{BCH}) conversion of DBT into BCH. Experimental conditions: $T= 310$ °C, $p_t = 65$ bar, $H_2/HGO=7.2$. Feed: Heavy Gas Oil.....	209
8.12 Conversions as a function of W/F_{DBT}^0 over CoMoNi/PdPt-HY catalyst. ($X_{4,6-DMDBT}$) total conversion of 4,6-DMDBT, ($X_{3,4-DMBPH}$) conversion of 4,6-DMDBT into 3,4-DMBPH. Experimental conditions: $T= 310$ °C, $p_t = 65$ bar, $H_2/HGO=7.2$. Feed: Heavy Gas Oil.....	210

LIST OF TABLES

TABLE	Page
2.1 Typical process conditions and hydrogen consumption for various hydrotreating reactions.....	8
2.2 Sulfur-containing compounds in Petroleum.....	10
2.3 General summary of product types and distillation Range	11
2.4 Typical hydrodesulfurization reactions.....	15
2.5 Reactivities of several heterocyclic sulfur compounds.....	22
2.6 Reactivities of selected methyl-substituted dibenzothiophenes.....	24
3.1 USY sample and their manufacture properties.....	40
3.2 List of chemicals and their essay data.....	40
3.3 Expected composition of the CoMoPtPd/HY (HDS-1) catalyst.....	42
3.4 Expected composition of the CoMoPtPd/Ni-HY (HDS-3) catalyst.....	45
3.5 Expected composition of the CoMoPd/Pt-HY (HDS-5) catalyst.....	48
3.6 Expected composition of CoMo/PdNiPt-HY (HDS-8) catalyst.....	51
3.7 Expected composition of CoMoNi/PtPd-HY (HDS-10) catalyst	53
3.8 Analytical techniques used for the chemical and physical characterization of experimental catalysts.....	54

TABLE	Page
3.9 Specification and typical analysis of a commercial CoMo/Al ₂ O ₃ catalyst...	55
3.10 Composition of the metal-HY samples used as matrix of the catalyst.....	61
3.11 Physical properties of HY, Ni-HY and Pt-HY (used as matrix for preparing the HDS catalysts) pressed at 3 and 4.5 Ton/cm ²	62
3.12 Ni 2p XPS core level BE values of calcined Ni-HY zeolite.....	66
3.13 XPS surface compositions of calcined Ni-HY zeolite.....	67
3.14 Composition of the HDS-1, HDS-3 and HDS-5 catalysts compared to the CoMo/Al ₂ O ₃ commercial catalyst.....	69
3.15 Physical properties of HY, CoMoPtPd/HY (HDS-1), CoMoPdPt/Ni-HY (HDS-3) and CoMoPd/Pt-HY (HDS-5) catalysts pressed at 3 and 4.5 Ton/cm ² compared with the commercial CoMo/Al ₂ O ₃ (Com).....	70
3.16 Composition of the HDS-1, HDS-8 and HDS-10 catalysts compared with the CoMo/Al ₂ O ₃ commercial catalyst.....	74
3.17 Physical properties of HY, CoMoPtPd/HY (HDS-1), CoMo/PdNiPt-HY (HDS-8) and CoMoNi/PdPt-HY (HDS-10) catalysts pressed at 3 and 4.5 Ton/cm ² vs the commercial CoMo/Al ₂ O ₃ (Com) catalyst.....	76
4.1 Conditions for the gas chromatographic analysis of hydrogen sulfide, hydrogen and methane in the desorbed gas from reaction products.....	84
4.2 Integration parameters used in the GC-MS for the analysis of feedstock and the hydrocarbon liquid products coming from the reactor.....	87
4.3 Retention times of the selected sulfur compounds, naphthalene and phenanthrene.....	92

TABLE	Page
4.4 Retention times of reaction products of DBT and 4,6-DMDBT. Operating conditions: Cat. HDS-1, $W/F_{DBT}=6000 \text{ kg}_{cat}h/kmol$, $T = 310 \text{ }^\circ\text{C}$, $H_2/HC=7.2$ mol ratio, $P= 65$ bar.....	92
4.5 Operating conditions used to measure the catalytic activity for the CoMoPtPd/HY (HDS-1) catalyst.....	97
5.1 Typical properties of heavy gas oil and a Mexican light cycle oil	100
5.2 Composition of a USA heavy gas oil and a Mexican light cycle oil as determined by GC-MS.....	110
6.1 Operating conditions used to evaluate the catalytic activity for the CoMo/Al ₂ O ₃ (HDS-0) catalyst.....	119
6.2 Operating conditions used to test the catalytic activity for the CoMo/PdNiPt-HY (HDS-8) catalyst.....	137
6.3 Operating conditions used to evaluate the catalytic activity in the HDS of heavy gas oil over the CoMoNi/PdPt-HY (HDS-10) catalyst.....	144
6.4 Operating conditions used to evaluate the catalytic activity for the CoMoPt Pd/Ni-HY (HDS-3) catalyst.....	152
6.5 Operating conditions used to evaluate the catalytic activity for the CoMo Pd/Pt-HY (HDS-5) catalyst.....	156
7.1 Molar-averaged conversion and conversions of sulfur compounds and phenanthrene in the HDS and HDA of heavy gas oil over conventional CoMo/Al ₂ O ₃ (HDS-0) catalyst, CoMoPtPd/HY (HDS-1) and CoMoPd/Pt-HY (HDS-5) catalysts.....	162

TABLE	Page
7.2 Molar-averaged conversions and conversions of sulfur compounds and phenanthrene in the HDS and HDA of heavy gas oil over CoMoPtPd/HY (HDS-1), CoMoPtPd/Ni-HY (HDS-3) and CoMoPd/Pt-HY (HDS-5) catalysts.....	166
7.3 Molar-averaged conversions and conversions of sulfur compounds and phenanthrene in the HDS and HDA of heavy gas oil over CoMo/PdNiPt-HY (HDS-8), CoMoNi/PdPt-HY (HDS-10), and CoMoPtPd/Ni-HY (HDS-3) catalysts.....	170
7.4 Molar-averaged conversions and conversions of sulfur compounds and phenanthrene in the HDS and HDA of heavy gas oil over CoMo/PdNiPt-HY (HDS-8), CoMoNi/PdPt-HY (HDS-10), and CoMoPd/Pt-HY (HDS-5) catalysts.....	174
7.5 Molar-averaged conversions and conversions of sulfur compounds and phenanthrene in the HDS and HDA of heavy gas oil over CoMoPtPd/HY (HDS-1), CoMoPtPd/Ni-HY (HDS-3), and CoMoPd/Pt-HY (HDS-5) catalysts.....	179
7.6 Molar-averaged conversions and conversions of sulfur compounds and phenanthrene in the HDS and HDA of heavy gas oil over CoMo/PdNiPt-HY (HDS-8), CoMoNi/PdPt-HY (HDS-10), and CoMoPtPd/Ni-HY (HDS-3) catalysts.....	183
7.7 Molar-averaged conversions and conversions of sulfur compounds and phenanthrene in the HDS and HDA of heavy gas oil over CoMo/PdNiPt-HY (HDS-8), CoMoNi/PdPt-HY (HDS-10), and CoMoPd/Pt-HY (HDS-5) catalysts.....	187
8.1 Conversions of DBT into its reaction products as a function of space time (W/F_{DBT}^0) over CoMo/Al ₂ O ₃ catalyst.....	192
8.2 Total conversions of 4,6-DMDBT and conversions into 3,4-dimethylbiphenyl as a function of space time (W/F_{DBT}^0) over CoMo/Al ₂ O ₃ catalyst.....	193

TABLE	Page
8.3 Conversions of DBT into their reaction products as a function of space time (W/F_{DBT}°) over CoMoPtPd/HY catalyst.....	195
8.4 Total conversions of 4,6-DMDBT and conversions into 3,4-dimethylbiphenyl as a function of space time (W/F_{DBT}°) over CoMoPtPd/HY catalyst.....	196
8.5 Conversions of DBT into their reaction products as a function of space time (W/F_{DBT}°) over CoMoPd/Pt-HY catalyst.....	198
8.6 Total conversions of 4,6-DMDBT and conversions into 3,4-dimethylbiphenyl as a function of space time (W/F_{DBT}°) over CoMoPd/Pt-HY catalyst.....	200
8.7 Conversions of DBT into their reaction products as a function of space time (W/F_{DBT}°) over CoMoPtPd/Ni-HY catalyst.....	202
8.8 Total conversions of 4,6-DMDBT and conversions into 3,4-dimethylbiphenyl as a function of space time (W/F_{DBT}°) over CoMoPtPd/Ni-HY catalyst.....	203
8.9 Conversions of DBT into reaction products as a function of space time (W/F_{DBT}°) over CoMo/PdNiPt-HY catalyst.....	205
8.10 Total conversions of 4,6-DMDBT and conversions into 3,4-dimethylbiphenyl as a function of space time (W/F_{DBT}°) over CoMo/PdNiPt-HY catalyst.....	206
8.11 Conversions of DBT into their reaction products as a function of space time (W/F_{DBT}°) over CoMoNi/PdPt-HY catalyst.....	208
8.12 Total conversions of 4,6-DMDBT and conversions into 3,4-dimethylbiphenyl as a function of space time (W/F_{DBT}°) over CoMoNi/PdPt-HY catalyst.....	210

CHAPTER I

INTRODUCTION

Hydrodesulfurization (HDS) of petroleum fractions is one of the most important processes in the petroleum industry to produce clean fuels. In particular, sulfur removal in diesel fuels is now strongly desirable for environmental and technical reasons. For instance, HDS is used to prevent atmospheric pollution by sulfur oxides produced during the combustion of petroleum-based fuels, to prevent poisoning of sulfur-sensitive metal catalysts used in subsequent reforming reactions and in the catalytic converter for exhaust emission treatment, finally, to avoid corrosion problems in engines.

The European Union has limited the sulfur content in diesel to 0.005 wt% since 2005 (Song, 2000). In the United States the sulfur content in diesel is limited to 0.050 wt% since 1993. For June 2006 the maximum sulfur content will be 0.0015 wt%. While the Japanese official legislation has proposed <10-ppm sulfur content in diesel for 2007, most Japanese refiners voluntarily began <10-ppm sulfur diesel before January 2005 and many other countries are planning to begin implementing ultra-low sulfur diesel fuel (ULSD) with a content of <10-ppm to supply in the near future. In view of the demands for USLD fuels, the development of technology for ultra-deep hydrodesulfurization to remove most of the sulfur compounds in the diesel fractions will become extremely important.

Removal of sulfur content is possible by using modified operating conditions for hydrotreaters with respect to the reaction temperature and space time. However, higher reaction temperature results in coke formation on the catalyst and rapid catalytic deactivation, and higher space time results in reduced hydrotreating efficiency, thus, requiring additional reactors or larger reactor replacement. Consequently, the best way

This dissertation follows the format of *Industrial And Engineering Chemistry Research*.

of achieving the ultra-deep HDS without changing the operating conditions and in a cost-effective manner is to develop a catalyst having a super high HDS and a high hydrodearomatization (HDA) activity.

A catalyst with these properties could be formulated using new active phases such as noble metals (Pt, Pd, Rh, Ru) in combination with basic metals such as CoMo or NiMo supported in zeolites. However, although noble metals show activity for hydrogenation at low temperatures, their use as catalysts will become attractive only if their sulfur resistance can be greatly enhanced.

1.1 Motivation and Significance of Research

This work is motivated by the necessity of getting novel sulfur-resistant noble metal catalysts for more efficient hydrotreating of sulfur-containing middle distillates. Middle distillates are petroleum products boiling between the kerosene (C₈-C₁₈, 126-258 °C) and the lubricating oil fraction (>C₂₀, >343 °C).

Properties of middle distillates depend on the nature of the original crude oil and the refining processes by which the fuel is produced. In the case of Diesel fuel, “PEMEX-Refinación” in Mexico has considered the refinery reconfiguration integrating streams from other processes to increase diesel fuel production with low sulfur content. These streams could come from visbreaking, coker, FCC, etc, and they have a higher amount of sulfur and unsaturated compounds than straight run gas oil because they could come from crude with high Maya/Istmo volume ratio (>60).

The sulfur-containing compounds in Middle Distillates such as Diesel, Light Cycle Oil (LCO), and Heavy Gas oil (HGO), etc, are complex molecules of alkyl-aromatics and substituted alkyl aromatics which are called refractory compounds because of the difficulty to remove the S heteroatom.

The conventional catalysts for hydrotreating of middle distillates are basically formulated with CoMo/Al₂O₃ and NiMo/Al₂O₃. However, although they have high

activity for HDS, they are insufficient to guarantee a diesel production with low sulfur content (deep HDS, <50 ppm). In order to address this demand of deep HDS a catalyst with high activity towards the hydrogenolysis (rupture of the C-S bond) and hydrogenation of aromatics is required. The combination of active elements such as CoMo is excellent for HDS but is somewhat less active for hydrogenation of aromatics. Metals like Pt, Pd or Ni, on the other hand, are very good for hydrogenation, but their use in HDS catalysts will become attractive only if their sulfur resistance is enhanced. Related with this, it has been reported that the HDA activity of Pt-Pd catalysts greatly depends on the kind of supports (Yasuda et al., 1999, Shimada and Yoshimura, 2003, Song and Schmitz, 1997). On the other hand, it has been accepted that metal-zeolite catalysts have high possibility as new hydrodesulfurization catalysts for petroleum fractions (Laniecki and Zmierczak, 1991; Okamoto, 1997; Sugioka, 1996). In this context, noble-metal catalysts on acidic supports, such as HY zeolite, have been reported as high sulfur-tolerant aromatic hydrogenation catalysts.

1.2 Scope of Research

In this work, a study of Middle Distillate Hydrotreatment Zeolite Catalysts containing Pt/Pd or Ni is proposed. The study is mainly aimed at examining the potential of zeolite-supported Pd, Pt, Ni, Co and Mo catalysts for removing refractory sulfur compounds such as 4,6-dimethyldibenzothiophene (4,6-DMDBT) and 4-methyldibenzothiophene (4-MDBT) of middle distillates. The specific purposes of this research are as follow:

(i) Synthesis and characterization of Pt-HY and Ni-HY as matrix of the deep hydrodesulfurization catalysts.

(ii) Synthesis and characterization of zeolite catalysts containing metal combinations of basic metals, such as Co, Mo, Ni, and noble metals, such as Pt, Pd, supported on HY, Ni-HY and Pt-HY

(iii) Determine the activity of the prepared catalysts for the deep HDS of heavy gas oil, under the effect of the operating conditions: temperature, space time, hydrogen/hydrocarbon mol ratio and pressure.

(iv) Determine the conversions of DBT, 4-MDBT and 4,6-DMDBT in the HDS of heavy gas oil over CoMoPtPd/HY, CoMoPtPd/Ni-HY, CoMoPd/Pt-HY, CoMo/PdNiPt-HY and CoMoNi/PdPt-HY catalysts.

(v) Generate the technical bases for the future development of a catalyst and process for deep hydrodesulfurization of heavy gas oil with sulfur levels according to European International regulation of < 50 ppm (2005-2006) and/or <15 ppm for 2010 year.

Some aspects considered in the development of this project were: zeolites have acidity and shape-selectivity properties for their use as catalysts in hydrocarbon hydrotreating reactions. In particular, ultra stable Y zeolite (USY) has homogeneous large pores and supercages window diameters interconnected in three dimensions and they are stable in thermal as well as hydrothermal operation.

The hydrodesulfurization of refractory 4-methyl- and 4,6-dimethyldibenzothiophene is essential to achieve the sulfur level of gas oil requested by current regulation. Their direct hydrodesulfurization through the interaction of their sulfur atom with the catalysts surface is sterically hindered by neighboring methyl groups. The steric hindrance can be reduced by destruction of the planar configuration through hydrogenation. According to Isoda et al. (1996) the hydrogenation of one of two phenyl rings breaks the coplanarity of the dibenzothiophene skeleton, moderating the steric hindrance of the methyl groups. Furthermore, the hydrogenation of the neighboring phenyl ring increases the electron density of the sulfur atom to enhance its elimination through electron donation to the active site.

4,6-DMDBT must compete for the hydrogenation active sites with other aromatic hydrocarbons in gas oil, such as naphthalene and tetralin, which compete for hydrogen and they competitively adsorb on the hydrogenation sites, thus slowing down the desired hydrogenation. There are two possible approaches for efficient desulfurization of 4,6-DMDBT: the selective hydrogenation of 4,6-DMDBT in the dominant aromatic

compounds and the hydrodesulfurization (HDS) reaction after the migration of substituted methyl groups. Basic and noble metals such as Ni and Pt favor the aromatic hydrogenation, and zeolites are good promoters for isomerization. So a combination of noble metals and zeolite could improve the HDS of 4,6-DMDBT. Moreover, the catalysts based on Pt-Pd alloys supported on zeolites enhance the sulfur resistance of the supported Pt catalysts. The formation of Pt-Pd alloys depends on the method of catalyst preparation, precursors and pretreatment conditions of the catalysts. Fast Fourier transform infrared (FFT-IR) spectroscopy, characterizing CO adsorbed on a Pt-Pd/Al₂O₃ catalyst sample has been used by Jan et al. (1996) to examine the formation of bimetallic interactions. The results indicated that Pd-Pt catalysts made from Pd(II) and Pt(II) acetate without calcination pretreatment presented more Pd-Pt bimetallic interaction than catalysts made from Palladium (II) acetate with calcinations at 450 °C in air and from palladium amine. The bimetallic interactions were formed from the catalytic reduction of Pt as inferred from the FFT-IR monitoring of the decomposition of carboxylate ligands of [Pd(OAc)₂]. The decrease of electron density on Pt induced by such bimetallic interactions enhances the sulfur resistance of the catalysts, leading to relatively high activities for aromatics hydrogenation.

For this reason it is considered of great interest to study catalysts based on PtPd and/or Ni containing USY zeolites and its application in CoMo and/or NiMo formulations for deep HDS of middle distillates, suggesting that the rate of the hydrogenation route could be increased by Pt or Ni containing zeolite. Thus, these catalysts could be good candidates for the application of deep hydrodesulfurization with good aromatics hydrogenation.

CHAPTER II

LITERATURE REVIEW

2.1 Hydrotreating Processes

The hydrotreating processes (HDT) of oil-derived middle distillates have deserved much attention during recent years because of more stringent environmental regulations that restrict heteroatoms (S, N, O, etc.) and aromatic compounds content. Hydrotreating or hydroprocessing refers to a variety of catalytic hydrogenation processes that covers desulfurization (HDS), denitrogenation (HDN), aromatics saturation (HDA), hydrodeoxygenation (HDO), hydrocracking (HDC), and metals removal (HDM) of different petroleum streams in a refinery. These processes represent some of the most important catalytic processes and the annual sales of hydrotreating catalysts represent close to 10% of the total world market for catalysts (Anderson and Boudart, 1996).

Hydrotreating also plays an essential role in pretreating streams for other refinery processes such as catalytic reforming, fluid catalytic cracking (FCC) and is used extensively for conversion of heavy feedstock and for improving the quality of final products.

2.1.1 Process Chemistry

Hydrotreating imply small changes in overall molecular structure, but hydrocracking reactions often occur simultaneously. The hydrotreating process is conducted in the presence of excess hydrogen over a catalyst at elevated temperature and pressure. The consumption of hydrogen is especially high when treating heavier feeds. The hydrotreating consists mainly of HDS and hydrogenation. All reactions are exothermic, so the control of temperature in the reactor, especially the catalyst bed, is very important in the practical operation (Kabe et al., 1999). Although equilibrium constants decrease at higher temperatures, the heteroatom removal reactions are favored under practical

operating conditions: temperature of 320-440 °C and pressure of 10-150 atm. Hydrogenation of aromatics, however, is limited by thermodynamics at high temperature and lower hydrogen pressure. Examples of hydrotreating reactions are shown in Figure 2.1.

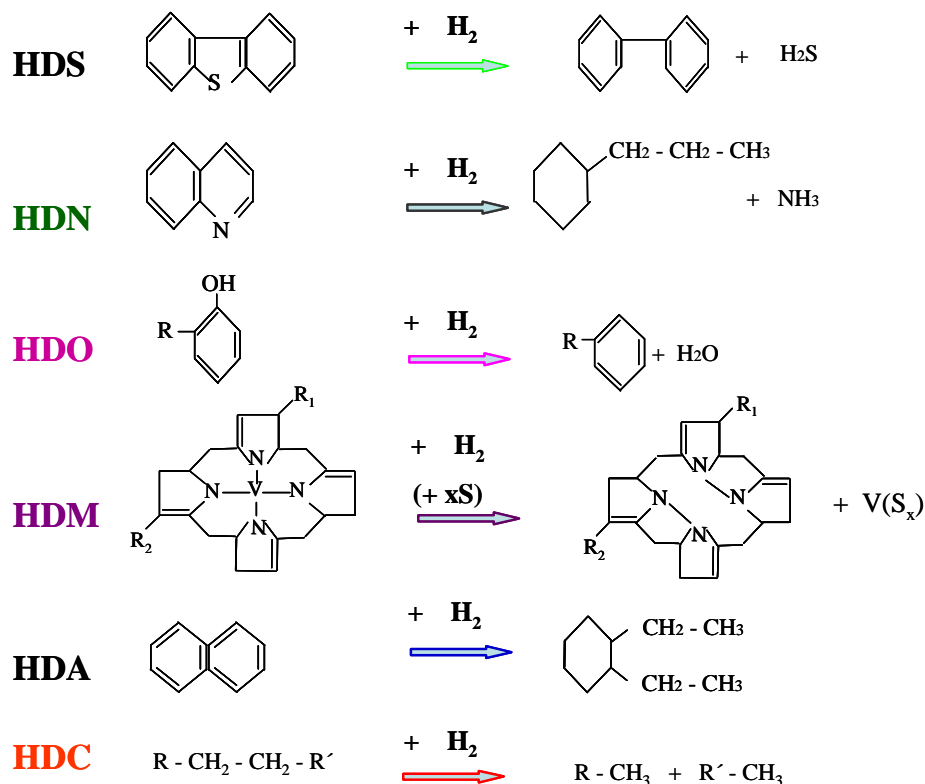


Figure 2.1 Some examples of hydrotreating reactions.

Removal of contaminants involves the controlled breaking of the molecular chain or ring at the point where the sulfur, nitrogen, or oxygen atom is joined to carbon atoms. This breaking is accomplished by the introduction of hydrogen with production of hydrogen sulfide, ammonia, or water, respectively. The resultant hydrocarbon reaction product usually remains either as one or more aliphatic hydrocarbons or as an alkyl

group on an aromatic or naphthenic hydrocarbon. These hydrocarbon reaction products usually have larger liquid molecular volumes than do the parent sulfur-, nitrogen-, or oxygen-containing reactants. Owing to the fact that only a small amount of cracking of carbon-to-carbon bonds occurs and that olefins and some aromatics are hydrogenated, yields of liquids from most hydrotreating operations are in excess of 100 volume percent of the charge stock. (Meyers, 1986)

The degree of hydrotreating required on petroleum fractions generally will depend entirely on the feed and the refiner's need to meet the specific requirements related to final product blending and application. Typical process conditions for various hydrotreating reactions are shown in Table 2.1.

Table 2.1 Typical process conditions and hydrogen consumption for various hydrotreating reactions (from Anderson and Boudart, 1996)

Hydrotreating process	Temperature (°C)	Hydrogen partial pressure (atm)	LHSV¹ (h⁻¹)	Hydrogen consumption (Nm³m⁻³)
Naphtha	320	10-20	3-8	2-10
Kerosene	330	20-30	2-5	5-15
Atm, GO	340	25-40	1.5-4	20-40
VGO	360	50-90	1-2	50-80
ARDS²	370-410	80-130	0.2-0.5	100-175
VGO HDC	380-410	90-140	1-2	150-300
Residue HDC	400-440	100-150	0.2-0.5	150-300

¹ Liquid hour space velocity (the ratio of the hourly volume flow of liquid in, say, barrels to the catalysts volume in barrels)

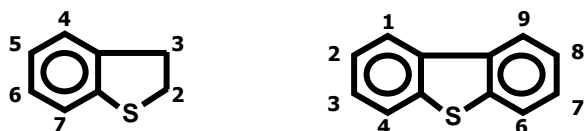
²Atm residue desulfurization.

The catalyst is the key to most hydroprocessing applications. Basically the catalyst combines high volumetric activity with low bulk density, resulting in low cost per unit of activity to the refiner. HDS and HDN catalysts generally consist of sulphides of Co and Mo or Ni and Mo on a high surface area support such as aluminum oxide.

2.1.2 Sulfur Compounds in Raw Oil Materials

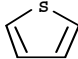
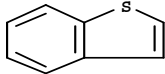
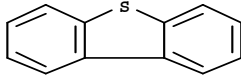
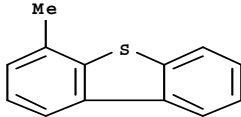
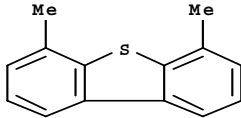
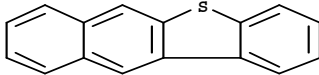
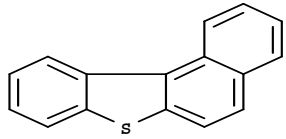
Sulfur compounds are among the most important heteroatomic constituents of petroleum. They are generally classified into one of two types: heterocycles or nonheterocycles (Kabe, 1999). The latter comprises thiols, sulfides and disulfides. Heterocycles are mainly composed of thiophenes with one to several rings and their alkyl or aryl substituents. Examples of sulfur compounds are shown in Table 2.2.

The numbering of the carbon atoms in benzothiophene and dibenzothiophene is as follows:



Sulfur containing polyaromatic compounds in straight run gas oil from Arabian Light were analyzed and determined by a gas chromatography-atomic emission detector (GC-AED) and a gas chromatography-mass spectroscopy (GC-MS (Kabe et al., 1992)). It was found that 42 kinds of alkylbenzothiophene and 29 kinds of alkyl dibenzothiophene were included in the oil. When this oil was desulfurized using CoMo/Al₂O₃ catalyst at 300-410 °C, 4-methyldibenzothiophene (4-MDBT) and 4,6-dimethyldibenzothiophene (4,6-DMDBT) were most difficult to desulfurize. This result suggested that HDS of DBT's substituted at the 4,6-positions is the key reaction to achieve deep desulfurization.

Table 2.2 Sulfur-containing compounds in Petroleum

Compound	Structure
Thiols (Mercaptanes)	RSH
Disulfides	RSSR'
Sulfides	RSR'
Thiophene	
Benzo[b]thiophene or Benzothiophene	
Dibenzothiophene	
4-Methyldibenzothiophene	
4,6-Dimethyldibenzothiophene	
Benzo[b]naphtho[2,3-d]thiophene	
Benzo[b]naphtho[1,2-d]thiophene	

2.1.3 Compositional Features of Distillate Fuel Oil

In this work, heavy gas oil will be used to test the experimental catalysts; however, a summary of compositional features of distillate fuel oil is given in this section because heavy gas oil has similar properties to those fractions.

The term “fuel oil” is sometimes used to refer to the light, amber-colored middle distillates or gas oils that are distinguished from the residual fuel oil by being characterized as distilled fuel oil (ASTM-D-396). In this specification the No. 1 grade fuel oil is a kerosene type used in vaporizing pot-type burners whereas the No. 2 fuel oil is a distillate oil (gas oil) used for general-purpose domestic heating. Kerosene may also be included in this definition.

Distillate fuel oils are vaporized and condensed during a distillation process and thus have a definite boiling range and do not contain high-boiling oils or asphaltic components. In general they correspond to light gas oil (Table 2.3).

Fuel oils are made for specific uses and may be either distillates or residuals or mixtures of the two. The terms domestic fuel oil, diesel fuel oil, and heavy fuel oil are more indicative of the uses of fuel oils.

Table 2.3 General summary of product types and distillation range (from Speight, 2002)

Product	Carbon limit		Boiling Point, °C		Boiling Point, °F	
	Lower	Upper	Lower	Upper	Lower	Upper
Refinery gas	C ₁	C ₄	-161	-1	-259	31
Liquefied petroleum gas	C ₃	C ₄	-42	-1	-44	31
Naphtha	C ₅	C ₁₇	36	302	97	575
Gasoline	C ₄	C ₁₂	-1	216	31	421
Kerosene/diesel fuel	C ₈	C ₁₈	126	258	302	575
Aviation turbine fuel	C ₈	C ₁₆	126	287	302	548
Fuel oil	C ₁₂	>C ₂₀	216	421	>343	>649
Lubricant oil	>C ₂₀		>343		>649	
Wax	C ₁₇	>C ₂₀	302	>343	575	>649
Asphalt	>C ₂₀		>343		>649	
Coke	>C ₅₀ ¹		>1000 ¹		>1832 ¹	

¹ Carbon number and boiling point difficult to assess; inserted for illustrative purposes only.

Domestic fuel oil is fuel oil that is used primarily in the home. This category of fuel oil includes kerosene, stove oil, and furnace fuel oil: These are distillate fuel oils.

Diesel fuel oil is also a distillate fuel oil, but residual oil has been successfully used to power marine diesel engines, and mixtures of distillate fuel oil and residual fuel oil have been used in locomotive diesel engines.

Heavy fuel oils include a variety of oils ranging from distillates to residual oils that must be heated to 260 °C (500 °F) or more before they can be used. In general heavy fuel oils consist of residual oils blended with distillates to suit specific needs. Included among heavy fuel oils are called bunker oils.

Because the boiling ranges, sulfur contents, and other properties of even the same fraction vary from crude oil to crude oil and with the way the crude oil is processed, it is difficult to specify which fractions are blended to produce specific fuel oils. In general, however, furnace fuel oil is a blend of straight-run gas oil and cracked gas oil to produce a product boiling in the 175-345 °C (350-650°F) range.

Heavy fuel oils usually contain cracked residua, reduced crude, or cracking coil heavy product that is mixed to a specified viscosity with cracked gas oils and fractionator bottoms. For some industrial purposes in which flames or flue gases contact the product (ceramics, glass, heat treating, and open-hearth furnaces) fuel oils must be blended to contain minimum sulfur content, and hence low-sulfur residues are preferable for these fuels.

Straight run-gas oil fraction is usually blended with the appropriate boiling-range material from catalytic cracking processing. The components are suitably treated before final blending, and additives may be added to further assist in the stabilization of the finished product.

2.2 Hydrodesulfurization Process

Hydrotreating for sulfur removal is called hydrodesulfurization. Hydrodesulfurization is a catalytic process whereby an oil fraction is flowing with hydrogen over or through a catalyst bed at elevated temperatures (315°-425°C) and pressures (up to 68 bar).

In a typical catalytic hydrodesulfurization unit, the feedstock is deaerated and mixed with hydrogen, preheated in a fired heater and then charged under pressure through a fixed-bed catalytic reactor. In the reactor, the sulfur and nitrogen compounds in the feedstock are converted into H_2S and NH_3 . The reaction products leave the reactor and after cooling to a low temperature enter a liquid/gas separator. The hydrogen-rich gas from the high-pressure separation is recycled to combine with the feedstock, and the low-pressure gas stream rich in H_2S is sent to a gas treating unit where H_2S is removed. The clean gas is then suitable as fuel for the refinery furnaces. The liquid stream is the product from hydrotreating and is normally sent to a stripping column for removal of H_2S and other undesirable components. In cases where steam is used for stripping, the product is sent to a vacuum drier for removal of water. Hydrodesulfurized products are blended or used as catalytic reforming feedstock. The flow-sheet for many HDS or hydrotreating processes is similar to that shown in Figure 2.2.

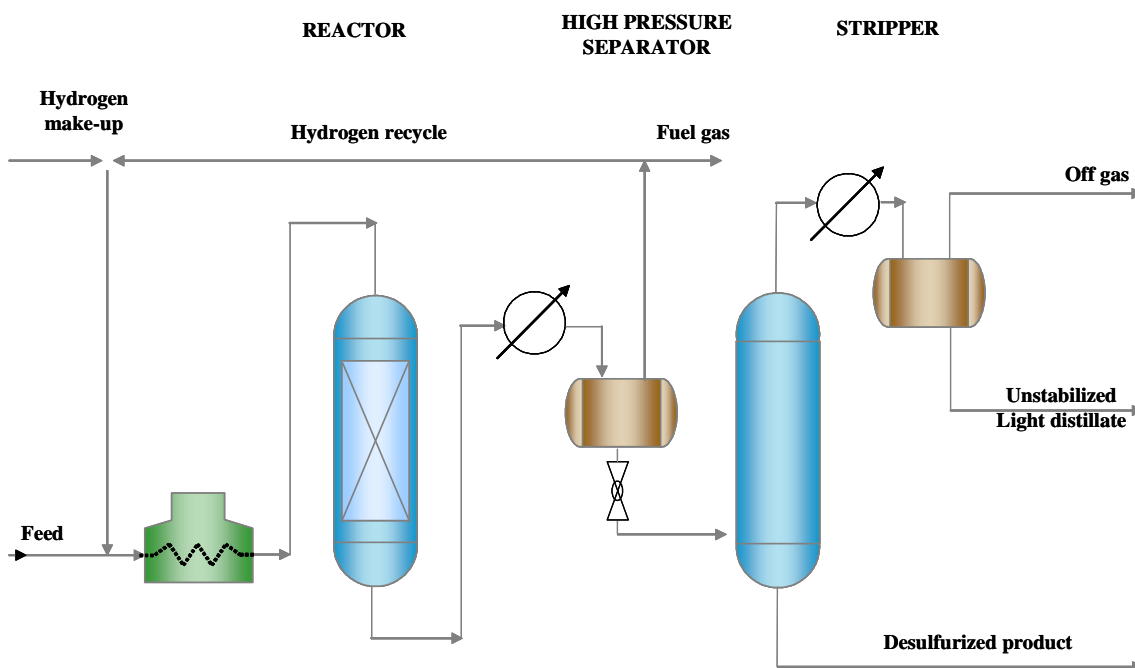


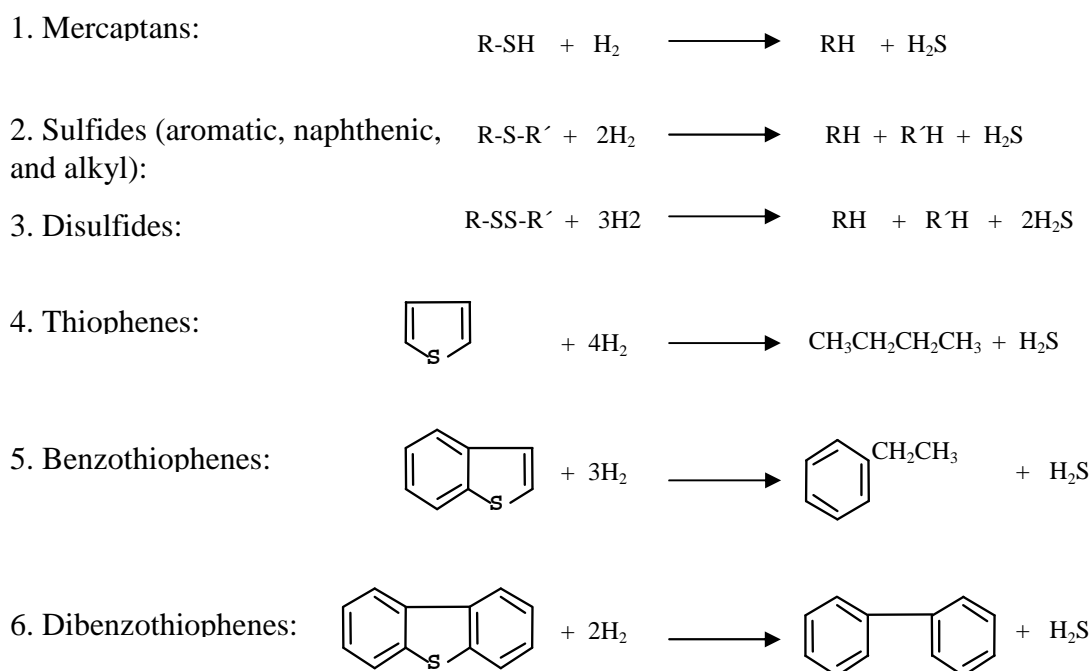
Figure 2.2 Scheme of a typical desulfurizer unit (from Set Laboratories, Inc., 1999).

The use of a recycle gas from the top of the high pressure separator minimizes the loss of valuable hydrogen, the consumption of which is especially high when treating heavier feeds.

2.2.1 Chemical Concepts

The basic chemical concept of the hydrodesulfurization process is to convert the organic sulfur in the feedstock to hydrogen sulfide. Hydrogenation processes for the conversion of crude oil fractions and products may be classified as nondestructive and destructive (Speight, 1981). Although the definition of the two processes is purely arbitrary, it is generally assumed that destructive hydrogenation (which is characterized by the cleavage of carbon-to-carbon linkages and is accompanied by hydrogen saturation of the fragments to produce lower-boiling products) requires temperatures in excess of 350 °C (660 °F). However nondestructive hydrogenation is more generally used for the purpose of improving product quality without any appreciable alteration of the boiling range. Mild processing conditions (temperatures below 350 °C or 660 °F) are employed so that only the more unstable materials are attacked and the sulfur, nitrogen, and oxygen compounds undergo hydrogenolysis to split out hydrogen sulfide, ammonia, and water respectively. Table 2.4 shows the various reactions that result in the removal of sulfur from the organic feedstock under the usual commercial hydrodesulfurization conditions (elevated temperatures and pressures, high hydrogen-to-feedstock ratios, and the presence of a catalyst).

Thiols and open-chain and cyclic sulfides are converted to saturated and/or aromatic compounds—depending, of course, on the nature of the particular sulfur compound involved. Benzothiophenes are converted to alkyl aromatics, while dibenzothiophenes are usually converted to biphenyl derivatives. In fact, the major reactions that occur as part of the hydrodesulfurization process involve carbon-sulfur bond rupture and saturation of the reactive fragments (as well as saturation of olefinic material) (Speight, 2000). HDS is accompanied by a certain amount of hydrogenation of aromatics.

Table 2.4 Typical hydrodesulfurization reactions

It is generally recognized that the ease of desulfurization is dependent upon the type of compounds, and the lower-boiling fractions are desulfurized more easily than the higher-boiling fractions. The difficulty of sulfur removal increases in the order:



The wide range of temperature and pressure employed for the hydrodesulfurization process virtually dictate that many other reactions will proceed concurrently with the desulfurization reaction. Thus, the isomerization of paraffins and naphthenes may occur and hydrocracking will increase as the temperature and pressure increase. Furthermore, at the higher temperatures (but low pressures) naphthenes may dehydrogenate to aromatics and paraffins dehydrocyclize to naphthenes, while at lower temperatures (high pressures) some of the aromatics may be hydrogenated.

These reactions do not all occur equally which is due, to some extent, to the nature of the catalyst. The judicious choice of a catalyst will lead to the elimination of sulfur (and other heteroatoms nitrogen and oxygen) and, although some hydrogenation and hydrocracking may occur, the extent of the denitrogenation, deoxygenation and hydrocracking reactions may be relatively minor.

The hydrodesulfurization process is a very complex sequence of reactions, due, no doubt, to the complexity of the feedstock; so, this work is limited to the sulfur removal.

2.2.2 Hydrodesulfurization Network of Dibenzothiophene

A detailed network for the hydrodesulfurization of dibenzothiophene (DBT) has been proposed by Houalla et al. (1978, 1980) (Figure 2.3). As Vanrysselberghe and Froment (1996, 2003) reported, dibenzothiophene reacts along two parallel path-ways: hydrogenolysis of DBT into biphenyl (BPH) and H_2S , and partial hydrogenation of the aromatics ring system into tetrahydrodibenzothiophene (THDBT) and hexahydrodibenzothiophene (HHDBT), which are rapidly converted into cyclohexylbenzene (CHB) and H_2S . Each of the hydrogenated dibenzothiophenes was rapidly converted into the other. Biphenyl is further hydrogenated to give cyclohexylbenzene and then bicyclohexyl (BCH).

The hydrogenation reaction of dibenzothiophene was about 1000 times slower than the hydrogenolysis reaction, but the hydrogenation became relatively fast as H_2S was added to the reactant mixture or as methyl groups were present in the 4 and/or 6 position(s) in dibenzothiophene. The experiments were carried out on a $CoMo/\gamma-Al_2O_3$ catalyst. The catalyst particles were crushed to a size between 149 and 178 μm so as to ensure the absence of diffusional limitations.

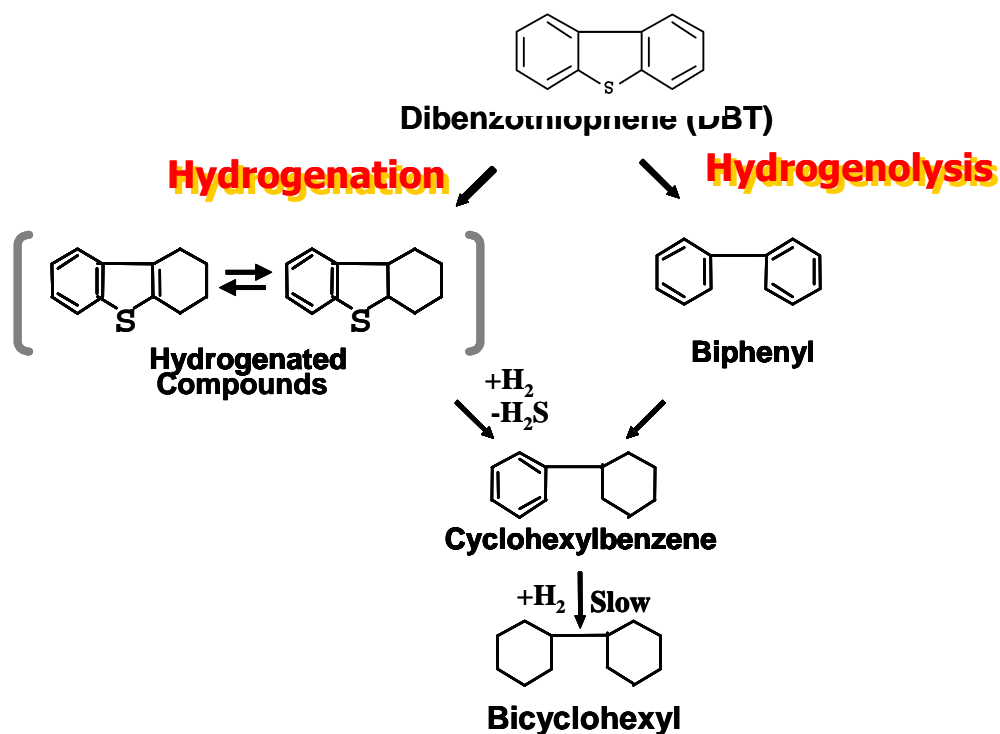


Figure 2.3 Proposed reaction network for the HDS of DBT by Houalla et al. (1978).

2.2.3 Hydrodesulfurization Network of 4-Methyldibenzothiophene and 4,6-Dimethyldibenzothiophene

Hydrodesulfurization of refractory 4-methyl- and 4,6-dimethyldibenzothiophene (4-MDBT and 4,6-DMDBT) is essential for deep HDS. Their direct desulfurization through the interaction of their sulfur atom with the catalyst surface is sterically hindered by neighboring methyl groups (Isoda et al., 1994). A number of attempts have been made to elucidate mechanisms for 4-MDBT and 4,6-DMDBT using kinetic data.

Vanrysselberghe et al., (1998) have investigated the HDS of 4-MDBT and 4,6-DMDBT in liquid phase at 533-593 °K and 60-80 bar on a commercial CoMo/Al₂O₃ catalyst. The networks for the HDS of 4-MeDBT and 4,6-DMDBT are shown in Figures 2.4 and 2.5 respectively.

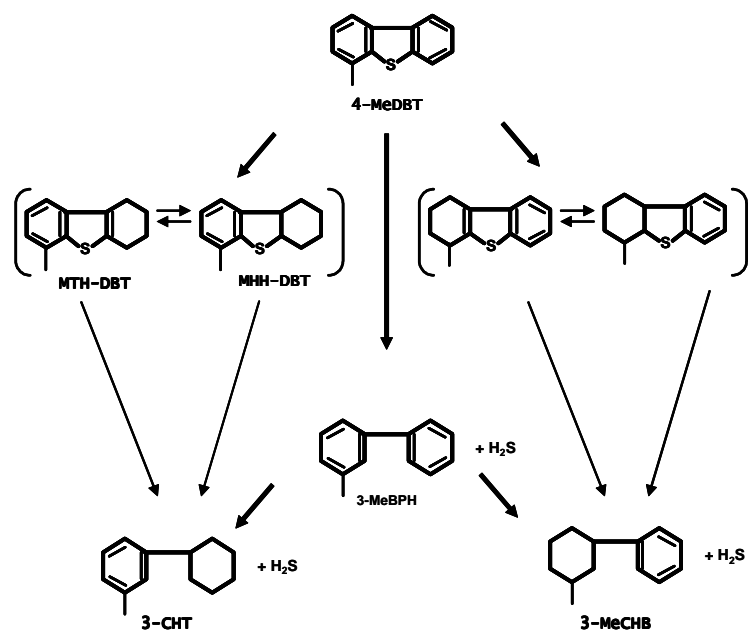


Figure 2.4 Reaction scheme for the HDS of 4-MeDBT.

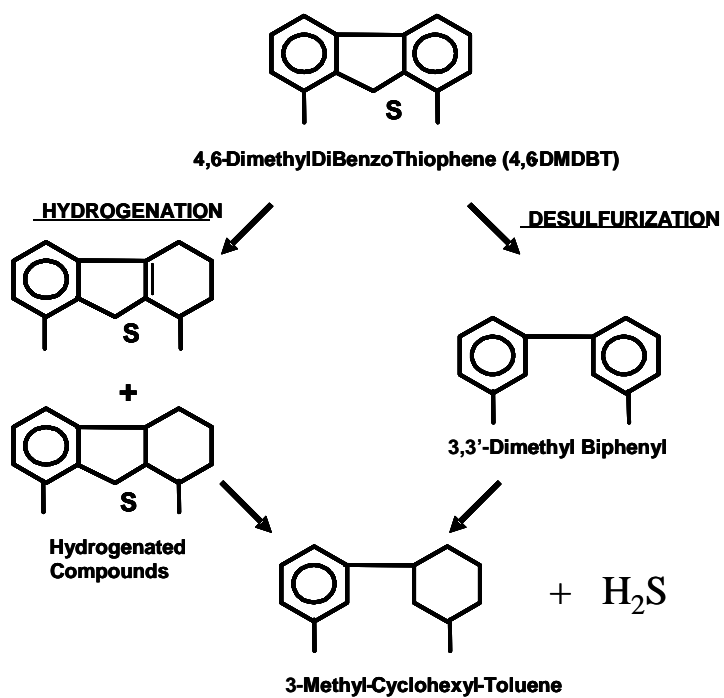


Figure 2.5 Reaction scheme for the HDS of 4,6-DMDBT.

Hydrodesulfurization reactivity of 4,6-DMDBT was examined in a batch autoclave by Isoda et al. (1996) over a Y-zeolite containing CoMo/Al₂O₃ at 270 °C under 3.0 Mpa of H₂ pressure for 0-3 hr, and 0.1 wt% of 4,6-DMDBT in decane. Isomerization and considerable transalkylation of 4,6-DMDBT into 3,6-DMDBT and into tri- or tetramethyldibenzothiophenes, respectively, were reported. Such migrations moderate the steric hindrances of methyl groups at the 4- and 4,6-positions of the dibenzothiophene skeleton. Figure 2.6 illustrates the reaction pathway proposed by Isoda (1996).

This reaction network proposes a new concept of HDS of refractory alkyldibenzothiophenes. However, it is mentioned that improvement of the performance life and optimization of the catalyst will be the target for application in the current refinery.

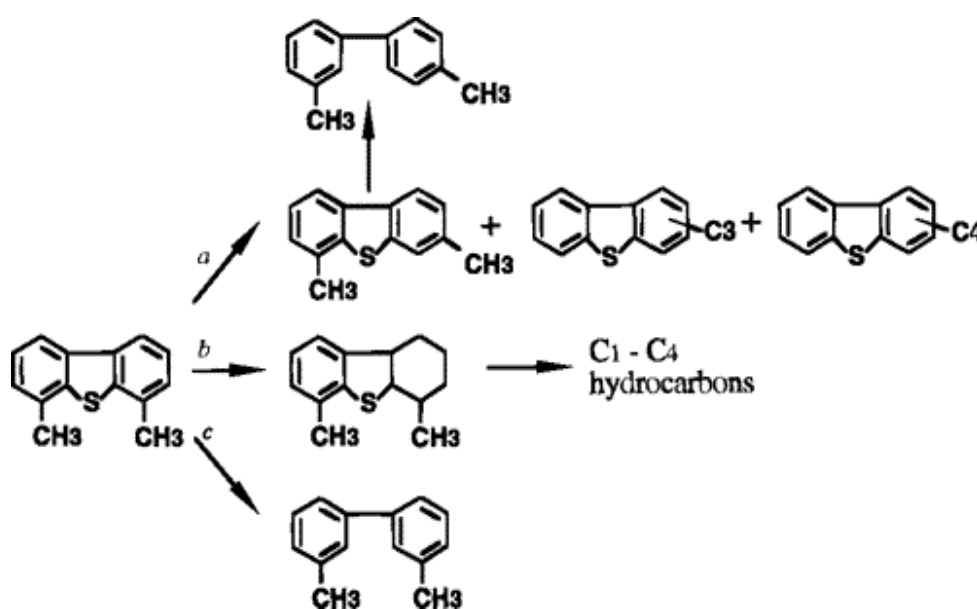


Figure 2.6 Reaction pathway of 4,6-DMDBT over zeolite containing CoMo/Al₂O₃ catalyst. a, HDS with isomerization route; b, hydrocracking route; c, direct desulfurization route. (From Isoda et al., 1996).

Thus, the new multiphase reaction network (Figure 2.7) for the HDS of 4,6-DMDBT over PtPdCoMo-containing zeolite might be proposed taking into consideration the reaction networks reported by Vanrysselberghe et al., (1998) and Isoda et al. (1996).

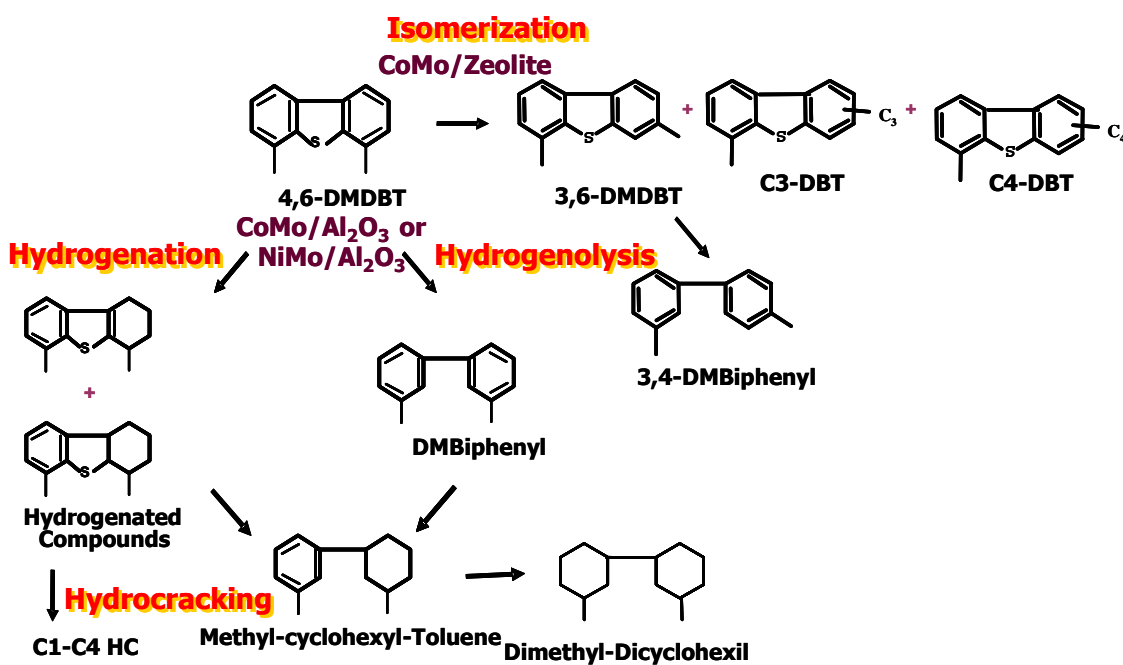


Figure 2.7 Multiphase reaction network proposed for the HDS of 4,6-dimethyldibenzothiophene (proposed for studying).

2.2.4 Thermodynamics

HDS of organosulfur compounds is exothermic and essentially irreversible under the reaction conditions employed industrially (e.g., 330-425 °C and 55-170 atm) and there is no thermodynamic limitation under industrial reaction conditions (Gates et al., 1979; Speight, 1981; Vrinat, 1983; Girgis and Gates, 1991). In the case of HDS of mercaptans, sulfides, disulfides and thiophenic compounds the equilibrium constants decrease with increase in temperature and have values more than unity. (Speight, 1981; Vrinat, 1983).

Thermodynamic data for organosulfur compounds present in higher boiling fractions (i.e., multiring heterocyclics) are unavailable, except for recent data for dibenzothiophene HDS (Vrinat, 1983). The later results indicate that dibenzothiophene HDS to give biphenyl is also favored thermodynamically under practical HDS conditions and is exothermic ($\Delta H^\circ = -11$ kcal/mol). Extrapolation of the latter results suggests that the HDS of higher molecular weight organosulfur compounds (e.g., benzonaphthothiophenes) is also favored.

As was shown in Figure 2.5, sulfur removal occurs along two parallel pathways, hydrogenolysis and hydrogenation (Froment, 2004). The pathways involving prior hydrogenation of the ring can be affected by thermodynamics because hydrogenation of the sulfur-containing rings of organosulfur compounds is equilibrium-limited at practical HDS temperatures. For example, the equilibrium constant for hydrogenation of thiophene to give tetrahydrothiophene is less than unity at temperatures above 350 °C (Vrinat, 1983), indicating that sulfur-removal pathways via hydrogenated organosulfur intermediates may be inhibited at lower pressures and high temperatures because of the low equilibrium concentration of the latter species.

2.2.5 Reactivities

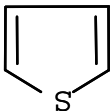
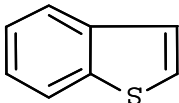
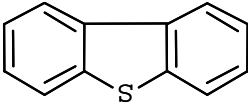
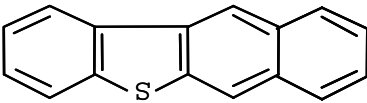
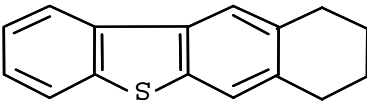
The reactivities of heterocyclic sulfur compounds in HDS are governed basically by the types of C-S bonds and the position of alkyl substituents (Kabe et al., 1999). The first factor is related to the strength of C-S bonds, and the second is related to the steric hindrance as well as the electron density on the sulfur atom.

2.2.5.1 Reactivities Based on the Strength of C-S Bonds

There are a large number of reports on HDS of thiophene (T), benzothiophene (BT) and dibenzothiophene (DBT) because they are among the simplest compounds in model reactions for petroleum refineries. Nag et al., (1979) reported the reactivities of typical thiophenic compounds as shown in Table 2.5. The rate constants decreased in the

order $T(1) > BT$ (0.59 of T) $> DBT$ (0.04 of T). DBT was one order of magnitude less reactive than BT. Benzonaphthothiophene (BNT) and its hydrogenated derivative have similar or rather higher reactivities than DBT. Even though a first order model for HDS is not accurate because it globalizes hydrogenolysis and hydrogenation of the sulfur-containing compounds and ignores the adsorption effects, the result suggests that HDS of three-ring compounds may be a key reaction in making deeply desulfurized oil from heavier fractions. Hydrogenated derivatives are more easily desulfurized than thiophenic compounds (Kilanowski et al., 1978; Weisser and Landa, 1973, Vanrysselberghe and Froment, 1998).

Table 2.5 Reactivities of several heterocyclic sulfur compounds* (from Nag, 1979)

Reactant	Structure	Pseudo-First-order rate constant (L/s g-cat)
Thiophene		1.38×10^{-3}
Benzothiophene		8.11×10^{-4}
Dibenzothiophene		6.11×10^{-5}
Benzo [b] naphtho-[2,3-d]thiophene		1.61×10^{-4}
7,8,9,10-Tetrahydrobenzo[b]naphtho-[2,3-d]thiophene		7.78×10^{-5}

* Reaction conditions: batch reactor using n-hexadecane solvent (0.25 mol % reactant concentration), 300 °C, 71 atm, CoMo/Al₂O₃ catalyst, each compounds reacted individually.

The reactivity of sulfur-containing compounds in HDS is significantly affected by the operating conditions (Kabe et al., 1999), by the molecular size and by the degree of substitution of the thiophenic ring (Topsoe et al., 1996). In addition, the substitution of these compounds by ring alkylation further affects the reactivity. For instance, Satterfield et al., (1980) have studied the effect of ring alkylation of thiophene on the rate of the HDS reaction and have found that the reactivity varies in the following order:

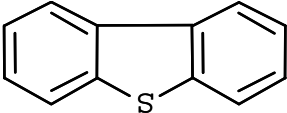
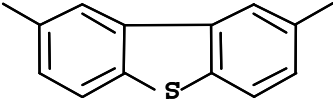
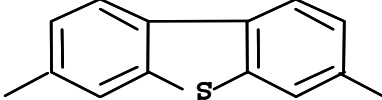
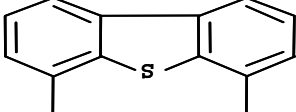
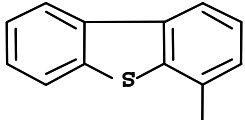


2.2.5.2 Reactivities Based on the Steric Hindrance

Ma et al., (1994, 1995, 1996) have concluded that sulfur compounds in the diesel fuel can be classified into four groups according to their HDS reactivities: (1) most of the alkyl BTs, (2) DBT and alkyl DBT's with substituents at the 4- and 6- positions, (3) alkyl DBTs with only one of the substituents at either the 4- or 6-position, and (4) alkyl DBTs with two of the alkyl substituents at the 4- and 6-positions, respectively. Since the pseudo-first-order rate constants of HDS for these groups were about 0.25, 0.058, 0.020, and 0.007 min⁻¹, respectively, the fourth group is the most difficult to desulfurize.

The effect of methyl substituents on the reactivity of dibenzothiophene has been investigated by Houalla et al., (1980). Table 2.6 shows the HDS reactivities based on the pseudo-first-order constants. 4-Methyldibenzothiophene and 4,6-Dimethyldibenzothiophene are the most difficult to desulfurize because of steric hindrance caused by the methyl groups in the 4- and 4,6-positions, respectively. Steric hindrance hampers the adsorption of the S atom onto the active sites of the catalyst; as a consequence the hydrogenolysis (rupture of C-S bond) is inhibited.

Table 2.6 Reactivities of selected methyl-substituted dibenzothiophenes*

Reactant	Structure	Pseudo-First-order rate constant (L/s g-cat)
Dibenzothiophene		7.38×10^{-5}
2,8-dimethyldibenzo- thiophene		6.72×10^{-5}
3,7-dimethyldibenzo- thiophene		3.53×10^{-5}
4,6-dimethyldibenzo- thiophene		4.92×10^{-6}
4-methyldibenzo- thiophene		6.64×10^{-6}

*Reaction conditions: flow reactor, n-hexadecane carrier oil, each reactant allowed to react individually at 300 °C at 102 atm in the presence of a CoMo/Al₂O₃ catalyst.

Vanrysselberghe et al., (1998) have reported that methyl-substituted dibenzothiophenes have a higher rate of hydrogenation than dibenzothiophenes itself. The experiments with the model components 4-MeDBT and 4,6-DMDBT demonstrated that methyl groups increase both the adsorption equilibrium constant on the active sites and the rate coefficient for the hydrogenation surface reaction.

2.3 Effect of H₂S on Hydroprocessing Reactions

H₂S in hydrotreater recycle gas is an activity depressant for hydroprocessing reactions (Albermarle Catalysts, 2003). The presence of H₂S inhibits the rate of reaction of hydrocarbon molecules with active sites on the catalyst surface. In addition, H₂S

reduces the hydrogen partial pressure in the reactor. This, in combination with higher operating temperature requirements can lead to a substantial increase in the deactivation rate of the catalyst.

Production of H_2S is the byproduct of hydrodesulfurization reactions. Sulfur containing molecules react on the active sites of hydroprocessing catalysts, cleaving S from the molecule, releasing it to react with hydrogen. The byproduct H_2S diffuses from the catalyst pores and enters the recycle gas stream.

H_2S concentration in the recycle gas builds as the gas moves from reactor inlet to outlet. The recycle gas loop often contains an amine scrubber to remove H_2S from the gas stream. In cases where the H_2S content is relatively low, a gas purge may be used in place of an amine scrubber to prevent H_2S build-up in the system. H_2S reduces the activity of hydroprocessing catalysts by competitive adsorption on catalytically active sites. This blocks the active sites available for hydroprocessing reactions, resulting in higher temperature requirement to obtain a constant product quality. As recycle gas H_2S concentration is raised the number of blocked active sites increases. Hydrodesulfurization, hydrodenitrogenation and aromatic saturation are all negatively affected by increasing H_2S concentration in the recycle gas. Figure 2.8 shows the effect of recycle gas H_2S content on the temperature required to maintain a constant product sulfur (Albermarle Catalysts, 2003). This graph was developed for HDS of diesel but similar effects would be expected for other hydrotreating processes.

In addition to the effect of competitive adsorption on hydroprocessing reactions, increasing H_2S content in the gas reduces hydrogen partial pressure in the reactor. Combined with higher temperatures requirement for constant product quality, the lower hydrogen partial pressure can cause increased catalyst deactivation rates and ultimately a reduction in cycle length. For this reason, it is recommended that H_2S content in the recycle gas stream be maintained below 2 vol%.

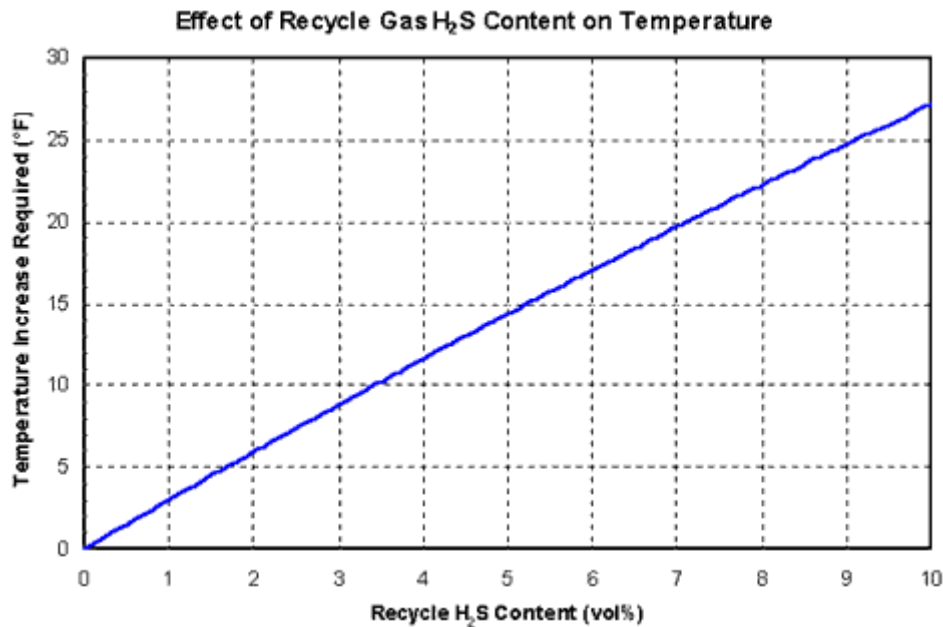


Figure 2.8 Effect of recycle gas H₂S content on the temperature (Albermarle Catalysts, 2003).

2.4 Poisons of the Hydrodesulfurization Catalyst

Sodium and Arsenic are two critical poisons well known in hydrotreating units.

2.4.1 Effect of Sodium on Catalyst Performance

Sodium (Na) is a severe poison to hydrotreating catalyst. In addition, Na can form a crust at the top of the hydrotreating bed, resulting in build-up of the pressure drop. Sodium naturally occurs in crude oil and dissolves in water in an emulsion with the oil. Additional sources of Na in a refinery include:

- caustic -- used in acid neutralization and cleaning
- seawater – from tanker and barge ballast
- chemical addition -- boiler chemicals, etc.

Desalting is used to control Na content of the feed and mitigate the effects on catalyst and unit performance. However, poor desalting or Na from another source can result in the contaminant being present in the feed to a hydrotreater, causing short cycles and poor performance. In this report the effect of sodium on hydrotreating catalyst is described below.

Sodium is a severe poison to hydrotreating catalyst, as can be seen in the Figure 2.9 (Albermarle catalysts, 2003). While Na affects activity within the cycle in which it is deposited, it has a more severe effect during catalyst regeneration. At the elevated temperatures of regeneration, Na sinters the catalyst surface, causing acid sites to be destroyed, a reduction in surface area and a reduction of active sites. Na also becomes mobile at elevated temperatures so a high concentration of Na on the outer edges of the spent material can move inward. For these reasons, regeneration is not recommended for spent catalysts containing more than 0.25 wt% Na.

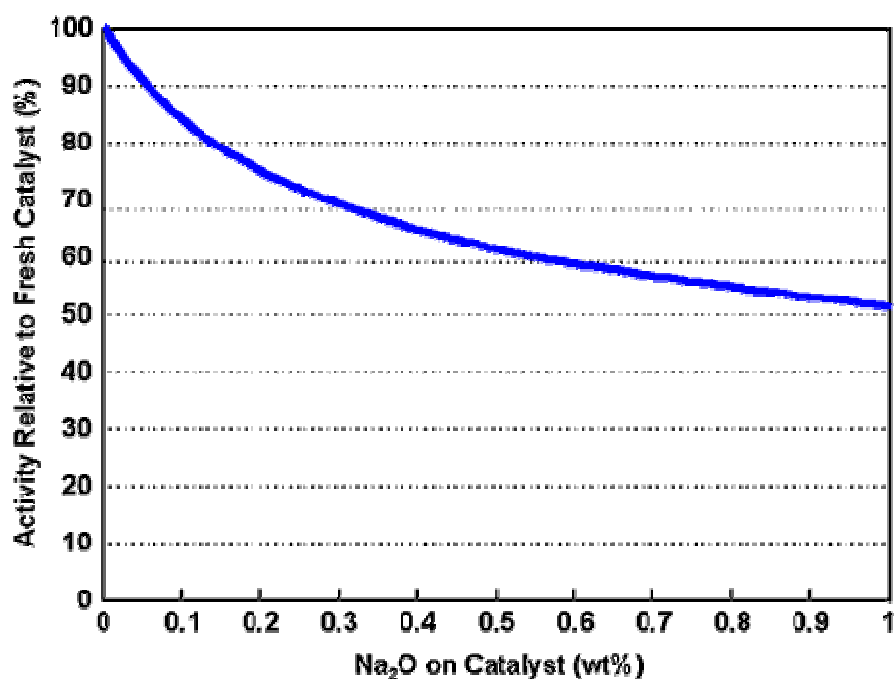


Figure 2.9 Effect of the sodium content on catalysts on the activity relative to fresh catalyst (from Albermarle Catalysts, 2003).

The majority of sodium is carried into hydrotreating units by water in emulsion with the feed. For this reason, Na tends to deposit in the upper portion of the catalyst bed. High concentration of Na in the feed results in the formation of a crust at the top of the hydrotreater. If not controlled (through size grading or other means) the crust causes a rapid build-up in pressure drop and eventual unit shutdown. Fortunately, the crust can usually be removed by skimming. Depending upon unit severity and throughput, downstream catalyst activity may not be seriously affected.

Prevention is the only effective means of control for Na poisoning. Ensure effective desalting unit performance and careful monitoring of chemical additions to prevent pressure drop build-up in the current cycle. Avoid regenerated catalyst with Na content greater than 0.25 wt%.

2.4.2 Effect of Arsenic on Catalyst Performance

Arsenic (As) is a very severe poison to hydrotreating catalyst. It is naturally occurring in crude oil, with the concentration highly dependent upon the crude source. Arsenic poisoning is primarily observed in distillate and VGO hydrotreating but is occasionally observed in lighter feedstocks. Due to the severe impact on catalyst activity, it is preferred to capture as much arsenic as possible in the upper portion of the catalyst bed. The arsenic has a more damaging effect on unit performance if it spreads out over a significant portion of the total catalyst bed. This work describes the effect of arsenic on hydrotreating catalyst and a means of mitigating these effects.

Arsenic (As) is a very severe poison to hydrotreating catalyst, as can be seen in the Figure 2.10 (Albermarle catalysts, 2003). Even 0.5 wt% As on catalyst results in more than 30% reduction in activity as compared to fresh! Arsenic poisons by blocking access to catalytically active sites on the pore surface. In general, it is not recommended to regenerate or to use regenerated catalyst containing more than 3000 ppm As. However, arsenic does not deposit uniformly in a catalyst bed. If an entire catalyst bed is discharged together, it is possible for the catalyst to have an average arsenic content in

excess of 3000 ppm while still retaining acceptable activity. In this case, catalyst from the top of the bed will have very low activity but the bulk of the catalyst will have reasonable activity.

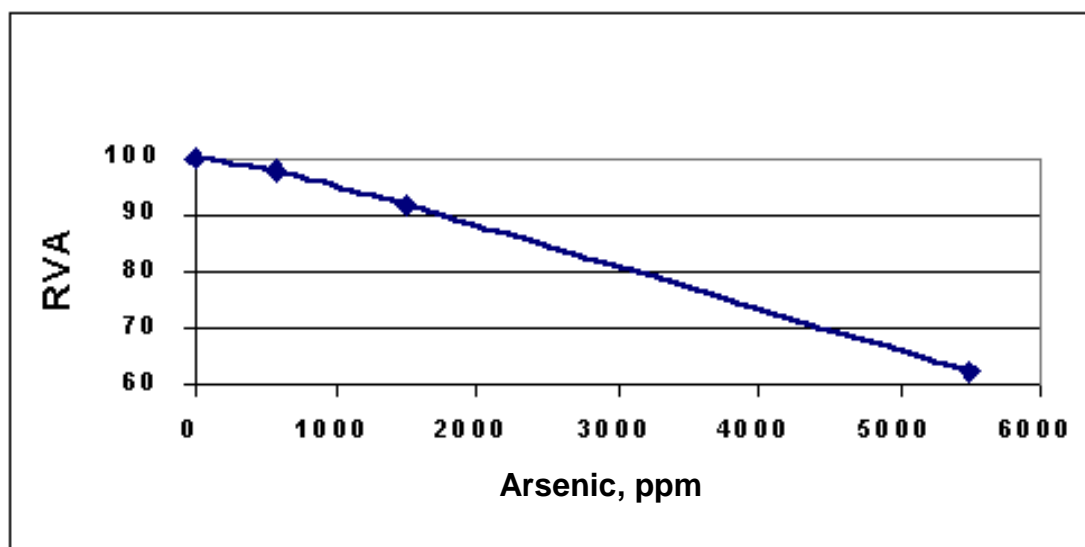


Figure 2.10 Effect of arsenic on relative volumetric activity (from Albermarle catalysts, 2003).

To reduce the impact of arsenic on activity, during a cycle, it is recommended to minimize the depth of penetration into the catalyst bed. The Deposition of arsenic on catalyst is controlled by three variables: severity (temperature, pressure), space velocity and metal capacity. The combination of these variables determines the profile of arsenic penetration into the catalyst bed. Higher severity will increase deposition in the upper portion of the bed. Higher space velocity will drive the arsenic more deeply into the bed. Metal capacity refers to the ability of the catalyst to hold deposited arsenic, with higher metal capacity reducing the penetration into the bed.

There are some catalysts that can be used where arsenic contamination is known to exist. For instance, KF 647, an Akzo Nobel demetallization catalyst, is one of them.

KF 647 has been shown to remove two to three times more arsenic per unit volume than traditional hydrotreating catalyst. A layer of KF 647 at the top of a reactor can prevent extensive penetration of arsenic into the catalyst bed and extend cycle length (Albermale catalysts, 2003).

2.5 Catalyst Formulations

The choice of catalyst for a given application depends on various factors, including feed and product properties. Hydrodesulfurization catalysts most often contain alumina as support, typically having a surface area of the order of 200 to 300 m²/g a pore volume of about 0.5 cc/g, and an average pore diameter of about 100 Å. Of the various types of alumina available, γ -Al₂O₃ is the one generally applied because of its acidity and porosity.

The basic compositions of current hydrotreating catalysts consists of molybdenum sulfide promoted by cobalt or nickel with various modifications by using additives (e.g., boron or phosphorus or silica), or more promoters (e.g., Ni-Co-Mo/Al₂O₃) or improved preparation methods. Eventhough the activity and selectivity of the hydrotreating catalysts have been improved significantly as a result of continuous research and development in research institutions and catalysts, and petroleum companies worldwide, they generally have low hydrogenation activity, so they are not adequate for deep HDS.

Vanrysselberghe and Froment (2003) have reported that Ni-promoted catalysts on alumina may be attractive since these catalysts have a much higher hydrogenation activity. It is generally accepted that the hydrogenation activity decreases in the order NiW > NiMo > CoMo > CoW. Furthermore, Ni-promoted catalysts are cheap and robust. Carbon-supported catalysts may be more active than alumina-supported catalysts because they seem to be more resistant to coke formation. Noble metal catalysts such as Pt and Pd not only have high hydrogenation activity, but also have HDS activity, as was shown by Topsoe et al., (1993). Figure 2.11 shows the HDS activities of some transition metals as a function of the heats of formation calculated on a sulfur atom basis.

The results were adapted by Topsoe et al., (1993) from Chianelli et al., (1984) who studied the HDS of dibenzothiophene at high pressures and 400 °C over unsupported sulfides.

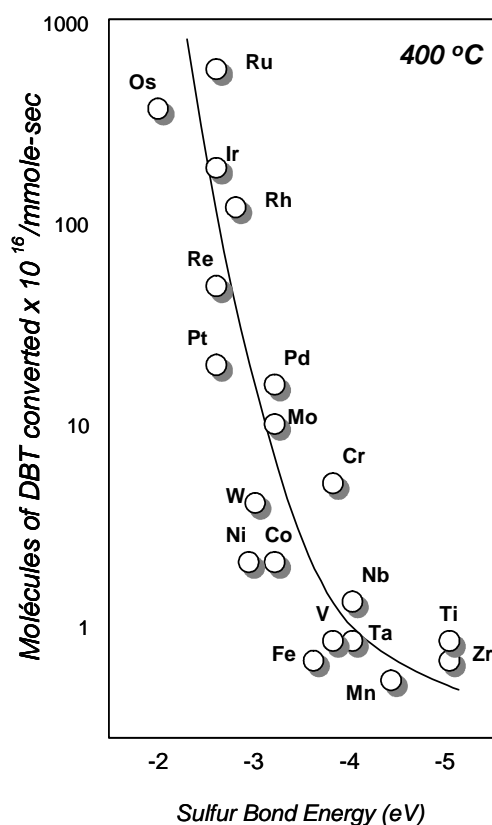


Figure 2.11 HDS activities as a function of the calculated metal-sulfur bond energies.

As was mentioned noble metals have high hydrogenation activity, but supported on γ -alumina they are very sensitive to sulfur poisoning. The sulfur resistance of noble metals can be increased by the use of supports like zeolites. In addition, Pd is thought to inhibit the H_2S adsorption on Pt owing to the electronic interaction between Pd and Pt. Moreover, addition of Pd helps to maintain a high dispersion of Pt, even in the presence of sulfur components.

The development of new HDS technologies of catalysts is aiming for the production of 10-ppm sulfur content for diesel. The genesis of the active phase of cobalt and molybdenum is controlled in such way that the desulfurization of refractory sulfur compounds is promoted. In this context, Criterion Co. (2003) has considered two aspects for the catalysts manufacturing process for ultra deep desulfurization: better dispersion, and hence utilization, of the promoter metals, and greater conversion of the promoter metal oxide sites to metal sulfides (active state). A consequence of the Criterion novel manufacturing process used for the CENTINEL catalysts, metal complexes, MX_n , physically adsorbed on the surface react directly with sulfur compounds to form highly dispersed metal sulfide species, $M-S_x$. These highly dispersed metal sulfide crystallites are “locked in place” during the activation process. This results in the active sulfide phase of the catalyst, MS_y . As a result, all metals placed on the catalyst are fully sulfided while maintaining high dispersion and better metals utilization than conventional catalysts.

2.6 Structure of Active Phase

In order to have a firm basis for understanding properties of hydrotreating catalysts, it is highly desirable to obtain a complete description of both the structures and the sites where the catalysis takes place, i.e. the “active sites”. Structural information on hydrotreating catalysts has in many instances been interpreted in terms of several models (i.e., the monolayer model, the intercalation model, the contact synergy model, and the Co-Mo-S model), which have been proposed in the literature.

The exact nature of active sites in Co-Mo or Ni-Mo catalysts is still a subject of debate, but the Co-Mo-S model (or Ni-Mo-S) model is currently the one most widely accepted Topsoe et al., (1996) and Prins (2001).

For this report, a brief description of the monolayer and intercalation models is presented.

2.6.1 Monolayer Model

The first detailed model of the structure of CoMo/Al₂O₃ catalysts was the monolayer model developed by Schuit and Gates (1973). In this model the calcined Mo or W was assumed to be bonded to the surface of the alumina forming a monolayer. Interaction of the Mo with the alumina was believed to occur via oxygen bridges resulting from reaction with surface OH groups. Co or Ni is present in the tetrahedral positions of the alumina support and stabilizes the Mo or W monolayer. The catalysts monolayer model is presented in Figure 2.12.

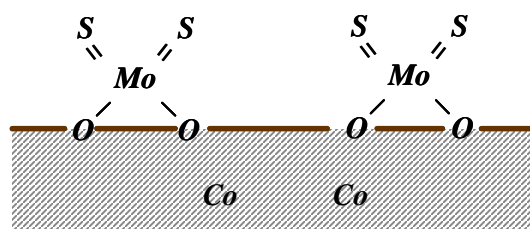


Figure 2.12 Schematic representation of the monolayer model (proposed by Schuit and Gates (1973)).

2.6.2 Intercalation Model

This model was initially developed by Voorhoeve and Stuver (1971). Mo or W is present in planes on the surface of the alumina carrier, each between two sulfur layers. The Co or Ni ions or promoters occupy octahedral intercalation positions between the MoS₂ or WS₂ planes. Later a pseudo-intercalation model was proposed by Farragher and Cossee (1973, 1977). In this model the promoter atoms are located at the edges of the MoS₂ or WS₂ planes. The intercalation and pseudo-intercalation models assume that the active sites are related to three-dimensional MoS₂ or WS₂ structures. The model is shown in Figure 2.13.

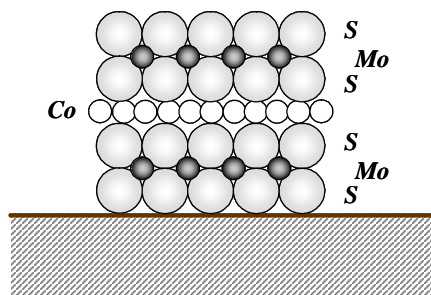


Figure 2.13 Locations of the promoter atoms in the MoS₂ structure proposed by the intercalation and psudo-intercalation models.

2.7 Zeolites

2.7.1 Introduction

The exploration of new catalysts with improved properties (e.g., a higher activity, selectivity and stability than the CoMo/Al₂O₃ catalysts) has stimulated many researchers to search for new active phases and supports. In this context, different types of zeolites have been recently proposed as support for the traditional sulfided phases (NiW, NiMo or CoMo) applied in hydrocracking (Honna et al., 1999), hydrodesulfurization (Cid et al., 1995; Taniguchi et al., 1999) and in hydrodesulfurization-hydrodenitrogenation (Cid et al., 1999) schemes.

In all those cases, the main goal has been the successful incorporation of the acidic properties of zeolites to conventional formulations for improving the catalyst performance, for instance, the promotion of the hydrocracking of S-C bonds. However, highly acidic zeolites can also increase the C-C bond scission reactions that could be reflected in an increased proportion of products from the cracking of intermediate reactions, as reported by Landau et al., (1996). Thus, in an industrial application the final consequence would be a reduction in the liquid yield by transformation of part of the feedstock to lighter byproducts.

Through careful control of acidic properties of the support cracking could be avoided taking advantage of the ability of the acid sites of medium strength to isomerize the methyl groups of very refractory heterocompounds (as 4,6-DMDBT) to positions of decreased steric hindrance, then facilitating sulfur removal (Isoda et al., 2000).

Faujasite-type Y zeolites seem to be especially suitable for this application. It has been reported (Li et al., 1999a; Li et al., 1999b; Li et al., 2000) that the relatively large pores of Y zeolite, the strong surface Brønsted acidity and high dispersion of the supported sulfided NiMo phase increases the HDS activity. Another approach is the modification of the alumina support by the introduction of zeolitic materials (Zanibelli et al., 1999). In this context, an improved performance in the hydrodesulfurization of dibenzothiophene is observed when a zeolite is added to the conventional NiMo supported on Al₂O₃ formulation (Li et al., 1999).

A successful application of HY zeolite to CoMoP/Al₂O₃ catalysts has resulted because of the industrial development of the C603A catalyst (patented by Cosmo Oil Company). The catalyst exhibited considerably higher HDS activity and stability than the conventional sulfided CoMo/alumina catalyst in the hydrotreatment of straight run gas oil (Fujikawa et al., 1998).

A proposal for designing sulfur resistant noble metal hydrotreating catalyst based on the concept of use of zeolites as support and on the roles of shape selectivity, hydrogen spillover and type of sulfur resistance has been reported (Song, 1999). Although the concept is not yet fully established, this is a promising direction of research for developing new catalysts for low-temperature hydrogenation and desulfurization of distillate fuels.

On the other hand, zeolite supports can be used to prepare bimodal distributions of noble-metal particles. Some metals are located in small pore openings (<5 Å), whereas others will be contained in large pore openings (>6 Å). Studies performed in the University of Pennsylvania (Song, 1999) have shown that “diffusion of organosulfur compounds (as thiophenic molecules) into the small pores would be inhibited by size (shape-selective exclusion). The large pores would preferentially allow fast diffusion and

reaction of bulky polycyclic aromatic and sulfur compounds. The thiophenic molecules could enter the large pores, but not the small pores. However, hydrogen molecules can readily enter both sizes of pores, dissociatively adsorb on metal contained within, and be transported between pore systems by spillover. When the metal in the large pores becomes inactivated by adsorbed sulfur, spillover hydrogen could recover the poisoned metal sites by eliminating of R-S-R and R-SH compounds.

2.7.2 Shape-selectivity

Zeolites have the ability to act as catalysts for chemical reactions which take place within the internal cavities. An important class of reactions is that catalyzed by hydrogen-exchanged zeolites, whose framework-bound protons give rise to very high acidity. This is exploited in many organic reactions, including cracking of crude oil fractions, isomerisation and fuel synthesis.

Behind all these types of reaction is the unique microporous nature of zeolites, where the shape and size of a particular pore system exerts a steric influence on the reaction, controlling the access of reactants and products. Thus zeolites are often said to act as shape-selective catalysts.

2.7.3 “Y” Zeolite (Faujasite) as Support of HDS Catalysts

Support materials used for hydrotreatment catalyst are alumina, silica-alumina, silica and zeolites. The combination used depends on its application and desired activity/selectivity. Generally zeolites and/or amorphous silica-alumina's supply acidic functions for cracking. Applying metal particles in acidic zeolites provides the opportunity to combine the HDS and cracking functions in one catalyst when a HDN function is present to prevent poisoning of the acidic sites present. In view of the above, an important point here is the possibility to prepare catalysts containing metal particles inside the zeolite cavities (e.g. the supercage of zeolite Y).

Although a large variety in zeolite structures is available at the moment (Bekkim, 1991) only a small number have been reported as useful for hydrotreating/hydrocracking purposes and are commercially used. Y-Type zeolites can be used for such purposes.

Many definitions of zeolite can be found in the literature, nevertheless the main characteristics of a zeolite are either clearly expressed or implied as a crystalline material of alumina-silicate featured by a three-dimensional microporous framework structure built of the primary SiO_4 and AlO_4 tetrahedra, and ion-exchange capability. Particularly, the three dimensional pore structure is formed by connecting Si and Al atoms through Oxygen atoms. These Si and Al atoms are tetrahedrally surrounded by oxygen. The framework of Faujasite can be described as a linkage of these tetrahedral (TO_4) in a truncated octahedron in a diamond-type structure (Szostak, 1992). The truncated octahedron is referred to as the sodalite cages which have high density of negative charge. Two important structural isotypes can be distinguished, which differ in Si/Al ratio. The so called zeolite X has a Si/Al atomic ratio between 1 and 1.5. Zeolite Y has an atomic ratio between 1.5 and 3.0 (Szostak, 1992).

In this study the Y-type zeolite was used. The unit cell of the faujasite type zeolites is cubic with a unit cell dimension of 25 \AA , and it contains 192 silica and alumina tetrahedra. The unit cell dimension varies with Si/Al ratio. It contains three different cages. Each sodalite unit in the structure is connected to four other sodalite units by six bridge oxygen ions connecting the hexagonal faces of two units, as shown in Figure 2.14. The truncated octahedral are stacked like carbon atoms in diamond. The oxygen bridging unit is referred to as a hexagonal prism, and it may be considered another secondary unit. This structure results in a supercage (sorption cavity) surrounded by ten sodalite units which is sufficiently large for an inscribed sphere with a diameter of 12 \AA . The opening into this large cavity is bounded by sodalite units, resulting in a 12-membered oxygen ring with a 7.4 \AA free diameter. Each cavity is connected to four other cavities, which in turn are themselves connected to three-dimensional cavities to form a highly porous framework structure.

This framework structure is most open of any zeolite and is about 51% void volume, including the sodalite cages; the supercage volume represents 45% of the unit cell volume. The main pore structure is three-dimensional and large enough to admit large molecules, e.g. naphthalene and fluorinated hydrocarbons. It is within this pore structure that the locus of catalytic activity resides for many reactions.

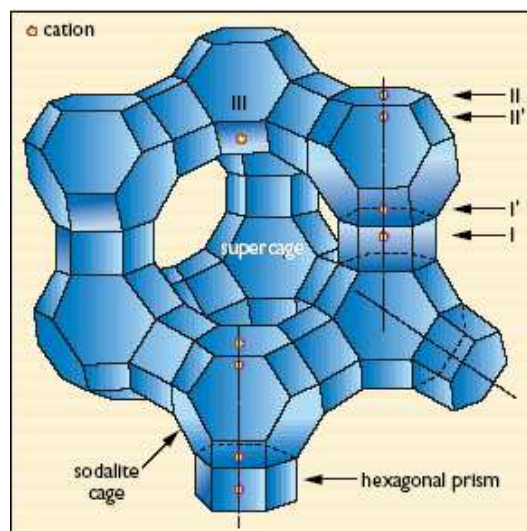


Figure 2.14 The structure of Y-type zeolite or Faujasite (USY). Cation positions are indicated by roman numerals.

The negatively charged framework is charge balanced by cations (usually Na^+) in the different mentioned cages. Some specific cation sites were defined and indicated in figure 2.14. Cation site I is situated in the hexagonal prism, cation I' and II' are situated in the sodalite cage, whereas cation site II and III are situated in the supercages.

CHAPTER III

SYNTHESIS AND CHARACTERIZATION OF THE CATALYSTS

The zeolite catalysts synthesized in this work are based on the three-dimensional ultrastable Y faujasite (USY). Studies of catalysts for hydrodesulfurization of Diesel fuel performed by Mexican Petroleum Institute are described by Marin et al., (2001). From that work, one should note that the USY zeolites (CBV-700 series) are candidates for deep hydrodesulfurization (HDS) and deep aromatic hydrogenation (HDA). For these reasons the USY-12 with $\text{SiO}_2/\text{Al}_2\text{O}_3$ mol ratio of 12 was selected for this research.

Generally, two methods were used to embed the active compounds and promoters into zeolite. These were incipient wetness impregnation and ion exchange. The impregnation method is used when the amount of metal required is greater than the ion exchange capacity of the zeolite. In this case the support is impregnated with a metal containing solution based on its pore volume. The ion exchange method involves contacting the zeolite with a specific concentration of the metal solution with vigorous stirring above 90 °C and under reflux conditions for several hours.

Commercial samples were used in this research to prepare the final hydrodesulfurization catalysts. The following discussion deals with the origin of the zeolite sample and raw chemicals purchased prior to the synthesis of the catalysts.

3.1 Raw Chemicals

3.1.1 Ultrastable Y Faujasite

The USY sample was obtained from Zeolyst International (formerly the PQ Corporation). This sample was received in the ammonium form and thus was used directly without further chemical treatment. The commercial designation of the USY

sample and its properties are listed in Table 3.1 along with the nomenclature used in this work.

Table 3.1 USY sample and their manufacture properties

Commercial Name given by Zeolyst Intl.	CBV-712
Sample Name used in this Study	USY-12
Nominal Cation form	Ammonium
SiO ₂ /Al ₂ O ₃ , mole ratio	12
Na ₂ O weight %	0.05
Unit Cell Size, Å	24.35
Surface Area m ² /g	730

3.1.2 Chemicals

All chemicals used as active compounds and promoters in the preparations of catalyst were of A.C.S reagent grade. The trade name of these compounds and the purity is listed in Table 3.2.

Table 3.2 List of chemicals and their assay data

Trade name	Formula	Purity	Brand
Tetraammineplatinum (II) chloride hydrate	Pt(NH ₃) ₄ Cl ₂ ·H ₂ O	98%	ALDRICH 27,590-5
Tetraamminepalladium (II) chloride monohydrate	Pd(NH ₃) ₄ Cl ₂ ·H ₂ O	98%	ALDRICH 20,582-6
Nickel (II) carbonate hydroxide tetrahydrate	2NiCO ₃ ·3Ni(OH) ₂ ·XH ₂ O	100	ALDRICH 33,977-6
Nickel (II) acetate tetrahydrate	Ni(CH ₃ CO ₂) ₂ ·4H ₂ O	98%	ALDRICH 24,406-6
Cobalt (II) acetate tetrahydrate	Co(CH ₃ CO ₂) ₂ ·4H ₂ O	100	ALDRICH 20,839-6
Molybdenum (VI) oxide	MoO ₃	99.5+%	ALDRICH 26,785-6
Ammonium hydroxide	NH ₄ OH	28-30% asNH ₃	CEM, AX1303P-1
Citric Acid anhydrous	HOC(CO ₂ H)(CH ₂ CO ₂ H) ₂	100	J.T. Baker, O122-01
Phosphoric acid	H ₃ PO ₄	85%p	CEM, PX0995-14

3.2 Synthesis of the Catalysts

The preparation of the catalysts was divided into three groups.

3.2.1 Synthesis of catalysts containing USY-12

3.2.2 Synthesis of catalysts containing Ni-USY

3.2.3 Synthesis of catalysts containing Pt-USY

3.2.1 Synthesis of Catalysts Containing USY-12

3.2.1.1 CoMoPtPd/HY (HDS-1)

Pt and Pd were impregnated together in the zeolite from an aqueous solution containing the specific quantity of the noble metals to get a Pt+Pd loading of 0.65 wt% and Pt:Pd mol ratio of 4:1 in the zeolite prepared. Here the metal precursors are dissolved in aqueous media using a volume equal to the pore volume of the zeolite, contacted with the carrier and dried at 120 °C for 4 hours after drying at room temperature overnight.

The HDS-1 (CoMoPtPd/USY-12 or CoMoPtPd/HY after thermal treatment) catalyst was prepared by incipient wetness impregnation utilizing a CoMo solution. The concentration of CoMo solution was calculated to formulate a hydrodesulphurization catalyst with loadings showed in Table 3.3. After the impregnating stage, the PtPdCoMo containing zeolite was dried at 120 °C for 4 hours after drying at room temperature overnight. Then it was crushed to 200 mesh and kept in dry ambient air for pressing into 850-1000 µm.

Table 3.3 Expected composition of the CoMoPtPd/HY (HDS-1)

Element and Zeolite	Loading, wt%
Co	3.0
Ni	--
Mo	12.5
Pt+Pd	0.5
P	1.6
zeolite	73.3

Finally the catalyst was calcined at 450 °C for 4 h. Figures 3.1 and 3.2 depict the route and the schematic presentation used in the preparation of the HDS-1.

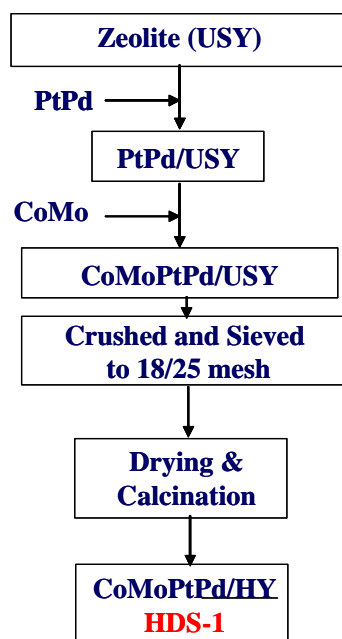


Figure 3.1 Preparation of CoMoPtPd/HY (HDS-1) catalyst. Introduction of PtPd and CoMo into USY zeolite.

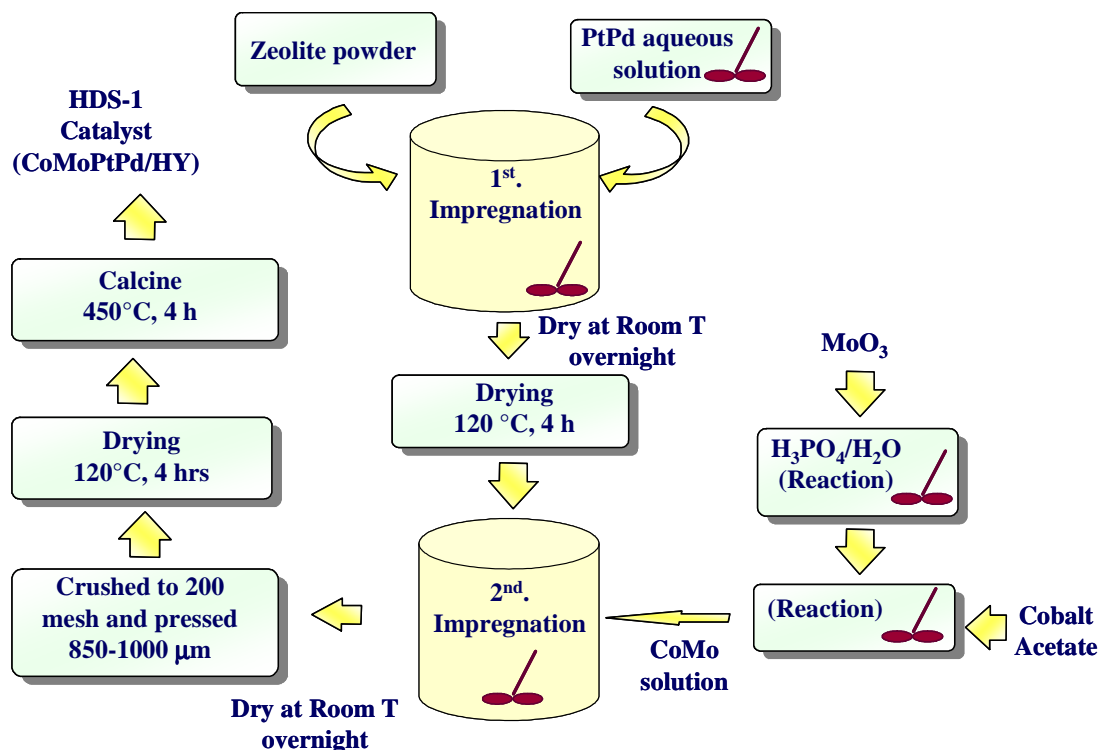


Figure 3.2 Schematic presentation of the preparation of CoMoPtPd/HY (HDS-1) catalyst. Introduction of Pt, Pd, Co and Mo into zeolite.

3.2.2 Synthesis of Catalysts Containing Ni-USY

The preparation of nickel sulfide in zeolite for hydrotreating reactions have been a subject of increasing attention in the last decade, since nickel ion exchanged zeolites leads to catalysts with high activity for hydrogenation of aromatics (Moraweck et al., 1997), and combining it with other transition metals and noble metals such as Co, Mo, Pt and Pd could be an excellent catalysts with good sulfur resistance for removal refractory sulfur compounds such as 4,6-dimethyldibenzothiophene contained in gas oil fractions for hydrodesulfurization (HDS).

In this section, Ni containing zeolite (Ni-USY) was prepared by ion exchange using the ammonium-zeolite USY-12 with $\text{SiO}_2/\text{Al}_2\text{O}_3$ mole ratio of 12 as template. The USY-12 zeolite was modified in the laboratory. The modification involved ion exchange of the as received zeolite in order to obtain a sample with Nickel and different acidic properties. The ion exchange using a nickel salt was performed on the USY zeolite sample prior to introduce Pt, Pd, Co and Mo. The nickel salt used in the ion exchange was Nickel (II) acetate tetrahydrate ($\text{Ni}(\text{CH}_3\text{CO}_2)_2 \cdot 4\text{H}_2\text{O}$), herein referred to as Nickel acetate. The ion exchange procedure involved the addition of the zeolite to a solution of nickel acetate with the appropriate concentration. The zeolite was left in contact with the aqueous solution for 66 hr at 98 °C with stirring and under reflux conditions. The pH was of 4.3. Following the ion exchange, the Ni-USY was dried at 120 °C for 4 hr and kept in dry ambient conditions after drying at room temperature overnight. Figure 3.3 illustrates the ion exchange procedure

Two samples of the Ni-USY were taken for characterization. The first sample was calcined in air at 450 °C during 4 h for analysis of metals content. The second sample, which was pressed and crushed into 850-1000 μm before calcination, was used for the characterization of its physical properties.

3.2.2.1 Synthesis of CoMoPtPd/Ni-HY (HDS-3) Catalyst

To prepare the HDS-3 catalyst a combination of ion exchange with incipient wetness impregnation method was used.

Because the Ni-USY zeolite contained around 13.6 wt % Ni (according to calculation), PtPd were introduced by incipient wetness impregnation of a quantity (82%) of fresh USY-12 before the impregnation of CoMo solution. The solutions of PtPd and CoMo were calculated to get the composition shown in Table 3.4.

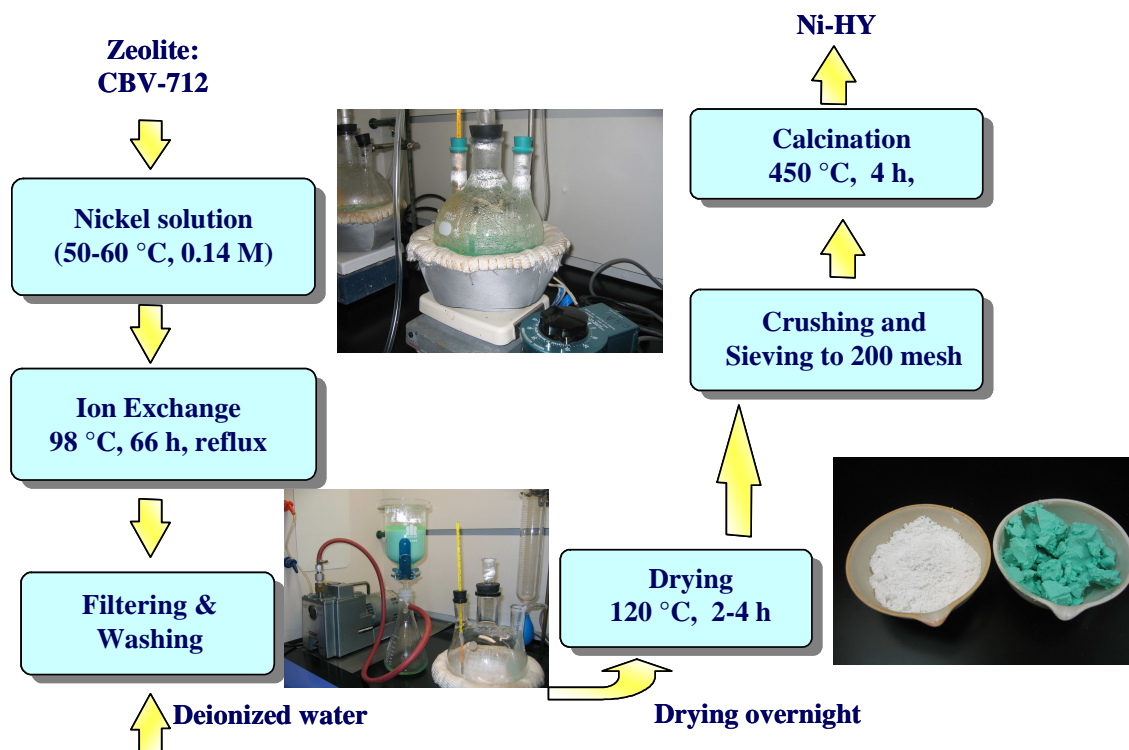


Figure 3.3 Schematic presentation of ion exchange procedure with an aqueous nickel solution.

Table 3.4 Expected composition of the CoMoPtPd/Ni-HY (HDS-3) catalyst

Element and Zeolite	Loading, wt %
Co	2.3
Ni	1.7
Mo	16.5
Pt+Pd	0.5
P	1.6
zeolite	66

Figures 3.4 and 3.5 depict the route and the schematic presentation used in the preparation of the HDS-3 catalyst.

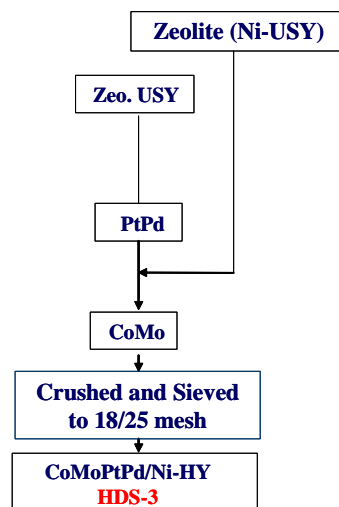


Figure 3.4 Preparation of CoMoPtPd/Ni-HY (HDS-3) catalyst. Introduction of PtPd and CoMo into Ni-USY zeolite.

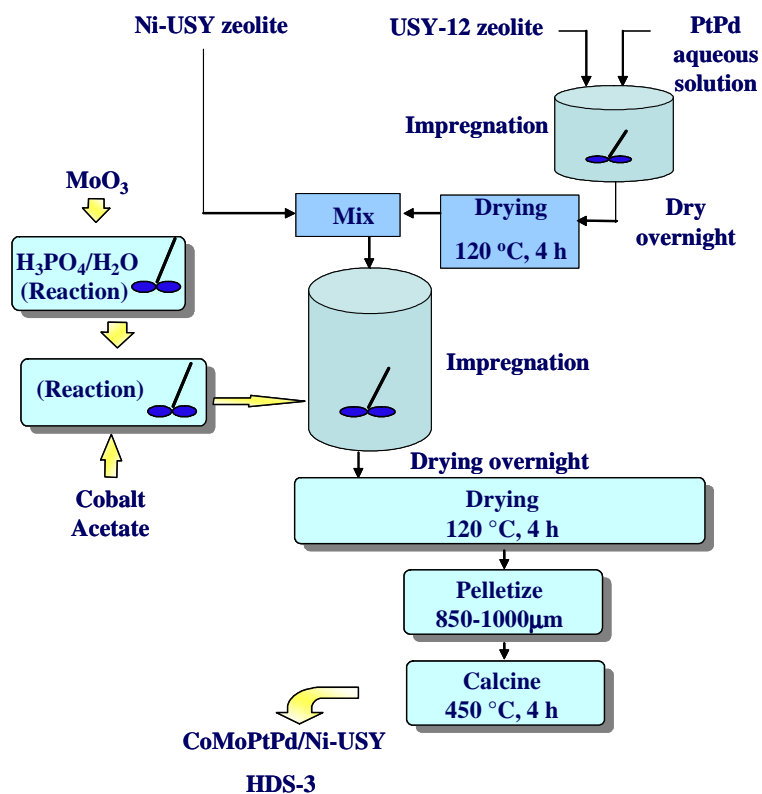


Figure 3.5 Schematic presentation of the preparation of (CoMoPtPd/Ni-HY (HDS-3) catalyst. Introduction of Pt, Pd, Co, and Mo into zeolite.

3.2.3 Synthesis of Catalysts Containing Pt-USY

In this section platinum ion exchanged USY zeolite (CBV-712: SiO₂/Al₂O₃ mole ratio=12.0) was prepared by stirring vigorously 10 g of zeolite with a 2.2×10^{-4} M platinum solution at 98 °C for 24 hours with reflux. The pH was of 3.5. The metal precursor of platinum was Tetraammineplatinum (II) chloride hydrate Pt(NH₃)₄Cl₂·H₂O. The metal containing solution was mixed with the zeolite in proportions of 176 cm³/g USY-12. The zeolite metal content is 0.73 wt % Pt. The exchanged sample from the ion exchange was dried at 120 °C for 4 h after drying overnight and kept at dry ambient conditions.

Two samples of the Pt-USY were taken for characterization. The first sample was calcined in air at 450 °C during 4 h for analysis of metals content. The second one, which was pressed and crushed into 850-1000 μm before calcination, was used for the characterization of its physical properties. Figure 3.6 shows a schematic representation to embed platinum into the zeolite.

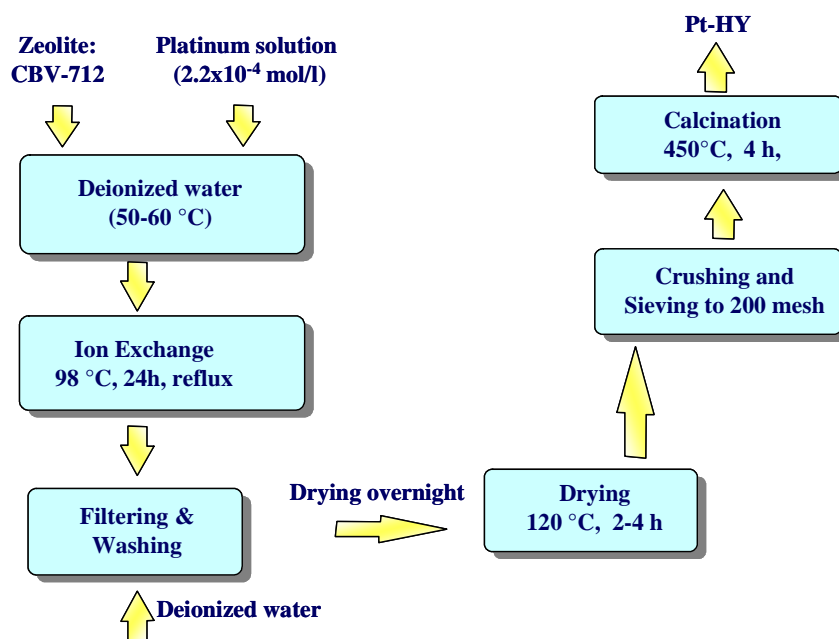


Figure 3.6 Schematic procedure of platinum containing zeolite.

3.2.3.1 Synthesis of CoMoPd/Pt-HY (HDS-5) Catalyst

To prepare the HDS-5 catalyst a combination of ion exchange and incipient wetness impregnation method was also used. The catalyst was made according to the route and Schematic presentation to introduce Pd and CoMo depicted in Figures 3.7 and 3.8. A quantity (35%) of fresh USY-12 zeolite was mixed with Pd/Pt-HY before the impregnation of CoMo solution. The metal precursors of Co, Mo and Pd were calculated to obtain the composition showed in Table 3.5.

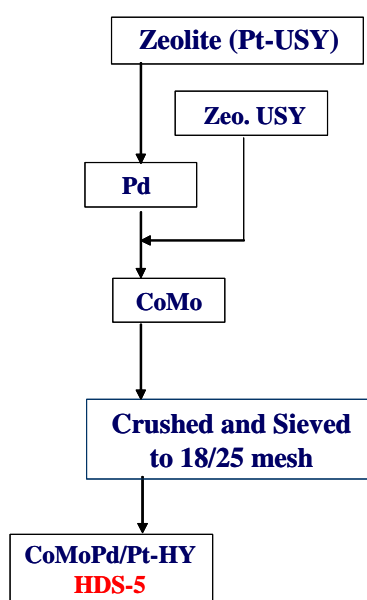


Figure 3.7 Preparation of CoMoPd/Pt-HY (HDS-5) catalyst. Introduction of Pd and CoMo into Pt-USY zeolite.

Table 3.5 Expected composition of the CoMoPd/Pt-HY (HDS-5) catalyst

Element and Zeolite	Loading, wt %
Co	3.0
Ni	--
Mo	12.5
Pt+Pd	0.5
P	1.6
Zeolite	73.3

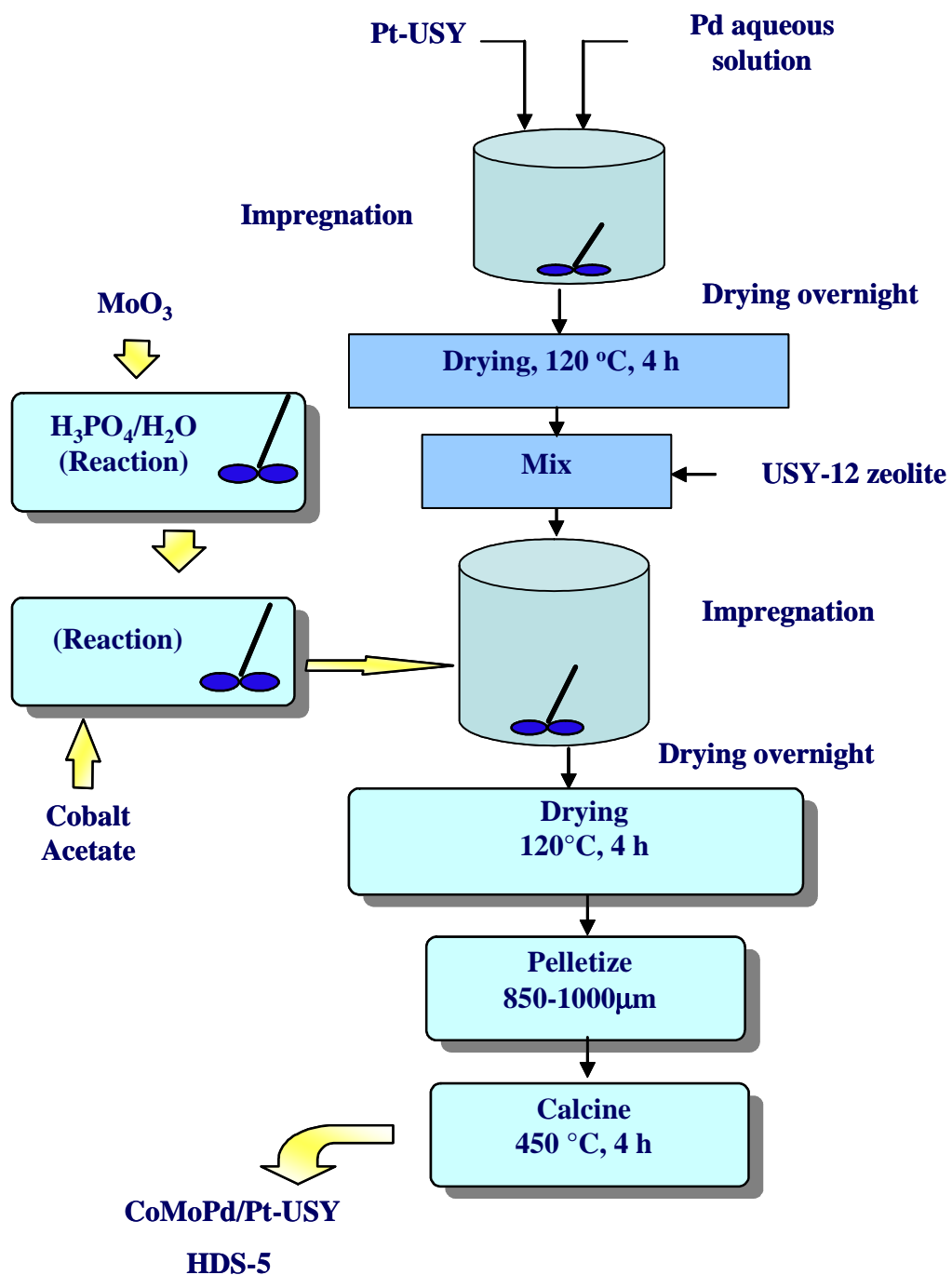


Figure 3.8 Schematic presentation of the preparation of CoMoPd/Pt-HY (HDS-5) catalyst. Introduction of Pd and CoMo into zeolite.

3.2.3.2 Synthesis of CoMo/PdNiPt-HY (HDS-8) Catalyst

Nickel was introduced into Pt-USY by ion exchange to get NiPt-USY. Then palladium was also embedded by ion exchange over the NiPt-USY to get PdNiPt-USY. To reach the expected concentration of Pd and Pt a second batch ion exchange of the PdNiPt-USY was carried out. Finally a CoMo solution was introduced by incipient wetness impregnation of a mixture of 54% of fresh USY and 46% of PdNiPt-USY to get the HDS-8 catalyst in CoMo/PdNiPt-USY formulation. The metal solutions were calculated to get the composition shown in Table 3.6.

Figures 3.9 and 3.10 show the route and the schematic presentation for the introduction of noble and basic metals.

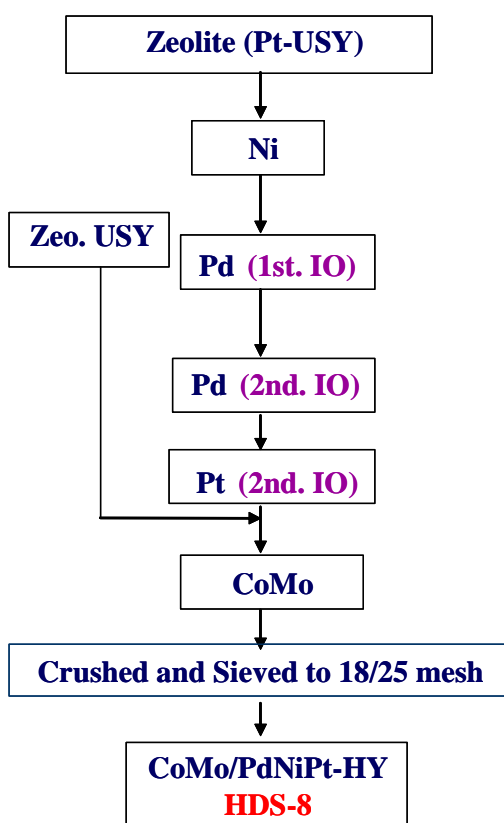
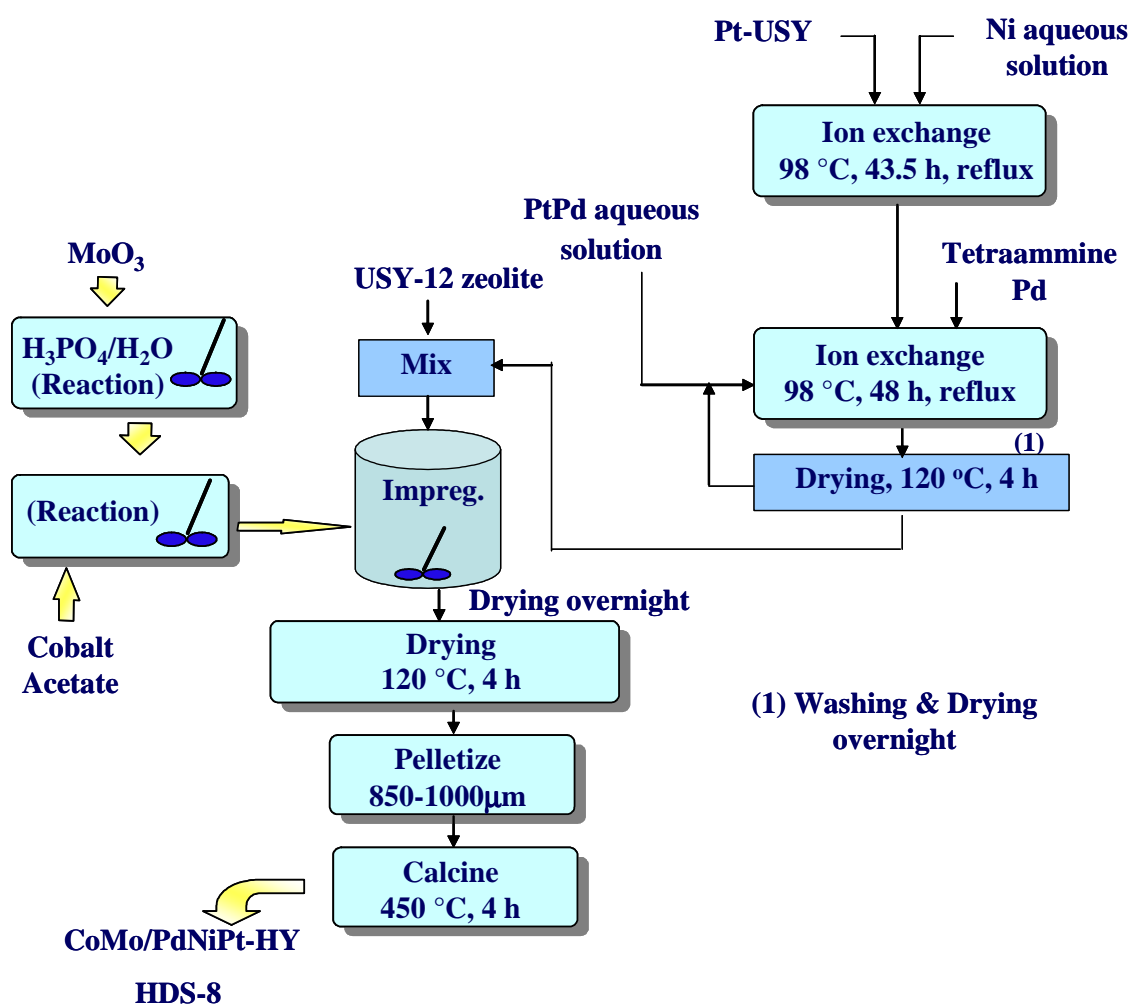


Figure 3.9 Preparation of CoMo/PdNiPt-HY (HDS-8) catalyst. Introduction of Pd, Ni and CoMo into Pt-USY zeolite.

Table 3.6 Expected composition of CoMo/PdNiPt-HY (HDS-8) catalyst

Element and Zeolite	Loading, wt %
Co	2.3
Ni	1.7
Mo	16.5
Pt+Pd	0.5
P	1.6
zeolite	66

**Figure 3.10** Schematic presentation of the preparation of CoMo/PdNiPt-HY (HDS-8) catalyst. Introduction of Ni, Pd, Pt and CoMo into zeolite.

3.2.3.3 Synthesis of CoMoNi/PdPt-HY (HDS-10) Catalyst

The Pd was introduced by ion exchange into Pt-USY to get PdPt-USY. The NiMo were introduced by incipient wetness impregnation of a mix of 28 wt% of USY fresh and 72 wt % of PdPt-USY. After drying at 120 °C for 4 hr a CoMo solution was introduced also by incipient wetness impregnation in a second step to obtain the HDS-10 catalyst. The concentration of both NiMo and CoMo solutions were calculated to reach the expected composition presented in Table 3.7. The route and the schematic presentation to introduce the basic and noble metals for the CoMoNi/PdPt-HY (HDS-10) catalyst are depicted in Figures 3.11 and 3.12.

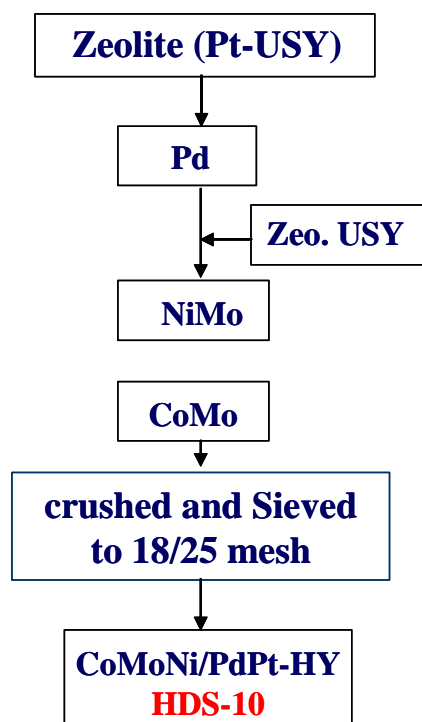
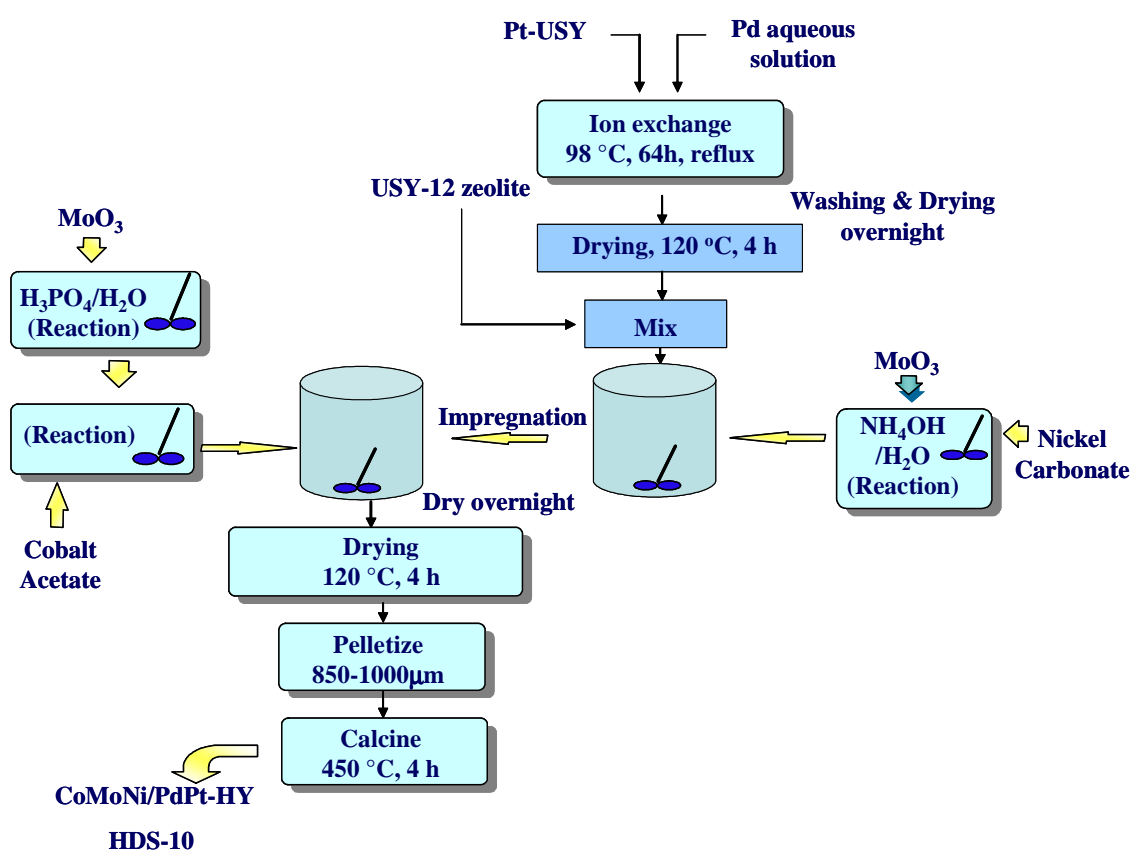


Figure 3.11 Preparation of CoMoNi/PdPt-HY (HDS-10) catalyst. Introduction of Pd, NiMo and CoMo into Pt-USY zeolite.

Table 3.7 Expected composition of CoMoNi/PtPd-HY (HDS-10) catalyst

Element and Zeolite	Loading, wt %
Co	2.3
Ni	1.7
Mo	16.5
Pt+Pd	0.5
P	1.6
zeolite	66

**Figure 3.12** Schematic presentation of the preparation of CoMoNi/PtPd-HY (HDS-10) catalyst. Introduction of Pd, Ni and CoMo into zeolite.

3.3 Characterization of the Catalysts

Samples of the zeolite catalysts were pressed into 3 Ton/cm² and 4.5 Ton/cm² and crushed into 18/25 mesh chips (850-1000 μm particles size) to define the best condition for pressing the pellets to be tested for their activity test. Final treatment of these samples involved drying to 120 °C for 4 hr and calcination to 450 °C for 4 hr in an air stream.

In this report, the abbreviations of the catalyst names will be used to describe the catalyst. “**HDS**” is the abbreviation employed to name the hydrodesulfurization catalyst. The number following an abbreviation is the number describing different catalysts, and actually is the order in preparation of catalyst.

To measure the metal contents of the catalysts Neutron Activation Analysis was used. To examine the textures of the pellets, surface area, total pore volume, average pore diameter, micropore surface area, micropore volume and pore size distribution were analyzed using a BET machine (ASAP 2010). Table 3.8 shows the analytical techniques used. The BJH calculation determines the mesopore volume/area distribution which account for both the change in adsorbate layer thickness and the liquid condensed in pore cores.

Table 3.8 Analytical techniques used for the chemical and physical characterization of experimental catalysts

Technique	Determination	Units
Neutron Activation Analysis	Metal contents	% wt
Brunauer-Emmett-Teller (BET)	Surface Area, m ² /g	m ² /g
	Average pore diameter	Å (Angstroms)
Barret-Joyner-Hallenda (BJH Desorption)	Total pore volume	cc/g
	Pore diameter distribution,	%*
t-Plot	Micropore area	m ² /g
	Micropore volume	cc/g

(*) Vol. ads as a function of pore diameter (Å)

The expected physical properties are based on the ones of a commercial CoMo/Al₂O₃ catalyst which are mentioned in Table 3.9.

Table 3.9 Specification and typical analysis of a commercial CoMo/Al₂O₃ catalyst

Physical properties	Specification	Typical analysis (1)
Surface Area, m²/g	≥195	216
Total pore volume, cc/g	≥0.43	0.49
Average pore diameter, Å	--	58
Pore diameter distribution, %	--	
< 50 Å	--	28
50-100 Å	--	61
>50 Å	--	10

(1) From IMP data

A brief description of the characterization techniques is described in the following sections.

3.3.1 Analytical Techniques

3.3.1.1 Neutron Activation Analysis

The metal contents of the calcined catalysts were determined using Neutron activation analysis. Neutron activation analysis is a sensitive multielement analytical method based on the detection and measurement of characteristic gamma rays emitted from radioactive isotopes produced in the unknown sample upon irradiation with neutrons. The unknown samples together with standard materials of known elemental concentrations are irradiated with thermal neutrons in a nuclear reactor. After some appropriate decay period, high resolution gamma ray spectroscopy is performed to measure the intensity and energies of the gamma lines emitted. A comparison between specific activities induced in the standards and the samples provides the basis for computation of elemental abundances.

The process of measurement of the gamma ray spectra following neutron irradiation of the catalyst samples was performed using a high resolution germanium semiconductor

detector. This device provided sufficient resolution to differentiate between most all commonly occurring gamma lines. An EG&G Ortec detector was operated. The signals produced from this detector were refined with various electronic modules to amplify and shape the pulses prior to input to a high speed analog to digital converter (ADC). A gamma spectroscopy system physically housed at the Nuclear Science Center was used. The irradiated samples were returned to the counting lab in a matter of a few seconds. This system was used for determination of those elements which undergo neutron activation reactions with relatively short half-lives (from seconds to a few hours). Spectral data of this particular system was accumulated on a personal computer version of Canberra's Genie, the Genie2000. Files containing the data as well as various sample parameter information were transferred via Ethernet back to the Alpha system for analysis.

3.3.1.2 Adsorption-Desorption Isotherms of Nitrogen

The texture of the calcined catalysts were evaluated using adsorption-desorption isotherms of nitrogen. The isotherms were obtained on an ASAP 2010 Micromeritics unit shown in Figure 3.13. Nitrogen Adsorption-Desorption isotherms were measured at liquid nitrogen temperature of $-196\text{ }^{\circ}\text{C}$ after degassing the samples below 300 mmHg at $250\text{ }^{\circ}\text{C}$ overnight to eliminate water and volatile substances. The volumetric BET (Brunauer-Emmet-Teller) method was used to determine the specific surface area of each catalyst using adsorption data in the relative pressure range of 0.01 to 0.67. The pore size distribution was obtained by analyzing the adsorption data of the nitrogen isotherm using the Barret-Joyner-Hallenda (BJH Desorption) method.

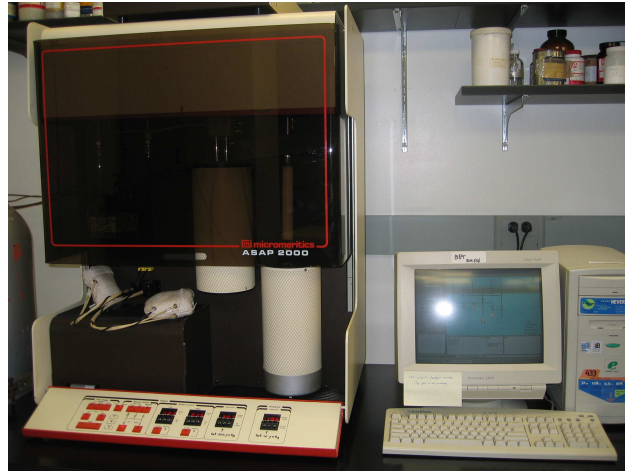


Figure 3.13 Micromeritics BET machine Model ASAP 2010.

Thomas and Thomas (1997) give in their book a summary on the theory of BET method. Surface area is determined when the BET equation No. 3.1, is applied by plotting $[p/V(p_o-p)]$ against p/p_o .

$$\frac{p}{V(p_o - p)} = \frac{1}{V_m c} + \frac{(c-1)}{V_m c} \frac{p}{p_o} \quad (3.1)$$

where p is the pressure of gas, V is the volume of gas adsorbed, p_o is the vapor pressure of the adsorbate at the adsorption temperature, V_m is the monolayer volume, and c is a constant defined according to equation 3.2.

$$c = \exp\left(\frac{H_1 - H_L}{RT}\right) \quad (3.2)$$

where H_1 is the fixed heat of adsorption of the first adsorbed layer, and H_L is the latent heat of vaporization of the subsequent layers. The slope and the intercept of the plot yield the monolayer volume capacity in the adsorption and the constant, c .

By using the ideal gas law, the number of moles adsorbed in the monolayer is $V_m/0.0224$ when the monolayer volume is calculated at standard temperature and pressure (1atm and 0 °C). Finally, the specific surface area in m^2/g is calculated by equation 3.3.

$$S_g = \frac{V_m}{0.0224} \times 6.023 \times 10^{23} \times A \quad (3.3)$$

where A is the area occupied by each adsorbed molecule.

3.3.1.3 X-ray Photoelectron Spectroscopy Technique (XPS)

XPS was used for studying the distribution and state of Ni and Pt in Ni-HY and Pt-HY catalysts. The analyses were made by Dinh L. from the Artie Mc Ferrin Department of Chemical Engineering of Texas A&M University.

X-ray photoelectron spectroscopy (XPS) also called electron spectroscopy for chemical analysis (ESCA) is an electron spectroscopic method that uses X-rays to eject electrons from inner-shell orbitals. The electron binding energies are dependent on the chemical environment of the atom, making the technique useful to identify the oxidation state of an atom.

XPS is a surface sensitive technique because only those photoelectrons generated near the surface can escape and become available for detection. Due to collisions within the sample's atomic structure, those photoelectrons originating much more than about 20 to 100 Å below the surface are unable to escape from the surface with sufficient energy to be detected (Penchev et al., 1973)

The X-ray photoelectron spectroscopy (XPS) analyses were performed with a Kratos AXIS HIs Instrument at room temperature shown in Figure 3.14.



Figure 3.14 X-ray photoelectron spectroscopy machine model Kratos AxisIIIs.

The XPS instrument consists of an X-ray source, an energy analyzer for the photoelectrons, and an electron detector. The analysis and detection of photoelectrons requires that the sample be placed in a high-vacuum chamber. Since the photoelectron energy depends on X-ray energy, the excitation source must be monochromatic. The energy of the photoelectrons is analyzed by an electrostatic analyzer, and the photoelectrons are detected by an electron multiplier tube or a multi-channel detector such as a micro-channel plate.

The samples to be analyzed were dried at 120°C for 4h before acquiring the spectrum to avoid any interference during XPS analysis due to humidity of the zeolite catalysts obtained when they are exposed at room temperature.

The X-ray gun is conditioned with a Mg anode (MgK α radiation: 1253.6eV), 12 mA emission current and 15kV anode HT. Spectra were taken at 25°C at high resolution (pass energy 40eV). Samples were transferred under nitrogen atmosphere and then evacuated at 10⁻⁶ Torr by a turbomolecular pump in a high-vacuum chamber for 90 min.

During the spectra acquisition the pressure of the analysis chamber was maintained at 1×10^{-7} Torr.

C1s spectra have been used as a reference with a binding energy value of 284.6 eV. Atomic concentrations were determined from integrated peak areas normalized by atomic sensitivity factors. The atomic concentration ratio on the surface of catalysts was calculated using equation No. 3.4.

$$\frac{n_A}{n_B} = I_A S_B / I_B S_A \quad (3.4)$$

where n_i is the atomic number of species i (A or B). I_i is the integrated intensity of species i , and S_i is the sensitivity factor determined by XPS measurement (Kerkhof and Moulijn, 1979). The sensitivity factor not only depends on the photoionization cross section (σ_i) but also depends on exciting X-ray energy, detector efficiency, and kinetic energy of the measured peaks.

3.4 Results and Discussion

In this section, the characterization results and discussion of the metal contents and textures of the calcined catalysts prepared by several methods are reported. Each section is dedicated to each category of comparisons on catalyst properties. First, the comparison among the Pt-HY and Ni-HY catalysts prepared by ion exchange are presented in section 3.4.1. In section 3.4.2, the comparison among the catalyst prepared with USY-12 zeolite by wetness impregnation (HDS-1) and the catalysts prepared from the Ni-USY (HDS-3) and Pt-USY (HDS-5) by combining the incipient wetness impregnation with ion exchange method is reviewed. Finally, the comparison among catalysts prepared with PdPt-USY (HDS-10) and PdNiPt-USY (HDS-8) by incipient wetness impregnation and ion exchange are discussed in section 3.4.3.

Each group of catalysts were powdered and pressed into two different pressure values to define the best condition for pressing the pellets to be tested for their activity test.

To measure the metal contents of the catalysts Neutron Activation Analysis was used. To examine the textures of the catalysts, surface area, total pore volume, micropore surface area, micropore volume and pore size distribution were analyzed using a BET machine. To study the state of Ni and Pt in Ni-HY and Pt-HY, XPS was used. The used characterization techniques and the methods of the catalysts preparation has been described in chapter IV and chapter III respectively.

3.4.1 Characterization of Ni-HY and Pt-HY

3.4.1.1 Metal Contents

The Ni and Pt concentrations of the Ni-HY and Pt-HY prepared by ion exchange and used as matrix in the catalyst preparation are shown in Table 3.10. Even though the metal content obtained differs from the expected the concentration is within the required to be used for preparing the HDS catalysts.

Table 3.10 Composition of the metal-HY samples used as matrix of the catalyst

Loading, wt%	Ni- HY		Pt-HY	
	Expected	Real	Expected	Real
Nickel	11.3	10.2	--	--
Platinum	--	--	0.33	0.734

3.4.1.2 Textures

To examine the texture of the catalysts, the samples were pressed into particle size chips of 850-1000 μm . Pressure of 3 and 4.5 Ton/cm² were selected to define the best

conditions for making the pellets of the experimental catalysts to be tested in the conversion test.

Table 3.11 presents the physical properties of the Ni-HY and Pt-HY vs the HY fresh zeolite pressed at the same conditions (3 and 4.5 Ton/cm²). The texture of the HY zeolite is modified when Nickel or Platinum are introduced by ion exchange. The BET surface area and total pore volume of Ni-HY are in the range of 520-540 m²/g and 0.28-0.33 cc/g, while the corresponding values of Pt-HY are in the range of 518-563 m²/g and 0.20-0.22 cc/g respectively.

Table 3.11 Physical properties of HY, Ni-HY and Pt-HY (used as matrix for preparing the HDS catalysts) pressed at 3 and 4.5 Ton/cm²

Physical properties	HY	Ni-HY	Pt-HY	HY	Ni-HY	Pt-HY
	3.0 Ton/cm ²			4.5 Ton/cm ²		
BET Surface Area, m²/g	566	540	563	534	520	518
Micropore Area, m²/g	422	351	389	399	336	357
Micropore Volume, cc/g	0.22	0.19	0.21	0.21	0.18	0.19
Total pore Volume⁽¹⁾, cc/g	0.17	0.33	0.22	0.16	0.28	0.20
Pore Size distribution⁽¹⁾, %						
<50 Å	50	35	54	51	41	54
50-100 Å	13	30	14	13	28	15
>100 Å	37	35	32	36	31	31

(1) BJH Desorption

Although the surface area of all the catalysts has a similar magnitude, 518-566 m²/g (Table 3.11, Figure 3.15a) the catalysts pressed into 3 Ton/cm² show a little bit better physical properties than the catalyst pressed into 4.5 Ton/cm², so they were selected to prepare a big lot for their activity test in the HDS setup.

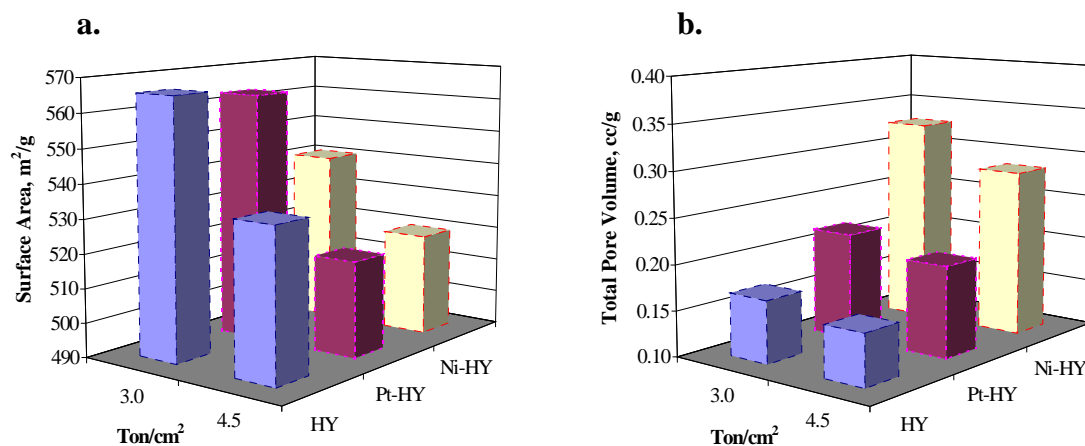


Figure 3.15 Texture of HY, Ni-loaded zeolite, and Pt-loaded zeolite pressed at 3 and 4.5 Ton/cm². (a) Surface area (BET), (b) Total pore volume (BJH Desorption).

In both cases, at 3 and 4.5 Ton/cm², the Ni-loaded zeolite has the highest total pore volume as shown in Figure 3.15b. Figure 3.16 shows that the Ni-loaded zeolite presents not only the lowest micropore area (Figure 3.16a), but also presents the lowest micropore volume (Figure 3.16b). This is because the concentration of Ni in the zeolite is higher than the concentration of Pt in the zeolite as was presented in Table 5.2.

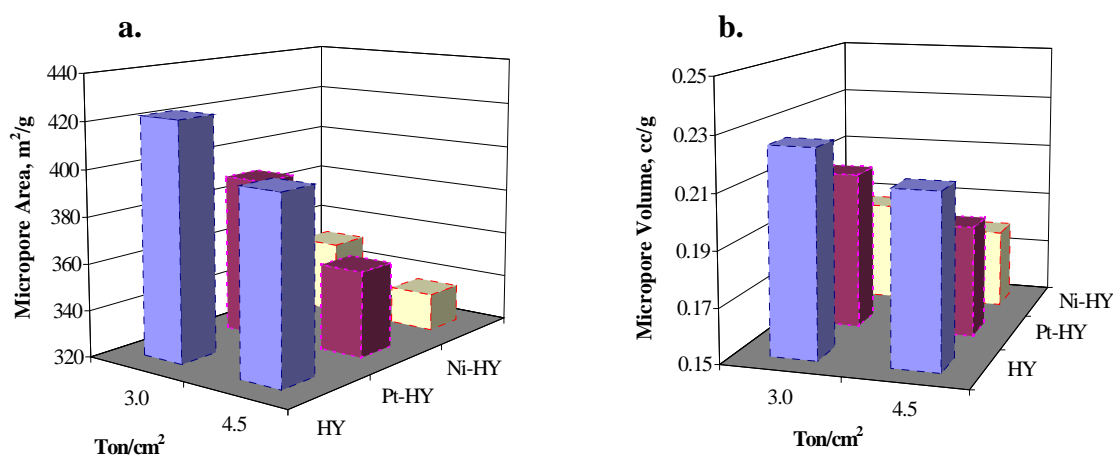


Figure 3.16 Textures of HY, Ni loaded zeolite and Pt-loaded zeolite pressed at 3 and 4.5 Ton/cm². (a) Micropore area, (b) Micropore volume.

Figure 3.17 shows the pore size distribution in the mesopore size range when catalysts were pressed into 3 and 4.5 Ton/cm². The Ni-loaded zeolite (Ni-HY) shows highest pore size distribution in the range of 50 to 100 Å of pore size (>27 %) as was shown in Table 5.3.

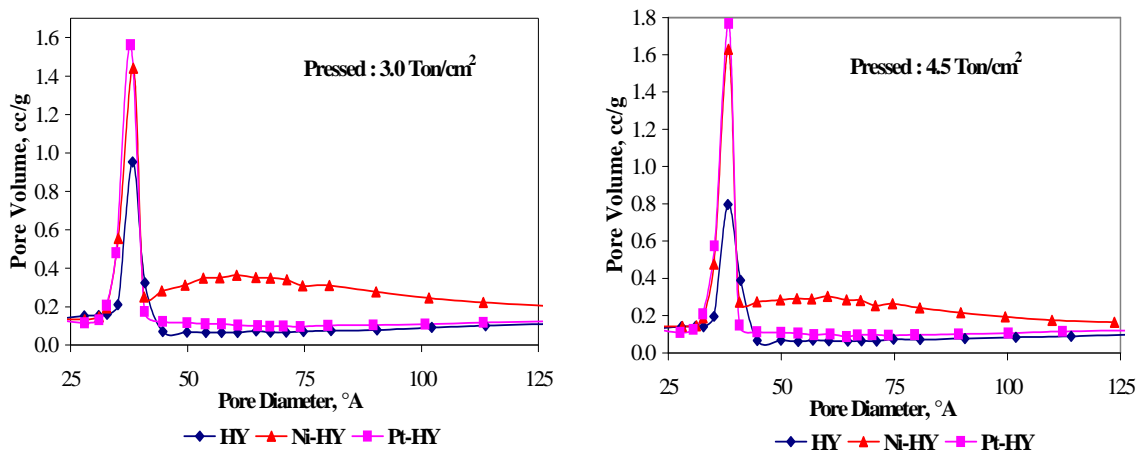


Figure 3.17 Pore size distribution of HY, Ni-loaded zeolite and Pt-loaded zeolite pressed at 3 and 4.5 Ton/cm².

The structure of “Y” zeolite consists of a supercage with a diameter of 12 Å and it is surrounded by 10 sodalite units of 7.4 Å free diameter. So, the pore size distribution measured in all zeolite catalysts does not represent the pore size distribution of the zeolite, but represents the size distribution of the “pores” between the pressed zeolite particles. Textures of the powdered HY, Pt-HY and Ni-HY zeolites are reported in Appendix A. The corresponding adsorption and desorption isotherms are also included in this Appendix.

3.4.1.3 X-ray Photoelectron Spectroscopy (XPS)

XPS analyses were made by Dinh L. in the Center Integrated Microchemical System of Texas A & M University.

Platinum and Nickel XPS investigations were performed in order to elucidate the state of platinum and nickel sites on the surface of HY support. Ni-loaded zeolite and Pt-loaded zeolite were prepared by ion exchange. The results for the calcined Pt-HY zeolite were not successful because the binding energy of Pt 4f XPS spectrum was coincident with the binding energy of Al 2p. As a result, Pt 4d photoline with binding energy at 313.2 ± 0.2 eV was tried for the analysis instead of Pt 2p. However, there was no good resolution of the Pt 4d XPS peak due to the low concentration of Pt in the sample (0.73 wt %) as is shown in Figure 3.18.

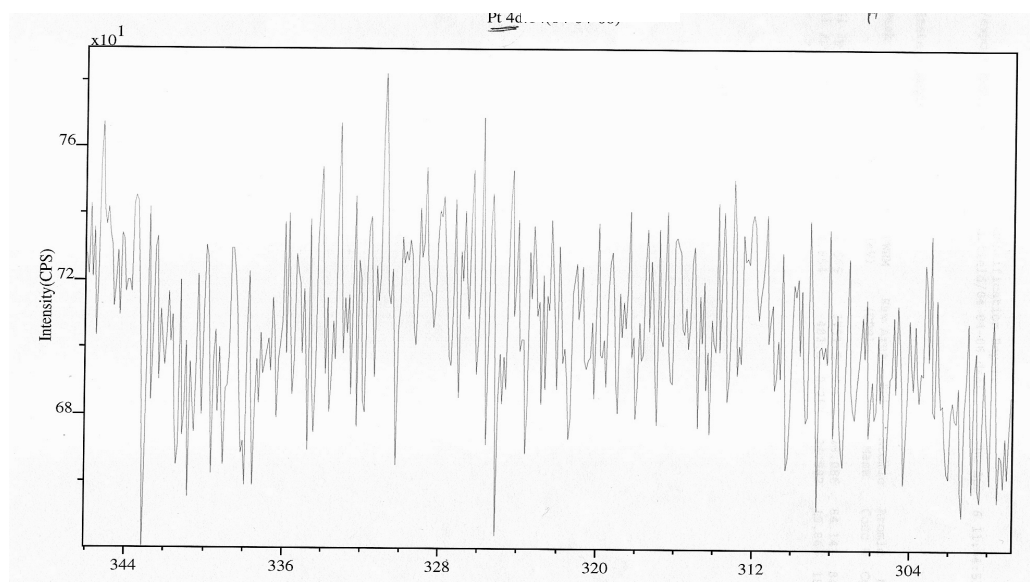


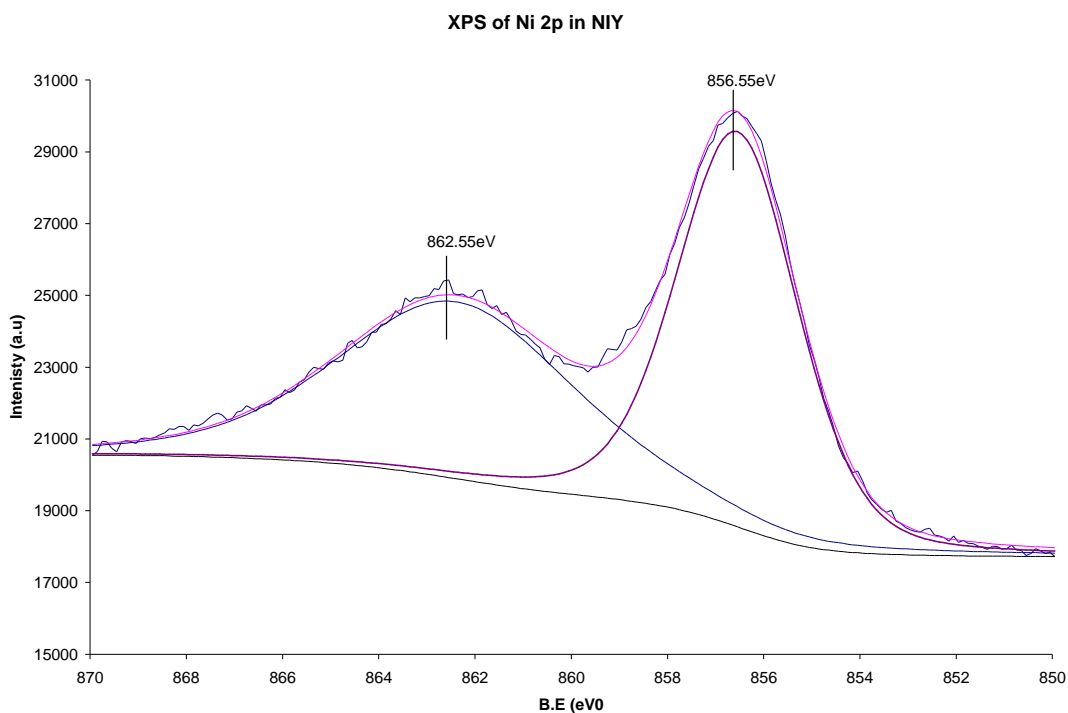
Figure 3.18 XPS spectrum of Pt 4d of the sample Pt-HY with 0.73 wt% of Pt.

XPS studies have been undertaken in order to elucidate the chemical nature and surface structure of Ni-containing zeolite. The Ni 2p XPS spectrum of Ni-loaded zeolite synthesized by ion exchange is shown in Figure 3.19, and the corresponding core level BE values are summarized in Table 5.4. For comparison, the BE values of NiO, NiAl₂O₄ spinel, and Ni metal reported by Velu et al., (2005) are also included in the Table 3.12.

Table 3.12 Ni 2p XPS core level BE values of calcined Ni-HY zeolite

Compound	Binding energy, BE(eV)		
	Ni 2p _{3/2}	satellite	ΔE
Ni-HY	856.55	862.55	6.0
NiO ¹	854.5	861.3	6.8
NiAl ₂ O ₄ ¹	856.0	862.7	6.3
Ni metal ¹	852.5		

⁽¹⁾ From Velu et al., 2005

**Figure 3.19** Ni 2p core level XPS spectrum of calcined Ni-HY zeolite.

In the calcined sample the Ni2p_{3/2} main peak appears as a broad single band around 856 eV together with a satellite centering around 862 eV. The peak at 856 eV coincides

with the BE of NiAl₂O₄ (Table 12), indicating that NiAl₂O₄-like species are present at the surface of Ni-containing zeolite. No peak appears at 854 eV, so NiO-like species are not present at the surface of Ni-HY. Moreover, no peak appears at 852 eV, demonstrating that the Ni²⁺ ions are present in the zeolite matrix instead of metal Ni. This result is really true because the samples were not reduced for this analysis. On the other hand, It is interesting to note that the signal intensity of Ni-HY is high. This indicates that the dispersion of Ni at the surface is good. It is also interesting to note that, although the Ni loading in Ni-HY is only 11.3 wt%, the sample exhibits high XPS signal intensity, because the sample was prepared by ion exchange rather than impregnation. Those observations are in agreement with those reported by Velu (2005) for Ni-containing zeolite.

Because the XPS spectral intensity is directly proportional to the surface concentrations, the same has been calculated by taking into account the atomic sensitivity factors of the elements, and the data are summarized in Table 3.13.

Table 3.13 XPS surface compositions of calcined Ni-HY zeolite

Sample (calcined)	Surface composition (atom %)			
	Ni	Si	Al	Ni/Si atomic ratio
Ni/HY	30.81	29.25	39.94	1.053

As can be seen, the surface Ni concentration is high and very close to the surface concentration of Si giving a Ni/Si ratio of 1.05. This value demonstrates that surface exposure of Si is similar to the surface exposure by Ni.

3.4.2 Characterization of CoMoPtPd/HY (HDS-1), CoMoPtPd/Ni-HY (HDS-3) and CoMoPd/Pt-HY (HDS-5) Catalysts

Preparation parameters, such as: a) procedure to introduce metals; b) metal loading; c) calcinations temperature; d) activation procedure; and e) presence of additives, may

strongly affect the structure, morphology and chemical state of the resulting CoMo or NiMo sulfided species in the HDS catalysts. In this context metals content and texture were determined for the experimental catalysts prepared by different methods of introducing metals. The catalysts did not contain any additive and the calcination temperature and activation procedures were the same in all of them.

3.4.2.1 Metal Contents

It is well known that the structures and their relative proportion in sulfided Mo and CoMo are very dependent on the loading of both active compounds (Mo) and promoters (Co) to obtain active catalysts for HDS. The loading of the metals is consequently one of the more important parameters in optimizing commercial hydrotreating catalysts.

The loading used in industrial applications are usually governed by the desire to achieve as high an activity as possible with as small amount of the expensive metals as possible. In this work a concentration of 0.5 wt% of noble metals was considered. The composition of the CoMoPtPd/HY (HDS-1), CoMoPtPd/Ni-HY (HDS-3) and CoMoPd/Pt-HY (HDS-5) is compared with the commercial CoMo/Al₂O₃ catalysts as is shown in Table 3.14. As it was described in the section 3.2.1, the HDS-1 (CoMoPtPd/HY) catalyst was prepared by incipient wetness impregnation of the USY-12 zeolite. The CoMoPtPd/Ni-HY (HDS-3) and CoMoPd/Pt-HY (HDS-5) were prepared combining both ion exchange and incipient wetness impregnation methods.

The metal content of the HDS-1 catalyst was almost as expected having a Co+Pt/Mo atomic ratio (0.38) similar to the Co/Mo atomic ratio specified for the commercial CoMo/Al₂O₃ catalyst (0.39).

Table 3.14 Composition of the HDS-1, HDS-3 and HDS-5 catalysts compared to the CoMo/Al₂O₃ commercial catalyst

Formulation	Commercial ⁽¹⁾ CoMo/Al ₂ O ₃	HDS-1		HDS-3		HDS-5	
		CoMoPtPd/HY		CoMoPtPd/Ni-HY		CoMoPd/Pt-HY	
		Expected	Real	Expected	Real	Expected	Real
Nickel, wt%	--	--	--	1.70	1.01	--	--
Cobalt, wt%	3.0 +/- 0.2	3.00	2.78	2.30	2.35	3.00	2.90
Molybdenum, wt%	12.5 +/- 0.5	12.50	12.10	16.50	17.40	12.50	12.60
Phosphorous, wt%	1.6 max.	1.60	nd	1.60	nd	1.60	nd
Platinum, wt%	--	0.16	0.12	0.16	0.13	0.16	0.40
Palladium ⁽²⁾ , wt%	--	0.34	0.36	0.34	0.35	0.34	0.36
Atomic ratio Co+Pt/Mo	--	0.40	0.38	--	--	0.40	0.39
Atomic ratio Co+Ni+Pt/Mo	--	--	--	0.40	0.32	--	--
Atomic ratio Co/Mo	0.39	--	--	--	--	--	--

(1) Specifications of IMP

(2) Pd:Pt= 4:1 mol ratio

nd = not determined

The metal content of CoMoPtPd/Ni-HY (HDS-3) and CoMoPd/Pt-HY (HDS-5) is close to the expected values, except for Ni in the HDS-3 and Pt in the HDS-5. The Ni concentration for the HDS-3 catalyst was 1.0 wt% vs 1.7 wt% estimated and the real Pt concentration for the HDS-5 was 0.4 wt% vs 0.16 wt% estimated. However, the variation in the concentration of those metals did not affect the Co+Ni+Pt/Mo atomic ratio since this was similar to the CoMo/Al₂O₃ commercial catalyst as showed in Table 3.13.

3.4.2.2 Textures

Table 3.15 shows the physical properties of the experimental zeolite catalysts compared with the fresh zeolite and a commercial CoMo/Al₂O₃ catalyst. The results are divided into two groups. The first group corresponds to texture of pellets pressed at 3 Ton/cm² and the second group contains texture of the corresponding pellets pressed at 4.5 Ton/cm².

Table 3.15 Physical properties of HY, CoMoPtPd/HY (HDS-1), CoMoPdPt/Ni-HY (HDS-3) and CoMoPd/Pt-HY (HDS-5) catalysts pressed at 3 and 4.5 Ton/cm² compared with the commercial CoMo/Al₂O₃ (Com)

Physical properties	Com. ⁽¹⁾	3 Ton/cm ²				4.5 Ton/cm ²			
		HY	HDS-1	HDS-3	HDS-5	HY	HDS-1	HDS-3	HDS-5
BET Surface Area, m ² /g	≥195	566	379	332	366	534	366	309	359
Micropore Area, m ² /g	--	422	288	254	274	399	280	236	265
Micropore Volume, cc/g		0.23	0.15	0.14	0.15	0.21	0.15	0.13	0.14
Total Pore Volume ⁽²⁾ , cc/g	≥0.43	0.17	0.10	0.10	0.11	0.16	0.09	0.09	0.11
Pore Size Distribution ⁽²⁾ , %									
<50 Å	28	50	57	51	59	50	63	50	64
50-100 Å	62	13	20	26	22	13	17	25	19
>100 Å	10	37	23	22	19	36	20	25	17

(1) Specifications of IMP

(2) BJH Desorption

The BET surface areas, total pore volumes, micropore areas, micropore volumes, and pore size distribution are plotted in Figures 3.20-3.24 for the pellets pressed into 3 and 4.5 Ton/cm² of fresh zeolite as well as for the experimental zeolite catalysts prepared from HY, Ni-HY and Pt-HY.

The physical properties were not considerably affected by the pressure given for making the pellets. However, the physical properties of the HY zeolite are significantly different when noble and basic metals are embedded in zeolite. For the CoMoPd/Pt-HY (HDS-3) and CoMoPtPd/Ni-HY (HDS-5) catalysts Pt in Pt-HY and Ni in Ni-HY were loaded into zeolite by ion exchange before the impregnation. The BET surface area and micropore area decreased in the order of HY > CoMoPtPd/HY > CoMoPd/Pt-HY > CoMoPtPd/Ni-HY as showed in Figures 3.20 and 3.21. That means that the surface area of the calcined samples was reduced more by the ion-exchange process than by the impregnation process. Although the physical properties of the HY zeolite are significantly affected by embedding metals as mentioned above, the methods used to integrate basic and noble metal into zeolite seems not to affect the total pore volume and micropore volume plotted in Figures 3.22-3.23.

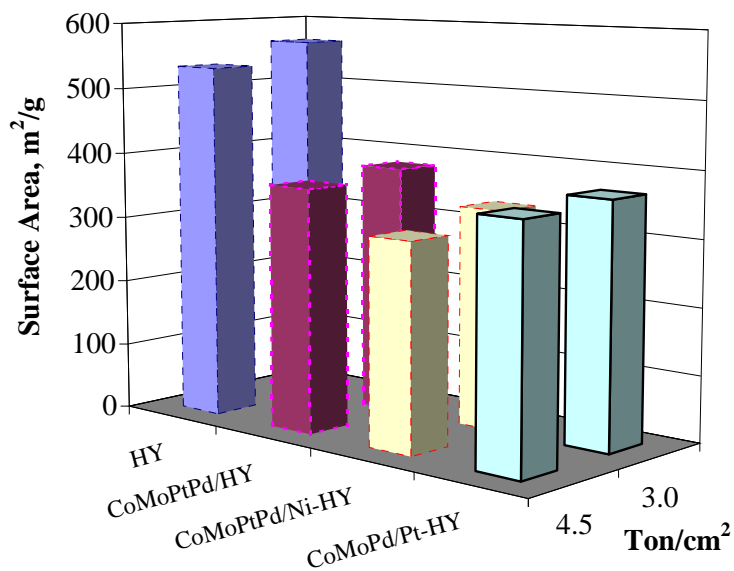


Figure 3.20 Surface area of HY, CoMoPtPd/HY (HDS-1), CoMoPdPt/Ni-HY (HDS-3) and CoMoPd/Pt-HY (HDS-5) pressed at 3 and 4.5 Ton/cm².

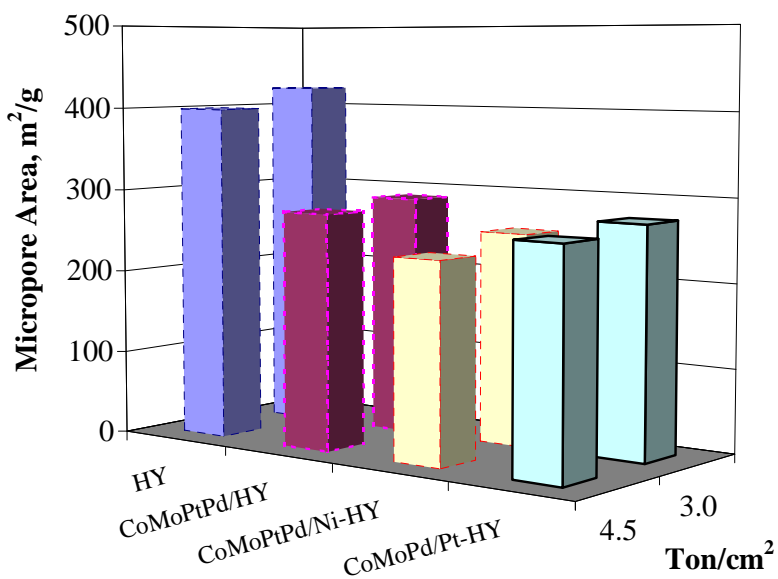


Figure 3.21 Micropore area of HY, CoMoPtPd/HY (HDS-1), CoMoPdPt/Ni-HY (HDS-3) and CoMoPd/Pt-HY (HDS-5) pressed at 3 and 4.5 Ton/cm².

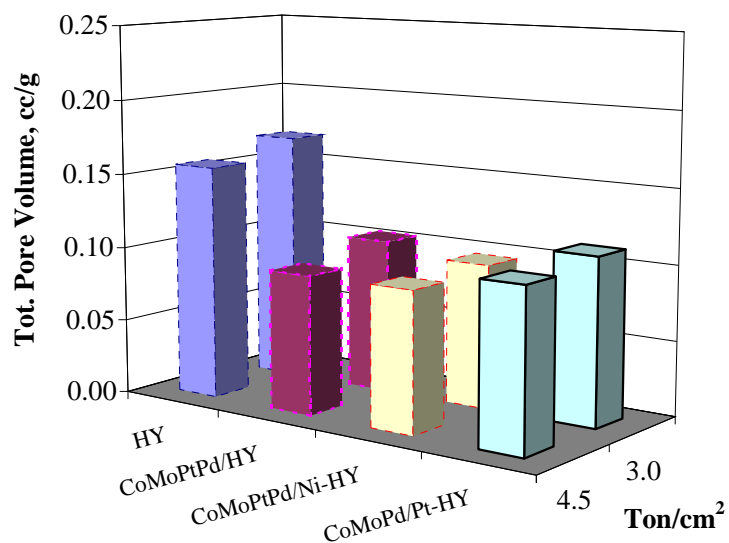


Figure 3.22 Total pore volumes (BJH desorption) of HY, CoMoPtPd/HY (HDS-1), CoMoPtPd/Ni-HY (HDS-3) and CoMoPd/Pt-HY (HDS-5) pressed at 3 and 4.5 Ton/cm².

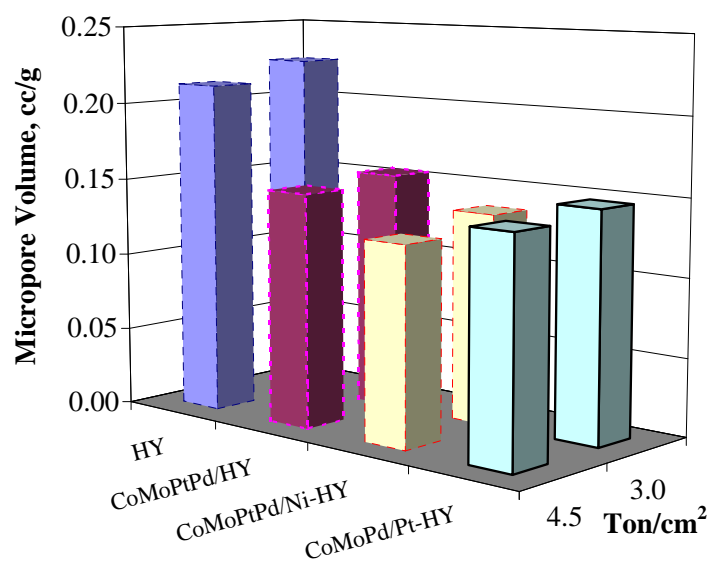


Figure 3.23 Micropore volume of HY, CoMoPtPd/HY (HDS-1), CoMoPtPd/Ni-HY (HDS-3) and CoMoPd/Pt-HY (HDS-5) pressed at 3 and 4.5 Ton/cm².

It is well-known that not only the chemistry surface of the support but also geometrical factors, like the pore-size distribution, are of major importance for the preparation and performance of hydrotreating catalysts. Since the pores influence the “deposition” of the active metals during preparation and they are paths for reactants and products it is important to measure the pore-size distribution of the HDS catalysts. Anderson and Pratt (1985) have classified pores on the basis of their diameters, d : the smallest are micropores ($d < 20 \text{ \AA}$), intermediate are mesopores ($20 \text{ \AA} \leq d \leq 500 \text{ \AA}$) and larger are macropores ($d > 500 \text{ \AA}$). Thus Figure 3.24 shows the pore size distribution in the mesopore range.

These results show that all the samples had very narrow pore size distribution as expected. Most of the pores were less than 50 Angstroms in diameter, which accounted for 50-65% of the pore area.

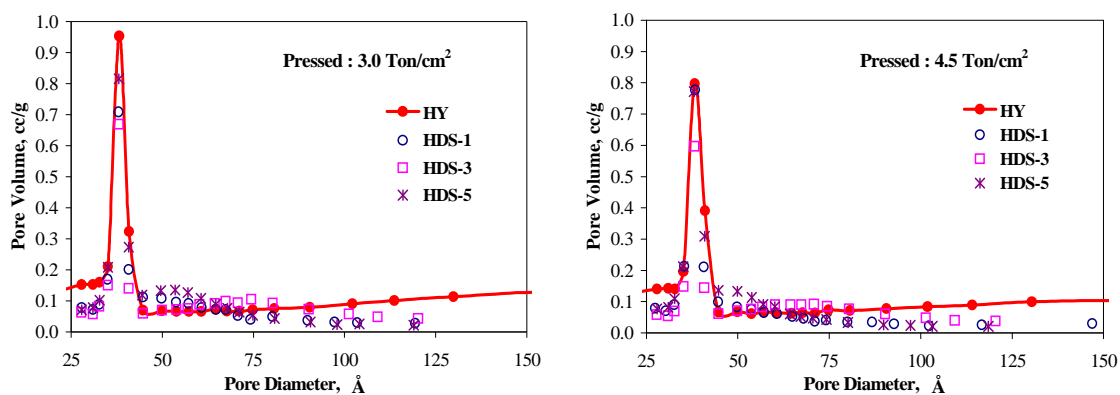


Figure 3.24 Pore size distribution of HY, CoMoPtPd/HY (HDS-1), CoMoPdPt/Ni-HY (HDS-3) and CoMoPd/Pt-HY (HDS-5) pressed at 3 and 4.5 Ton/cm².

3.4.3 Characterization of CoMo/PdNiPt-HY (HDS-8) and CoMoNi/PdPt-HY (HDS-10) Catalysts

In the same way as CoMoPtPd/NiHY (HDS-3) and CoMoPd/Pt-HY (HDS-5) catalysts the CoMoPtPd/HY (HDS-1) catalyst was used as reference of the CoMo/PdNiPt-HY (HDS-8) and CoMoNi/PdPt-HY (HDS-10).

3.4.3.1 Metal Contents

The composition of CoMo/PdNiPt-HY and CoMoNi/PdPt-HY compared with the commercial CoMo/Al₂O₃ catalyst and experimental CoMoPtPd/HY is shown in Table 3.16. As it was described previously, the CoMoPtPd/HY (HDS-1) catalyst was prepared by incipient wetness impregnation of the USY-12 zeolite and the CoMo/PdNiPt-HY (HDS-8) and CoMoNi/PdPt-HY (HDS-10) were prepared combining ion exchange and the incipient wetness impregnation methods.

The metal content of the HDS-8 and HDS-10 catalyst differs from the HDS-1, because this last one does not contain Ni, and Mo and Pt+Pd concentrations are higher.

Table 3.16 Composition of the HDS-1, HDS-8 and HDS-10 catalysts compared with the CoMo/Al₂O₃ commercial catalyst

Formulation	Commercial ⁽¹⁾ CoMo/Al ₂ O ₃	HDS-1		HDS-8		HDS-10	
		CoMoPtPd/HY Expected	Real	CoMo/PdNiPt-HY Expected	Real	CoMoNi/PdPt-HY Expected	Real
Nickel, wt%	--	--	--	1.70	2.28	1.70	1.49
Cobalt, wt%	3.0 +/- 0.2	3.00	2.78	2.30	2.34	2.30	2.37
Molybdenum, wt%	12.5 +/- 0.5	12.50	12.10	16.50	17.70	16.50	17.60
Phosphorous, wt%	1.6 max.	1.60	nd	1.60	nd	1.60	nd
Platinum, wt%	--	0.16	0.12	0.16	0.33	0.16	0.39
Palladium ⁽²⁾ , wt%	--	0.34	0.36	0.34	0.31	0.34	0.24
Atomic ratio Co+Pt/Mo	--	0.40	0.38	--	--	--	--
Atomic ratio Co+Ni+Pt/Mo	--	--	--	0.40	0.43	0.40	0.37
Atomic ratio Co/Mo	0.39	--	--	--	--	--	--

(1) Specifications of IMP

(2) Pd:Pt= 4:1 mol ratio

nd = not determined

Although the metal concentration of the CoMo/PdNiPt-HY (HDS-8) and CoMoNi/PdPt-HY (HDS-10) catalysts is higher than CoMoPtPd/HY and CoMo/Al₂O₃ commercial catalyst, the atomic ratio, expressed as promoters/active compounds ratio (Co+Ni+Pt/Mo), is similar. This means that the HDS-8 and HDS-10 catalysts might be good candidates for deep hydrodesulfurization and high hydrogenation. It is important to remember that the Co, Ni and Pt act as promoters and the Mo is the active component. Moreover, the sulfides of Co, Ni and Mo are the active phases for HDS and metal Pt is the active phase for the aromatic hydrogenation reactions. It is known that the function of Pd in combination with Pt enhances the sulfur tolerance of the noble metals when supported in zeolite due to electron transfer.

3.4.3.2 Textures

A sample of the powder of the CoMoPtPd/HY (HDS-1), CoMo/PdNiPt-HY (HDS-8) and CoMoNi/PdPt-HY (HDS-10) catalysts was pressed at 3.0 and 4.5 Ton/cm² to define the best condition of the pellets to be tested for their activity test. Table 3.17 shows the physical properties compared with a CoMo/Al₂O₃ commercial catalyst. The properties of the HY fresh zeolite pressed at the same conditions as the other catalysts are included also.

The physical properties of the HY zeolite are significantly different when noble or basic metals are introduced by ion exchange. Figures 3.25-3.29 show the comparison of the experimental catalysts prepared by incipient wetness impregnation and by combining of incipient wetness impregnation and ion exchange when pressed into 3 and 4.5 Ton/cm². The HY fresh zeolite pressed at the same conditions is also presented. The CoMoNi/PdPt-HY (HDS-10) catalyst shows the lowest BET surface area (SA), total pore volume (TPV), micropore area (MA), and micropore volume (MV) as is shown in Figures 3.25, 3.26, 3.27 and 3.28 respectively.

Table 3.17 Physical properties of HY, CoMoPtPd/HY (HDS-1), CoMo/PdNiPt-HY (HDS-8) and CoMoNi/PdPt-HY (HDS-10) catalysts pressed at 3 and 4.5 Ton/cm² vs the commercial CoMo/Al₂O₃ (Com) catalyst

Physical properties	Com. ⁽¹⁾	3 Ton/cm ²				4.5 Ton/cm ²			
		HY	HDS-1	HDS-8	HDS-10	HY	HDS-1	HDS-8	HDS-10
BET Surface Area, m²/g	≥195	566	379	298	130	534	366	291	131
Micropore Area, m²/g	--	422	288	219	74	399	280	214	73
Micropore Volume, cc/g		0.23	0.15	0.12	0.04	0.21	0.15	0.11	0.04
Total Pore Volume⁽²⁾, cc/g	≥0.43	0.17	0.10	0.10	0.08	0.16	0.09	0.10	0.08
Pore Size Distribution⁽²⁾, %									
<50 Å	28	50	57	60	41	50	63	59	43
50-100 Å	61	13	20	20	17	13	17	20	17
>100 Å	10	37	23	21	42	36	20	21	40

(1) Specifications of IMP

(2) BJH Desorption

The physical properties of CoMoNi/PdPt-HY (HDS-10) at 3 Ton/cm² are: SA of 129.6 m²/g, TPV of 0.08cc/g, MA of 73.2 m²/g, and MV of 0.04 cc/g. and the corresponding for CoMo/PdNiPt-HY (HDS-8) were SA of 298.2 m²/g, TPV of 0.1 cc/g, MA of 218.6 m²/g and MV of 0.12 cc/g pressed at the same conditions.

The texture of the CoMoPtPd/HY (HDS-1) catalyst prepared by incipient wetness impregnation in general is the closest to the HY fresh zeolite than the CoMo/PdNiPt-HY and CoMoNi/PdPt-HY catalysts prepared at least by an ion exchange step (HDS-8 and HDS-10, respectively)

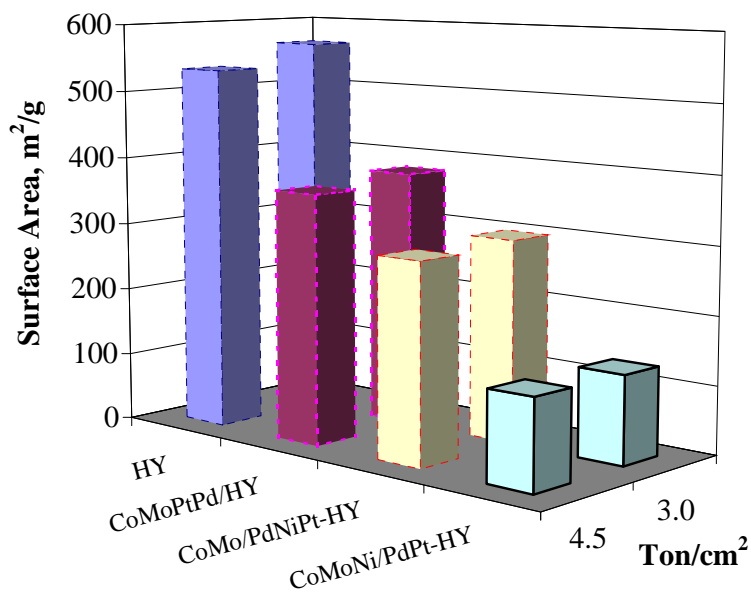


Figure 3.25 Surface area of HY, CoMoPtPd/HY (HDS-1), CoMo/PdNiPt-HY (HDS-8) and CoMoNi/PdPt-HY (HDS-10) catalysts pressed at 3 and 4.5 Ton/cm².

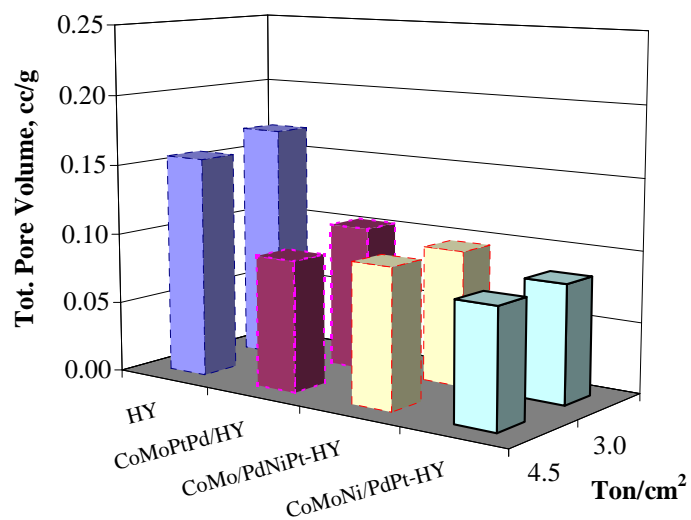


Figure 3.26 Total pore volumes (BJH desorption) of HY, CoMoPtPd/HY (HDS-1), CoMo/PdNiPt-HY (HDS-8) and CoMoNi/PdPt-HY (HDS-10) catalysts pressed at 3 and 4.5 Ton/cm².

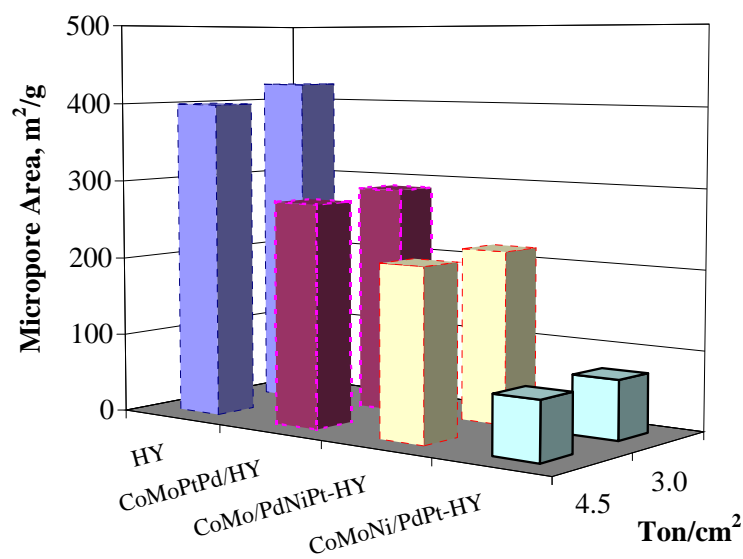


Figure 3.27 Micropore area of HY, CoMoPtPd/HY (HDS-1), CoMo/PdNiPt-HY (HDS-8) and CoMoNi/PdPt-HY (HDS-10) catalysts pressed at 3 and 4.5 Ton/cm².

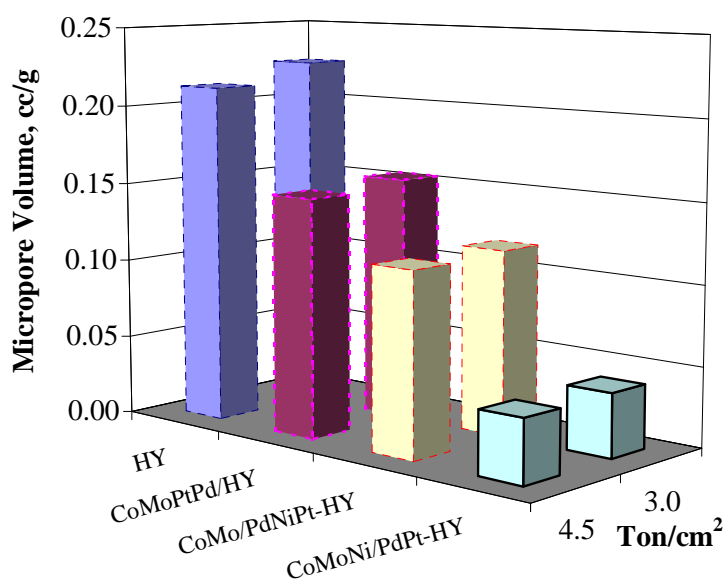


Figure 3.28 Micropore volume of HY, CoMoPtPd/HY (HDS-1), CoMo/PdNiPt-HY (HDS-8) and CoMoNi/PdPt-HY (HDS-10) catalysts pressed at 3 and 4.5 Ton/cm².

The pore size distribution of the catalyst shown in Figure 3.29, indicates that the majority of pores are in the mesoporous range.

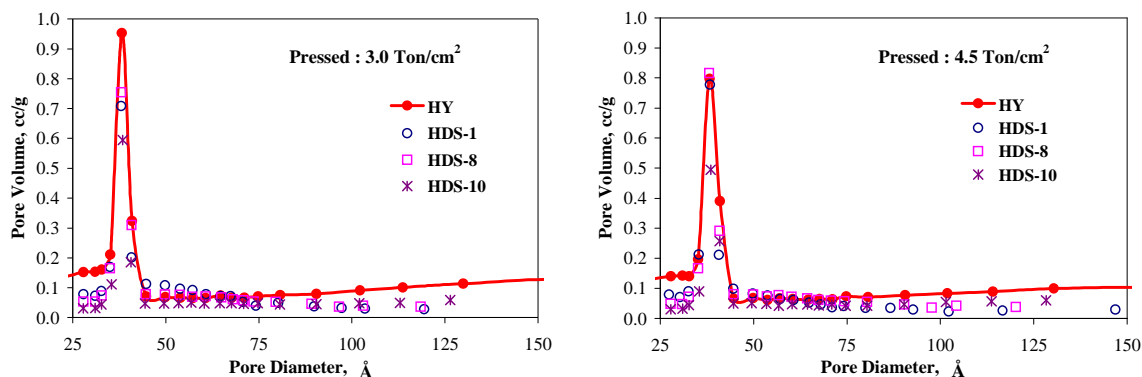


Figure 3.29 Pore distribution of HY, CoMoPtPd/HY (HDS-1), CoMo/PdNiPt-HY (HDS-8) and CoMoNi/PdPt-HY (HDS-10) catalysts pressed at 3 and 4.5 Ton/cm².

According to Table 3.17 and Figure 3.29 the pore size distribution is affected by the procedure of embedding metals, but not by the pressure conditions used for the pellets as expected. The pore size distribution is enhanced when metals are introduced into zeolite by combining incipient wetness impregnation and ion exchange as observed with the CoMoNi/PdPt-HY (HDS-10) catalyst. For instance, while the HY fresh zeolite has a pore size distribution of 37 % in pore size >100 Å, the HDS-10 catalyst shows 42% when pressed into 3 Ton/cm² and 40% when pressed into 4.5 Ton/cm².

The commercial CoMo/Al₂O₃ catalyst has a typical pore size distribution of 10 % in pore size >100 Å and 89% in pore size < 100 Å.

3.5 Concluding Remarks

The analysis has sought to examine physically and chemically, the CoMo formulations supported in HY and Ni, Pt, PdNiPt and PdPt-containing zeolites. The catalysts were characterized using Neutron Activation Analysis for determining the total

metal loading. Based on the BET method, surface area, pore volume, pore size distribution, micropore area and micropore volume, all catalysts were also analyzed.

The CoMoNi/PdPt-HY (HDS-10) and CoMoPd/Pt-HY (HDS-5) catalysts prepared from the PdPt-HY show good metal contents with a pore size distribution greater than 40% in pore size $>50 \text{ \AA}$. The noble metal concentration (Pt+Pd) was greater than 0.6 wt%. So, it is believed that these catalysts could have good performance not only in the hydrodesulfurization reactions, but also in the hydrogenation reactions.

CHAPTER IV

EXPERIMENTAL SET UP AND METHODS FOR THE ACTIVITY TEST OF THE CATALYSTS

4.1 Description of the Setup

The catalysts were evaluated in a one liter perfectly mixed flow reactor (CSTR). The Robinson-Mahoney Reactor is the most widely used for catalyst testing in multiple phases. Its design of perfectly mixed reactor lets circulate liquid reactants past a stationary catalyst bed. Impellers (1,200 rpm) draw fluid into the center of an annular catalyst basket. Figure 4.1 shows a schematic representation of the special CSTR reactor.

The stainless steel 316 Robinson-Mahoney stationary basket reactor was obtained from Autoclave Company. It is housed in a cylindrical electric furnace capable of heating up 450 °C. Inside the reactor, a stainless steel of ¼ inch outside diameter thermocouple well was inserted along the axial direction to control the temperature.

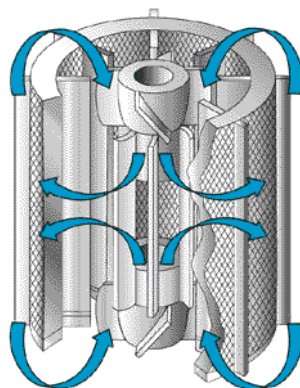


Figure 4.1 Schematic representation of the Robinson-Mahoney catalyst testing reactor. (from the Autoclave Engineers Company).

Figure 4.2 provides a schematic of the high-pressure and -temperature continuous flow reactor assembled for this study.

A Milton Roy minipump with a flow rate range of 49 to 920 ml/h and 6,000 psi was used to pump the liquid feedstock into the reactor against hydrogen/methane pressure. A Denver Instrument balance series TR-8101 with a weighing range of 8100 g was used to measure the liquid feed rate. A Brooks mass flow controller (5850E) calibrated for 0-2 SLPM @ 70 °F was used to measure and control hydrogen gas flow. Another mass flow controller (5850E) calibrated for 0-28 SLPH @ 70 °F was used to measure and control methane gas flow, which was selected as an internal standard. A Tescom S91W11505 backpressure regulator was used to maintain the overall system pressure required for deep desulfurization.

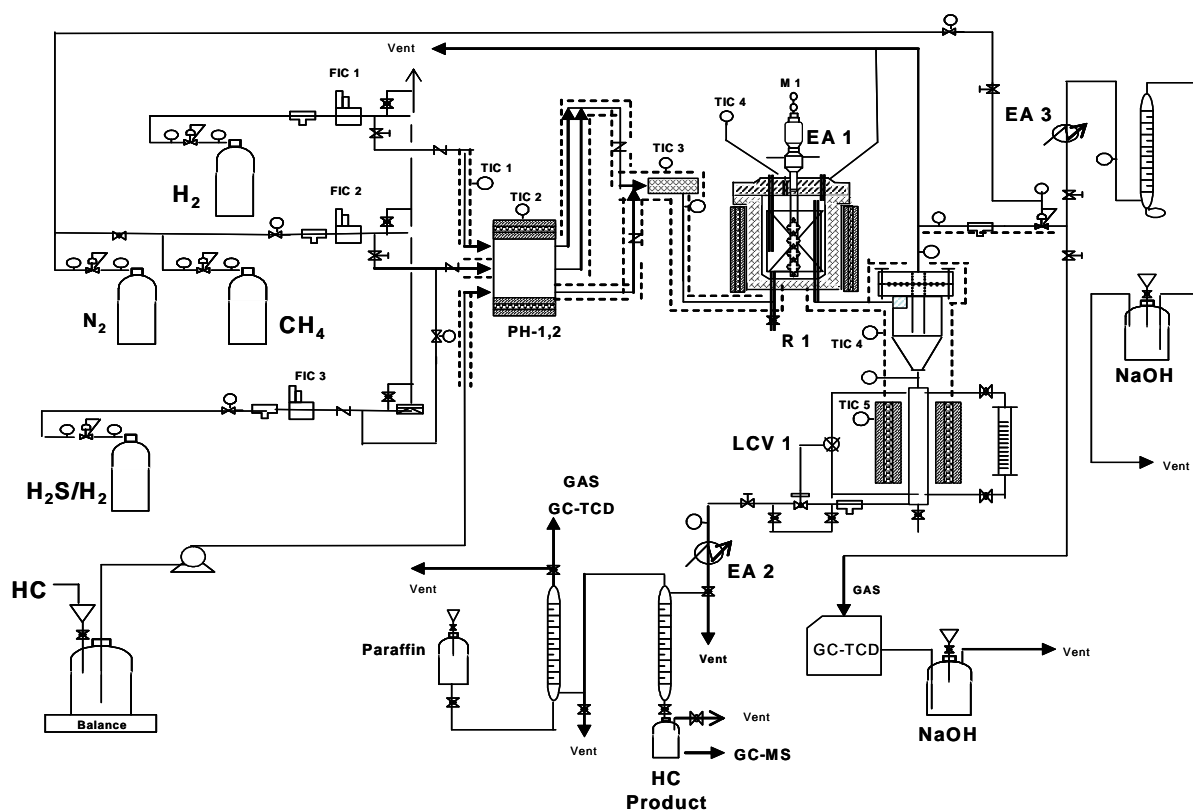


Figure 4.2 Schematic of high pressure experimental setup for the hydrodesulfurization of heavy gas oil.

A gas-liquid separator shaped as cyclone was designed and fabricated to separate the reaction products into gas and liquid phases. The gaseous reactor effluents were analyzed and bubbled through a 20wt% sodium hydroxide aqueous solution before venting in a hood.

A typical catalyst evaluation experiment used 8g of the catalyst. All experimental catalysts evaluated in the perfectly mixed flow reactor had a particle size of 710-850 μm , to avoid diffusional effects. A commercial CoMo/Al₂O₃ catalyst (HDS-0) was used as reference. The HDS-0 catalyst was obtained as trilobe-shaped presulfided 1/20 inch nominal diameter extrudates from the Mexican Petroleum Institute.

The commercial sample was crushed and sieved using sieves of mesh sizes 18 and 25 to give the same particle size as the experimental catalysts (850-1000 μm). γ -Alumina in the same size as the experimental catalysts was used as diluent. The weight ratio of Al₂O₃/catalyst was 16.6.

The catalyst is placed inside the reactor in an annular 80 ml stainless steel basket. The basket containing the catalyst is shown in Figure 4.3.



Figure 4.3 Stainless steel Catalyst Basket modified by the Chemical Engineering workshop at A&M University.

4.2 Analysis of Product

4.2.1 Gaseous Product

The gas samples were analyzed by an on line Shimadzu chromatograph (GC) model 17A with a thermal conductivity detector (TCD). The transfer line from the gas-liquid separator to the GC-TCD was maintained at room temperature. The Shimadzu 17A was redesigned with a complex 10 port valve containing a sample loop of 98.5 μl to take samples every hour and packed columns system to facilitate the port valve operation. A Hayesep D column was used to separate H_2 , CH_4 , and H_2S , and an OV-101 column was used to retain heavier hydrocarbons and backflushing after each analysis. The gaseous sample was controlled by a micrometric valve located in the HDS setup. A special timing-program for switching the 10 port's valve and an isothermal temperature for the GC oven was run through the GC-TCD analysis. Table 4.1 shows further details of the characteristics of the columns and the operating conditions of the GC-TCD. The set-up of the switching valve and columns is depicted in Figures 4.4 and 4.5. From these Figures, it can be seen that the GC had a sample injection loop.

Table 4.1 Conditions for the gas chromatographic analysis of hydrogen sulfide, hydrogen and methane in the desorbed gas from reaction products

Chromatograph:	Shimadzu model 17A
Columns:	<ul style="list-style-type: none"> • 20% OV-101 CHROM P-AW 80/100 6' x 1/8" x 0.085" SS OV-101; • 30' x 1/8" x 0.085 SS Hayesep D 100/120
Column Temperature:	110 °C Isothermal
Carrier gas:	8.2% H_2 /Helium balance at 20 cm^3/min
Detector Temperature:	120 °C
Injection port Temperature:	120 °C
Switching valve Temperature:	120 °C
Current in TCD:	100 mA
Range / Polarity:	1 / 1
Integration:	Sensitivity: 90%; Baseline: 60%
Auxiliary pressure controller:	80 kPa

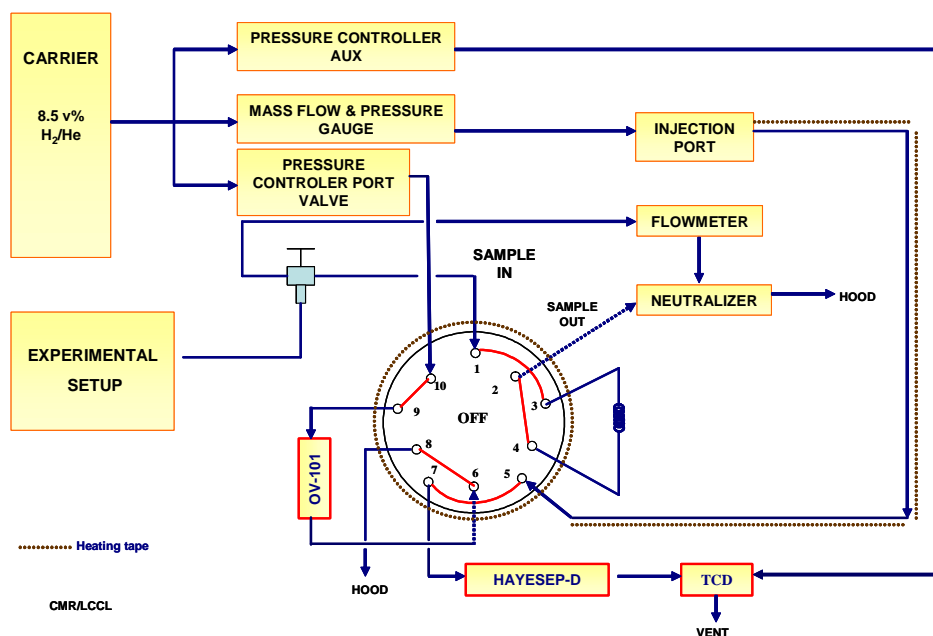


Figure 4.4 Schematic representation of the configuration on Shimadzu 17A GC-TCD in load position (loading sample and backflush).

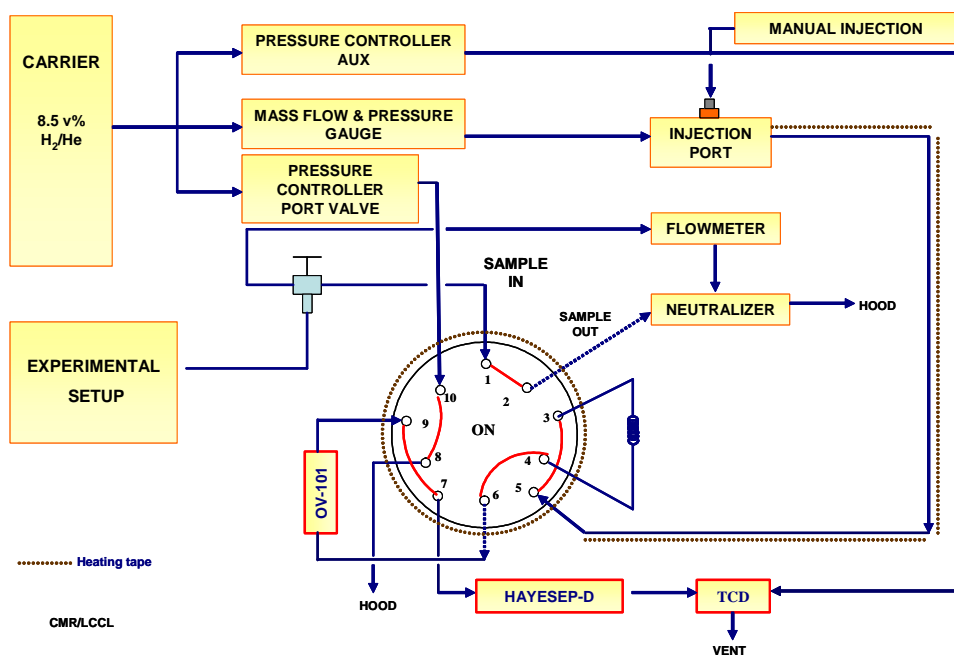


Figure 4.5 Schematic representation of the configuration on Shimadzu 17A GC-TCD in inject position (analysis online and manual injection).

4.2.2 Liquid Product

It is well known that middle distillates contain hundreds of sulfur compounds. In some of these compounds sulfur is relatively easily removed, while others are highly refractory. The requirement for production of ultra-low sulfur fuels makes it imperative to identify these sulfur compounds individually. Speciation of sulfur compounds has been a hard but rewarding task. DePauw and Froment (1997) characterized light cycle oil by GC-MS and GC-AED techniques. Buteyn and Kosman (1990) and Nishioka et al., (1985) reported the characterization of sulfur compounds in light gas oil (LGO) by GC-AED and GC-MS. Kabe et al., (1992, 1993) reported a group of alkyl-substituted benzothiophenes and another group of alkyl-substituted dibenzothiophenes contained in light gas oil and determined by GC-AED and GC-MS.

Internal standards are often used in chromatography, mass spectroscopy and atomic emission spectroscopy. In the project of HDS of the heavy gas oil (HGO) the identification of the sulfur compounds as for other aromatics was made by GC-MS only and fluorene was considered as an internal standard. This molecule is present in the heavy gas oil feed and is not produced nor hydrogenated or significantly evaporated under reaction conditions. In addition, it does not co-elute with other components with the same mass. The most important fragment of fluorene with m/z ratio of 166 was used for the calculations.

The hydrocarbon liquid samples taken from the reactor were collected in labeled vials, refrigerated and analyzed by gas chromatograph (Hewlett-Packard G1800A GCD system) equipped with an Electron Ionization detector. The GC separation was performed on a 50 m x 0.2 mm fused-silica capillary column coated with a 0.5 μm film of cross-linked 100% dimethylsiloxane (HP-PONA). Helium was used as a carrier gas at 0.645 ml/min @ 25°C.

The injection port temperature employed was 250 °C, and the detector temperature used was 270 °C. The column was temperature programmed from 35°C (5 min) to 80 °C (15 min) at a rate of 2.5 °C/min and then to 200 °C (5min) at a rate of 2.0 °C/min and

finally to 250°C at a rate of 1 °C/min. 2µl of the 100x diluted liquid samples in dichloromethane were injected at a split ratio of 63:1. The ions created by the Electron Ionization detector were scanned in the mass range of 10-450 m/z.

4.3 GC-MS Data Processing

The identification of the hydrocarbon compounds were performed by the comparison of the spectral data with database of reference spectra called spectral libraries (Wiley 138K mass spectral database for HP Vectra/IBM, 1990). The chromatograms were integrated by a ChemStation integrator. Table 4.2 shows the parameters of integration.

Table 4.2 Integration parameters used in the GC-MS for the analysis of feedstock and the hydrocarbon liquid products coming from the reactor

Integration Events	Value	Time
Initial Area Reject	1	Initial
Initial Peak Width	0.02	Initial
Shoulder Detection	on	Initial
Initial Threshold	12	Initial
Integrator off	--	0.001
Threshold	0.1	--
Integrator on	--	11.3

After GC-MS analysis is over, the retention time and peaks areas of components in a sample is saved. A typical total ion chromatogram of the analysis of HGO and one of the reaction products are presented in Figures 4.6 and 4.7 respectively. Two aromatic compounds and nine sulfur compounds were selected to follow the hydrodesulfurization and hydrogenation reactions. As mentioned 9H-Fluorene was chosen as an internal standard. Figures 4.8 and 4.9 show the corresponding sulfur compounds, Figure 4.10 illustrates the corresponding aromatic compounds, and finally Figure 4.11 shows the reaction products of DBT and 4,6-DMDBT.

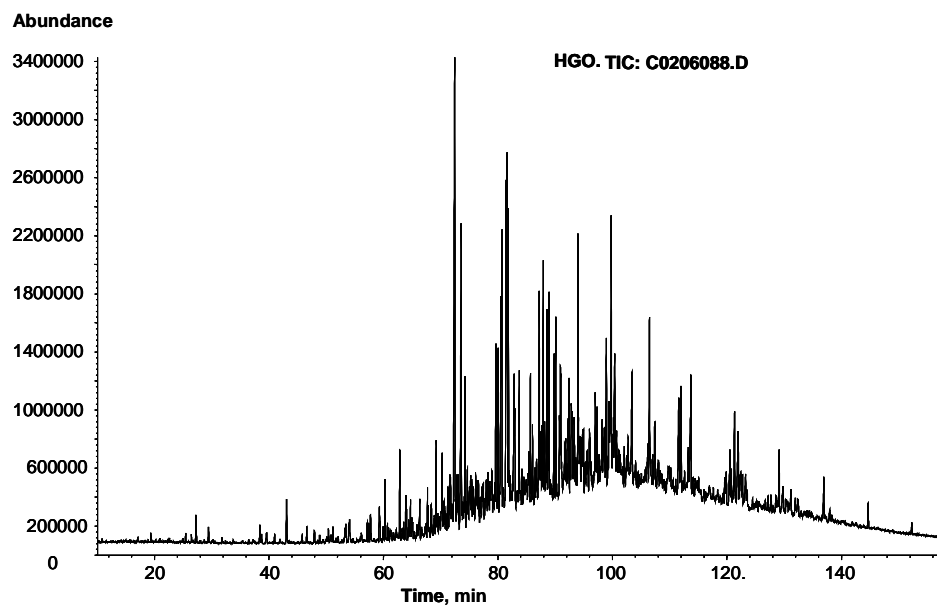


Figure 4.6 Total ion Chromatogram of heavy gas oil.

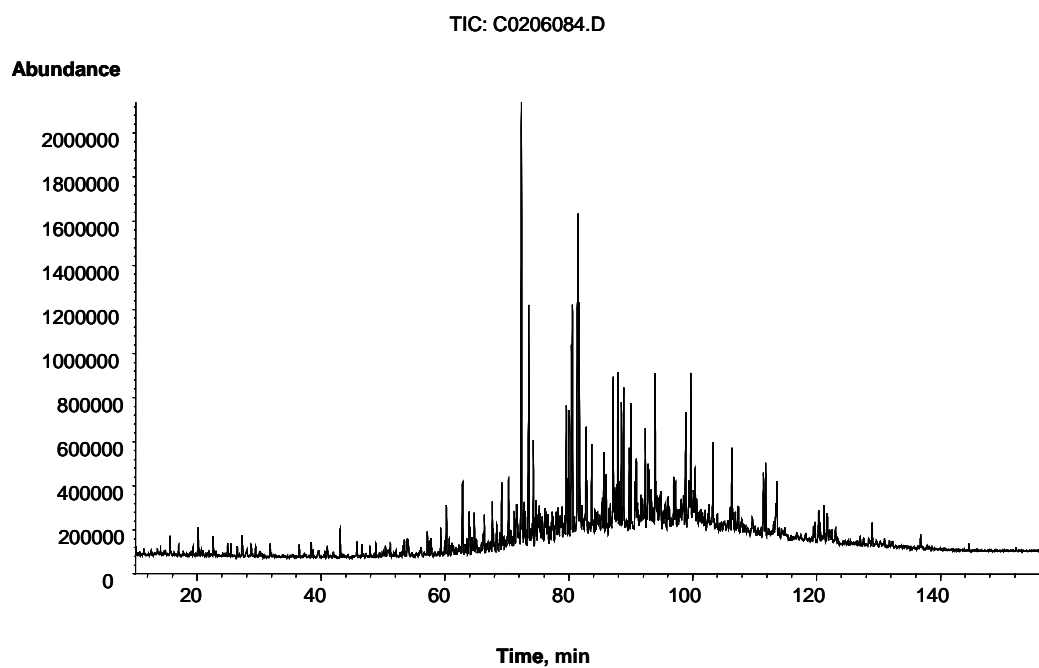


Figure 4.7 Total ion Chromatogram of one obtained product in the hydrodesulfurization of heavy gas oil.

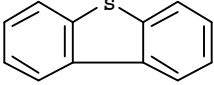
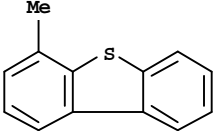
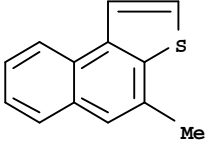
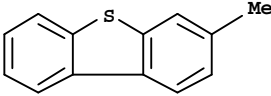
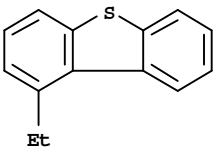
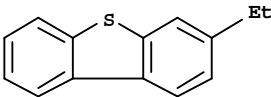
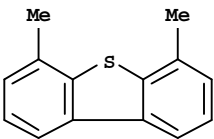
Compound	Structure	Formula	MW	Boiling Point (°C) @ 760 Torr
Dibenzothiophene		C ₁₂ H ₈ S	184.26	332.5±11.0
4-Methyldibenzothiophene		C ₁₃ H ₁₀ S	198.28	349.0±11.0
4-Methylnaphtho[2,1-b]thiophene		C ₁₃ H ₁₀ S	198.28	355.4±11.0
3-Methyldibenzothiophene		C ₁₃ H ₁₀ S	198.28	349.0±11.0
1-Ethyldibenzothiophene		C ₁₄ H ₁₂ S	212.31	359.3±11.0
3-Ethyldibenzothiophene		C ₁₄ H ₁₂ S	212.31	359.3±11.0
4,6-Dimethyldibenzothiophene		C ₁₄ H ₁₂ S	212.31	364.9±11.0

Figure 4.8 Molecular structures of the sulfur compounds present in heavy gas oil.

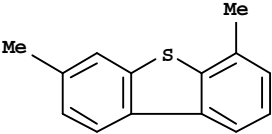
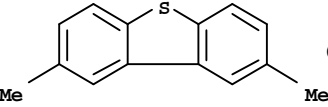
Compound	Structure	Formula	MW	Boling Point (°C) @ 760 Torr
3,6- Dimethyldibenzothiophene		C ₁₄ H ₁₂ S	212.31	364.9±11.0
2,8- Dimethyldibenzothiophene		C ₁₄ H ₁₂ S	212.31	364.9±11.0

Figure 4.9 Molecular structures of 2,8-dimethyldibenzothiophene and 3,6-dimethyldibenzothiophene present in heavy gas oil.

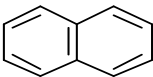
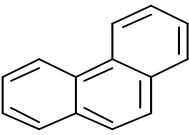
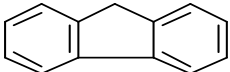
Naphthalene		C ₁₀ H ₈	128.17	220.7±7.0
Phenanthrene		C ₁₄ H ₁₀	178.23	337.4±9.0
9H-Fluorene		C ₁₃ H ₁₀	166.22	293.6±10.0

Figure 4.10 Molecular structures of the aromatics compounds present in heavy gas oil.

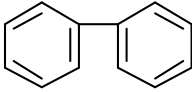
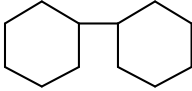
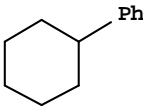
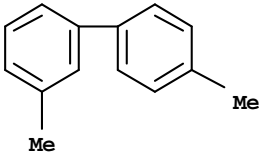
Compound	Structure	Formula	MW	Boiling Point (°C) @ 760 Torr
DBT:				
1,1'-Biphenyl		C12 H10	154.21	258.0±7.0
1,1'-Bicyclohexyl		C12 H22	166.30	239.0±0.0
Benzene, cyclohexyl-		C12 H16	160.26	242.6±7.0
4,6-DMDBT:				
1,1'-Biphenyl, 3,4'- dimethyl-		C14 H14	182.26	284.2±15.0

Figure 4.11 Molecular structures of the reactions products of DBT and 4,6-DMDBT.

The identification of the sulfur components was done with a combination of various techniques, GC-MS, matching of the increases of the HDS products to the decreases in the sulfur components after hydrotreatment, comparison of the retention times with literature data and by understanding of the elution order of the isomers.

The identification of aromatic compounds such as naphthalene and phenanthrene was obtained directly by the library search report of the GC-MS. Table 4.3 shows the retention times of the selected sulfur compounds and aromatics in heavy gas oil (HGO) and some reaction products.

Table 4.3 Retention times of the selected sulfur compounds, naphthalene and phenanthrene. Operating conditions: Cat. HDS-1, $W/F_{DBT}=6000 \text{ kg}_{\text{cat}}/\text{kmol}$, $T = 310 \text{ }^\circ\text{C}$, $H_2/\text{HC} = 7.2 \text{ mol ratio}$, $P = 65 \text{ bar}$

Library/ID	HGO	Hydrocarbon Products			
		Retention Time, min			
	C0206028	C0206043	C0206044	C0206045	
Naphthalene	62.86	62.92	62.92	62.93	
9H-Fluorene	91.68	91.71	91.68	91.74	
Dibenzothiophene	101.43	101.45	101.41	101.49	
Phenanthrene	103.44mi	103.44	103.38	103.49	
4-Methylthiophene	108.69	108.68	108.65	108.73	
4-Methylnaphtho[2,1-b]thiophene	109.88	109.89	109.85	109.92	
3-Methylthiophene	110.20	110.20	110.16	110.24	
1-Ethylthiophene	112.88	112.83	112.76	112.87	
3-Ethylthiophene	115.46	115.45	115.42	115.49	
4,6-Dimethylthiophene	116.01	116.01	115.96	116.05	
3,6-Dimethylthiophene	116.97	116.94	116.89	117.00	
		117.10	117.07	117.12	
2,8-Dimethylthiophene	118.84	118.86	118.81	118.89	

Table 4.4 shows the corresponding retention times of the reaction products of DBT and 4,6-DMDBT.

Table 4.4 Retention times of reaction products of DBT and 4,6-DMDBT. Operating conditions: Cat. HDS-1, $W/F_{DBT}=6000 \text{ kg}_{\text{cat}}/\text{kmol}$, $T = 310 \text{ }^\circ\text{C}$, $H_2/\text{HC} = 7.2 \text{ mol ratio}$, $P = 65 \text{ bar}$

Library/ID	HGO	Hydrocarbon Products			
		Retention Time, min			
	C0206028	C0206043	C0206044	C0206045	
DBT:					
1,1'-Bicyclohexil	74.58	74.64	74.62	74.64	
Benzene, cyclohexyl-	74.70	74.75	74.74	74.76	
1,1'-Biphenyl	78.27	78.31	78.29	78.32	
4,6-DMDBT:					
1,1'-Biphenyl, 3,4'-dimethyl-	92.13	92.15	92.13	92.17	

Based on the peak areas, the composition of one component can be calculated. The general calculation procedure is a tie component method. For this work, 9H-fluorene has been selected as internal standard (tie) component. The weight fraction of a component to that of the tie component can be expressed as:

$$\left[\frac{w_i}{w_{fl}} \right] = \frac{A_i}{A_{fl}} \left[\frac{f_i}{f_{fl}} \right] \quad (4.1)$$

where w is weight fraction of a i component in the sample, A the GC-MS peak area, the subscript fl represents the tie component, and f is the GC peak area weight correction factor. For instance, for Dibenzothiophene (DBT) and fluorene as tie component or internal standard the weight fraction can be expressed as:

$$\left[\frac{w_{DBT}}{w_{fluorene}} \right] = \frac{A_{DBT}}{A_{fluorene}} \left[\frac{f_{DBT}}{f_{fluorene}} \right] \quad (4.2)$$

Since the GC-MS area correction factors for sulfur compounds are not available in the literature and because they are difficult to determine also due to the complexity of the samples, the conversion of the sulfur compounds was calculated relative to the sulfur compounds present in the feedstock (heavy gas oil). Calculations of conversions for a selected component from the peak areas were carried out using an Excel spreadsheet. The general formula is expressed in Equation 4.3.

$$x_i = 1 - \left[\frac{A_i}{A_{fl}} \right]^{Prod} \times \left[\frac{A_{fl}}{A_i} \right]^{HGO} \quad (4.3)$$

where x is the conversion of a component i in the sample, A is the Peak-area, A_{fl} is the Peak-area of internal standard and the superscript denotes the corresponding values to the product and feedstock.

A selection of nine sulfur components in the HGO and reaction products (DBT, 4-MDBT, 3-MDBT, 1-EDBT, 3-EDBT, 4,6-DMDBT, 3,6-DMDBT, 2,8-DMDBT and 4-Methylnaphtho[2,1-b]thiophene) was made to calculate the molar-averaged conversion.

The molar-averaged conversion was calculated according to Equation 4.4 and represents the conversion of the sulfur compounds in the heavy gas oil.

$$\bar{x} = \frac{1}{\sum_{i=1}^n y_i^{HGO}} \sum_{i=1}^n x_i y_i^{HGO} \quad (4.4)$$

where \bar{x}_i is the molar-averaged conversion of the selected set of sulfur compounds, x is the conversion and y_i^{HGO} is the mole fraction of the i component in the heavy gas oil.

The conversions of every selected compound into the corresponding product were calculated using fluorene in a similar manner as follows:

$$x_{i \rightarrow j} = \left[\frac{A_j}{A_f} \right]^{Prod} \times \left[\frac{A_f}{A_i} \right]^{HGO} - \left[\frac{A_j}{A_i} \right]^{HGO} \quad (4.5)$$

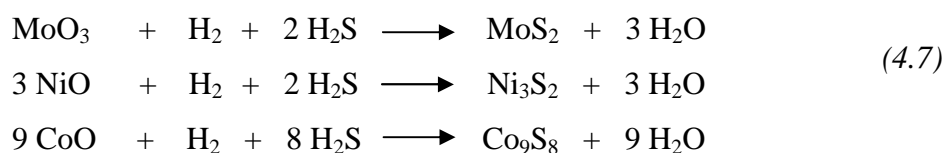
where A_i is the peak-area of component i and A_j , the peak-area of its corresponding product. A_f is the peak-area of fluorene. For instance, the conversion of DBT into biphenyl can be expressed in this fashion:

$$x_{DBT \rightarrow BPH} = \left[\frac{A_{BPH}}{A_f} \right]^{Prod} \times \left[\frac{A_f}{A_{DBT}} \right]^{HGO} - \left[\frac{A_{BPH}}{A_{DBT}} \right]^{HGO} \quad (4.6)$$

4.4 Catalysts Activation

It has long been recognized that to obtain the maximum activity from CoMo or NiMo catalyst, they must be sulfided prior to their use. Several methods are commonly

used to sulfide hydrotreating catalysts. These procedures include in-situ gas phase sulphiding or liquid phase sulphiding - with or without a sulfur spiking agent and ex-situ presulfurized catalyst which can also be activated in gas or liquid phase. Moreover, there are several classes of sulfur compounds that can be used for sulphiding. These include mercaptans, sulphides, disulphides, polysulphides and sulfoxides. The total required quantity of sulfur is determined for each catalyst based upon its promoter metals content. The following reactions show the stoichiometric amount of sulfur needed for successful sulphiding:



These sulfide metals are unstable components when they are exposed to air. So, It is recommendable to avoid exposing the material to air for extended periods. Long-term exposure to air could cause the material to generate sulfur dioxide and heat. Moreover, the sulfided catalysts should be stored in a cool place and kept dry. The material may generate sulfur dioxide and heat if it is wetted. Exposure to air and water may also cause discoloration and agglomeration of the material. One recommendation more is that if the material does get wet or generate heat, the container should be purged with nitrogen or CO₂ and resealed. Finally, the material should be inspected for signs of degradation just before it is loaded into the reactor.

For this work, an in-situ sulphiding procedure in gas phase was selected to activate the catalysts. The activation procedure implied two steps, drying and reaction. The drying step was carried out at 120 °C for 2 hours in an atmosphere of hydrogen, and the reaction step, where the CoMoPtPd/HY (HDS-1) and CoMo/Al₂O₃ (HD-0) catalysts were activated with 15 vol % H₂S/H₂ balance gas mixture, was performed at temperatures of 330 °C and pressure of 1 bar for 3.5 h. Methane, which was used as an internal standard for analysis of the gas products coming from the reactor, was not fed during the activation of the catalysts.

4.4.1 Description of the Sulphiding Procedure

The pressure in the setup was decreased at 1 bar after the leaks in the set up were corrected at 68 bar. A H₂ flow rate was set to 2.8 LSTP/h for approximately 1 h to eliminate N₂ gas which was used in the leaks testing. Then the drying step was carried out increasing the H₂ flow rate to 28 LSTP/h.

The reactor temperature was increased also at 25 °C/h until 120 °C. One hour was considered enough to dry completely the catalysts. The agitation started at 500 RPM and the temperature of preheater, mixer, separator and demister was increased when the reactor reached 70 and 120 °C. When the drying step finished the reactor temperature increased again at 25 °C/h until 330 °C. Finally, the conditions were set for 3.5 hr after 2 hr of stabilization. Figure 4.12 represents a diagram of the activation procedure followed by the reaction step of the activity test and shutdown.

4.5 Catalysts Testing for HDS of Real Feedstock

The evaluation procedure for the commercial CoMo/Al₂O₃ (HDS-0) and experimental catalysts was almost the same. The operating conditions for each catalyst are mentioned in its corresponding section. However, for exemplifying the procedure for the activity test the operating conditions of the experimental CoMoPtPd/HY (HDS-1) catalyst were taken and shown in Table 4.5. A set of twelve experiments were carried out at temperature of 330 and 310 °C, space time (W/F_{DBT}⁰) from 4000 to 6000 kg_{cat}h/kmol, H₂/HC from 7.2 to 11.2 mol reaction, and partial pressure of hydrogen of 65 and 75 bar.

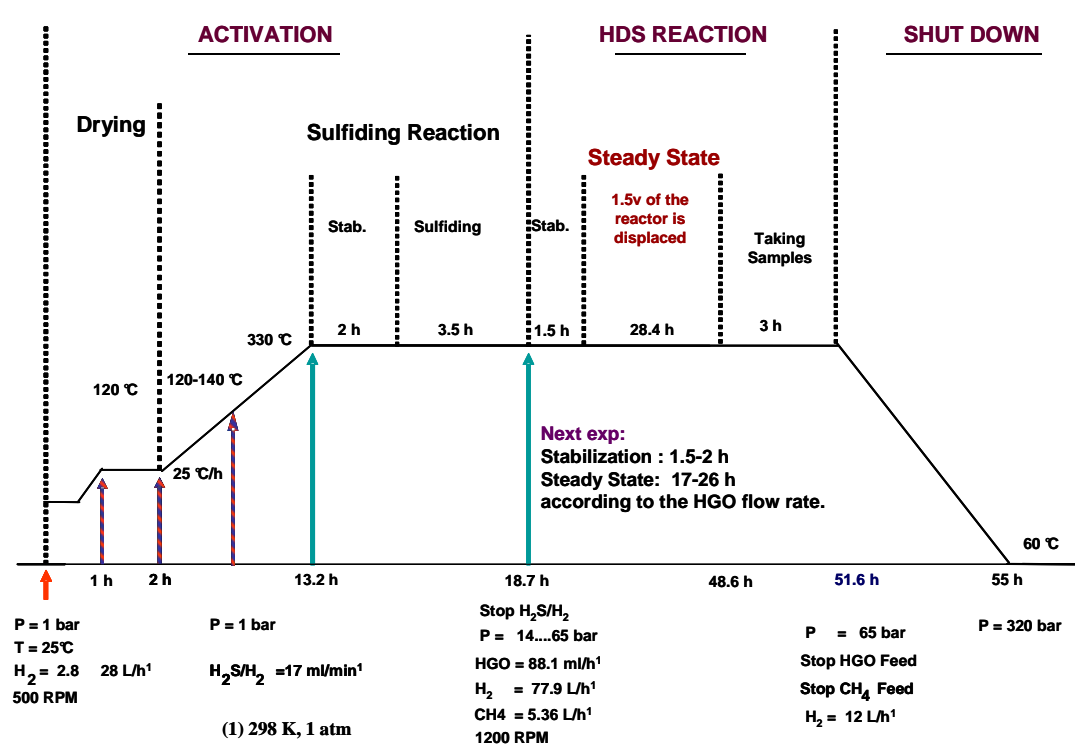


Figure 4.12 Diagram of the procedure carried out for activating the experimental zeolite containing catalysts, reaction-activity test and shut down.

Table 4.5 Operating conditions used to measure the catalytic activity for the CoMoPtPd/HY (HDS-1) catalyst

Experiment	T °C	Pt bar	W/F _{DBT} ^o kg _{cat} h/kmol	H ₂ /HGO mol ratio	HGO ml/h	H ₂ @ 294 K, 1atm L/h
E13T1			4000		88.1	77.9
E14T1	330	65	5000	7.2	70.5	62.3
E15T1			6000		58.7	51.9
E15T4			6000		58.7	51.9
E14T4	310	65	5000	7.2	70.5	62.3
E13T4			4000		88.1	77.9
E15T4			6000	7.2	58.7	51.9
E16T4	310	65	6000	9.2	58.7	66.0
E17T4			6000	11.2	58.7	80.2
E18T4			6000	7.2	58.7	51.9
E19T4	310	75	6000	9.2	58.7	66.0
E20T4			6000	11.2	58.7	80.2

The procedure for the activity test described as follow is given as an example and it uses the operating conditions for the E13T1 experiment.

Once the activation of catalyst was completed the H₂S/H₂ flow was stopped. The backpressure was set at 950 psig, H₂ flow rate was set to 77.9 LSTP/h, and the HGO flow rate was set at 88.1 ml/h. The agitation was set to 1200 rpm. The temperature of the reactor was increased to 330°C at 25°C/h. Operating conditions were maintained for 28.4 h for reaching steady state. Then, a set of 6 gas and hydrocarbon product samples were taken during 3 h for its analysis. Readings of temperature controllers (TIC), mass flow controllers (FIC), temperature indicators (TI), pressure gauges, were taken every 30 min. The desorbed gases from the liquid product were analyzed on line, while the hydrocarbon liquid samples were labeled and analyzed off line.

Although both the commercial HDS-0 (CoMo/Al₂O₃) and HDS-1 (CoMoPtPd/HY) catalysts were evaluated with the same procedure, the activation was a little different, because the drying step was not given for the HDS-0 catalyst.

CHAPTER V

CHARACTERIZATION OF FEEDSTOCK AND REACTION PRODUCTS

This chapter shows the results and discussion of the characterization broken down into two groups:

5.1 Characterization of Heavy Gas Oil and Light Cycle Oil by GC-MS

5.2 Characterization of HDS Reaction Products

5.1 Characterization of Heavy Gas Oil and Light Cycle Oil by GC-MS

Light cycle oil (LCO) has been used as feedstock in the investigation of the HDS of real feedstocks because LCO contains most sulfur-containing compounds of interest (Chen et al., 2003; Froment et al., 1994). In this project heavy gas oil was obtained from Shell Chemical LP. So, in order to know how different these potential feedstocks are, this section presents a comparison of the Mexican LCO with USA HGO in terms of composition as determined by GC-MS.

According to the initial and final boiling points of heavy gas oil (HGO), which is listed in Table 5.1, belongs to the range of diesel fuel and distillate fuel oil and is a feedstock for a hydrocracker unit. The LCO is a petroleum fraction typically produced in Fluid Catalytic Cracking (FCC) with a high concentration of total sulfur and a wide diversity of benzothiophenes, dibenzothiophenes and naphtho benzothiophenes. The HGO has a higher specific gravity and wider boiling interval than LCO, but with lower concentrations of total sulfur. Because the properties of both fractions are different, it was required to determine their composition.

Table 5.1 Typical properties of Heavy Gas oil (from Shell Chemical LP) and a Mexican Light Cycle Oil (from Mexican Petroleum Institute)

Physical and Chemical Properties	Heavy Gas Oil	Light Cycle Oil
Specific Gravity @ 60°F	0.9318	0.9096
Initial Boiling Point, °F (°C)	304 (151)	360 (182)
Final Boiling Point, °F (°C)	763 (406)	750 (399)
Total Sulfur, wt %	0.453	2.94
Hydrogen	10.84	na
Carbon	88.29	na

na= not available

The characterization of both feedstocks was performed by using a Hewlett-Packard G1800A GCD system gas chromatograph equipped with a capillary column (HP PONA) and an Electron Ionization detector. The method of the analysis was the same as that reported in chapter IV for the analysis of liquid products. The integration parameters defined in the Chemstation software were basically the same. The identification of the most important peaks which are shown in the chromatogram was done with the Chemstation software. The area and area% data were taken for every peak to obtain the corresponding concentration. Peaks with an identification quality higher than 90% of confidence were considered as correct.

A classification in paraffins (P), naphthenes (N), aromatics (A) and sulfur-aromatics (S-A) was selected for every compound to be included. The GC-MS report was transferred to Excel and a program was constructed to develop the P/N/A/S-A classification. The LCO/HGO weight ratio in terms of total sulfur is 6.5/1.

Heavy gas oil (HGO) contains a significant amount of C₆-C₉ hydrocarbons while light cycle oil (LCO) is completely absent of them. The identification of DBT and BT's was moderately complicated in LCO. However in the HGO this was a hard task. Using those integration parameters (Table 4.2, Chapter IV) when reviewing data of liquid samples analysis, around 500 peaks are successfully integrated in the light cycle oil (LCO) analysis, and a few interesting peaks corresponding to sulfur compounds have been manually integrated only. The heavy gas oil (HGO) integration accounted for more

than 550 integrated peaks; however, in the zone in which dibenzothiophenes are present the manual integration was also applied. Figure 5.1 shows a typical total chromatogram of LCO feed and Figure 5.2 shows a typical total chromatogram of HGO.

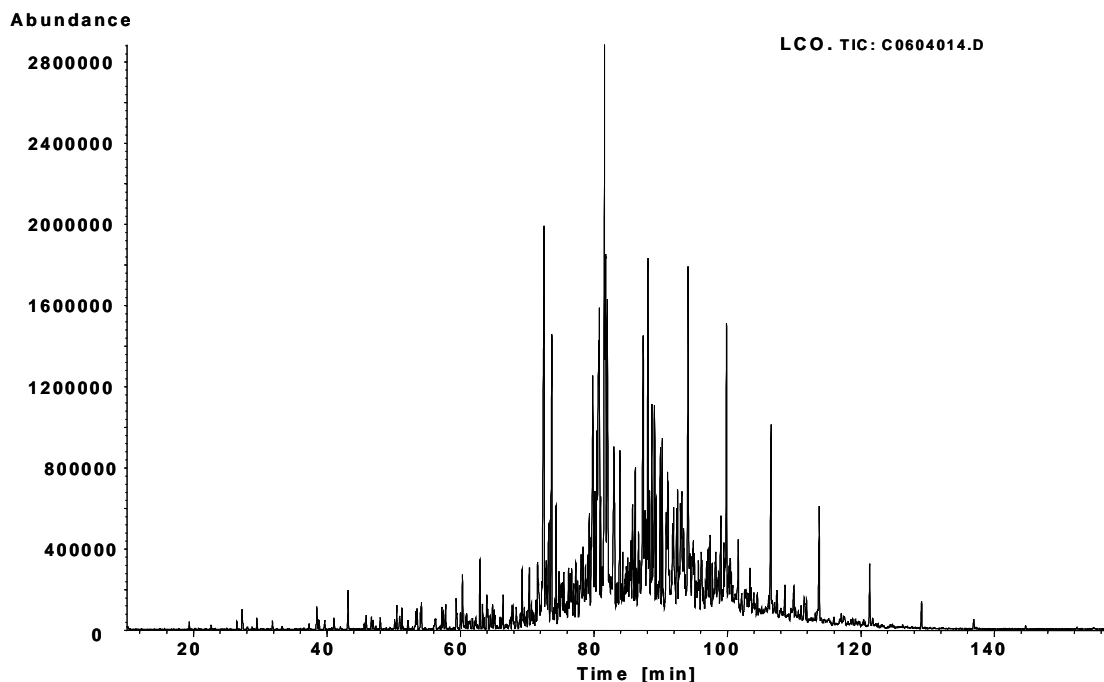


Figure 5.1 Typical total chromatogram of light cycle oil (LCO) using GC-MS.

The abundance for all peaks shown in the heavy gas oil (HGO) chromatograms are higher than those present in the light cycle oil (LCO) analysis. In the interval of retention time 20-60 minutes, the HGO has higher number of identified components and higher concentration of them. The baseline for the HGO showed more drifting than the corresponding baseline for LCO. This behavior can be caused due to the high number of components in the interval of retention time 80-120 minutes which have very close boiling point. Moreover, their concentration varies strongly.

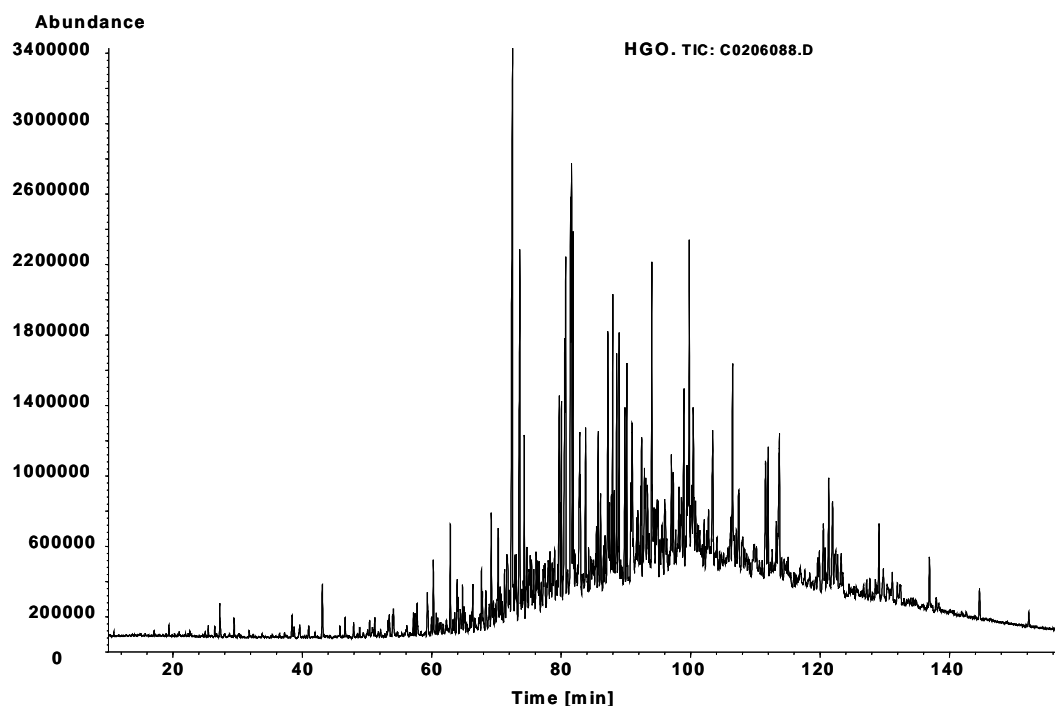


Figure 5.2 Typical total chromatogram of heavy gas oil (HGO) using GC-MS.

At retention times of 120 minutes and longer the HGO shows a higher number of components and higher abundances. Since the HGO has a wider boiling point interval than LCO, the contribution to this property is the major presence of components such as paraffins (C_8 - C_{11}), alkyl-naphthenes (C_8 - C_{10}) and alkyl aromatics (C_8 - C_{11}) with retention times of 20-60 minutes and longer than 120 minutes as well, as paraffins (C_{20} - C_{23}), Dimethylphenanthrenes (C_{16}), and di- and tri-methyl carbazoles (C_{14} - C_{15}).

The total chromatogram of HGO and LCO is divided into “windows” and are shown in Figures 5.3 to 5.10. Every “window” comprises an interval of retention time with some of the peaks identified used for groupings into paraffins, naphthenes, aromatics and sulfur-aromatics. The identification of all compounds was made by combining the data library report of the GC-MS and data of retention times reported by Depauw & Froment (1997) using a GC-AED. In this work, the qualities reported by the GC-MS

higher than 90 % were used to identify each compound and locate it in the corresponding group.

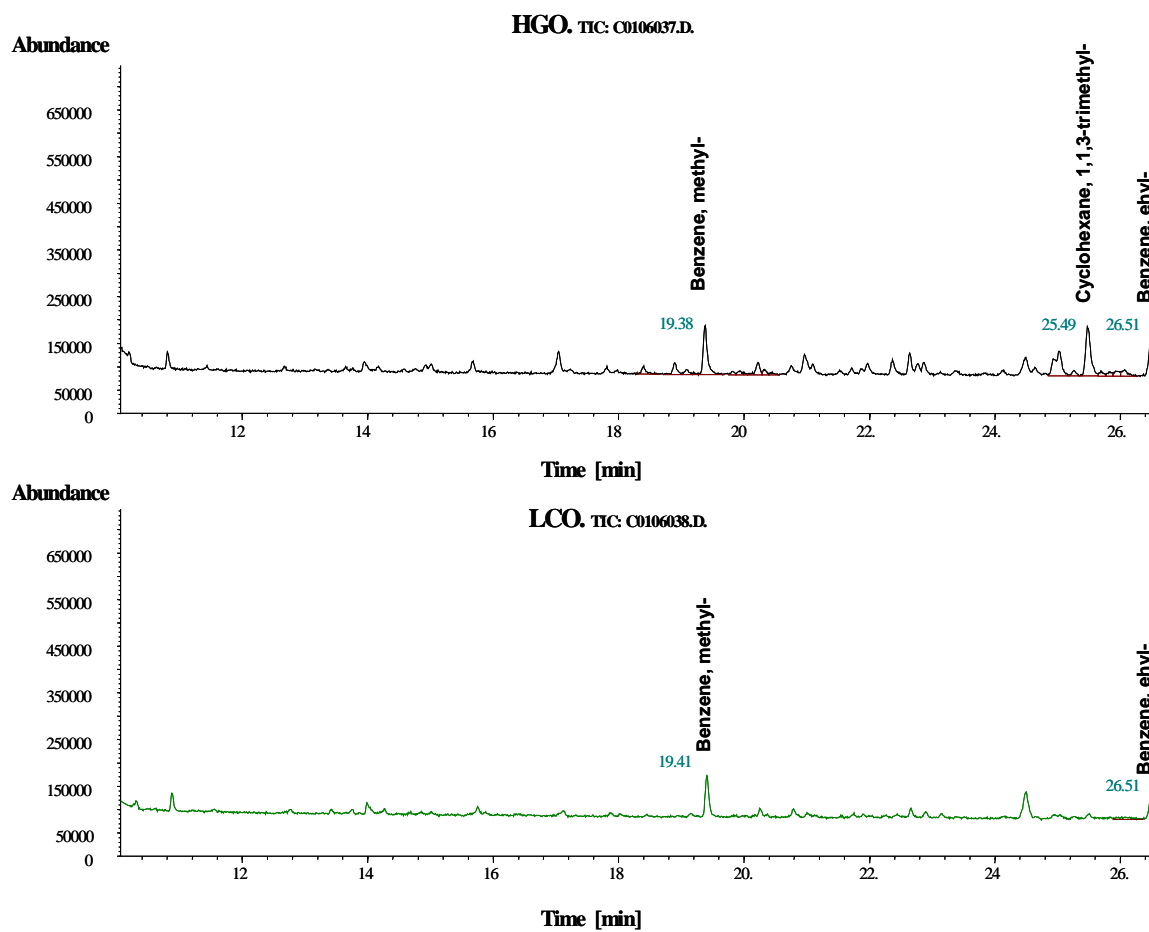


Figure 5.3 Part of the total ion chromatogram of the HGO and the LCO showing part of the peaks with retention times in the interval of 12-26 min.

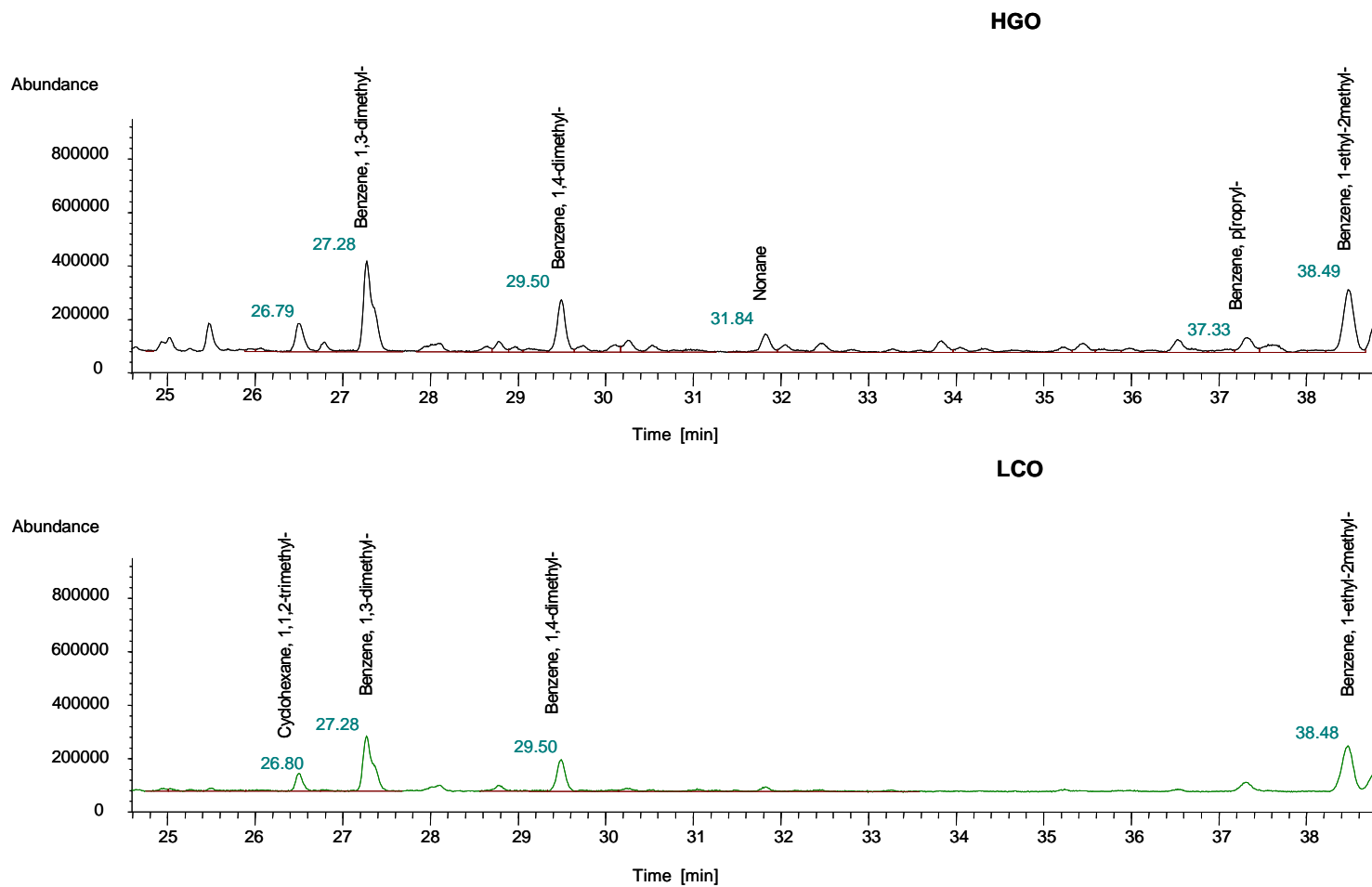


Figure 5.4 Part of the total ion chromatogram of the HGO and the LCO showing part of the peaks with retention times in the interval of 25-38 min.

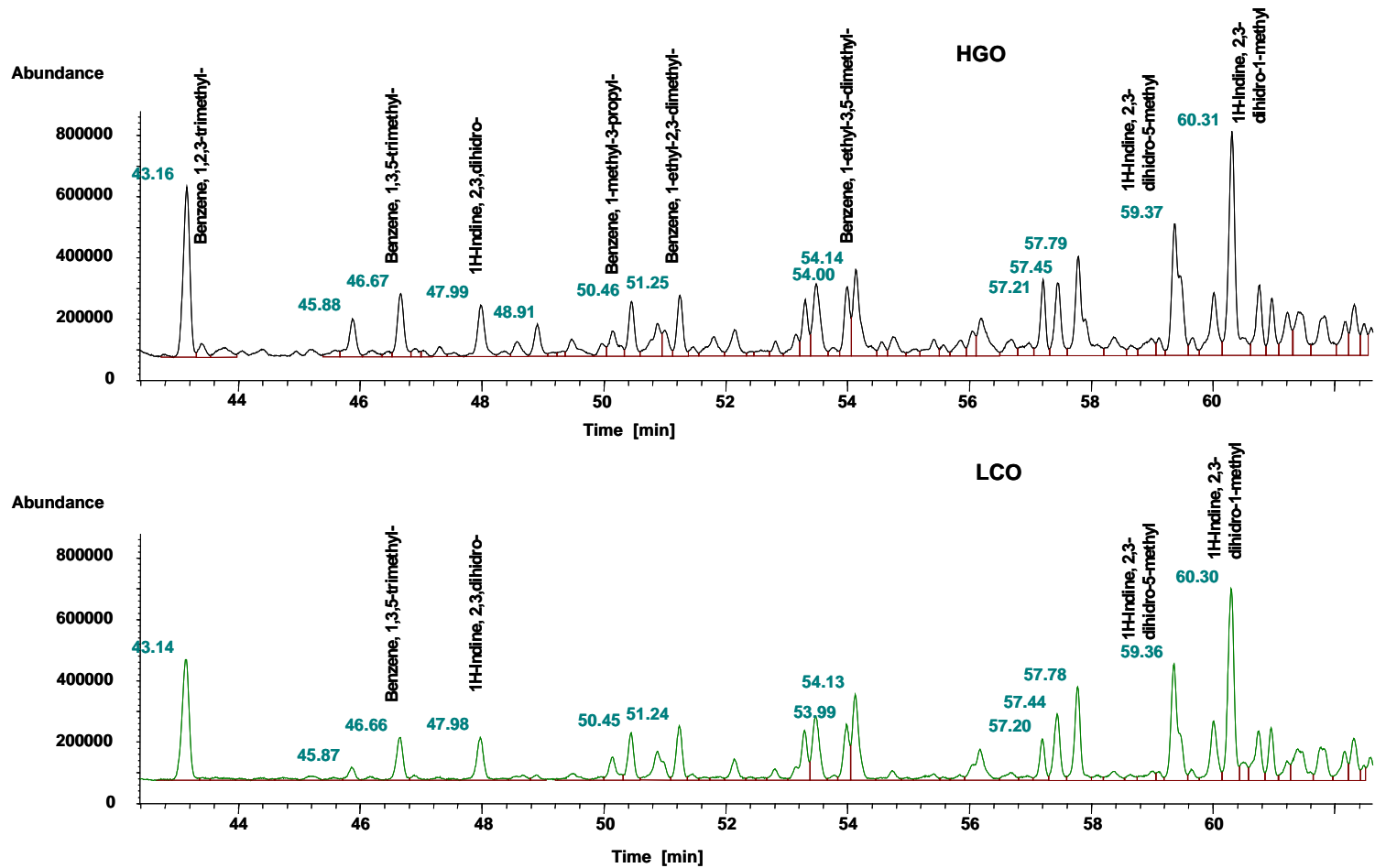


Figure 5.5 Part of the total ion chromatogram of the HGO and the LCO showing part of the peaks with retention times in the interval of 44-60 min.

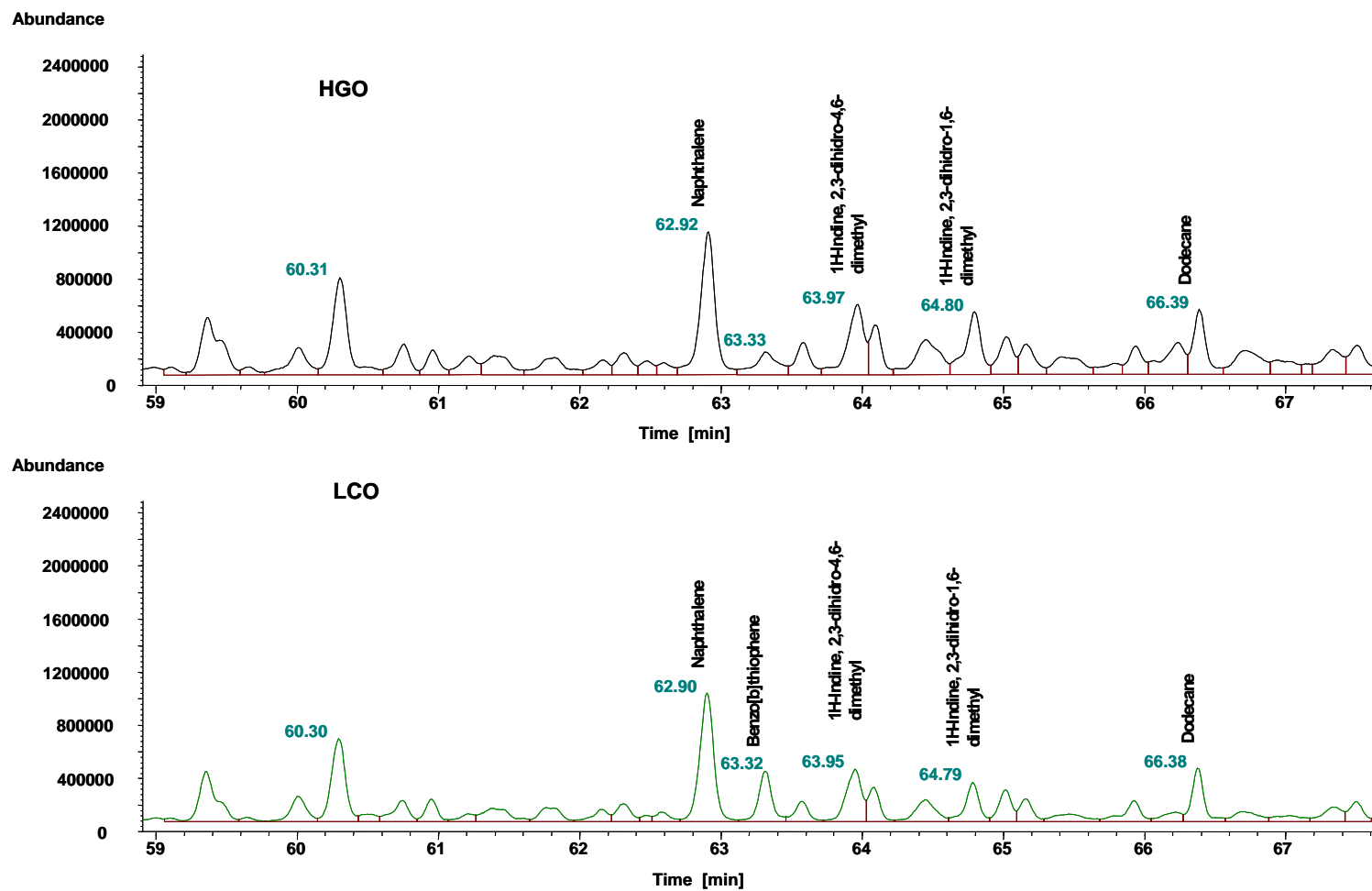


Figure 5.6 Part of the total ion chromatogram of the HGO and the LCO showing part of the peaks with retention times in the interval of 60-67 min.

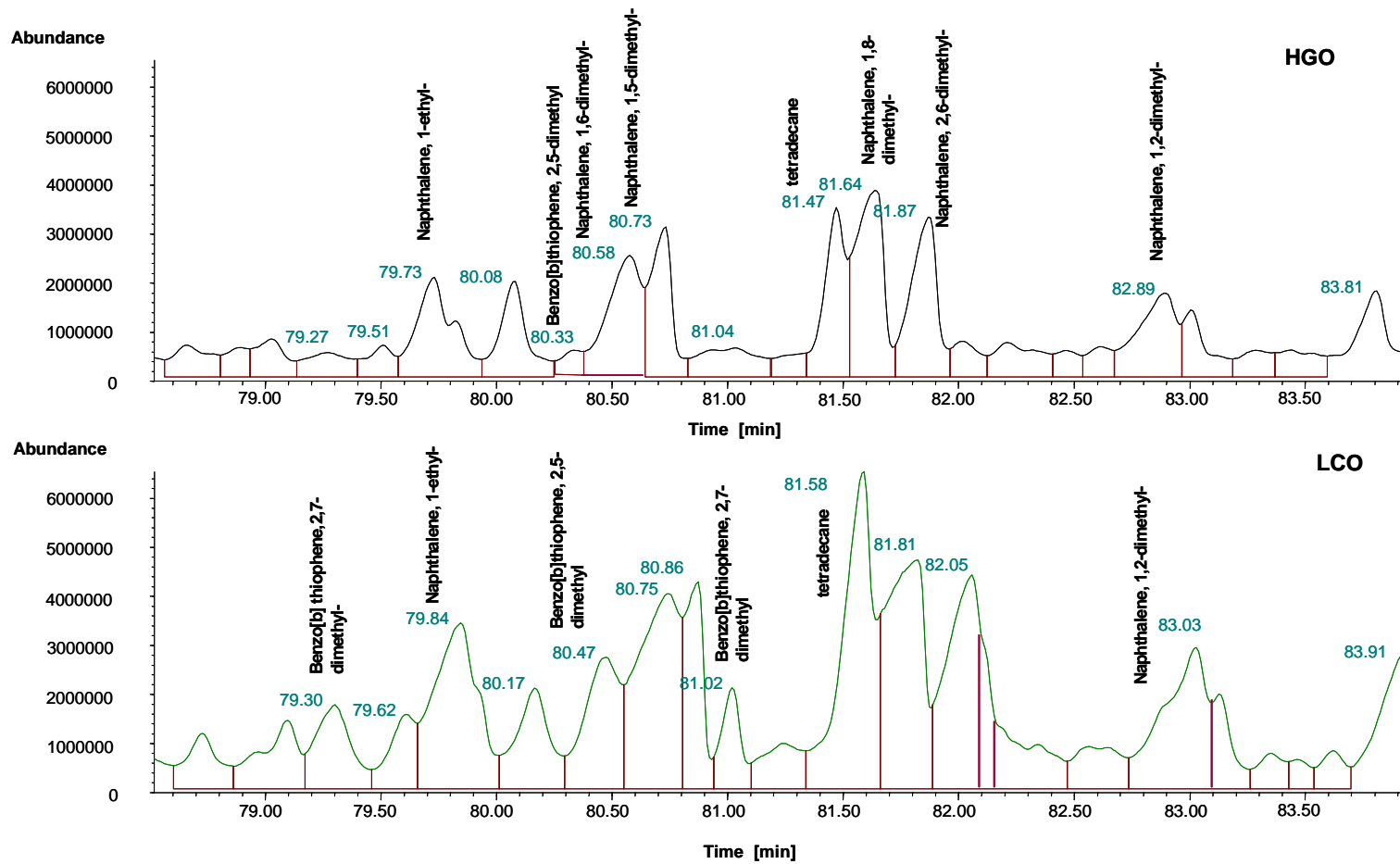


Figure 5.7 Part of the total ion chromatogram of the HGO and the LCO showing part of the peaks with retention times in the interval of 79-83.5 min.

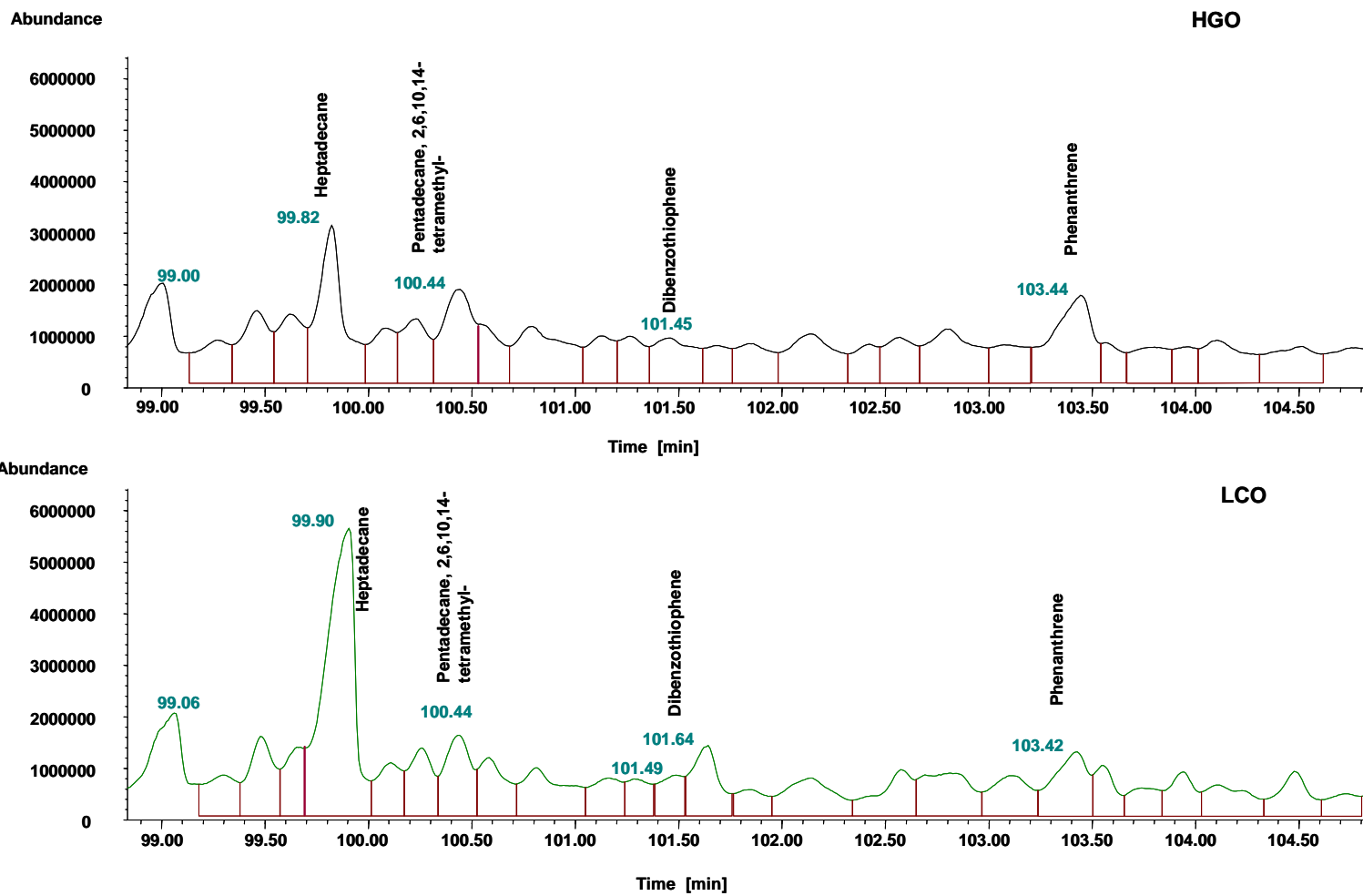


Figure 5.8 Part of the total ion chromatogram of the HGO and the LCO showing part of the peaks with retention times in the interval of 99-104.5 min.

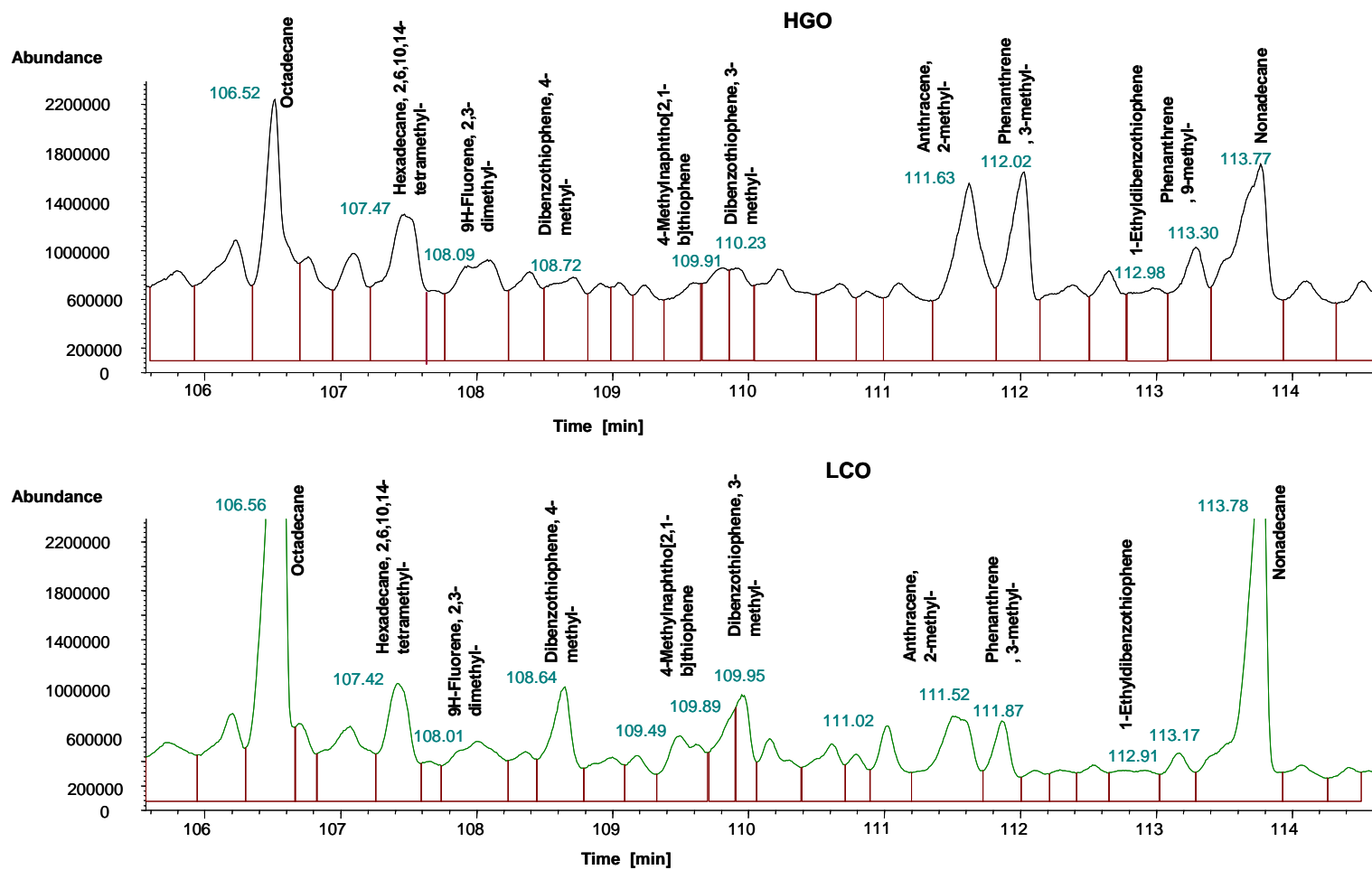


Figure 5.9 Part of the total ion chromatogram of the HGO and the LCO showing part of the peaks with retention times in the interval of 106-114 min.

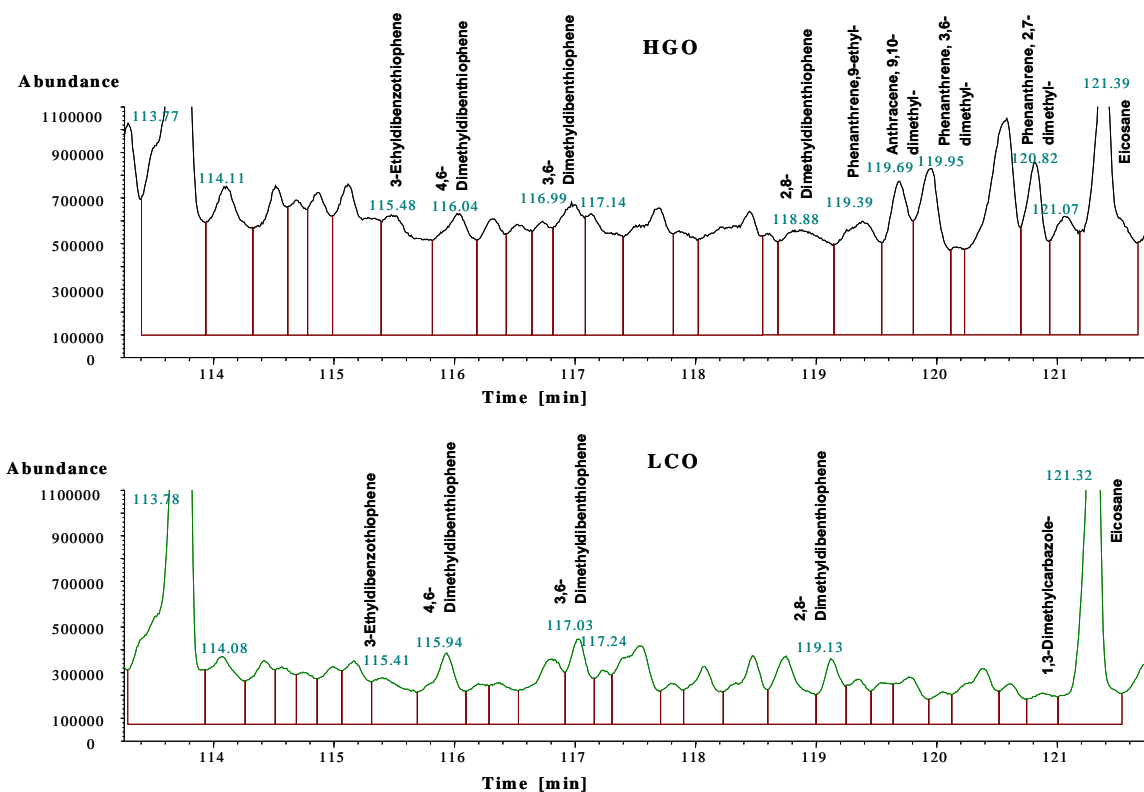


Figure 5.10 Part of the total ion chromatogram of the HGO and the LCO showing part of the peaks with retention times in the interval of 114-121 min.

The characterization of light cycle oil (LCO) and heavy gas oil (HGO) as feedstock to be used in the hydrodesulfurization projects leads to the results given in Table 5.2.

Table 5.2 Composition of a USA heavy gas oil and a Mexican light cycle oil as determined by GC-MS

Composition , wt%	Heavy Gas Oil	Light Cycle Oil
Paraffin	15.3	24.22
Aromatics	30.61 ¹	30.73
Sulfur Aromatic Compounds	1.44	3.57

(1) 28.76 wt% determined by UV and reported by Shell Oil Co.

The only reference that was known is that the total sulfur of LCO as determined by the neutron activation technique was 2.94 wt%, while the corresponding value for HGO provided by Shell was 0.453 wt%.

5.2 Characterization of HDS Reaction Products

The identification of the reaction products from the HDS of DBT and 4,6-DMDBT was carried out following every single compound on the GC-MS chromatogram. Fluorene was used as an internal standard to calculate the conversions of the sulfur containing compounds.

Fluorene, or 9H-Fluorene, is a tricyclic aromatic hydrocarbon. It has the form of odorless white crystals with a melting point 116 °C and boiling point 295 °C. Its chemical formula is C₁₃H₁₀. It is manufactured artificially, although it occurs in the higher boiling fractions of petroleum and coal tar. It is usually found in vehicle exhaust emissions, crude oil, motor oil, coal and oil combustion products. It is insoluble in water and soluble in benzene and ether.

Fluorene arises in fossil fuels. Its release to the environment is wide spread since it is an ever-present product of incomplete combustion. It is released to the atmosphere in emissions from the combustion of oil, gasoline and coal. If released to the atmosphere, fluorene will exist primarily in the vapor phase where it will degrade readily by photochemically produced hydroxyl radicals.

There are scarce reports in the literature regarding the hydrogenation and hydrocracking reactions for Fluorene. Lapinas et al., (1991) investigated the reactions of fluorene in the presence of hydrogen and NiW/Al₂O₃ and NiMo/ zeolite Y catalysts at 335-380 °C and 153 atm in a 300-cm³ stirred batch reactor. NiW catalyst was active for isomerization and hydrogenation, whereas NiMo/zeolite was active for isomerization and hydrogenation and also for hydrocracking. The fluorene hydrogenation network is shown in Figure 5.11. The operating conditions for these reactions to occur are more severe than those for the HDS of HGO. Therefore, it is not expected that these reactions will occur in HDS of HGO.

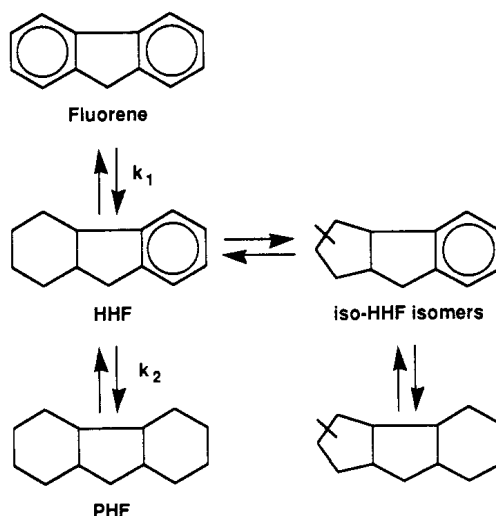


Figure 5.11 Fluorene hydrogenation network (From Lapinas et al., (1991)). HHF: hexahydrofluorene, PHF: Perhydrofluorene.

Benzene,cyclohexyl- (CHB) and 1,1'-Bicyclohexil (BCH) were co-injected in separate samples of liquid products to confirm their identification and calculate the conversions of DBT into 1,1'-Biphenyl, Benzene.cyclohexyl- and 1,1'-Bicyclohexil and the conversions of 4,6-DMDBT into 1,1'-Biphenyl,3,4'-dimethyl-. The later compound is a product from HDS of 4,6-DMDBT through the isomerization route reported by Isoda et al., (1996).

The samples of reaction products were more difficult to identify and quantify. Thus, some peaks were manually integrated when Chemstation ignored these compounds or when they were integrated together with others.

Figures 5.12 and 5.13 show two “windows” of the total ion chromatogram of a typical HDS product compared with HGO. Every window comprises an interval of retention time with the identified reaction products of DBT and 4,6-DMDBT.

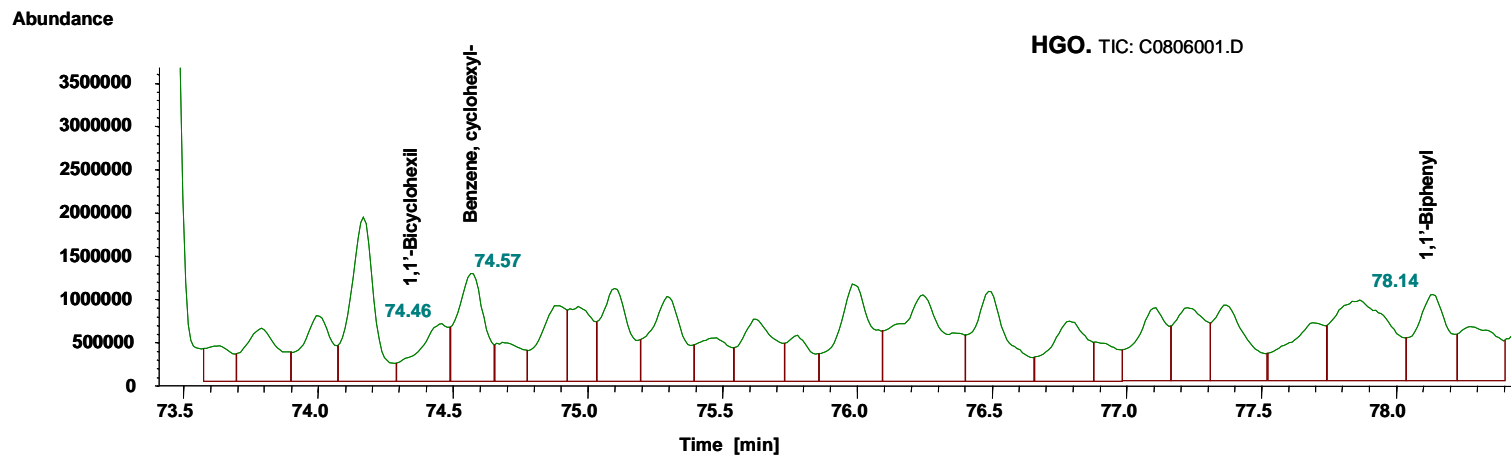
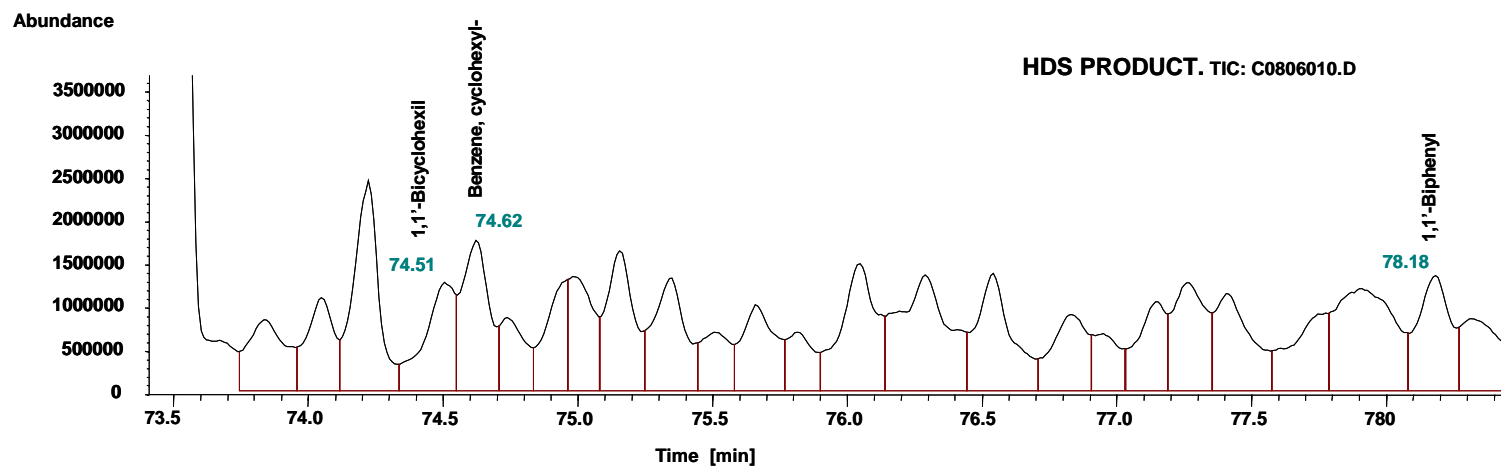


Figure 5.12 Part of the total ion chromatogram of a typical HDS product and the HGO showing the peaks of the reaction products of HDS of DBT. Experimental conditions: 310 °C, 65 bar, 7.2 H₂/HC mol ratio and W/F_{DBT}^o of 4000 kg_{cat}/h/kmol.

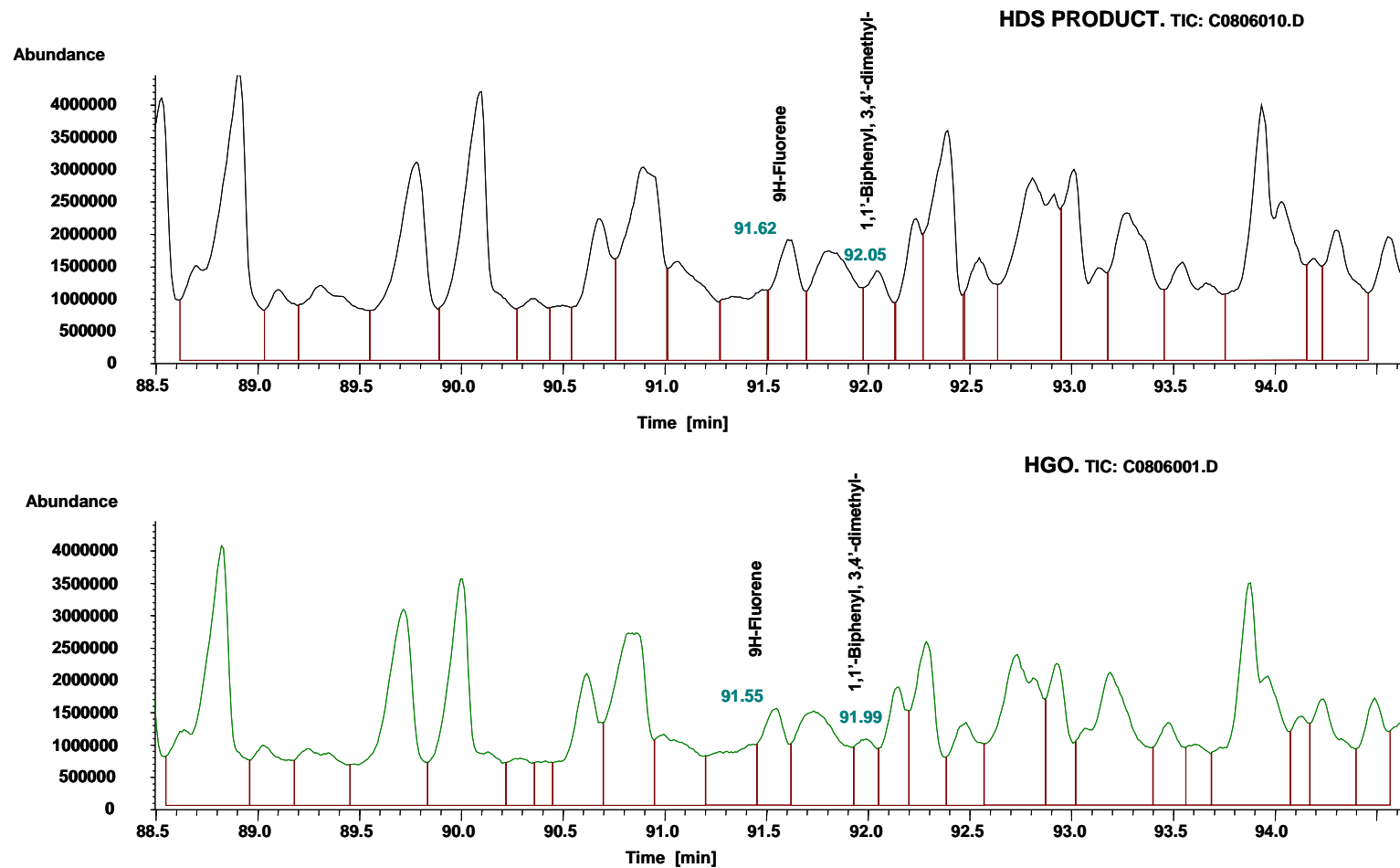


Figure 5.13 Part of the total ion chromatogram of a typical HDS product and the HGO showing the peaks of fluorene and reaction products of HDS of 4,6-DMDBT. Experimental conditions: 310 °C, 65 bar, 7.2 H₂/HC mol ratio and W/F⁰_{DRT} of 4000 kg_{cat}/h/kmol.

CHAPTER VI

TEST OF THE CATALYSTS

This part presents the results on the Hydrodesulfurization of Heavy Gas oil (HGO) over a commercial CoMo/Al₂O₃ and over CoMoNiPtPd supported on ultrastable Faujasite (HY) catalysts. The effect of the reaction conditions: temperature (290-350 °C), space time (W/F_{DBT}^o: 3000-8000 kg_{cat}/h/kmol), hydrogen/hydrocarbon ratio (2.8-11.2 mol/mol) and pressure (65-75 bar) were studied. The activity of the catalysts in terms of conversions of dibenzothiophene (DBT), methyl dibenzothiophene's (MDBT's), phenanthrene and molar-averaged conversion under the effect of variables is discussed.

For discussion purposes the activity test has been divided into six categories. The activity test of the conventional CoMo/Al₂O₃ (HDS-0) catalyst constitutes the first category. For this catalyst the effect of the space time at molar H₂/HC ratio of 2.8 and the effect of space time at molar H₂/HC ratio of 7.2 is discussed. Moreover, the conversions of DBT, phenanthrene and molar-averaged conversion under the effect of space time and molar hydrogen/hydrocarbon ratio at 330 °C are also discussed.

The remaining categories include the activity test of the experimental zeolite catalysts (HDS-1, HDS-8, HDS-10, HDS-3 and HDS-5).

For CoMoPtPd/HY (HDS-1) catalyst, the effect of space time and temperature and the effect of the molar hydrogen/hydrocarbon ratio at 65 bar and 75 bar is discussed. For reasons of safety 75 bar was the upper limit for the operating pressure.

For CoMo/PdNiPt-HY (HDS-8) and CoMoNi/PdPt-HY (HDS-10) catalysts, the effect of the space time at 330 °C and 310 °C under molar H₂/HC ratio of 7.2, the effect of the space time at 310 °C and a molar H₂/HC ratio of 11.2 and the effect of the molar hydrogen/hydrocarbon ratio at 310 °C at 65-75 bar are discussed.

Finally for CoMoPtPd/Ni-HY (HDS-3) and CoMoPd/Pt-HY (HDS-5) catalysts, the effect of the space time at 310 °C under molar H₂/HC ratio of 7.2 and the study of the effect of the molar hydrogen/hydrocarbon ratio at 310 °C at 65 bar is discussed.

The activity tests were conducted by using a Robinson Mahoney stationary basket reactor for hydrodesulfurization and hydrogenation of a heavy gas oil provided by the Shell Company. A set of 9 sulfur compounds was selected to express the conversion as a molar-averaged conversion.

6.1 Sulfiding

The sulfiding reactions of metals are exothermic. However, run away of temperatures was not observed neither with the zeolite catalysts nor CoMo/Al₂O₃ (HDS-0) catalyst. Figures 6.1 and 6.2 show typical temperature profiles obtained during the activation of the CoMoPtPd/HY (HDS-1) and conventional CoMo/Al₂O₃ catalysts, respectively. Despite the fact that sulfiding time for the catalysts was 3.5 h at 330°C, the zeolite catalyst required a higher total activation time than the HDS-0 catalyst due to drying and stabilization stages.

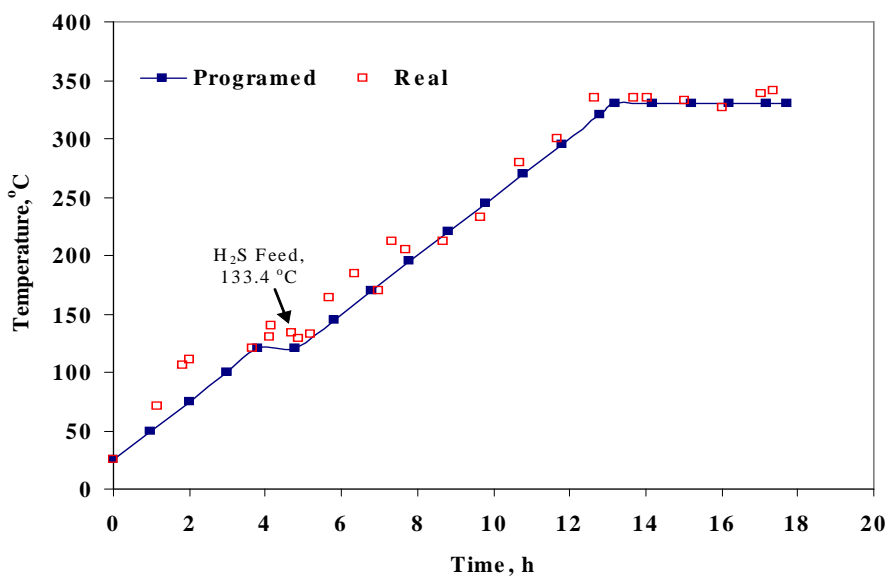


Figure 6.1 Evolution of temperature with time obtained during the activation of the CoMoPtPd/HY (HDS-1) catalyst.

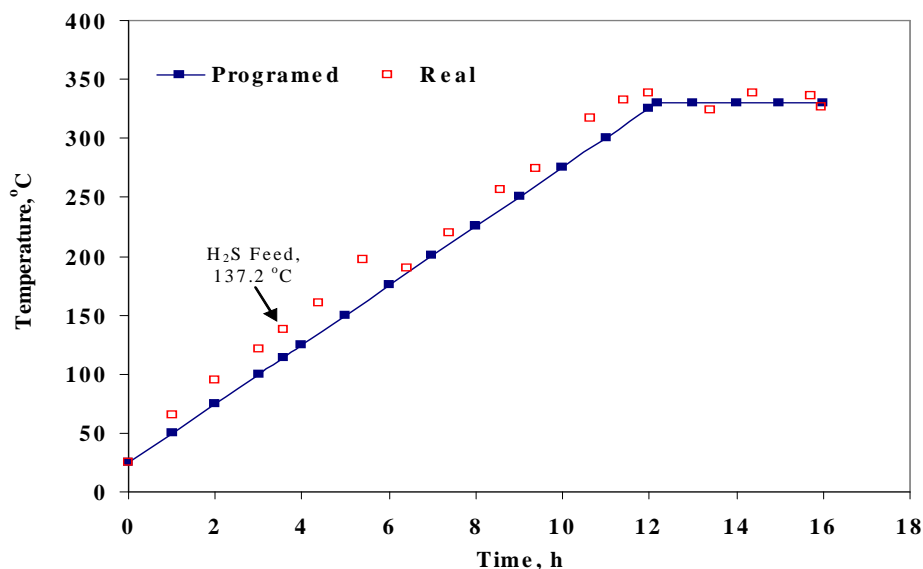


Figure 6.2 Evolution of temperature with time obtained during the activation of the CoMo/Al₂O₃ (HDS-0) catalyst.

The variation of H₂S concentration in the produced gas during the activation of the catalysts is shown in Figures 6.3 and 6.4. Monitoring of the H₂S concentration in the gas leaving the separator was followed from 169 to 330 °C for the CoMo/Al₂O₃ (HDS-0) and from 191 to 330 °C for CoMoPtPd/HY (HDS-1). In Figure 6.3 it is observed that in the interval from 169 to 330 °C the hydrogen sulfide concentration in the gas decreased from 15 wt% to around 8 wt%, while Figure 6.4 shows that in the interval from 191-330 °C the hydrogen sulfide concentration in the gas decreased from 15 wt% to around 4 wt%. The 15 wt% plotted at zero time corresponds to the concentration of the sulfiding agent (H₂S) in the H₂S/H₂ mixture fed.

A minimum was observed in the concentration of H₂S at 10h and 11.5 h during the activation at 330°C of the CoMo/Al₂O₃ (HDS-0) (Figure 6.3) and CoMoPtPd/HY (HDS-1) (Figure 6.4) catalysts, respectively. These points suggest that each catalyst reached the maximum consumption of H₂S required for activation. After those points, the observed

H₂S concentration was increasing towards the original level of the sulfiding mixture, meaning that the catalysts were activated after 3.5 h.

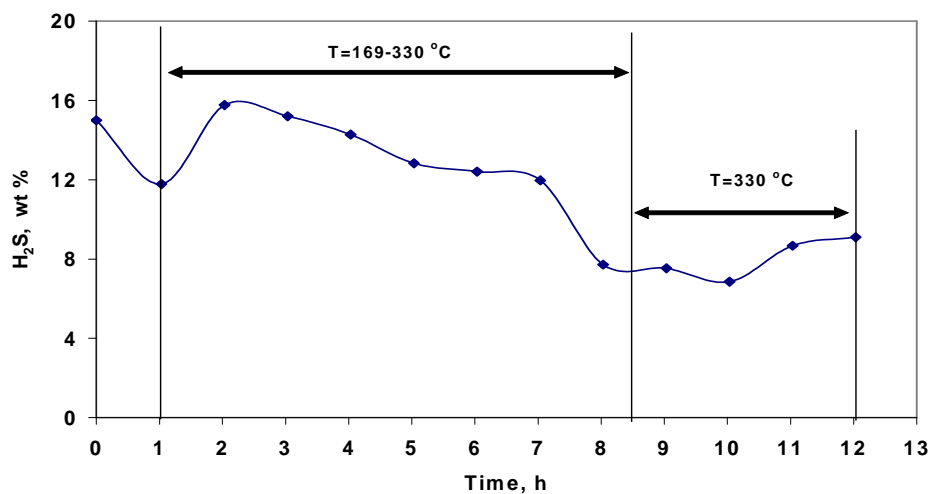


Figure 6.3 Concentration of H₂S in the gas phase during the activation of the CoMo/Al₂O₃ (HDS-0) catalyst. P= 1 atm, T=330°C.

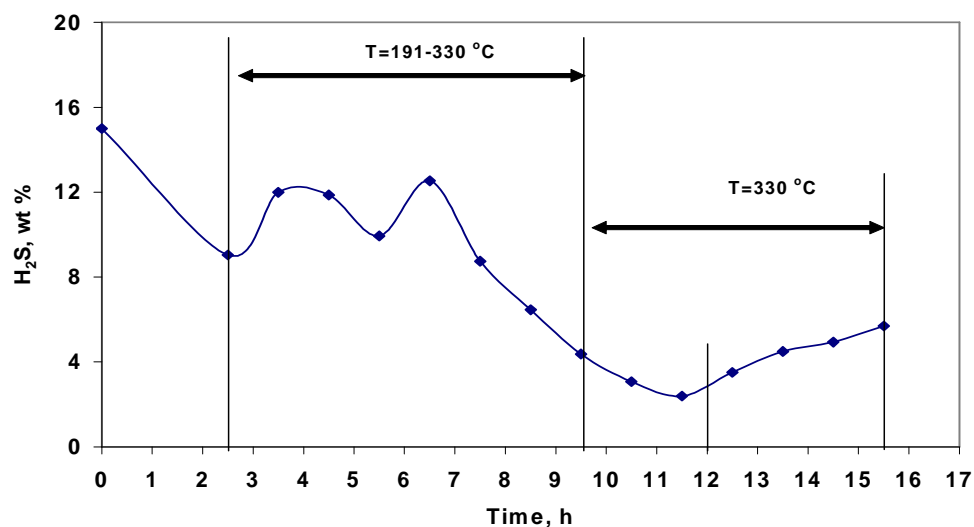


Figure 6.4 Concentration of H₂S in the gas phase during the activation of the CoMoPtPd/HY (HDS-1) catalyst. P= 1 atm, T=330°C.

6.2 Activity Test of the CoMo/Al₂O₃ and the Zeolite Catalysts in the HDS of Heavy Gas Oil

6.2.1 CoMo/Al₂O₃ Catalyst (HDS-0)

Table 6.1 shows a set of nineteen experiments and their operating conditions carried out to evaluate the catalytic activity of HDS-0 and to define the operating conditions for the CoMoPtPd/HY (HDS-1) catalyst presented in section 4.2.5 (Table 4.7).

Table 6.1 Operating conditions used to evaluate the catalytic activity for the CoMo/Al₂O₃ (HDS-0) catalyst.

Experiment	T °C	Pt bar	W/F _{DBT} ^o kg _{cat} h/kmol	H ₂ /HGO mol ratio	HGO ml/h	H ₂ @ 294 K, 1atm L/h
E1T1			3000		117.4	40.0
E2T1	330	65	4000	2.8	88.1	30.0
E3T1			5000		70.5	24.0
E3T2	350	65	5000	2.8	70.5	24.0
E2T2			4000		88.1	30.0
E5T2	350	65	4000	3.6	88.1	38.8
E6T2			5000		70.5	31.1
E6T1			5000		70.5	31.1
E5T1	330	65	4000	3.6	88.1	38.8
E4T1			3000		117.4	51.8
E10T1			4000		88.1	77.9
E11T1	330	65	5000	7.2	70.5	62.3
E12T1			6000		58.7	51.9
E12T4			6000		58.7	51.9
E11T4	310	65	5000	7.2	70.5	62.3
E10T4			4000		88.1	77.9
E10T5			4000		88.1	77.9
E11T5	290	75	5000	7.2	70.5	62.3
E12T5			6000		58.7	51.9

The molar H_2/CH_4 ratio was 14.5 for all experiments. Methane was used as an internal standard for all on-line gas analyses in the GC-TCD.

6.2.1.1 Effect of Space Time at Molar H_2/HC Ratio of 2.8

The conversions of dibenzothiophene (DBT), methyl dibenzothiophene's (MDBT) and phenanthrene as a function of space-time (W/F_{DBT}^o) and temperature are shown in Figure 6.5.

As expected, the conversion of DBT is higher than the conversion of 4-MDBT and 4,6-DMDBT. These conversions increase with space time, obtaining conversions of 27.7-35.8% of DBT, 25.9-32.5% of 4-MDBT and 22.0-30.1% of 4,6-DMDBT in the interval of space time of 3000-5000 $kg_{cat}h/kmol$, respectively. Phenanthrene shows no apparent change with conversion for increasing W/F_{DBT}^o , providing conversions of 6.7-5.7% in the same interval of space time. This effect maybe related with the difficult integration of the peak observed in the GC-MS analysis.

The corresponding molar-averaged conversion, which was defined by equation 4.8 presented in the GC-MS Data Processing section is shown in Figure 6.6. The conversion measured at 330 °C shows a moderate increase with rising W/F_{DBT}^o (29.1 to 41.6% from 3000 to 5000 $kg_{cat}h/kmol$); while the conversion at 350 °C was really high (89.8 to 93.2% from 4000 to 5000). The operation at 350 °C led to the production of carbon and a fast deactivation of the catalyst.

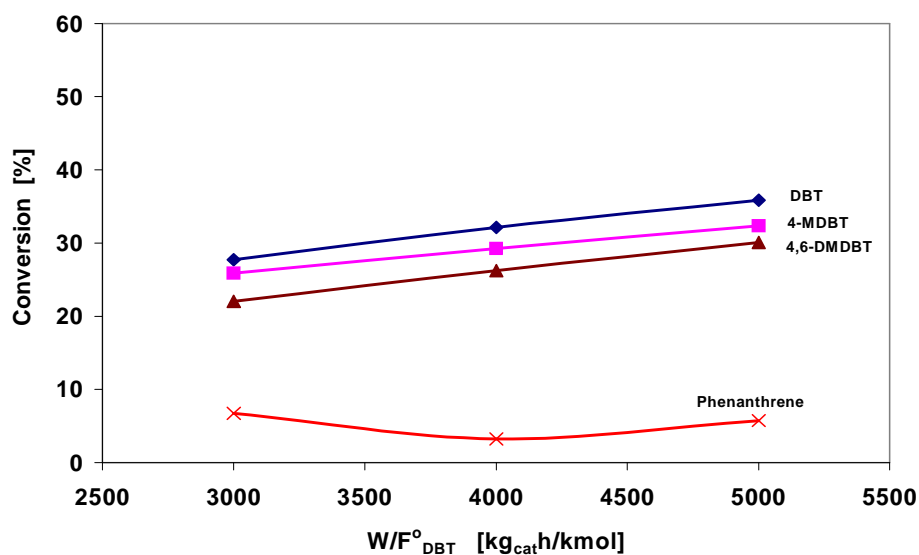


Figure 6.5 Conversions of DBT, MDBT's and phenanthrene as a function of space time (W/F_{DBT}°) for the commercial $CoMo/Al_2O_3$ (HDS-0) catalyst. Reaction conditions were 65 bar, 330 °C and 2.8 molar H_2/HGO ratio. Feed: Heavy Gas Oil.

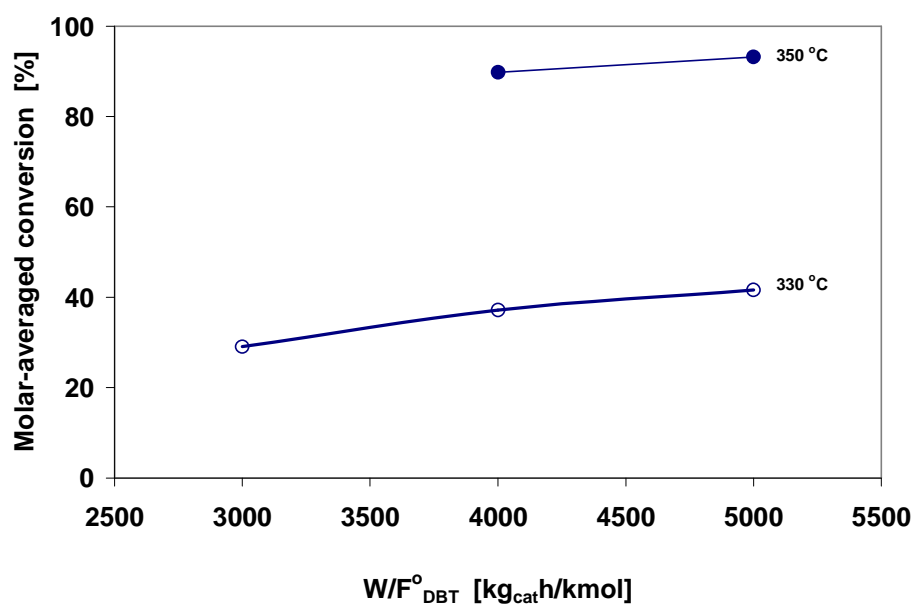


Figure 6.6 Molar-averaged conversions as a function of space time (W/F_{DBT}°) and temperature for the commercial $CoMo/Al_2O_3$ (HDS-0) catalyst. Reaction conditions were 65 bar, and 2.8 molar H_2/HGO ratio. Feed: Heavy Gas Oil.

6.2.1.2 Effect of Space Time at Molar H₂/HC Ratio of 7.2

Conversion of DBT, MDBT and phenanthrene as a function of space time (W/F_{DBT}^0) for the commercial CoMo/Al₂O₃ catalyst is shown in Figure 6.7. Comparing with the performance showed in Figure 6.5 at space times in the range of 4000-6000 kg_{cat}h/kmol, the conversions of DBT (48.9-63.7%), 4-MDBT (44.6-57.9%) and 4,6-DMDBT (38.7-50.7%) are higher at H₂/HC molar ratio of 7.2 than the corresponding conversions obtained at 2.8 molar ratio as expected. Since an increasing H₂/HC ratio implies higher H₂ partial pressure, the conversion of polyaromatics will be enhanced by an increase in H₂/HC ratio.

On the other hand, phenanthrene shows an opposite effect than expected when increasing W/F_{DBT}^0 . The difficulty with integrating the phenanthrene peak obtained in the analysis and its coelution together with other reaction products obtained at the mentioned operating conditions made its resolution impossible. However, in order to get this resolution, it is recommendable to split the peak for confirming the ion fragment (m/z) 178, which is typical for the phenanthrene molecule. The results of the conversion calculations for phenanthrene using the ion fragment could elucidate the increasing behavior as space time.

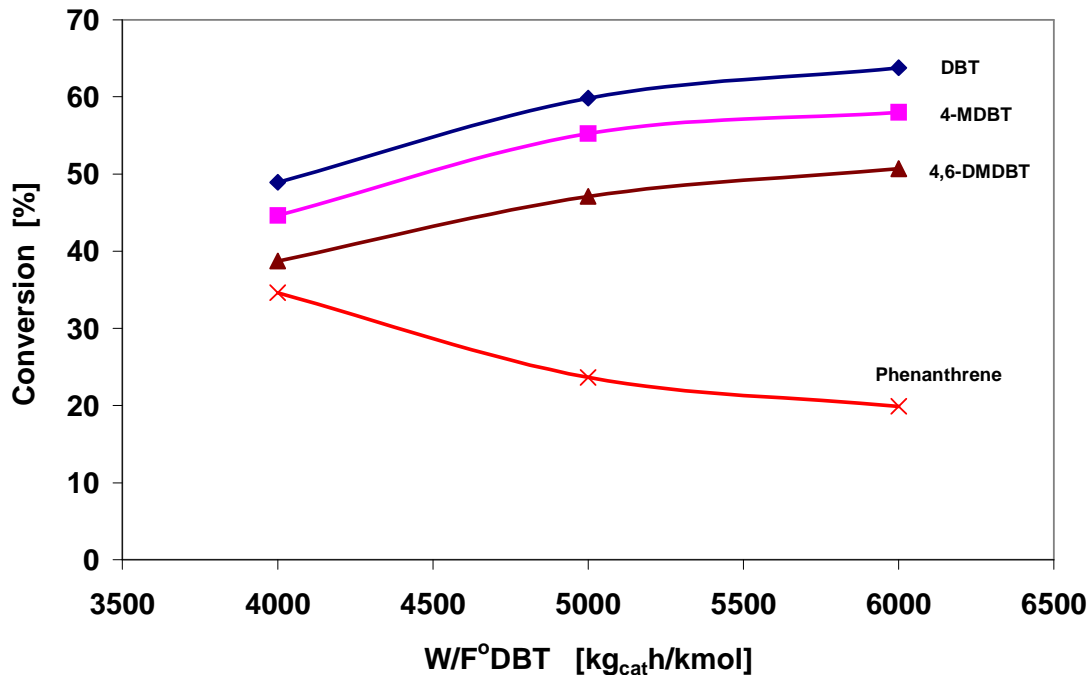


Figure 6.7 Conversions of DBT, MDBT's and phenanthrene as a function of space time (W/F_{DBT}°) for the commercial $CoMo/Al_2O_3$ (HDS-0) catalyst. Reaction conditions were 65 bar, 330 °C and 7.2 molar H_2/HGO ratio. Feed: Heavy Gas Oil.

Figure 6.8 shows the conversions for DBT and MDBT's at 310 °C. By comparing the behavior shown in Figure 6.7 with the behavior presented in Figure 6.8, the effect of the reaction temperature is observed. At 310 °C the conversion for DBT and MDBT's are in the interval of 12-25 % whereas at 330 °C those conversions were between 38-64%. The behavior of phenanthrene at 310 °C was as expected, increasing W/F_{DBT}° its conversion increased as well from 7.6 to 18.3% in the interval of space time of 4000-6000 $kg_{cat} h/kmol$. The results suggest selecting this temperature to evaluate the zeolite catalysts.

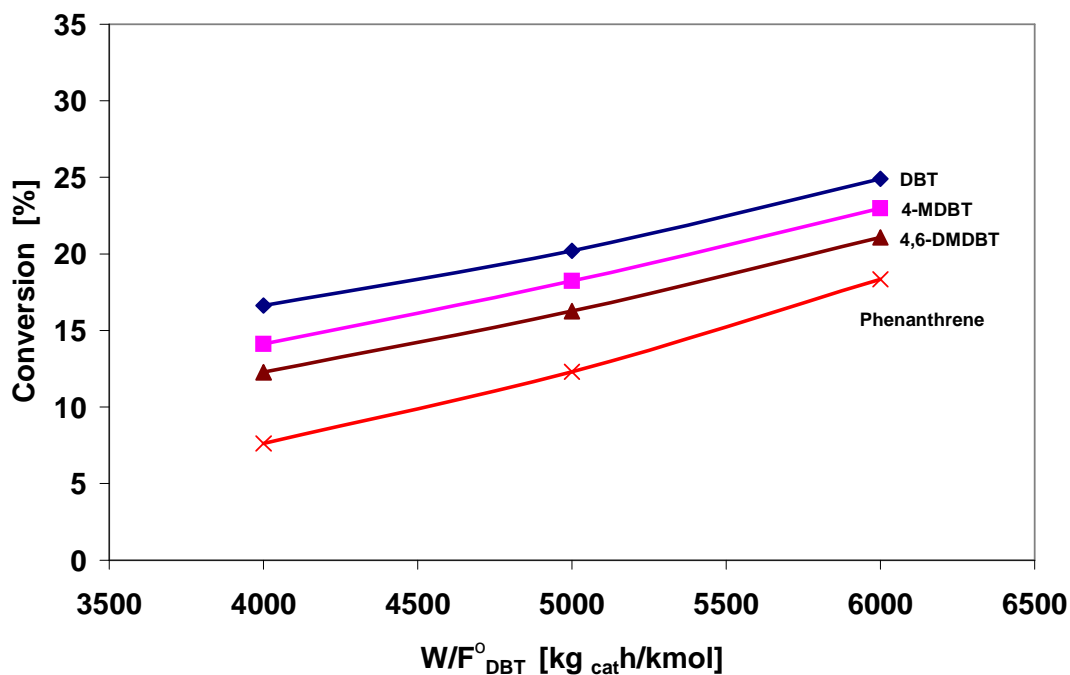


Figure 6.8 Conversions of DBT, MDBT's and phenanthrene as a function of space time (W/F_{DBT}^0) for the commercial CoMo/Al₂O₃ (HDS-0) catalyst. Reaction conditions were 65 bar, 310 °C and 7.2 molar H₂/HGO ratio. Feed: Heavy Gas Oil.

Conversion of DBT, MDBT's and phenanthrene as a function of the space time (W/F_{DBT}) at 290 °C is shown in Figure 6.9. This Figure shows similar performance as Figure 6.8 for 310 °C. The effect of decreasing the temperature to 290 °C shows conversions in the interval of 13-20 % for DBT and 8-19 % for MDBT's. The behavior of phenanthrene at 290 °C is similar to that behavior at 310 °C for increasing W/F_{DBT} .

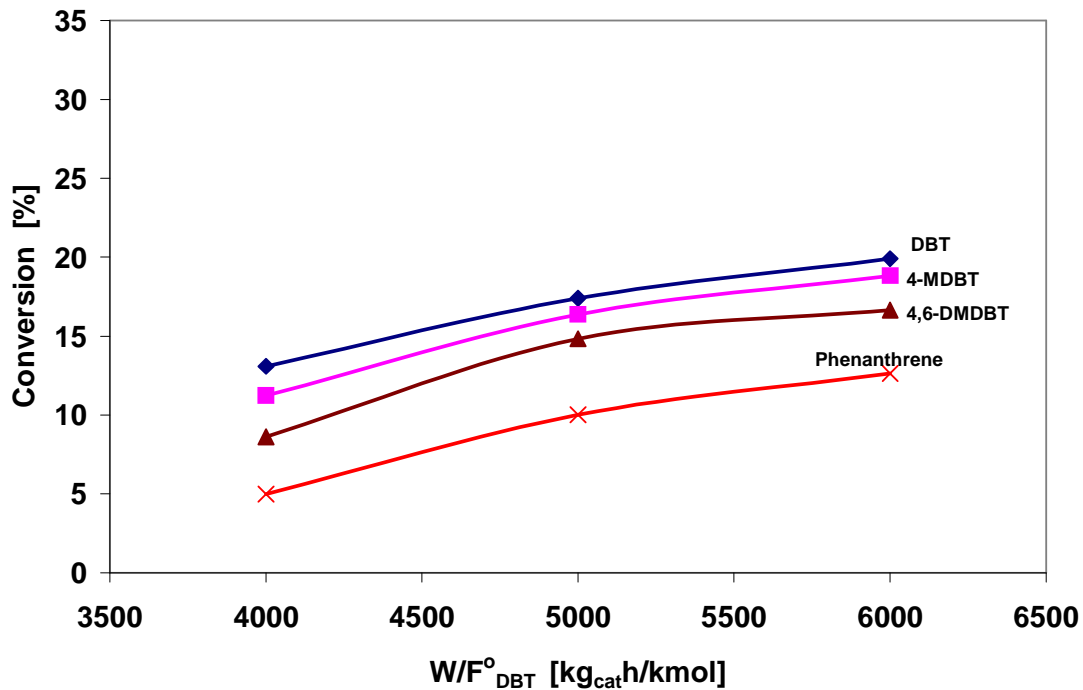


Figure 6.9 Conversions of DBT, MDBT's and phenanthrene as a function of space time (W/F_{DBT}°) for the commercial $CoMo/Al_2O_3$ (HDS-0) catalyst. Reaction conditions were 65 bar, 290 °C and 7.2 molar H_2/HGO ratio. Feed: Heavy Gas Oil.

The variation of the molar averaged-conversion is shown in Figure 6.10. The interval of conversion at 290 °C and 310 °C is narrow, 20-28%, while at 330 °C the conversions are remarkable higher with an interval between 64-79%. Since the test performed at 350 °C and 2.8 H_2/HC molar ratio presented too high conversions (>95%) and because the deactivation was notorious, the corresponding experiment at 7.2 H_2/HC molar ratio and 350 °C was not carried out.

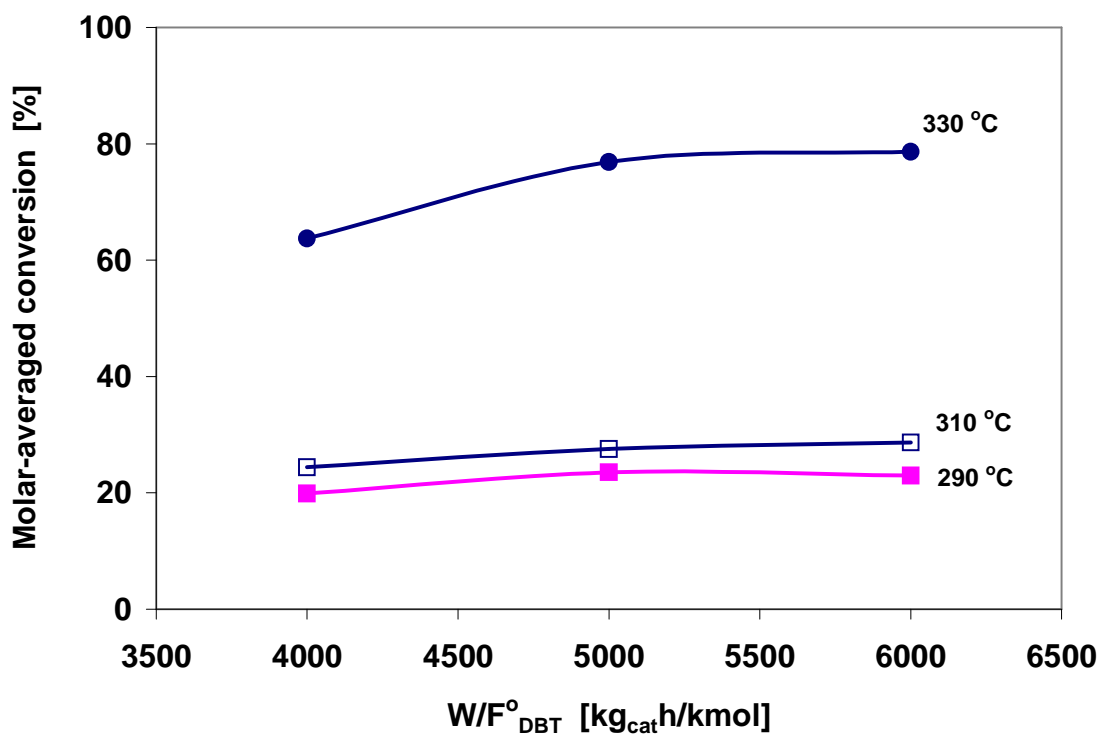


Figure 6.10 Molar-averaged conversions as a function of space time (W/F_{DBT}°) and temperature for the commercial $CoMo/Al_2O_3$ (HDS-0) catalyst. Reaction conditions were 65 bar, and 7.2 molar H_2/HGO ratio. Feed: Heavy Gas Oil.

6.2.1.3 Effect of Space Time and Molar Hydrogen/Hydrocarbon Ratio at 330 °C

Figure 6.11 shows the effect of the H_2/HGO mol ratio only for DBT as a function of space time. The conversion of DBT at 2.8 and 3.6 H_2/HC molar ratio was substantially the same. In contrast at the value of 7.2 the effect of H_2/HC ratio is important. During the operation of the setup this effect can be related to the quality of the liquid product, since a light yellow color is indicative of the confidence of the reaction. Moreover a darker color in the product or solid particles observed in the product collector suggests a probable deactivation of the catalyst.

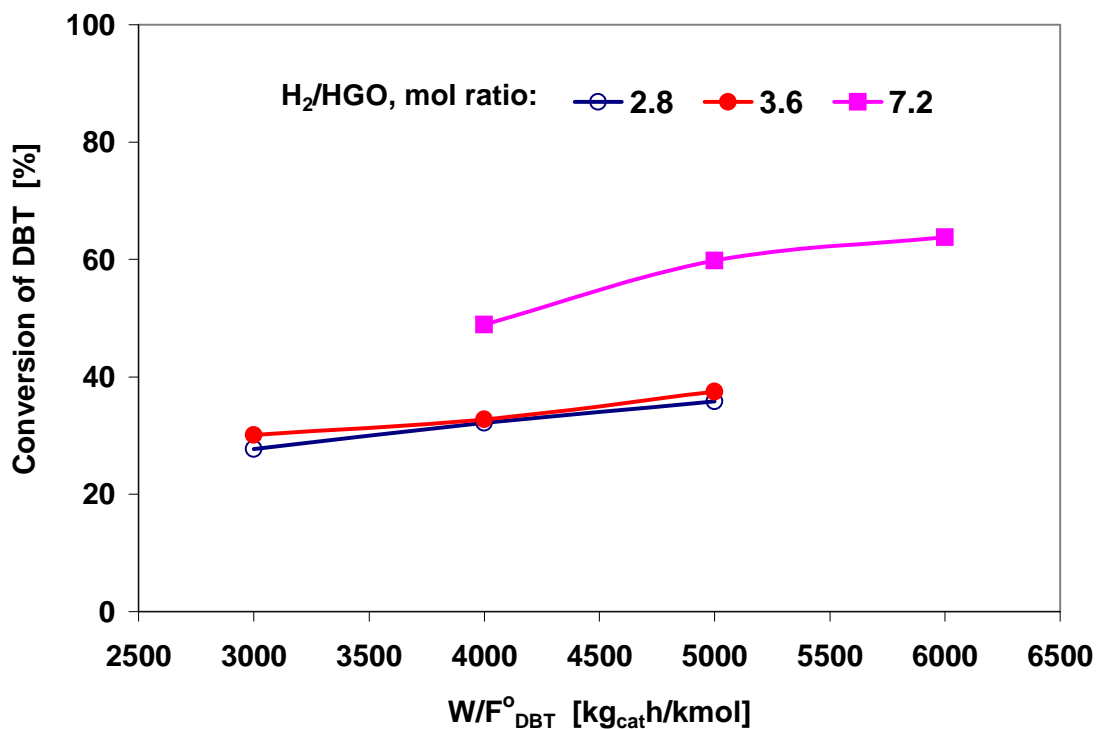


Figure 6.11 Conversions of DBT as a function of space time (W/F_{DBT}°) and H_2/HGO mol ratio for the commercial $CoMo/Al_2O_3$ (HDS-0) catalyst. Reaction conditions were 65 bar, 330 °C. Feed: Heavy Gas Oil.

The hydrogenation of heavy gas oil in terms of phenanthrene conversion is shown in Figure 6.12. At H_2/HC mol ratio of 2.8 and 3.6 the phenanthrene conversion was low and almost constant for increasing W/F_{DBT}° . This effect can be related to the reactivity of lighter aromatics to be hydrogenated. In this situation a deficit of H_2 in the reactor is an impediment of heavier aromatics to be saturated. Although the H_2/HC molar ratio of 7.2 is better for hydrogenation of phenanthrene, the negative effect of coelution or superposed peaks was present at this condition as was before explained for Figure 6.7.

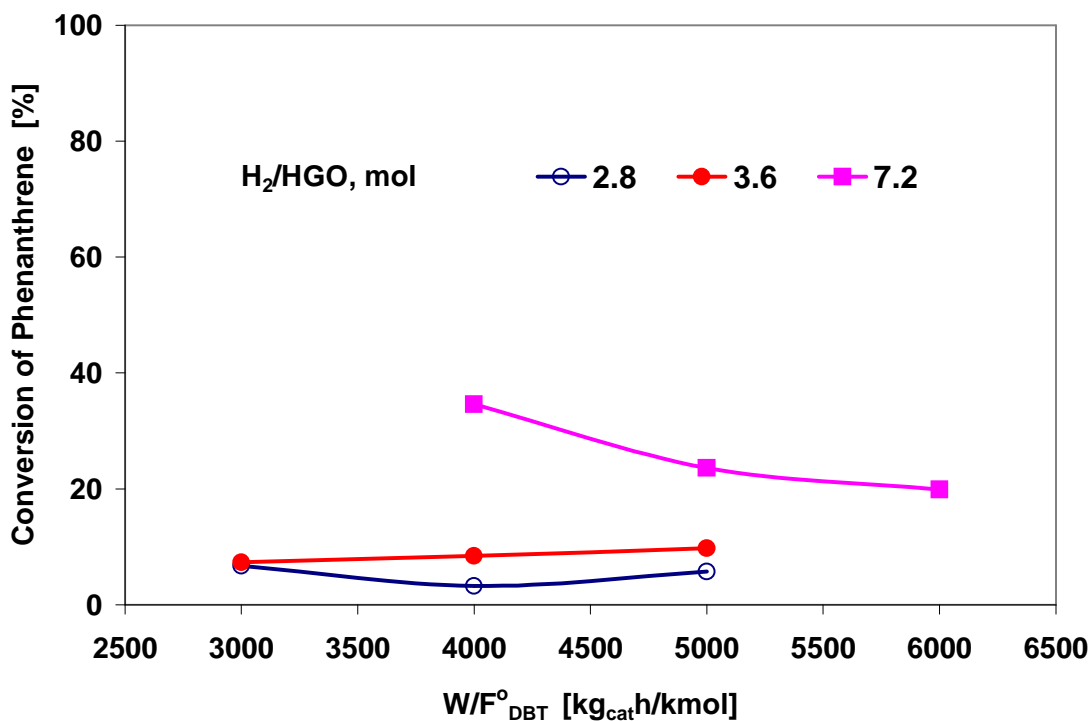


Figure 6.12 Conversion of phenanthrene as a function of space time (W/F_{DBT}°) and H_2/HGO mol ratio for the commercial $CoMo/Al_2O_3$ (HDS-0) catalyst. Reaction conditions were 65 bar, 330 °C. Feed: Heavy Gas Oil.

Figure 6.13 shows the molar averaged-conversions of the selected set of sulfur compounds as a function of space time (W/F_{DBT}°) and H_2/HC molar ratio. The highest value of 7.2 H_2/HC molar ratio shows the highest conversion for the MDBT's. However, for W/F_{DBT}° values higher than 5000 $kg_{cat}h/kmol$ the conversion is almost constant.

The results suggest studying higher H_2/HC mol ratios than 7.2 for the zeolite catalysts. The zeolite catalysts will contain noble metals such as Pt and Pd which will demand high consumptions of hydrogen for HDS of heavy gas oil.

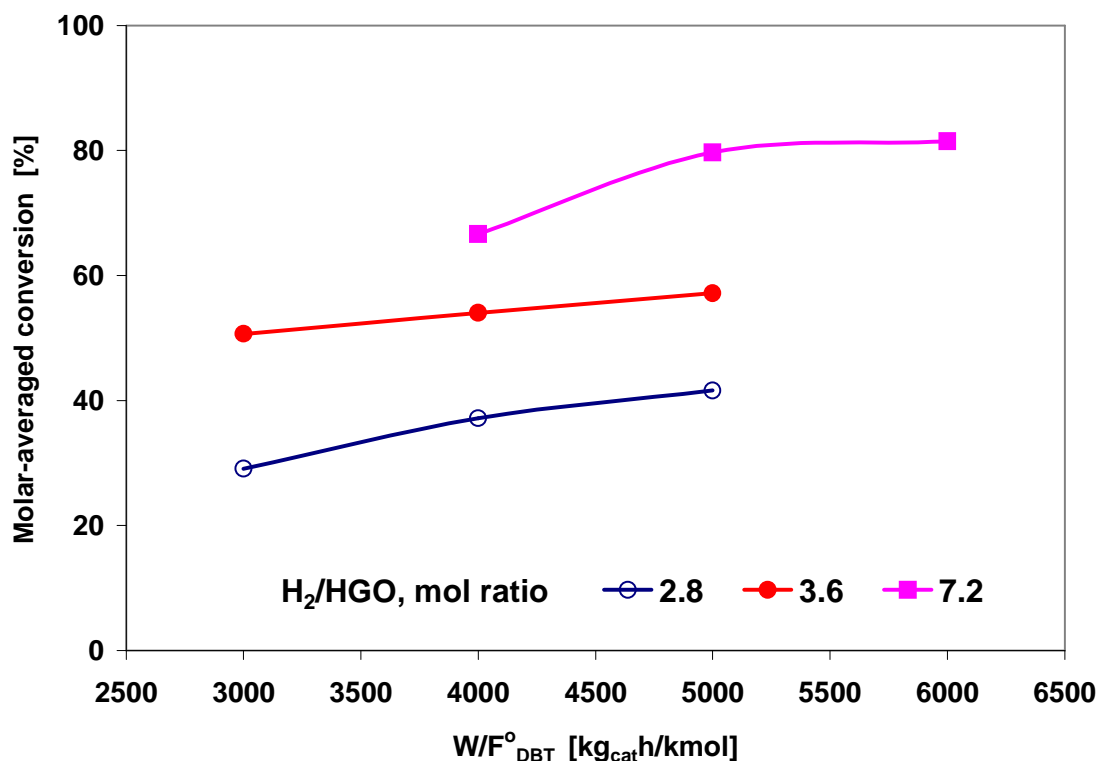


Figure 6.13 Molar averaged-conversions as a function of space time (W/F_{DBT}^0) and molar H_2/HGO ratio for the commercial $CoMo/Al_2O_3$ (HDS-0) catalyst. Reaction conditions were 65 bar, 330 °C. Feed: Heavy Gas Oil.

6.2.2 *CoMoPtPd/HY catalyst (HDS-1)*

6.2.2.1 *Effect of Space Time and Temperature*

The activity test of the $CoMoPtPd/HY$ catalyst in terms of conversion of DBT, MDBT's and phenanthrene is shown in Figure 6.14. The performance shows an increasing dependence on W/F_{DBT}^0 , giving conversions of 35.7-59.3% of DBT, 34.5-57.5% of 4-MDBT, 31.5-53.9% of 4,6-DMDBT, and 24.8-57% of phenanthrene in the interval of 4000-6000 kg_{cat}h/kmol. The conversions measured at 4000 kg_{cat}h/kmol are lower on this catalyst than the corresponding conversion on the commercial $CoMo/Al_2O_3$ for all components, as was observed in Figure 6.7. However, the

conversions of 4,6-DMDBT and phenanthrene at 6000 kg_{cat} h/kmol are higher than the conventional CoMo/Al₂O₃ (53.9 and 57.0% as compared to 50.7 and 19% respectively). Both catalysts provided the same conversion of 4-MDBT at this space time (57.5%). The results suggest that zeolite catalysts require high space time to reach high conversions of the refractory sulfur compounds in heavy gas oil.

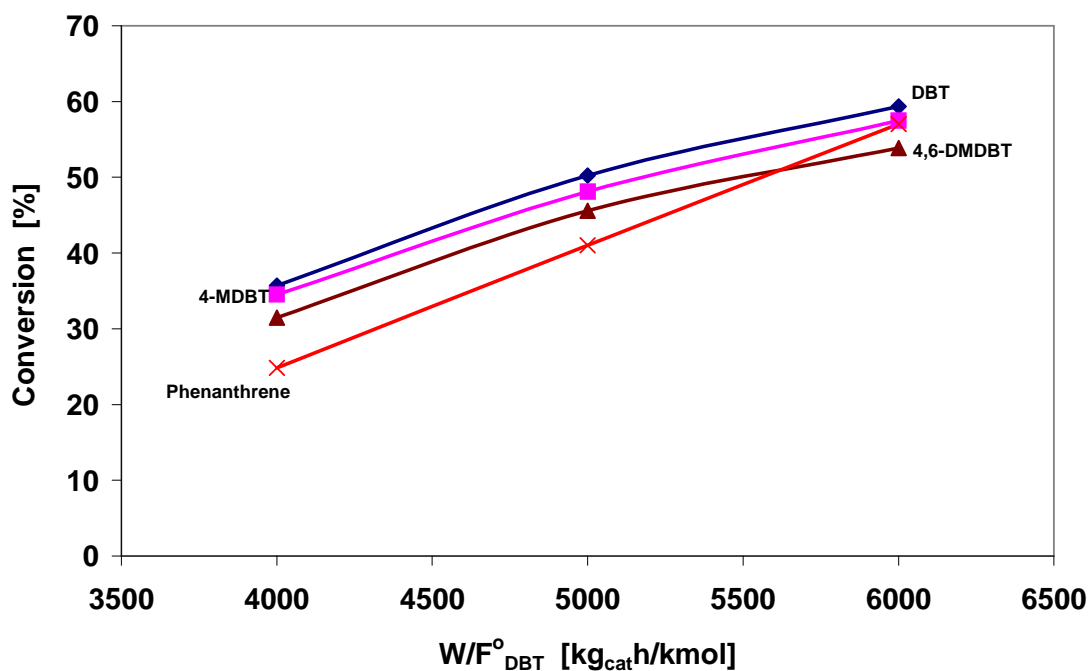


Figure 6.14 Conversion of DBT, MDBT's and phenanthrene as a function of space time (W/F_{DBT}^0) for the CoMoPtPd/HY (HDS-1) catalyst. Reaction conditions were 65 bar, 330 °C and 7.2 molar H₂/HGO ratio. Feed: Heavy Gas Oil.

As seen in Figure 6.15 the conversion of DBT, MDBT's and phenanthrene at 310 °C is lower than the corresponding conversion at 330 °C (Figure 6.14) for the same interval of space time. The difference in conversion for every W/F_{DBT}^0 is important; for instance at the maximum space time of 6000 kg_{cat} h/kmol, the conversion of DBT is 15% at 310 °C as compared to 59.7 % at 330 °C. The conversion of 4-MDBT is 14.1 % at 310 °C

while at 330 °C the corresponding value is 57.5%. For 4,6-DMDBT the conversion is 11.7% at 310 °C as compared to 53.9% at 330 °C, and for phenanthrene the conversion is 7.8 at 310 °C as compared to 57.04% at 330 °C.

In general, the catalytic performance of the CoMoPtPd/HY evaluated at 310°C, 65 bar and 7.2 of H₂/HC mol ratio was inferior compared to the commercial CoMo/Al₂O₃ presented in Figure 6.8. The results suggest that probably deactivation of the zeolite catalyst occurred at the conditions used.

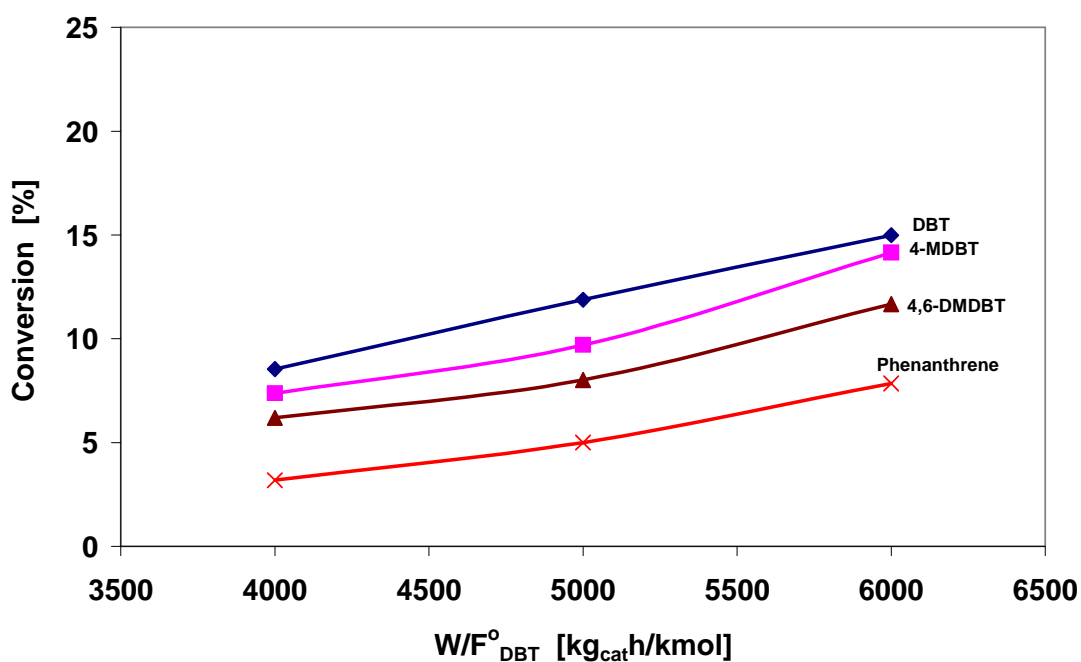


Figure 6.15 Conversions of DBT, MDBT's and phenanthrene as a function of space time (W/F°_{DBT}) for the CoMoPtPd/HY (HDS-1) catalyst. Reaction conditions were 65 bar, 310 °C and 7.2 molar H₂/HGO ratio. Feed: Heavy Gas Oil.

The dependence of the conversion of MDBT's for the CoMoPtPd/HY catalyst shown in Figure 6.16 is similar to the commercial catalysts (Figure 6.10), but the conversions of the CoMoPtPd/HY catalyst are less than the commercial catalyst for 330 and 310 °C.

The test at 290 °C for the CoMoPtPd/HY catalyst was not carried out because the conversion at 310 °C was so low.

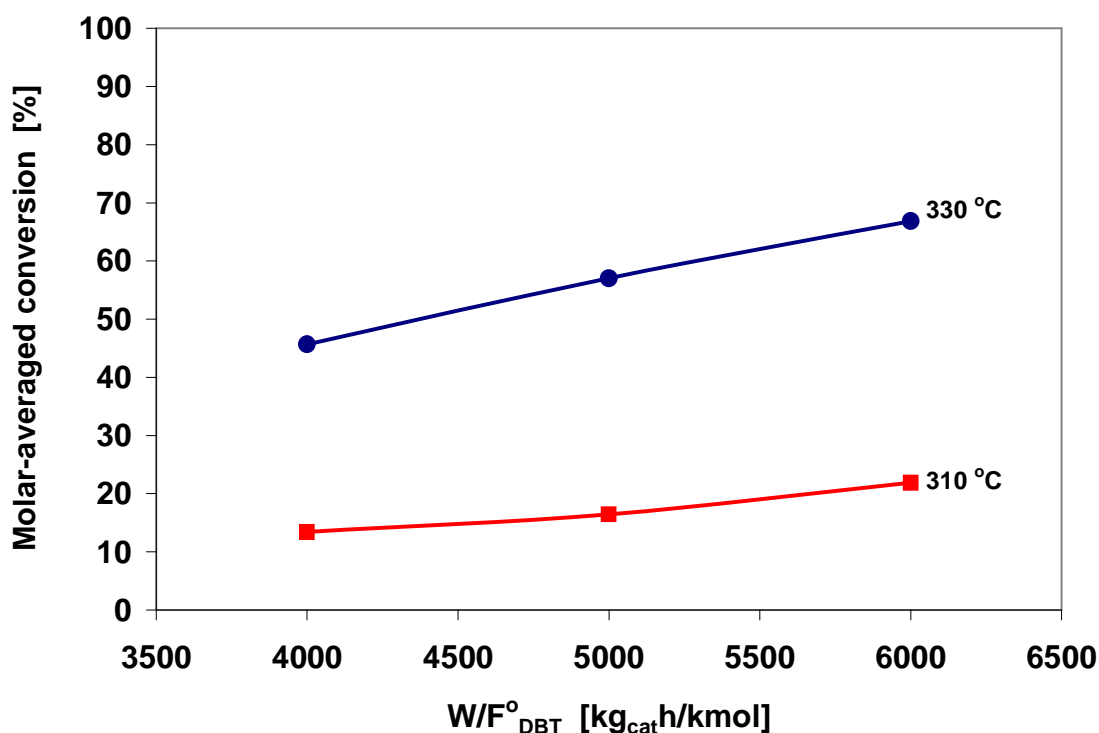


Figure 6.16 Molar-averaged conversion as a function of space time (W/F_{DBT}^o) and temperature for the CoMoPtPd/HY (HDS-1) catalyst. Reaction conditions were 65 bar and 7.2 molar H_2 /HGO ratio. Feed: Heavy Gas Oil.

6.2.2.2 Effect of the Molar Hydrogen/Hydrocarbon Ratio for the CoMoPtPd/HY Catalyst at 65 and 75 Bar

The evolution of the conversion of DBT, MDBT's and phenanthrene for a given W/F_{DBT}^o is shown in Figure 6.17. These tests were performed to determine the best H_2 /HC molar ratio to be considered in the remaining experiments. The conversion of

DBT and MDBT's at 9.2 and 11.2 H₂/HC molar ratio are very similar. The trend for phenanthrene is different because from 7.2 to 11.2 H₂/HC mol ratio its behavior is rising and higher H₂/HC ratio would increase the conversion. The results suggest that noble metals containing zeolites would enhance the hydrogenation reactions at high H₂/HC ratios.

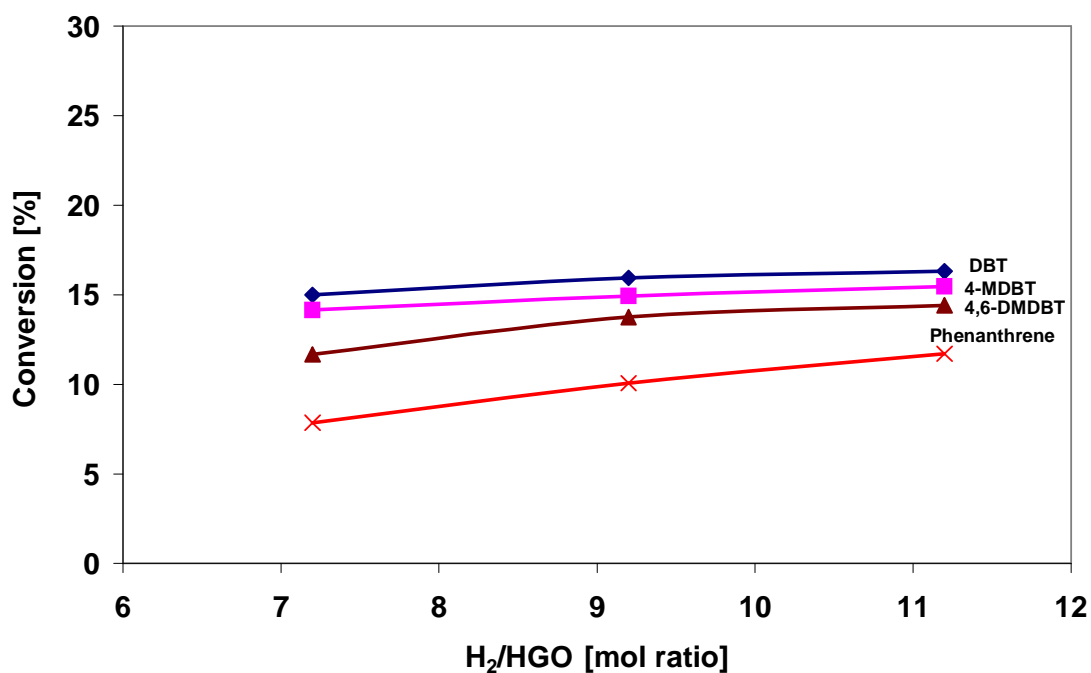


Figure 6.17 Conversion of DBT, MDBT's and phenanthrene as a function of H₂/HGO mol ratio for the CoMoPtPd/HY (HDS-1) catalyst. Reaction conditions were 65 bar, 310 °C, 6000 kg_{cat} h/kmol. Feed: Heavy Gas Oil.

The dependence of the conversion of DBT, 4-MDBT, 4,6-DMDBT and phenanthrene on total pressure is shown in Figures 6.17 and 6.18 (65 and 75 bar respectively). The 4,6-DMDBT and phenanthrene practically show the same values for different H₂/HC molar ratio in both Figures. DBT and 4-MDBT show higher conversions at 75 bar than 65 bar.

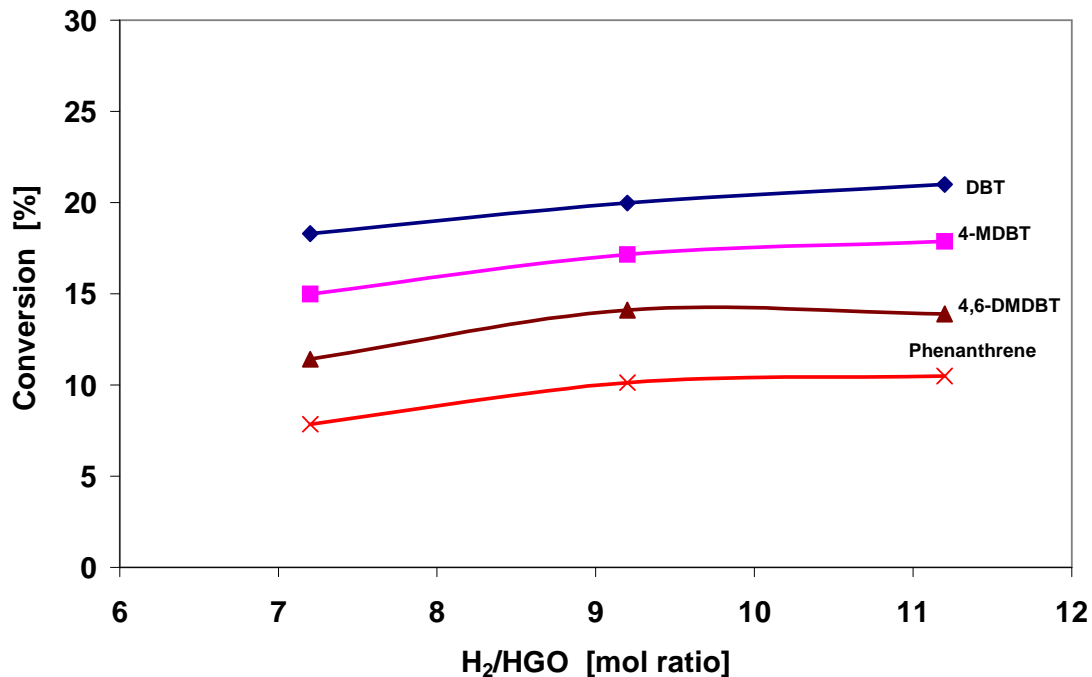


Figure 6.18 Conversion of DBT, MDBT's and phenanthrene as a function of H₂/HGO mol ratio for the CoMoPtPd/HY (HDS-1) catalyst. Reaction conditions were 75 bar, 310 °C, 6000 kg_{cat}/h/kmol. Feed: Heavy Gas Oil.

The molar averaged-conversion as well as the individual conversion of DBT, 4-MDBT and 4,6-DMDBT shows a moderate dependence on the H₂/HC molar ratio. Figure 6.19 shows this behavior. In this manner H₂/HC molar ratio between 7.2– 9.2 could be used to evaluate the zeolite catalyst. However, the hydrogenation of aromatics requires higher H₂/HC ratios.

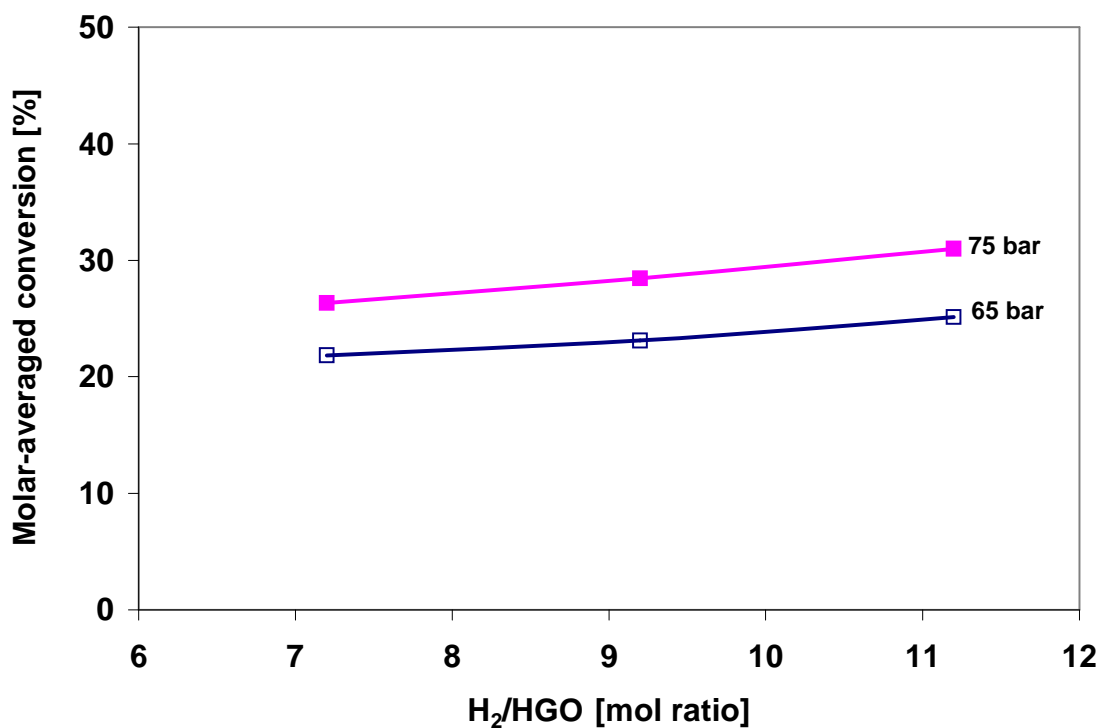


Figure 6.19 Molar-averaged conversion as a function of the molar H₂/HGO ratio and pressure for the CoMoPtPd/HY (HDS-1) catalyst. Reaction conditions were 310 °C, 6000 kg_{cat}/h/kmol. Feed: Heavy Gas Oil.

As already mentioned in all experiments the desorbed gases leaving the liquid-gas separator were analyzed online by the GC-TCD. However, in all of the programmed experiments no H₂S peak was observed, even though the liquid samples released the typical odor of H₂S when it is present. The absence of H₂S in the gas samples can be explained by the solubility of H₂S in the heavy gas oil, which means that all the H₂S was leaving from the gas-liquid separator dissolved in the liquid product. Figure 6.20 shows a typical chromatogram of a gaseous sample.

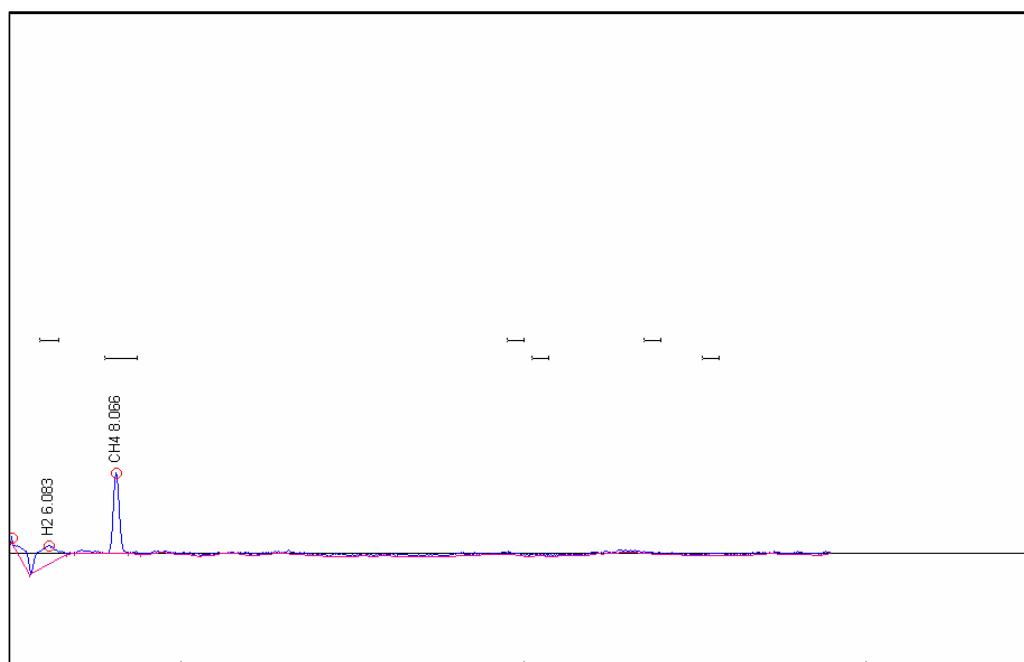


Figure 6.20 Typical chromatogram of a gaseous reaction product (E16T4 experiment) showing the retention time for H₂ and CH₄. Reaction conditions were 310 °C, 6000 kg_{cat} h/kmol, 65 bar, 9.2 molar H₂/HGO ratio and CoMoPtPd/HY (HDS-1) catalyst.

For H₂, low concentration was also detected for all experiments, meaning that almost all H₂ is consumed by the hydrodesulfurization and hydrogenation reactions of HGO.

6.2.3 CoMo/PdNiPt-HY (HDS-8) Catalyst

A set of thirteen experiments was carried out to test the CoMo/PdNiPt-HY (HDS-8) catalyst at temperatures of 330 and 310 °C, space time (W/F_{DBT}^o) of 4000 to 8000 kg_{cat}h/kmol, H₂/HC of 7.2 to 11.2 mol ratio, and total pressure of hydrogen of 65 and 75 bar. A summary of the operating conditions is shown in Table 6.2.

Table 6.2 Operating conditions used to test the catalytic activity for the CoMo/PdNiPt-HY (HDS-8) catalyst

Experiment	T °C	Pt bar	W/F⁰_{DBT} kg_{cat}h/kmol	H₂/HGO mol ratio
E21T1			4000	
E22T1	330	65	5000	7.2
E23T1			6000	
E23T4			6000	
E22T4	310	65	5000	7.2
E21T4			4000	
E23T4			6000	7.2
E24T4	310	65	6000	9.2
E25T4			6000	11.2
E30T4			6000	7.2
E27T4	310	75	6000	9.2
E26T4			6000	11.2
E29T4			8000	
E28T4	310	65	7000	11.2
E25T4			6000	

The evaluation procedure was the same as given in previous sections. The agitation was set to 1200 rpm. The temperature of the reactor was increased to 330 °C at 25°C/h. Operating conditions were maintained for 17-34 h to reach steady state, which corresponds to 1.5 liters of liquid product recovered from the reactor. Samples of gases, hydrocarbon product and readings of temperature controllers (TIC), mass flow controllers (FIC), temperature indicators (TI), and pressure gauges, were taken every 30 min for 3 h once the steady state was reached. The desorbed gases from the liquid product were analyzed on line, while the hydrocarbon liquid samples were labeled and analyzed off line.

6.2.3.1 Effect of the Space Time at 330 and 310 °C under Molar H₂/HC Ratio of 7.2

Run away of temperature was not observed during the activation of the CoMoPtPd/HY HDS-8 catalyst. A typical temperature profile of the reactor for zeolite

catalyst was presented in section 6.1. The conversions of dibenzothiophene (DBT), methylthiophene's (MDBT) and phenanthrene as a function of space-time (W/F_{DBT}^0) at 65 bar and 7.2 H_2/HC mol ratio and temperatures of 330 °C and 310 °C are shown in Figures 6.21 and 6.22 respectively. As expected the conversion of DBT is higher than the conversion for 4-MDBT and 4,6-DMDBT at both temperatures, obtaining 33-55.6% of DBT vs 29.3-51.1% of 4-MDBT and 26.2-47.2% of 4,6-DMDBT at 330 °C in the interval of 4000-6000 $kg_{cat}h/kmol$. These conversions increase with increasing space time, and decrease with decreasing temperature (Figure 6.22). phenanthrene shows also similar performance having conversions of 45.5-66.5% at 330 °C in same the interval of space time. To analyze the probability of methyl migration for 4- and/6-positions of 4,6-DMDBT, conversion of DBT and 4,6-DMDBT into their reaction products are shown in chapter VIII.

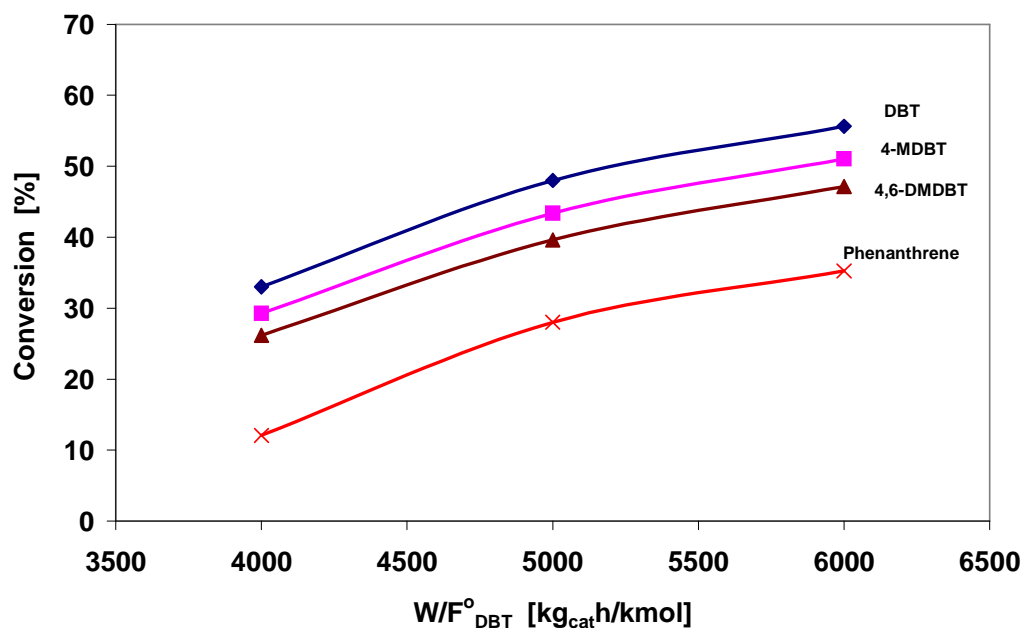


Figure 6.21 Conversion of DBT, MDBT's and phenanthrene as a function of space time (W/F_{DBT}^0) for CoMo/PdNiPt-HY (HDS-8) catalyst. Reaction conditions were 330 °C, 65 bar, and 7.2 molar H_2/HGO ratio. Feed: Heavy Gas Oil.

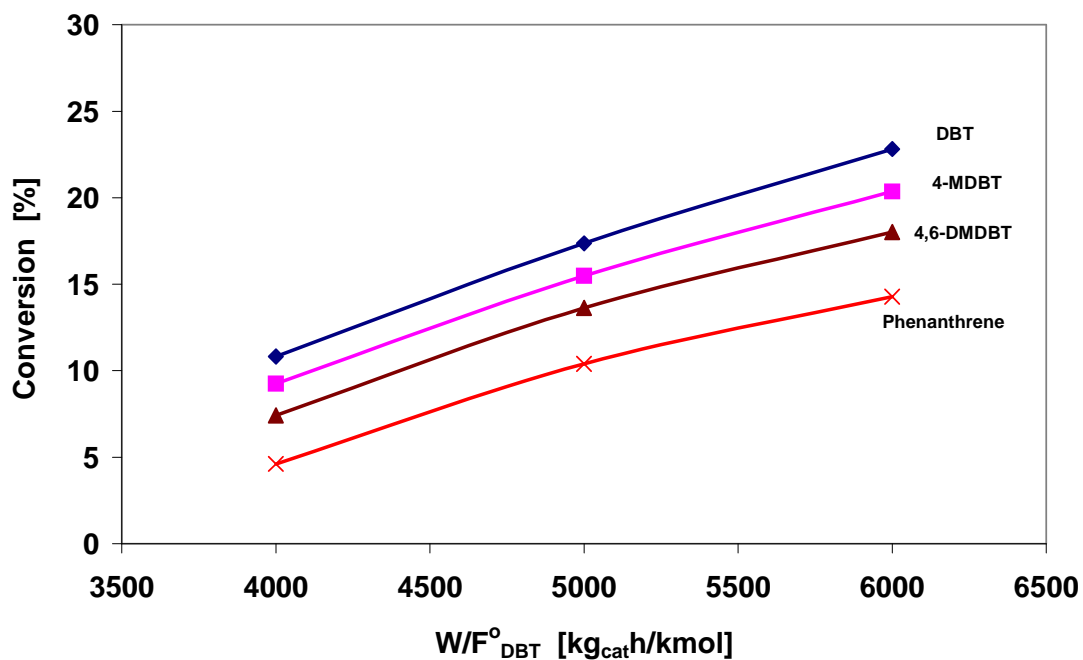


Figure 6.22 Conversion of DBT, MDBT's and phenanthrene as a function of space time (W/F°_{DBT}) for CoMo/PdNiPt-HY (HDS-8) catalyst. Reaction conditions were 310 °C, 65 bar, and 7.2 molar H₂/HGO ratio. Feed: Heavy Gas Oil.

The corresponding molar-averaged conversion is shown in Figure 6.23. The activity evaluated at 330 °C shows higher values than 310 °C for all space times studied. As expected the molar-averaged conversion increases with increasing W/F°_{DBT} .

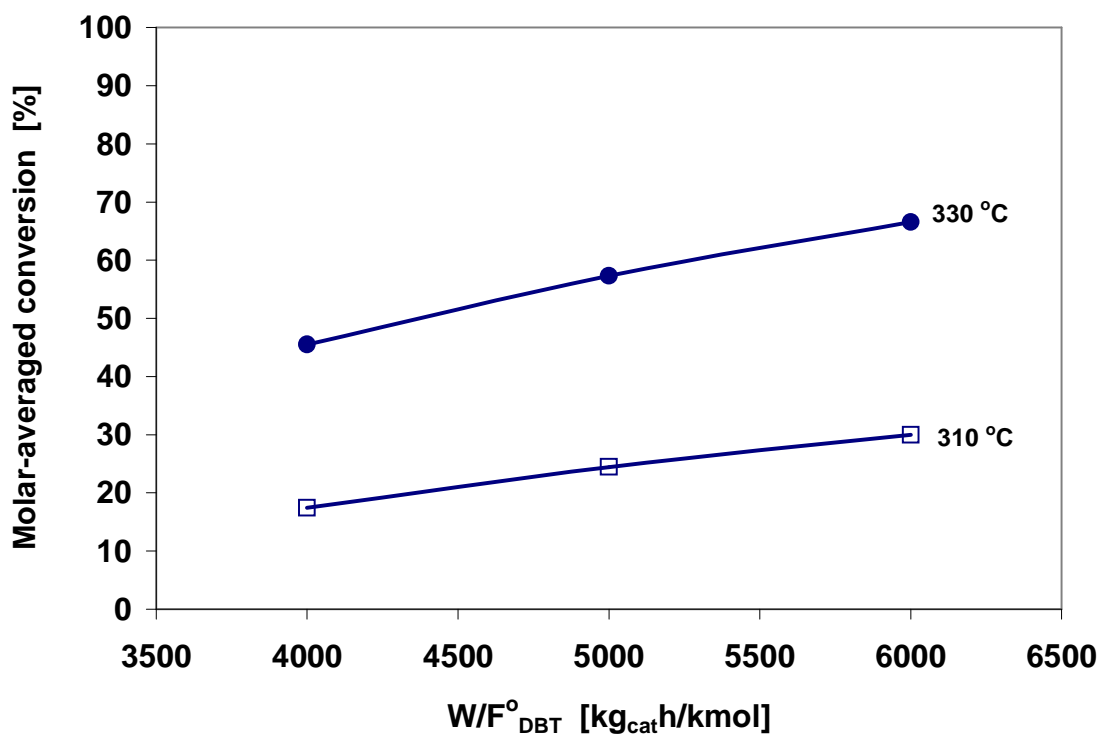


Figure 6.23 Molar-averaged conversion as a function of space time (W/F_{DBT}°) and temperature for CoMo/PdNiPt-HY (HDS-8) catalyst. Reaction conditions were 65 bar and 7.2 molar H_2 /HGO ratio. Feed: Heavy Gas Oil.

6.2.3.2 Effect of the Space Time at 310 °C and Molar H_2 /HC Ratio of 11.2

Figure 6.24 shows the conversion of DBT, MDBT's and phenanthrene as a function of space time (W/F_{DBT}°) for the CoMo/PdNiPt-HY catalyst. The performance of the CoMo/PdNiPd-HY catalyst at 65 bar with mol H_2 /HC ratio of 11.2 and space time in the range of 6000-8000 kg_{cat}h/kmol (W/F_{DBT}°) is higher than the performance obtained at 7.2 and 4000-6000 kg_{cat}h/kmol (W/F_{DBT}°) shown in Figure 6.22. As consequence the molar-averaged conversion is also higher when space time and the molar H_2 /HC ratio are higher as shown in Figure 6.25.

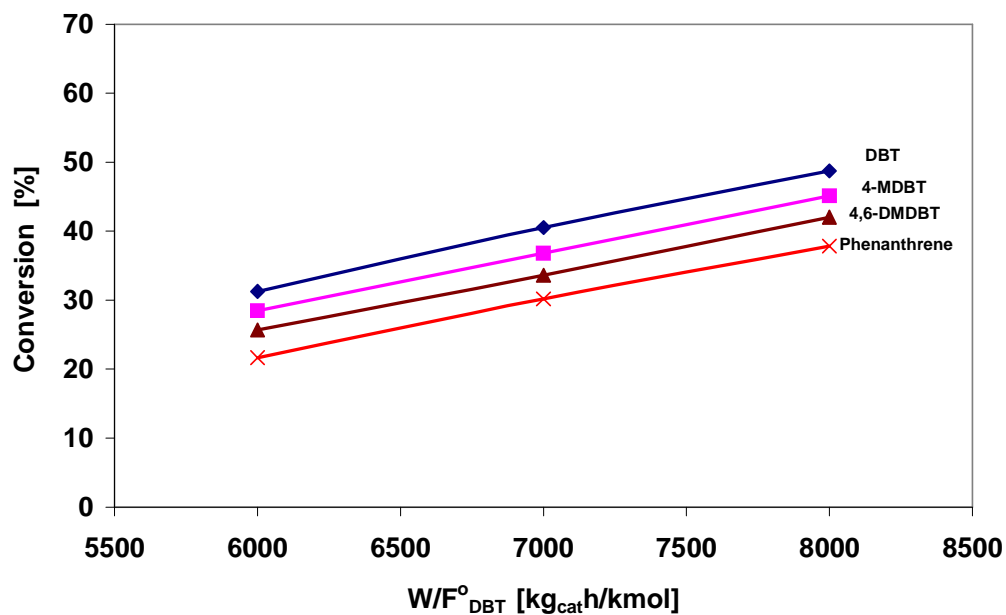


Figure 6.24 Conversion of DBT, MDBT's and phenanthrene as a function of space time (W/F_{DBT}°) for CoMo/PdNiPt-HY (HDS-8) catalyst. Reaction conditions were 310 °C, 65 bar, and 11.2 molar H₂/HGO ratio. Feed: Heavy Gas Oil.

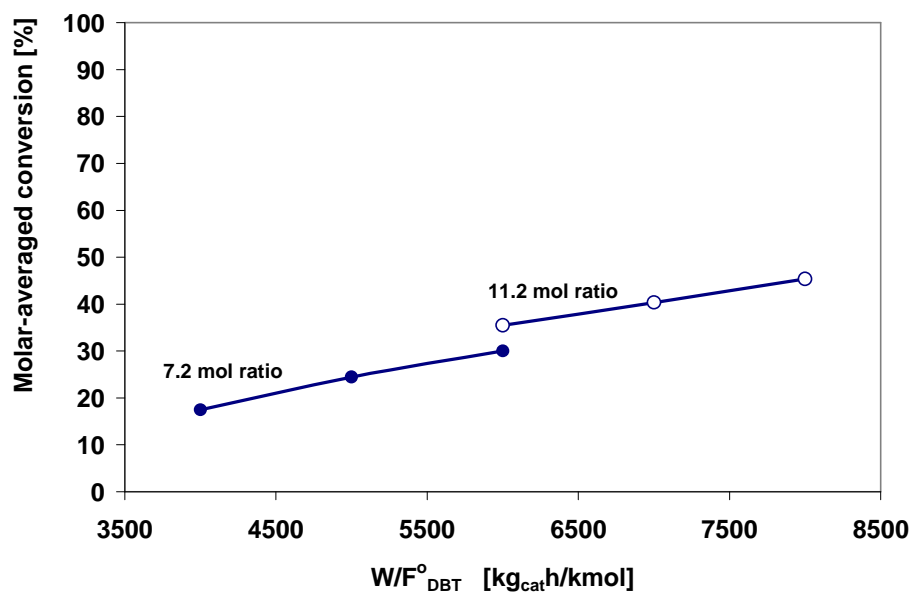


Figure 6.25 Molar-averaged conversion as a function of space time (W/F_{DBT}°) and H₂/HGO mol ratio for CoMo/PdNiPt-HY (HDS-8) catalyst. Reaction conditions were 310 °C, 65 bar, and 7.2 and 11.2 molar H₂/HGO ratio. Feed: Heavy Gas Oil.

6.2.3.3 Effect of the Molar Hydrogen/Hydrocarbon Ratio at 310 °C and 65-75 bar

Conversions of DBT, substituted DBT's (sDBT) and phenanthrene as a function of the molar H₂/HC ratio at 310 °C and pressure of 65 bar and 75 bar are shown in Figures 6.26 and 6.27 respectively. The corresponding sulfur compounds show small increase in their conversions when the pressure increased from 65 bar to 75 bar at the same molar H₂/HC ratio. However, the variation in the conversion of phenanthrene at the same conditions is higher. For instance, at molar H₂/HC ratio of 7.2 the conversion for DBT increased from 23 to 24% (variation= 4.3 %) and the conversion of phenanthrene increased from 14 to 17% (variation= 21%).

The variation of the molar-averaged conversion is shown in Figure 6.28. The variation of the conversion between 65 bar and 75 bar is small at the same molar H₂/HC ratio for all the interval studied.

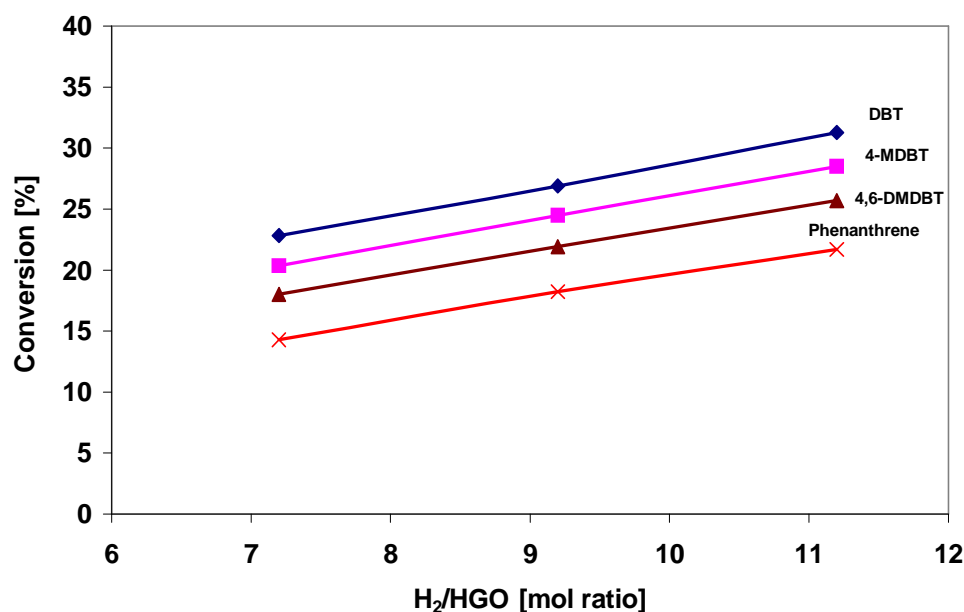


Figure 6.26 Conversion of DBT, sDBT and phenanthrene as a function of molar H₂/HGO ratio for CoMo/PdNiPt-HY (HDS-8) catalyst. Reaction conditions were 310 °C, 65 bar and 6000 kg_{cat}/kmol. Feed: Heavy Gas Oil.

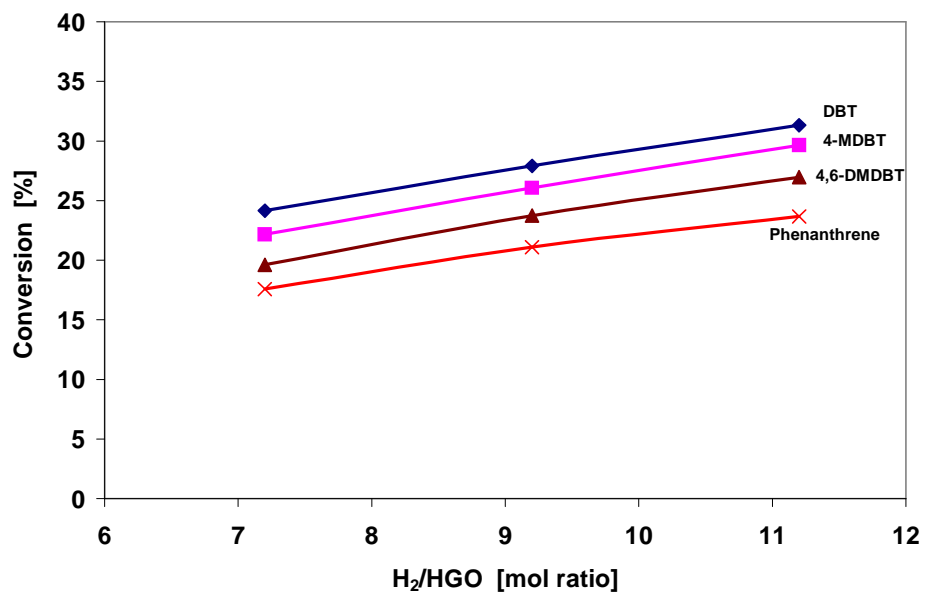


Figure 6.27 Conversion of DBT, sDBT and phenanthrene as a function of molar H₂/HGO ratio for CoMo/PdNiPt-HY (HDS-8) catalyst. Reaction conditions were 310 °C, 75 bar and 6000 kg_{cat}h/kmol. Feed: Heavy Gas Oil.

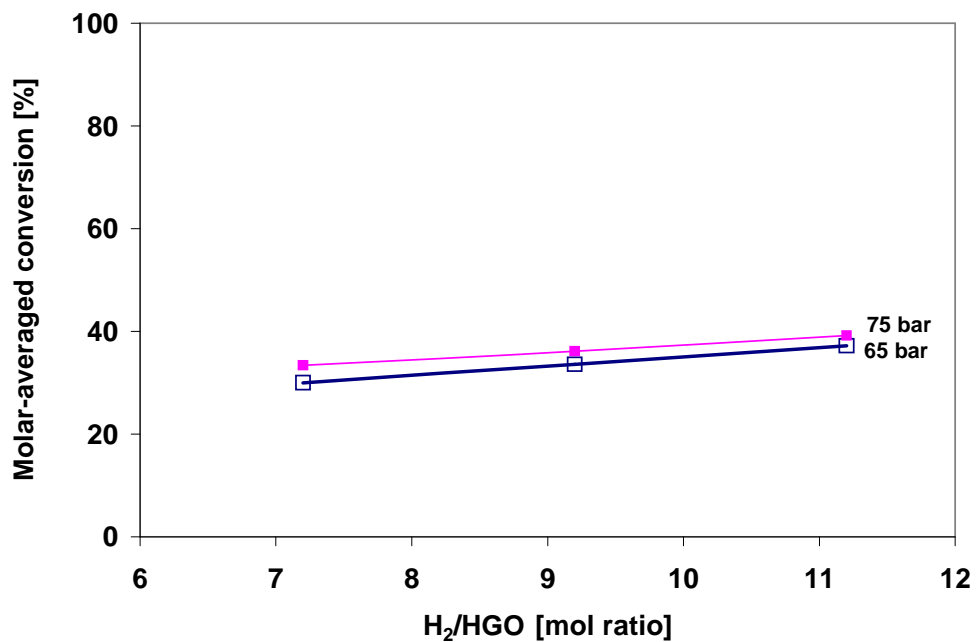


Figure 6.28 Molar-averaged conversion as a function of H₂/HGO mol ratio and pressure for CoMo/PdNiPt-HY (HDS-8) catalyst. Reaction conditions were 310 °C, 6000 kg_{cat}h/kmol. Feed: Heavy Gas Oil.

6.2.4 CoMoNi/PdPt-HY (HDS-10) Catalyst

Fifteen experiments were carried out to test the CoMoNi/PdPt-HY (HDS-10) catalyst at temperatures of 330 and 310 °C, space time (W/F_{DBT}^0) of 4000 to 8000 $kg_{cat}h/kmol$, H_2/HC of 7.2 to 11.2 mol ratio, and total pressure of hydrogen of 65 and 75 bar. A summary of the operating conditions is shown in Table 6.3.

Table 6.3 Operating conditions used to evaluate the catalytic activity in the HDS of heavy gas oil over the CoMoNi/PdPt-HY (HDS-10) catalyst.

Experiment	T °C	Pt bar	W/F_{DBT}^0 $kg_{cat}h/kmol$	H_2/HGO mol ratio
E31T1			4000	
E32T1	330	65	5000	7.2
E33T1			6000	
E33T4			6000	
E32T4	310	65	5000	7.2
E31T4			4000	
E33T4			6000	7.2
E34T4	310	65	6000	9.2
E35T4			6000	11.2
E40T4			6000	7.2
E37T4	310	75	6000	9.2
E36T4			6000	11.2
E39T4			8000	
E38T4	310	65	7000	11.2
E35T4			6000	

The evaluation procedure was the same as described for the CoMo/PdNiPt-HY (HDS-8) catalyst in the previous section. Operating conditions were maintained for 17-

34 h for reaching steady state, which is considered when 1.5 liters of liquid product is recovered from the reactor.

Analysis of gas samples and hydrocarbon product were taken every 30 min for 3 h once the steady state was reached. The desorbed gases from the liquid product were analyzed on line, while the hydrocarbon liquid samples were labeled and analyzed off line by GC-MS.

6.2.4.1 Effect of the Space Time at 330 °C and 310 °C for a Molar H₂/HC Ratio of 7.2

Run away of temperature was not observed during the sulfiding stage of the CoMoNi/PdPt-HY (HDS-10) catalyst. A typical temperature profile of the reactor for the zeolite catalyst was presented in section 6.1. The conversion of dibenzothiophene (DBT), and its derivatives such as 4-MDBT and 4,6-DMDBT as a function of space-time (W/F_{DBT}^0) over CoMoNi/PdPt-HY catalyst is shown in Figures 6.29 for 330 °C and 6.30 for 310 °C, both at 7.2 H₂/HC mol ratio under 65 bar. Conversion of phenanthrene at the same operating conditions is also shown in Figures 6.29 and 6.30.

As expected, the conversion for the different sulfur compounds increases as follows: DBT > 4-MDBT > 4,6-DMDBT, giving conversions of 44.1-54.9% of DBT, 31.1-51.3 % of 4-MDBT, and 37.7-48% of 4,6-DMDBT at space times of 4000-6000 kg_{cat}/h/kmol and 330 °C. Conversions of 24.1-28.3% of DBT, 22.5-27.1% of 4-MDBT and 20.8-25.6% of 4,6-DMDBT were obtained at 310 °C for the same interval of space time. To analyze the probability of the methyl migration of 4- and/6-positions of 4,6-DMDBT, conversion of DBT and 4,6-DMDBT into their reaction products are shown in chapter VIII.

The conversion of phenanthrene increased also with space time giving values from 33.9 to 39.6% at 310 °C and 22.8 to 30.9% at 330 °C. The maximum conversion was obtained at temperature of 310 °C, due to the exothermic hydrogenation of aromatics that is thermodynamically favored at a lower temperature.

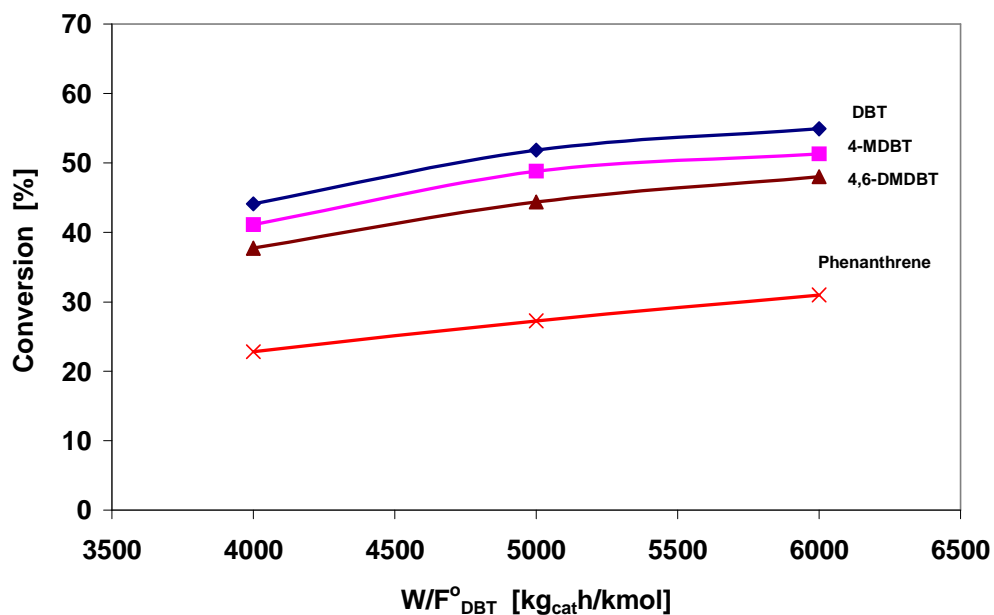


Figure 6.29 Conversion of DBT, MBDT's and phenanthrene as a function of space time (W/F_{DBT}°) for CoMoNi/PdPt-HY (HDS-10) catalyst. Reaction conditions were 330 °C , 65 bar, and 7.2 molar H_2/HGO ratio. Feed: Heavy Gas Oil.

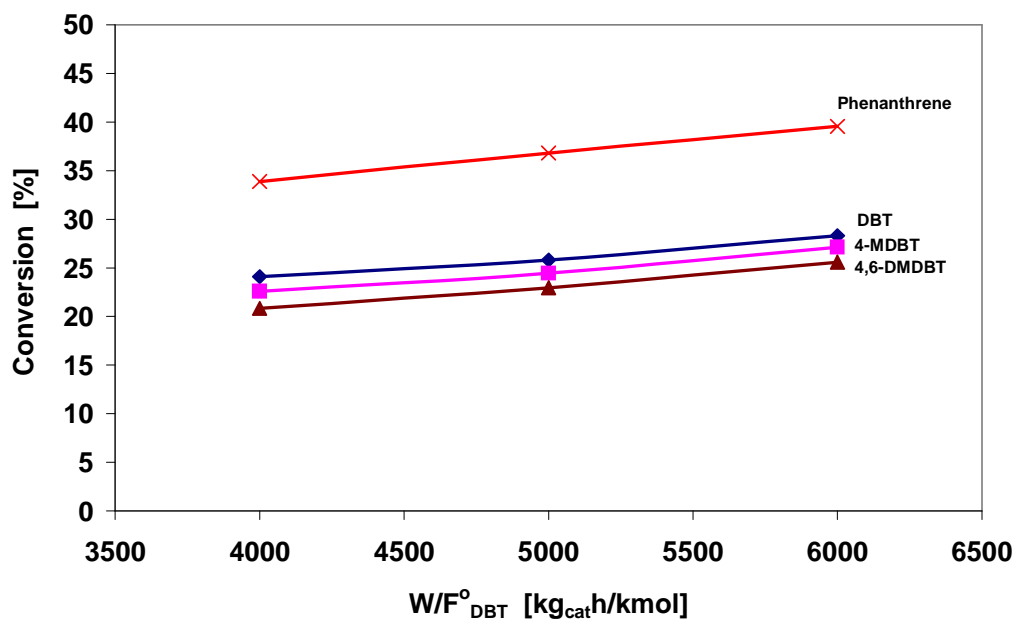


Figure 6.30 Conversion of DBT, MBDT's and phenanthrene as a function of space time (W/F_{DBT}°) for CoMoNi/PdPt-HY (HDS-10) catalyst. Reaction conditions were 310 °C , 65 bar, and 7.2 molar H_2/HGO ratio. Feed: Heavy Gas Oil.

The corresponding molar-averaged conversion is shown in Figure 6.31. As expected the molar-averaged conversions increase with increasing W/F_{DBT}^0 . The activity evaluated at 330 °C shows higher values than 310 °C in all space time studied.

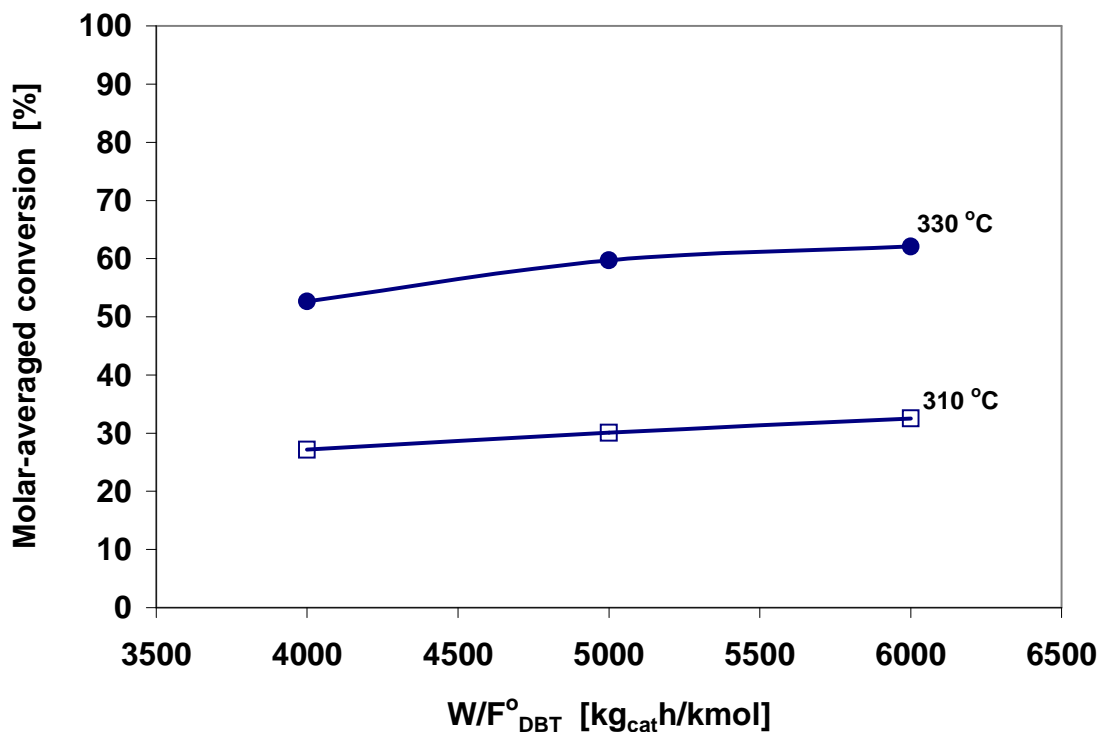


Figure 6.31 Molar-averaged conversion as a function of space time (W/F_{DBT}^0) and temperature for CoMoNi/PdPt-HY (HDS-10) catalyst. Reaction conditions were 65 bar and 7.2 molar H_2 /HGO ratio. Feed: Heavy Gas Oil.

6.2.4.2 Effect of the Space Time at 310 °C for a Molar H_2 /HC Ratio of 11.2

Figure 6.32 shows the conversion of DBT, MDBT's and phenanthrene as a function of space time (W/F_{DBT}^0) for CoMoNi/PdPt-HY (HDS-10) catalyst. This catalyst led to conversions of 32.2-53.3% of DBT, 31.3-51.5 % of 4-MDBT, 30.1-49.7% of 4,6-DMDBT and 43.2-63.0% of phenanthrene at space time of 6000-8000 kg_{cat}h/kmol, and mol H_2 /HC ratio of 11.2. The molar-averaged conversion is also higher when space time and molar H_2 /HC ratio are higher, as shown in Figure 6.33.

The performance of the catalyst at space time of 6000-8000 $\text{kg}_{\text{cat}}\text{h}/\text{kmol}$, and mol H_2/HC ratio of 11.2 was higher than that at 7.2 and 4000-6000 $\text{kg}_{\text{cat}}\text{h}/\text{kmol}$ (W/F°_{DBT}) shown in Figure 6.30.

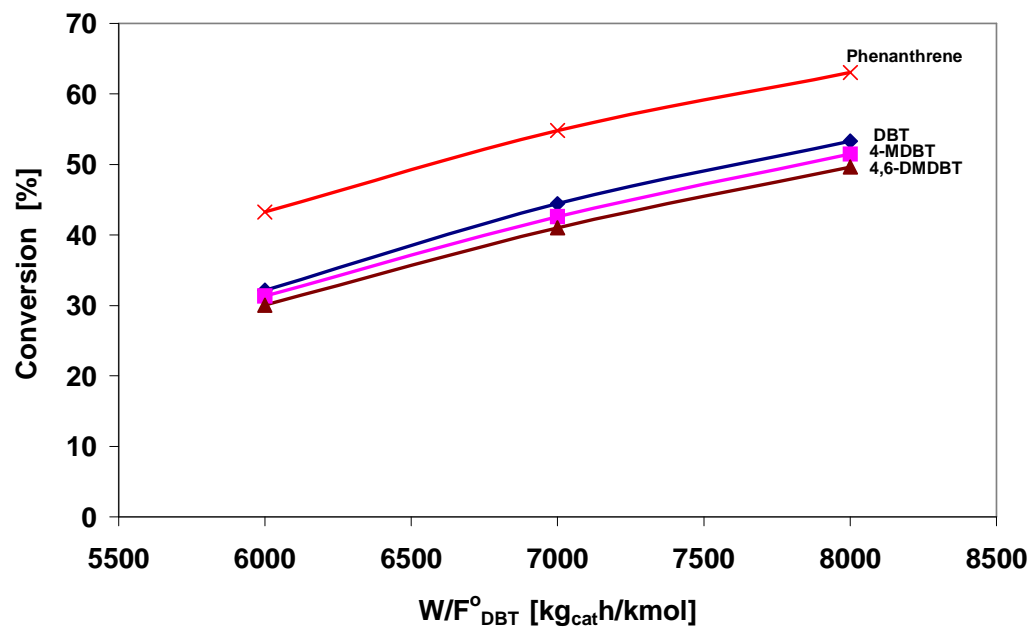


Figure 6.32 Conversion of DBT, MDBT's and phenanthrene as a function of space time (W/F°_{DBT}) for CoMoNi/PdPt-HY (HDS-10) catalyst. Reaction conditions were 310 °C, 65 bar, and 11.2 molar H_2/HGO ratio. Feed: Heavy Gas Oil.

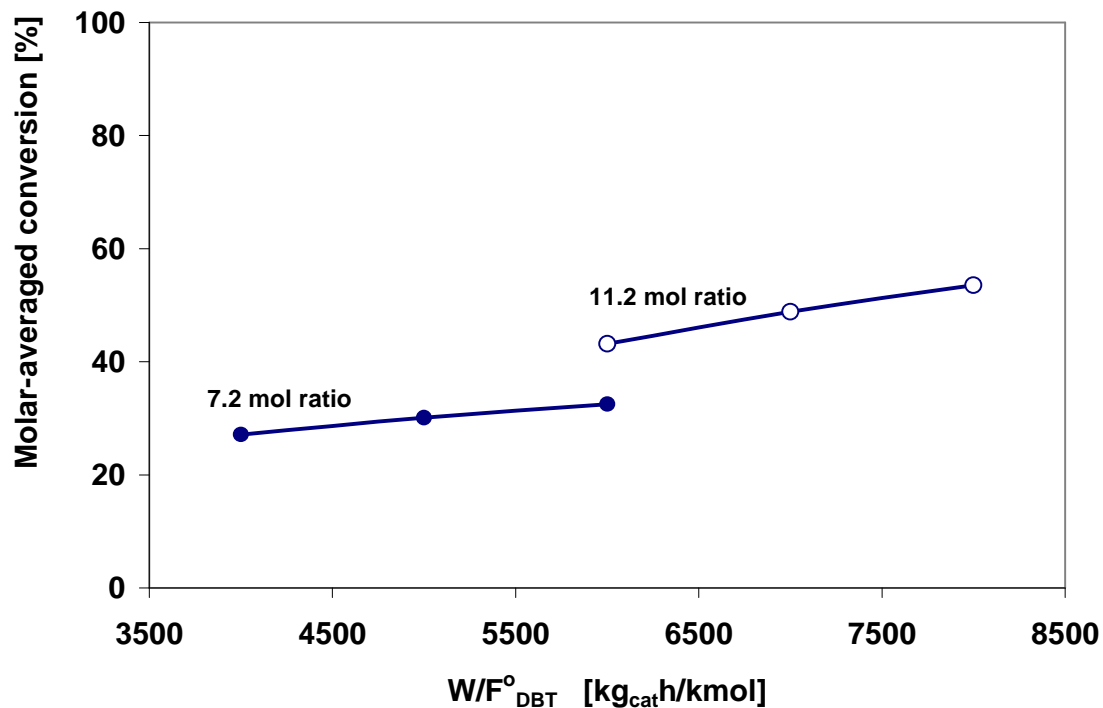


Figure 6.33 Molar-averaged conversion, as a function of space time (W/F_{DBT}^0) and H_2/HGO mol ratio CoMoNi/PdPt-HY (HDS-10) catalyst. Reaction conditions were 310 °C, 65 bar, and 7.2 and 11.2 molar H_2/HGO ratio. Feed: Heavy Gas Oil.

6.2.4.3 Effect of the Molar Hydrogen/Hydrocarbon Ratio at 310 °C and 65-75 Bar

Conversions of DBT, substituted DBT's (sDBT) and phenanthrene as a function of the molar H_2/HC ratio at 310 °C and pressure of 65 bar and 75 bar are shown in Figures 6.34 and 6.35, respectively. The variation of the conversions of sulfur compounds from 65 bar to 75 bar was not so significant at the interval of the molar H_2/HC ratio studied. The performance of the CoMoNi/PdPt-HY catalyst led to conversions from 28.3-32.2% of DBT, 27.1-31.3 % of 4-MDBT, and 25.6-30.1% of 4,6-DMDBT in the interval of the molar H_2/HC ratio of 7.2-11.2 at space time of 6000 $kg_{cat}h/kmol$ under 65 bar. While the conversions obtained at the same space time and same H_2/HC ratio under 75 bar were as follows: 32.8-41.9% of DBT, 29.7-30.1 % of 4-MDBT, and 27.7-36.59% of 4,6-

DMDBT. In contrast, the variation in the conversion of phenanthrene from 65 to 75 bar is higher, at the same space time and H_2/HC ratio, obtaining conversion of 39.6-43.2% of phenanthrene at 65 bar vs 47.4-66.7% at 75 bar, both in the interval of the molar H_2/HC ratio of 7.2-11.2 at space time of $6000 \text{ kg}_{\text{cat}}/\text{kmol}$. The variation of the molar-averaged conversion is shown in Figure 6.36. The variation of the conversion between 65 bar and 75 bar is small at the same molar H_2/HC ratio for all the interval studied.

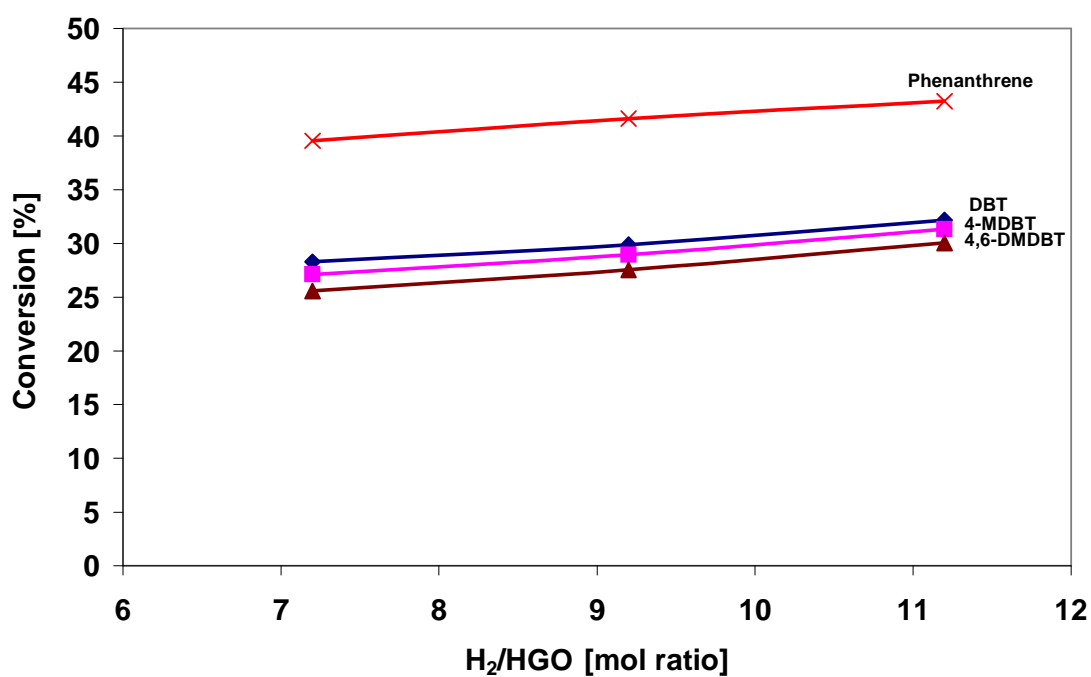


Figure 6.34 Conversion of DBT, sDBT and phenanthrene as a function of molar H_2/HGO ratio for CoMoNi/PdPt-HY (HDS-10) catalyst. Reaction conditions were 310°C , 65 bar and $6000 \text{ kg}_{\text{cat}}/\text{kmol}$. Feed: Heavy Gas Oil.

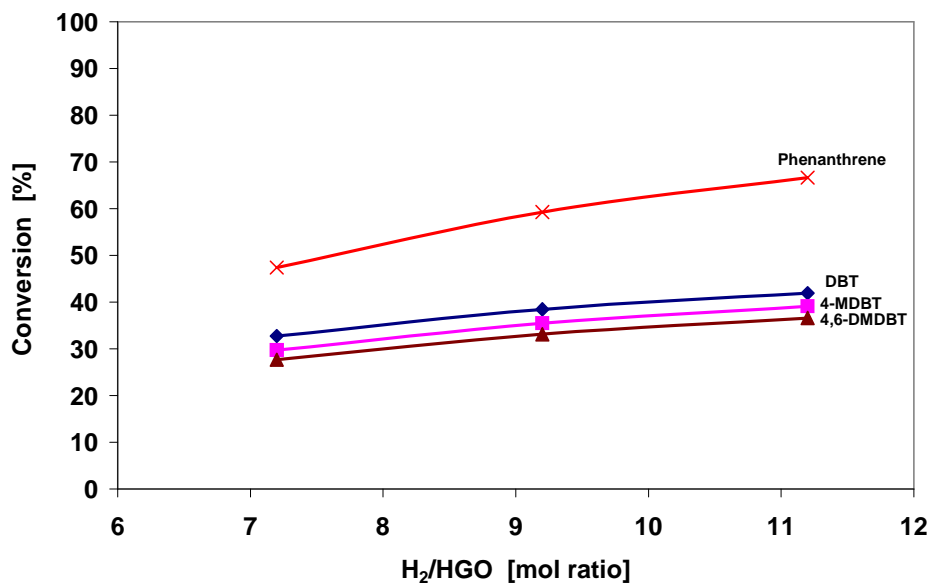


Figure 6.35 Conversion of DBT, sDBT and phenanthrene as a function of molar H₂/HGO ratio for CoMoNi/PdPt-HY (HDS-10) catalyst. Reaction conditions were 310 °C, 75 bar and 6000 kg_{cat}/h/kmol. Feed: Heavy Gas Oil.

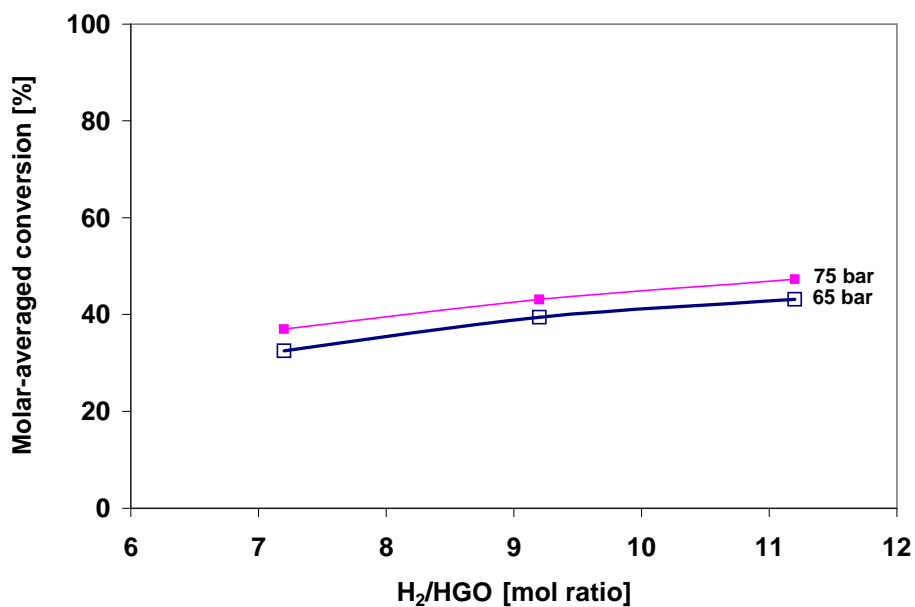


Figure 6.36 Molar-averaged conversion as a function of H₂/HGO mol ratio and pressure for CoMoNi/PdPt-HY (HDS-10) catalyst. Reaction conditions were 310 °C, 6000 kg_{cat}/h/kmol. Feed: Heavy Gas Oil.

6.2.5 CoMoPt Pd/Ni-HY (HDS-3) Catalyst

Six experiments were carried out to test the CoMoPt Pd/Ni-HY (HDS-3) at temperature of 310 °C, space time (W/F_{DBT}^0) of 4000 to 6000 $kg_{cat} h/kmol$, H_2/HC of 7.2 to 11.2 mol ratio, and total pressure of hydrogen of 65 bar. A summary of the operating conditions is shown in Table 6.4.

Table 6.4 Operating conditions used to evaluate the catalytic activity for the CoMoPt Pd/Ni-HY (HDS-3) catalyst

Experiment	T °C	Pt bar	W/F_{DBT}^0 $kg_{cat}h/kmol$	H_2/HGO mol ratio
E43T4	310	65	6000	7.2
E42T4			4000	
E41T4			5000	
E43T4	310	65	6000	7.2
E44T4			6000	9.2
E45T4			6000	11.2

The evaluation procedure was the same as described for the CoMo/PdNiPt-HY (HDS-8) catalyst. Operating conditions were maintained for 17-26 h for reaching steady state, which is considered when 1.5 liters of liquid product is recovered from the reactor. Analysis of gas samples and hydrocarbon product were carried out every 30 min for 3 h once the steady state was reached. The desorbed gases from the liquid product were again analyzed on line, while the hydrocarbon liquid samples were labeled and analyzed off line by GC-MS.

6.2.5.1 Effect of the Space Time at 310 °C for a Molar H_2/HC Ratio of 7.2

In the same way as the others catalysts, run away temperature was not observed during the sulfiding stage of the CoMoPt Pd/Ni-HY (HDS-3) catalyst. The conversions of dibenzothiophene (DBT) and alkyl-substituted DBT, such as 4-MDBT and 4,6-

DMDBT, are shown in Figure 6.37 as a function of space-time (W/F_{DBT}^o) at 310 °C, 7.2 H_2/HC mol ratio and pressure of 65 bar. Conversion of phenanthrene at the same operating conditions is also shown.

As expected, the conversion for the different sulfur compounds increases as follows: $DBT > 4\text{-MDBT} > 4,6\text{-DMDBT}$, giving conversions of 19.1-22.5% of DBT, 15.5-18.7% of 4-MDBT, and 14.7-17.7% of 4,6-DMDBT at space time of 4000-6000 $kg_{cat}h/kmol$ and 310 °C. To analyze the probability of the methyl migration of 4- and/6-positions of 4,6-DMDBT, conversion of DBT and 4,6-DMDBT into their reaction products are shown in chapter VIII.

The activity of phenanthrene increased also as space time; providing conversions from 53.0 to 58.4% at the same temperature and space time.

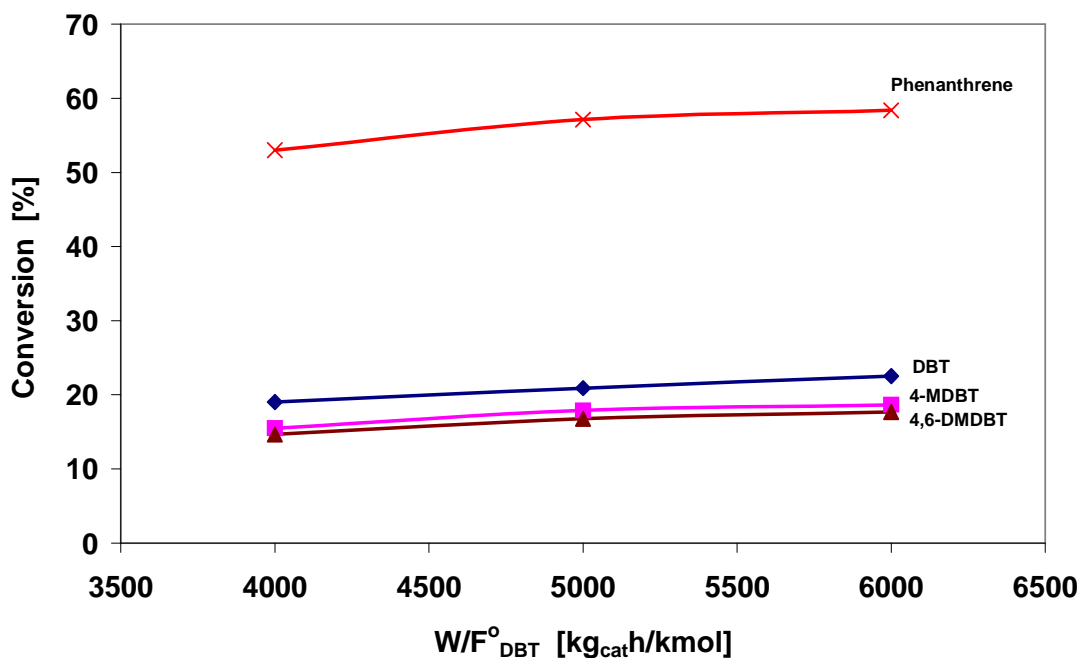


Figure 6.37 Conversion of DBT, MDBT's and phenanthrene as a function of space time (W/F_{DBT}^o) for CoMoPt Pd/Ni-HY (HDS-3) catalyst. Reaction conditions were 310 °C, 65 bar, and 7.2 molar H_2/HGO ratio. Feed: Heavy Gas Oil.

The corresponding molar-averaged conversion is shown in Figure 6.38. The molar-averaged conversion increased with rising W/F_{DBT}^0 from 4000 to 5000 $\text{kg}_{\text{cat}}\text{h}/\text{kmol}$ (22.8 to 26.2%). However, in the interval of 5000 to 6000 $\text{kg}_{\text{cat}}\text{h}/\text{kmol}$ the variation of conversions was quite close, 26.2 to 27.6% respectively.

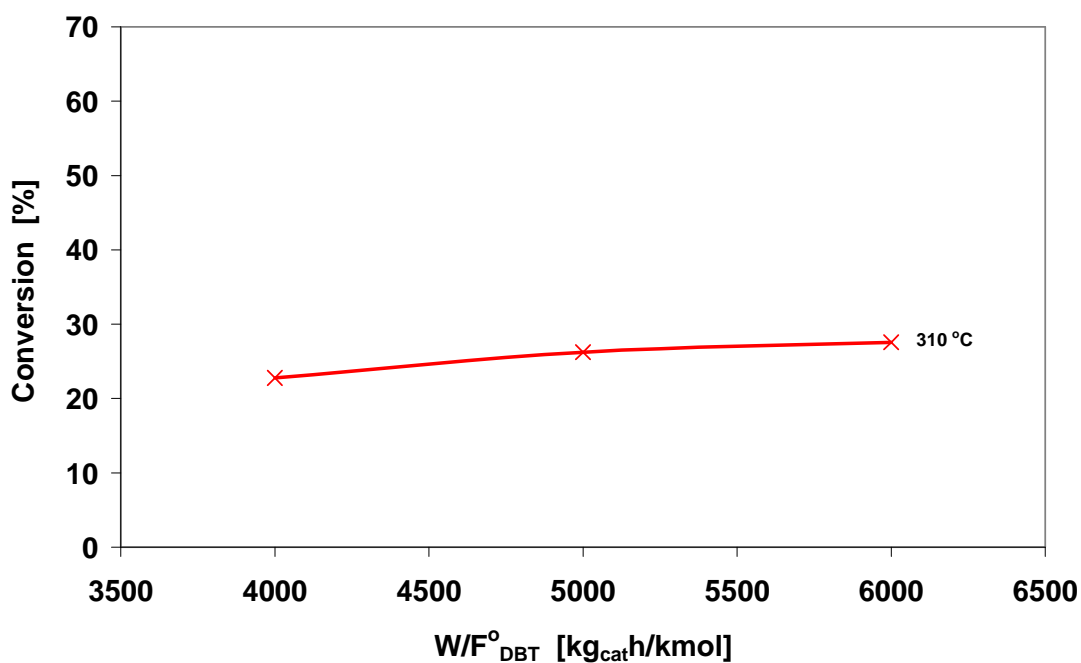


Figure 6.38 Molar-averaged conversion as a function of space time (W/F_{DBT}^0) for CoMoPt Pd/Ni-HY (HDS-3) catalyst. Reaction conditions were 310 °C, 65 bar and 7.2 molar H_2/HGO ratio. Feed: Heavy Gas Oil.

6.2.5.2 Effect of the Molar Hydrogen/Hydrocarbon Ratio at 310 °C and 65 Bar

Conversions of DBT, substituted DBT's (sDBT) and phenanthrene as a function of the molar H_2/HC ratio at 310 °C under pressure of 65 bar are shown in Figure 6.39. The performance of the CoMoPt Pd/Ni-HY catalyst produced conversions from 22.5-33% of DBT, 18.7-28.7% of 4-MDBT, and 17.7-27.5% of 4,6-DMDBT in the interval of the molar H_2/HC ratio of 7.2-11.2 at space time of 6000 $\text{kg}_{\text{cat}}\text{h}/\text{kmol}$ under 65 bar. The

conversion of phenanthrene increased from 27.6% to 35.7% as H_2/HC ratio increased from 7.2 to 11.2.

The molar-averaged conversion also increased as H_2/HC ratio increased from 7.2 to 9.2 mol ratio, obtaining conversions of 27.6 to 35.4% as shown in Figure 6.40. However, the molar-averaged conversions in the interval from 9.2 to 11.2 mol ratio were the same, 35.4 vs 35.7% respectively.

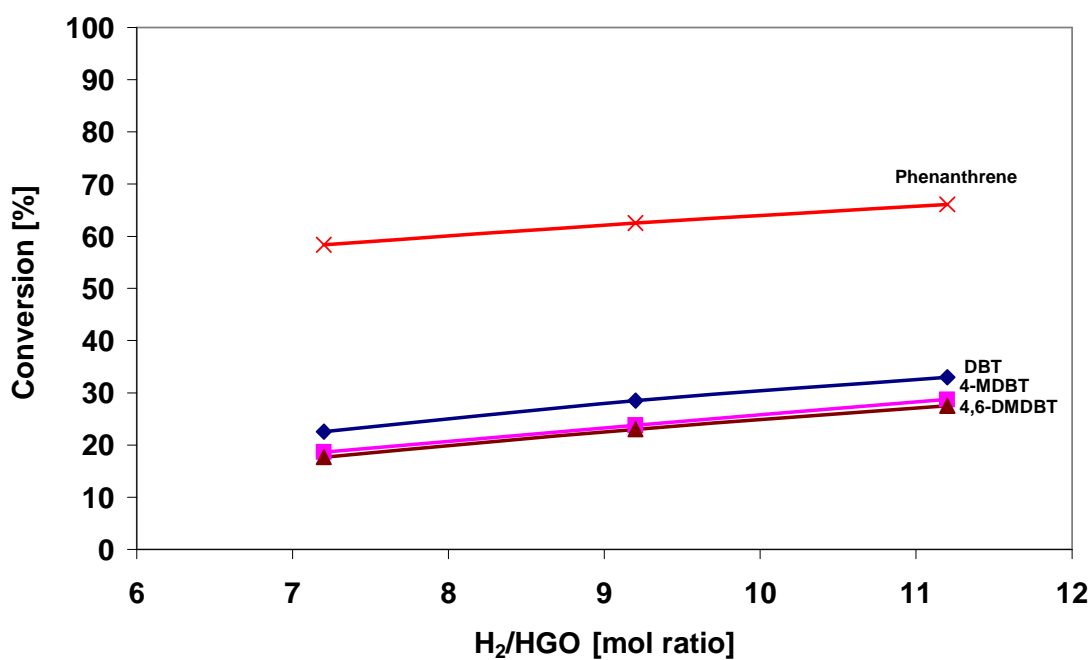


Figure 6.39 Conversion of DBT, sDBT and phenanthrene as a function of molar H_2/HGO ratio for CoMoPt Pd/Ni-HY (HDS-3) catalyst. Reaction conditions were 310 °C , 65 bar and 6000 $kg_{cat}/h/kmol$. Feed: Heavy Gas Oil.

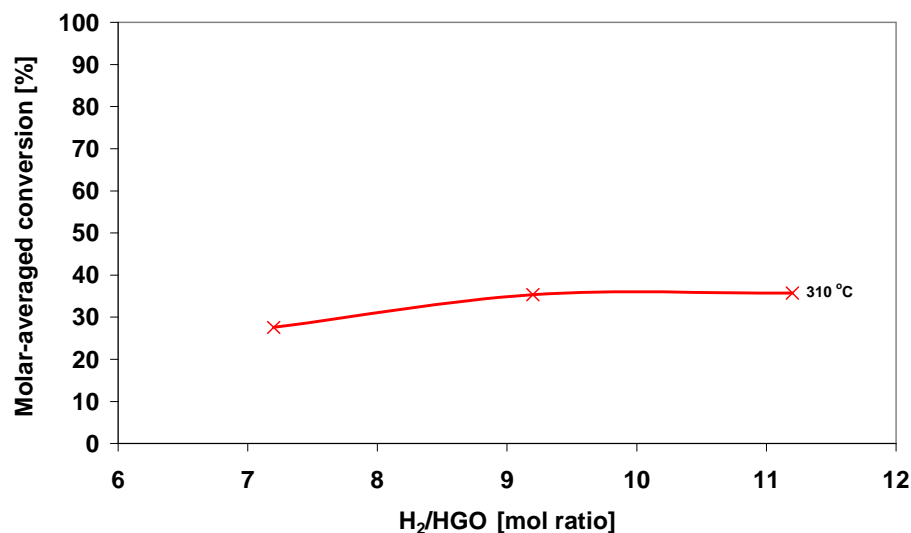


Figure 6.40 Molar-averaged conversion as a function of H₂/HGO mol ratio for CoMoPtPd/Ni-HY (HDS-3) catalyst. Reaction conditions were 310 °C, 65 bar, 6000 kg_{cat}h/kmol. Feed: Heavy Gas Oil.

6.2.6 CoMoPd/Pt-HY (HDS-5) Catalyst

As the CoMoPtPd/Ni-HY (HDS-3) catalyst, six experiments were carried out to test the CoMoPd/Pt-HY (HDS-5) at temperature of 310 °C, space time (W/F_{DBT}^0) of 4000 to 6000 kg_{cat} h/kmol, H₂/HC of 7.2 to 11.2 mol ratio, and total pressure of hydrogen of 65 bar. A summary of the operating conditions is shown in Table 6.5.

Table 6.5 Operating conditions used to evaluate the catalytic activity for the CoMoPd/Pt-HY (HDS-5) catalyst.

Experiment	T °C	Pt bar	W/F _{DBT} ⁰ kg _{cat} h/kmol	H ₂ /HGO mol ratio
E48T4	310	65	6000	7.2
E47T4			4000	
E46T4			5000	
E48T4	310	65	6000	7.2
E49T4			6000	9.2
E50T4			6000	11.2

The evaluation procedure was the same as described for the CoMo/PdNiPt-HY (HDS-8) catalyst. Operating conditions were maintained for 17-26 h for reaching steady state. Analysis of gas samples and hydrocarbon product were taken every 30 min for 3 h once the steady state was reached. The desorbed gases from the liquid product were also analyzed on line, while the hydrocarbon liquid samples were labeled and analyzed off line by GC-MS.

6.2.6.1 Effect of the Space Time at 310 °C under for a Molar H₂/HC Ratio of 7.2

Run away of temperature was not observed during the sulfiding stage of the CoMoPd/Pt-HY (HDS-5) catalyst. The conversions of dibenzothiophene (DBT) and sDBT, such as 4-MDBT and 4,6-DMDBT are shown in Figure 6.41 as a function of space-time (W/F_{DBT}^o) at 310 °C, 7.2 H₂/HC mol ratio and pressure of 65 bar. Conversion of phenanthrene at the same operating conditions is also shown.

The conversion for the different sulfur compounds increases as follows: DBT>4-MDBT>4,6-DMDBT, giving conversions of 19.6-26.9% of DBT, 17.8-25.6% of 4-MDBT, and 16.1-24.3% of 4,6-DMDBT at space time of 4000-6000 kg_{cat}h/kmol and 310 °C. To analyze the probability of the methyl migration of 4- and/6-positions of 4,6-DMDBT, conversion of DBT and 4,6-DMDBT into their reaction products are shown in chapter VIII.

The conversion of phenanthrene increased also with increasing space time; providing values from 39.1-47.7% at the same temperature and space time.

The corresponding molar-averaged conversion is shown in Figure 6.42. The molar-averaged conversion increased with rising W/F_{DBT}^o from 4000 to 6000 kg_{cat}h/kmol (24.1 to 32.3%).

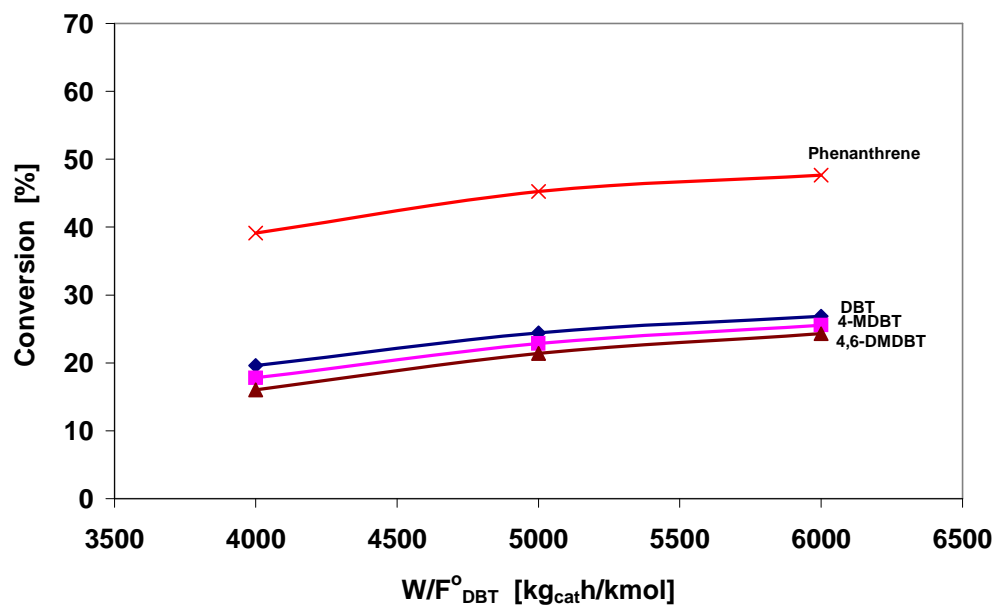


Figure 6.41 Conversion of DBT, sDBT and phenanthrene as a function of space time (W/F_{DBT}°) for CoMoPd/Pt-HY (HDS-5) catalyst. Reaction conditions were 310 °C , 65 bar, and 7.2 molar H₂/HGO ratio. Feed: Heavy Gas Oil.

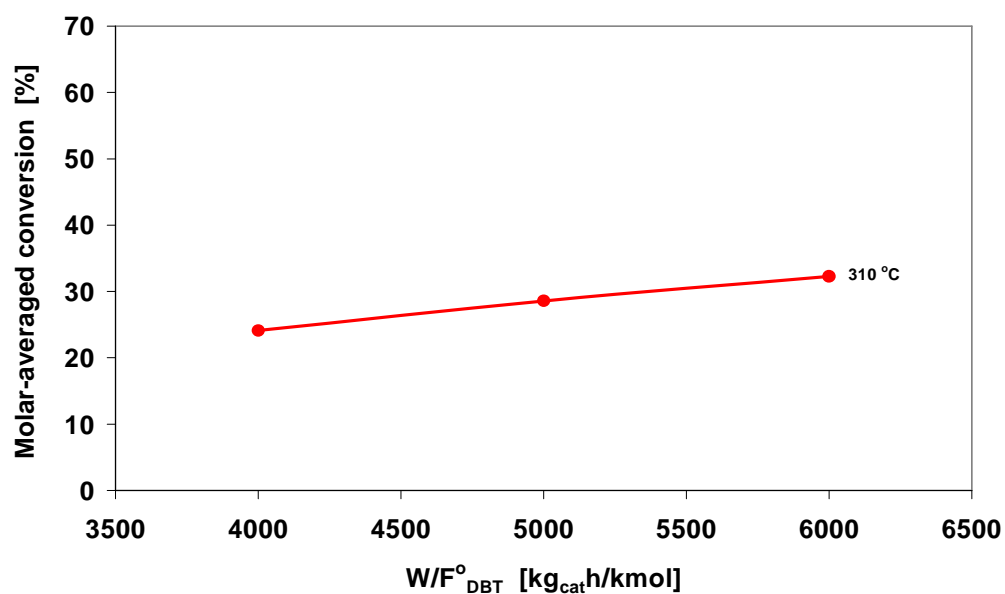


Figure 6.42 Molar-averaged conversion as a function of space time (W/F_{DBT}°) for CoMoPd/Pt-HY (HDS-5) catalyst. Reaction conditions were 310 °C, 65 bar and 7.2 molar H₂/HGO ratio. Feed: Heavy Gas Oil.

6.2.6.2 Effect of the Molar Hydrogen/Hydrocarbon Ratio at 310 °C and 65 Bar

Conversions of DBT, substituted DBT's (sDBT) and phenanthrene as a function of the molar H₂/HC ratio at 310 °C under pressure of 65 bar are shown in Figure 6.43. The performance of CoMoPd/Pt-HY catalyst provided conversions from 26.9-34.7% of DBT, 25.6-33.2% of 4-MDBT, and 24.3-32% of 4,6-DMDBT in the interval of the molar H₂/HC ratio of 7.2-11.2 at space time of 6000 kg_{cat}/kmol. The conversion of phenanthrene increased from 47.7% to 56.5% as H₂/HC ratio increased from 7.2 to 11.2.

The molar-averaged conversion also increased as H₂/HC ratio increased from 7.2 to 11.2 mol ratio, obtaining conversions of 32.3 to 39.1% as shown in Figure 6.44.

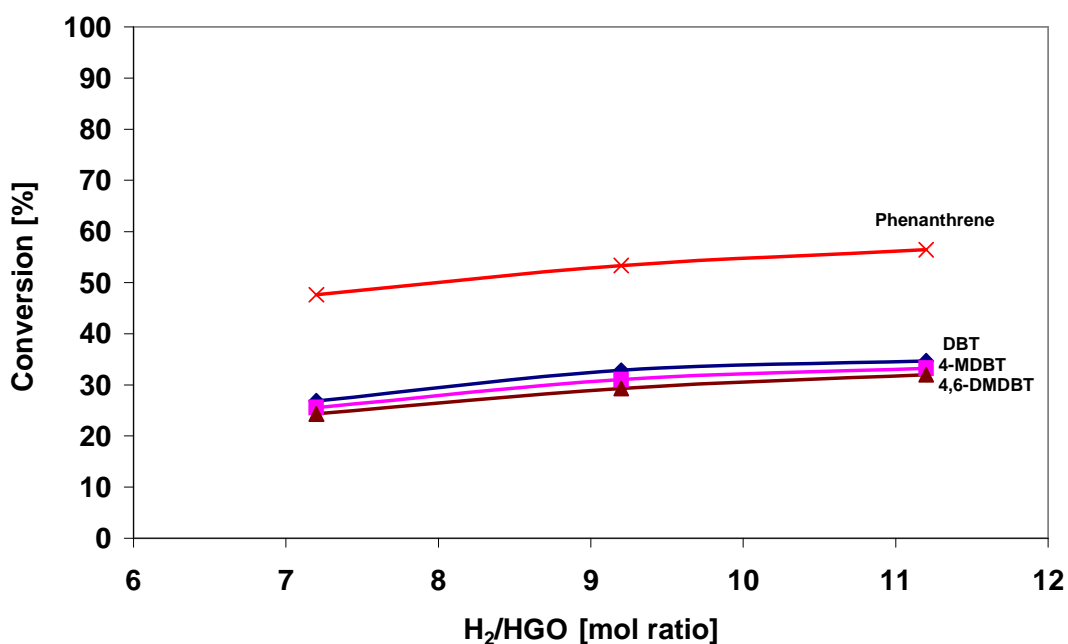


Figure 6.43 Conversion of DBT, sDBT and phenanthrene as a function of molar H₂/HGO ratio for CoMoPd/Pt-HY (HDS-5) catalyst. Reaction conditions were 310 °C , 65 bar and 6000 kg_{cat}/kmol. Feed: Heavy Gas Oil.

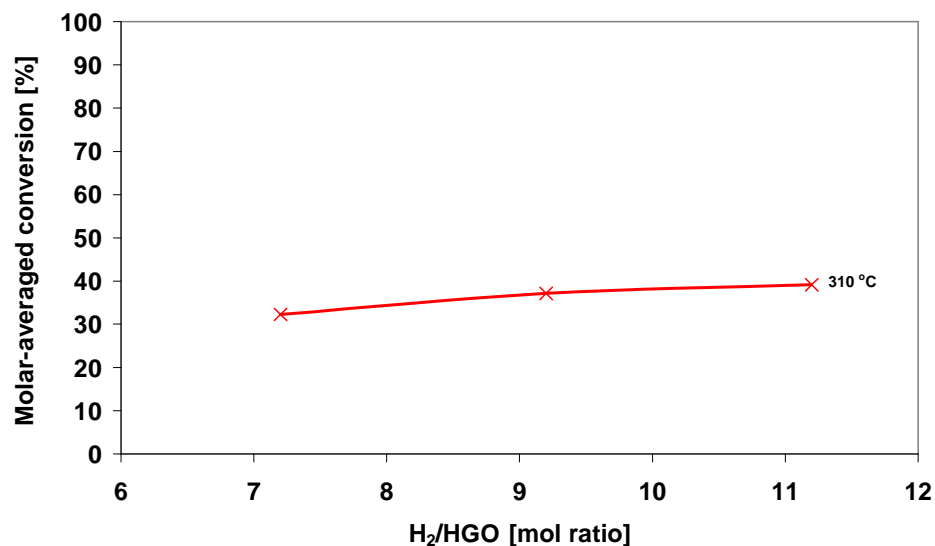


Figure 6.44 Molar-averaged conversion as a function of H₂/HGO mol ratio for CoMoPd/Pt-HY (HDS-5) catalyst. Reaction conditions were 310 °C, 65 bar, 6000 kg_{cat}h/kmol.

6.3 Concluding Remarks

From this study is concluded that the activity of basic and noble metals catalysts supported on zeolites in HDS of heavy gas oil is highly affected by temperature, H₂/HC ratio and space time rather than pressure. The recommendable values to get a HDS product of good quality are: temperature of 310 °C, H₂/HC mol ratios greater than 7.2 and space time greater than 6000 kg_{cat}h/kmol.

The alkyl-DBTs with alkyl substituents at the 4 and/or 6 positions are the most refractory sulfur species in heavy gas oil. Therefore, it is necessary to pay attention to the reactivity of such sulfur species when the HDS process and active catalysts are to be designed. It is worthwhile to point out that the refractory sulfur species exist in the lighter fraction of heavy gas oil; hence, it may be advantageous to separate the fraction rich in these species from the more reactive fraction to allow the desulfurization of these low reactivity species under more optimum conditions.

CHAPTER VII

COMPARISON OF THE ACTIVITY IN TERMS OF CONVERSION OF DBT AND REFRACTORY SULFUR SPECIES

Two groups of experiments were performed to compare the catalysts. The first group shows the results of the effect of space time at molar H₂/HC ratio of 7.2. The second group shows the corresponding results of the effect of the molar H₂/HC ratio at space time (W/F_{DBT}°) of 6000 kg_{cat}h/kmol. For each group, four sets of catalysts listed below were defined to compare their HDS and HDA activities in heavy gas oil. Every catalyst name contains 2 parts divided by a slash. Left part shows the components loaded by incipient wetness impregnation and the right side the components loaded by ion exchange into zeolite.

Set	Catalysts
1	CoMo/Al ₂ O ₃ , CoMoPtPd/HY and CoMoPd/Pt-HY.
2	CoMoPtPd/HY, CoMoPtPd/Ni-HY and CoMoPd/Pt-HY.
3	CoMo/PdNiPt-HY, CoMoNi/PdPt-HY, and CoMoPtPd/Ni-HY.
4	CoMo/PdNiPt-HY, CoMoNi/PdPt-HY, and CoMoPd/Pt-HY.

7.1 Effect of Space Time at Molar H₂/HC Ratio of 7.2

Tables from pages 162-174 and Figures from pages 163-177 show the hydrodesulfurization conversions of sulfur compounds, hydrogenation conversions of phenanthrene and the molar-averaged conversions in heavy gas oil. These conversions were obtained as a function of space time over basic and noble metals containing zeolite as well as reference catalysts at 65 bar, 310 ° C, 7.2 molar H₂/HC ratio.

7.1.1 HDS of Heavy Gas oil over Conventional CoMo/Al₂O₃ Catalyst, CoMoPtPd/HY and CoMoPd/Pt-HY Catalysts

Table 7.1 shows the molar-averaged conversions (X_{avg}), and conversions of DBT, 4-MDBT, 4,6-DMDBT and phenanthrene over a commercial CoMo/Al₂O₃ catalysts as

well as CoMoPtPd/HY and CoMoPd/Pt-HY catalysts prepared in lab. CoMoPd/Pt-HY exhibited an excellent activity for the HDS of DBT, 4-MDBT, 4,6-DMDBT and hydrogenation of phenanthrene among the catalyst examined, giving conversions from 19.6-26.88%, 17.81-25.56%, 16.1-24.31%, and 39.1-47.65% respectively in the range of space time (W/F_{DBT}^0) of 4000-6000 $Kg_{cat}h/Kmol$. CoMo/ Al_2O_3 and CoMoPtPd/HY were certainly inferior to the former catalyst and their conversions are shown in Table 7.1. Figures 7.1-7.4 illustrate the conversion of alkyldibenzothiophenes in heavy gas oil as a function of space time. HDS reactivity markedly decreased in the order DBT, 4-MDBT, and 4,6-DMDBT over all catalysts.

HDS reactivities of DBT, 4-MDBT, and 4,6-DMDBT were certainly smaller over the CoMoPtPd/HY catalyst. The low performance could be attributed to the sulfidation degree reached for this catalyst, since the degree of metal sulfidation or reduction is affected by the preparation procedure as reported by Pawelec et al., 1997. CoMoPd/Pt-HY exhibited its highest activity for the HDS of sulfur compounds at 6000 $kg_{cat}h/kmol$. The molar-averaged conversion for this catalyst at this space time was 32.7% compared to 21.9% and 28.6 % over CoMoPtPd/HY and CoMo/ Al_2O_3 respectively (Table 7.1 and Figure 7.5). At the same space time phenanthrene also exhibited the highest conversion.

Table 7.1 Molar-averaged conversion and conversions of sulfur compounds and phenanthrene in the HDS and HDA of heavy gas oil over conventional CoMo/ Al_2O_3 (HDS-0) catalyst, CoMoPtPd/HY (HDS-1) and CoMoPd/Pt-HY (HDS-5) catalysts

W/F_{DBT}^0 $Kg_{cat}h/Kmol$	Conversion [%]				$X_{avg}^{(1)}$ [%]
	DBT	4-MDBT	4,6-DMDBT	Phenanthrene	
Catalyst: CoMo/ Al_2O_3					
4000	16.6	14.1	12.3	7.6	24.4
5000	20.2	18.2	16.3	12.3	27.6
6000	24.9	23.0	21.1	18.3	28.6
Catalyst: CoMoPtPd/HY					
4000	8.5	7.4	6.2	3.2	13.4
5000	11.9	9.7	8.0	5.0	16.4
6000	15.0	14.2	11.7	7.9	21.9
Catalyst: CoMoPd/Pt-HY					
4000	19.6	17.8	16.1	39.1	24.1
5000	24.4	22.9	21.4	45.3	28.6
6000	26.9	25.6	24.3	47.7	32.3

⁽¹⁾Molar-averaged conversion

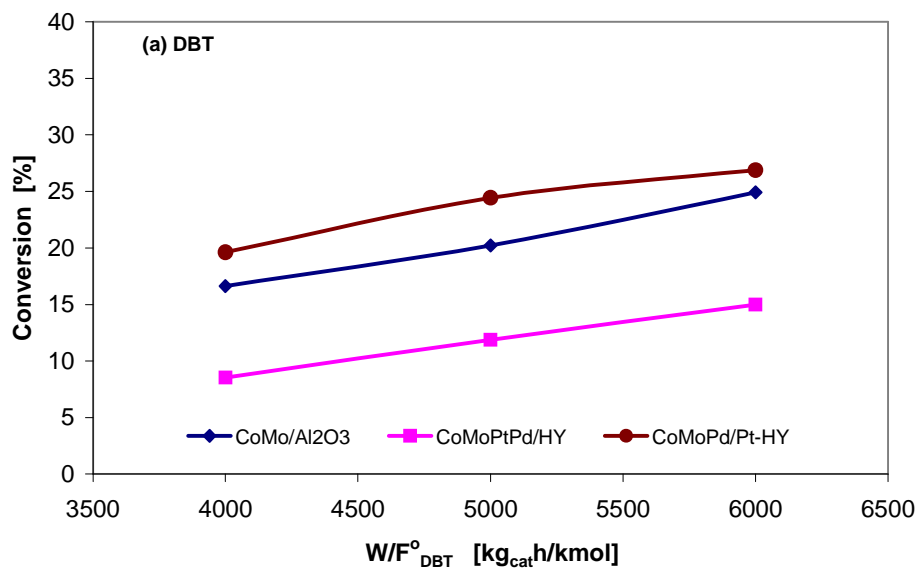


Figure 7.1 Hydrodesulfurization conversions of dibenzothiophene (DBT) in heavy gas oil over CoMo/Al₂O₃, CoMoPtPd/HY, and CoMoPd/Pt-HY catalysts. (65 bar, 310 °C, 7.2 molar H₂/HGO ratio).

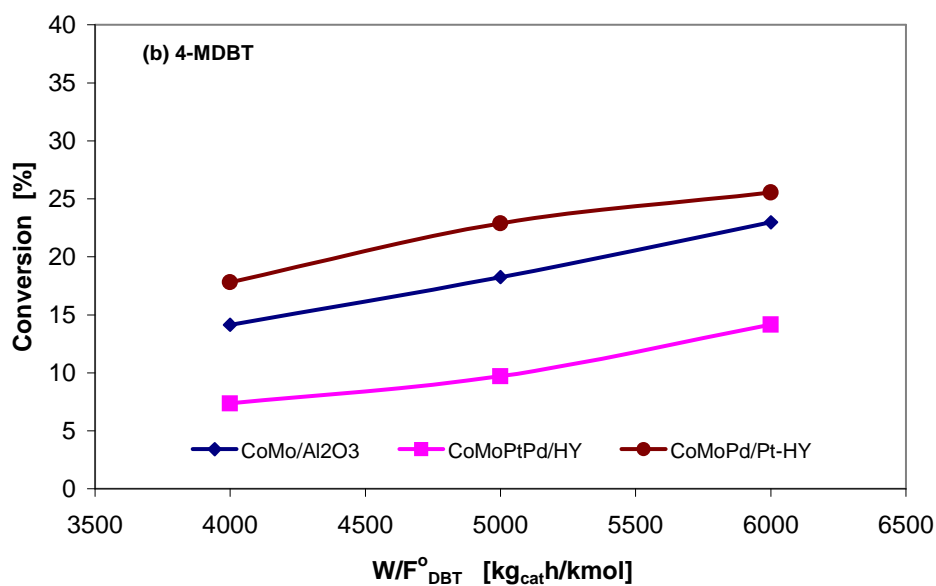


Figure 7.2 Hydrodesulfurization conversions of 4-methyldibenzothiophene (4-MDBT) in heavy gas oil over CoMo/Al₂O₃, CoMoPtPd/HY, and CoMoPd/Pt-HY catalysts. (65 bar, 310 °C, 7.2 molar H₂/HGO ratio).

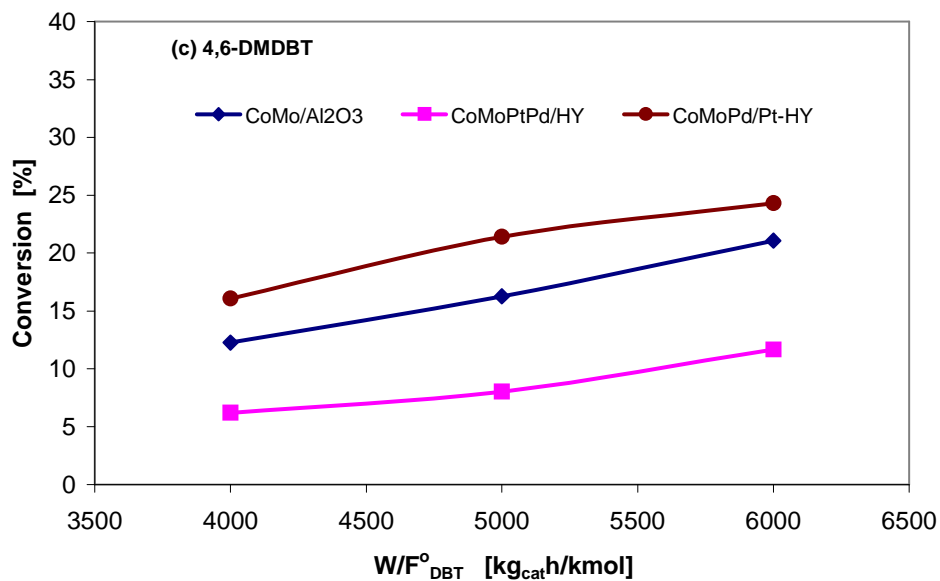


Figure 7.3 Hydrodesulfurization conversions of 4,6-dimethyldibenzothiophene (4,6-DMDBT) in heavy gas oil over CoMo/Al₂O₃, CoMoPtPd/HY, and CoMoPd/Pt-HY catalysts. (65 bar, 310 °C, 7.2 molar H₂/HGO ratio).

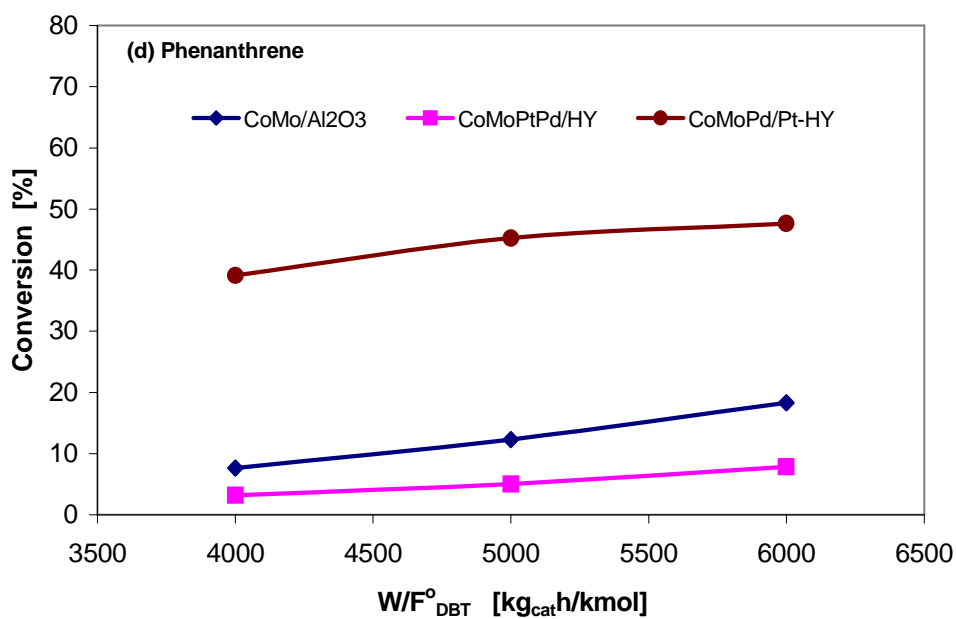


Figure 7.4 Hydrogenation conversions of phenanthrene in heavy gas oil over CoMo/Al₂O₃, CoMoPtPd/HY, and CoMoPd/Pt-HY catalysts. (65 bar, 310 °C, 7.2 molar H₂/HGO ratio).

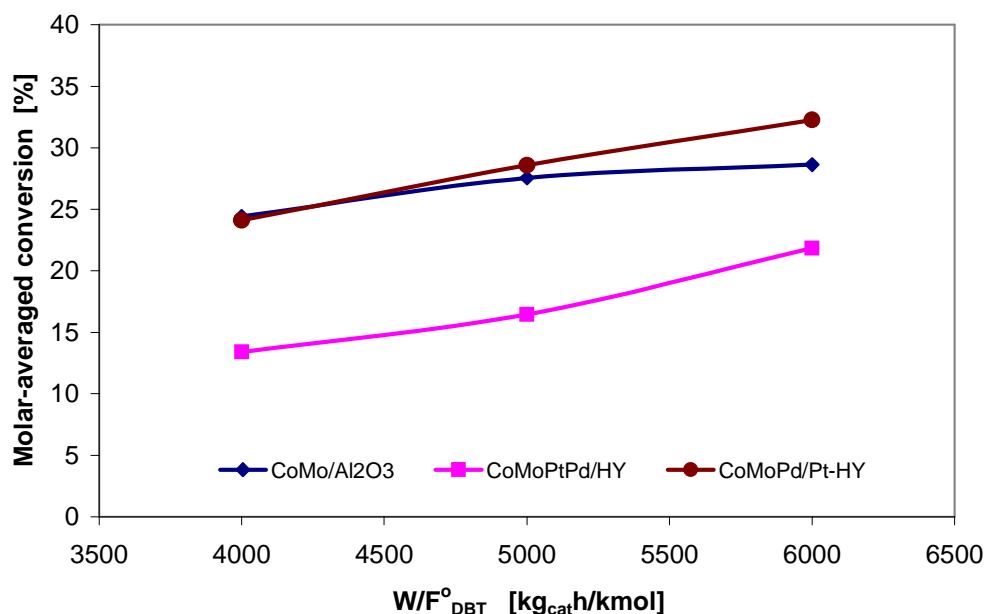


Figure 7.5 Molar-averaged conversions in heavy gas oil over CoMo/Al₂O₃, CoMoPtPd/HY, and CoMoPd/Pt-HY catalysts. (65 bar, 310 °C, 7.2 molar H₂/HGO ratio).

7.1.2 HDS of Heavy Gas Oil over CoMoPtPd/HY, CoMoPtPd/Ni-HY and CoMoPd/Pt-HY Catalysts

Table 7.2 shows the molar-averaged conversions (X_{avg}), and conversions of DBT, 4-MDBT, 4,6-DMDBT and phenanthrene over CoMoPtPd/Ni-HY and CoMoPd/Pt-HY catalysts as well as CoMoPtPd/HY. CoMoPd/Pt-HY exhibited the highest conversion for the HDS of DBT, 4-MDBT, 4,6-DMDBT but did not for the hydrogenation of phenanthrene among the catalyst examined giving conversions from 19.6-26.88%, 17.81-25.56%, 16.1-24.31%, and 39.1-47.65% respectively in the range of space time (W/F°_{DBT}) of 4000-6000 Kg_{cat}/h/Kmol. CoMoPtPd/HY and CoMoPtPd/Ni-HY were certainly inferior to the former catalyst, providing the conversions showed in Table 7.2. However, CoMoPtPd/Ni-HY showed the highest activity for the hydrogenation of phenanthrene giving conversions from 53-58.4% in the same range of space time.

Figures 7.6-7.9 illustrate the conversion of alkyldibenzothiophenes in heavy gas oil as a function of space time. HDS reactivity clearly decreased in the order DBT, 4-MDBT, and 4,6-DMDBT over all catalysts.

HDS reactivities of DBT, 4-MDBT, and 4,6-DMDBT decreased certainly in the order of CoMoPtPd/HY < CoMoPtPd/Ni-HY < CoMoPd/Pt-HY, while hydrogenation reactivities of phenanthrene were CoMoPtPd/HY < CoMoPd/Pt-HY < CoMoPtPd/Ni-HY.

CoMoPd/Pt-HY exhibited the highest molar-averaged conversions giving 24.1-32.3% in the interval of space time studied compared to 13.4-21.9% over CoMoPtPd/HY and 22.7-27.6% over CoMoPtPd/Ni-HY (Table 7.2 and Figure 7.10).

Table 7.2 Molar-averaged conversions and conversions of sulfur compounds and phenanthrene in the HDS and HDA of heavy gas oil over CoMoPtPd/HY (HDS-1), CoMoPtPd/Ni-HY (HDS-3) and CoMoPd/Pt-HY (HDS-5) catalysts

W/F ⁰ _{DBT} Kg _{cat} h/Kmol	Conversion [%]				X _{avg} ⁽¹⁾ [%]
	DBT	4-MDBT	4,6-DMDBT	Phenanthrene	
Catalyst: CoMoPtPd/HY					
4000	8.5	7.4	6.2	3.2	13.4
5000	11.9	9.7	8.0	5.0	16.4
6000	15.0	14.2	11.7	7.9	21.9
Catalyst: CoMoPtPd/Ni-HY					
4000	19.0	15.5	14.6	53.0	22.8
5000	20.9	17.9	16.8	57.1	26.2
6000	22.5	18.7	17.7	58.4	27.6
Catalyst: CoMoPd/Pt-HY					
4000	19.6	17.8	16.1	39.1	24.1
5000	24.4	22.9	21.4	45.3	28.6
6000	26.9	25.6	24.3	47.7	32.3

⁽¹⁾Molar-averaged conversion

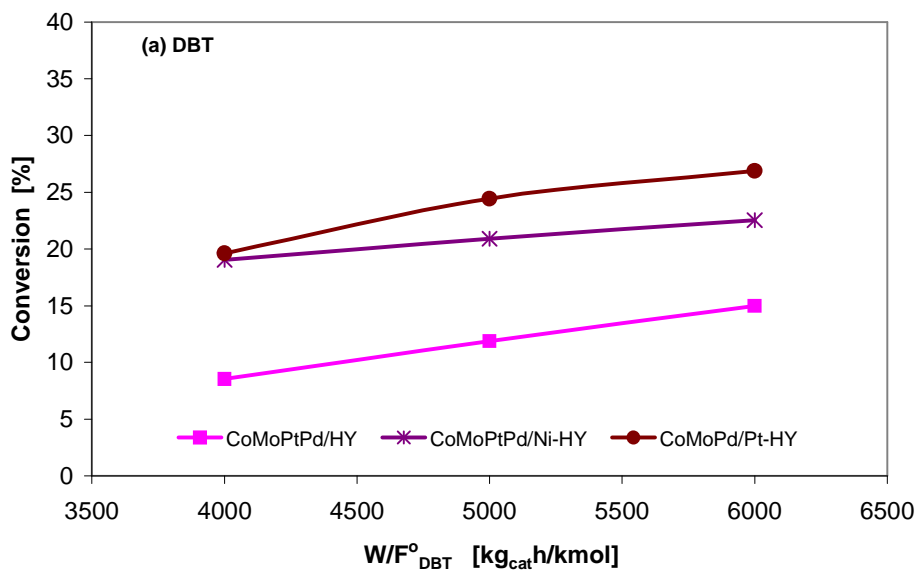


Figure 7.6 Hydrodesulfurization conversions of dibenzothiophene (DBT) in heavy gas oil over CoMoPtPd/HY, CoMoPtPd/Ni-HY and CoMoPd/Pt-HY catalysts. (65 bar, 310 °C, 7.2 molar H₂/HGO ratio).

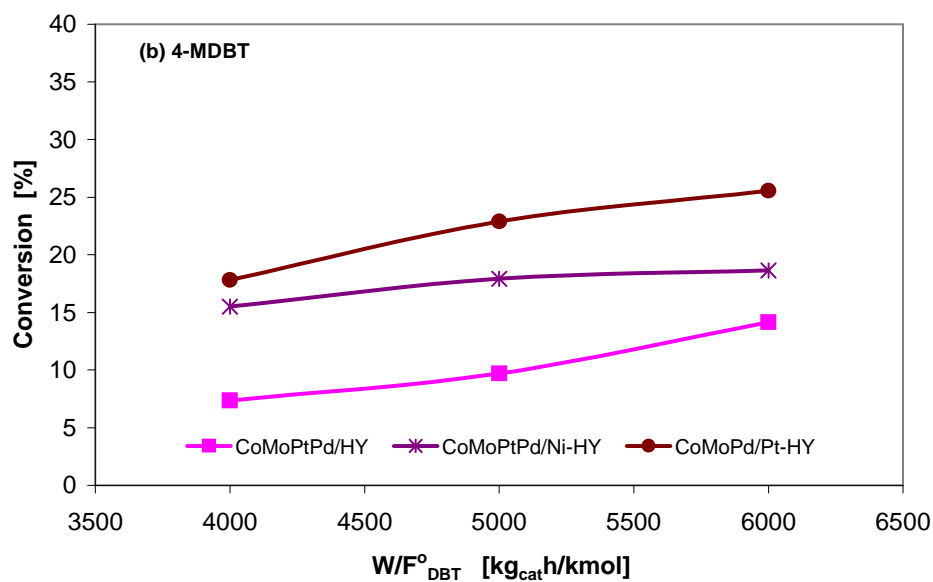


Figure 7.7 Hydrodesulfurization conversions of 4-methyldibenzothiophene (4-MDBT) in heavy gas oil over CoMoPtPd/HY, CoMoPtPd/Ni-HY and CoMoPd/Pt-HY catalysts. (65 bar, 310 °C, 7.2 molar H₂/HGO ratio).

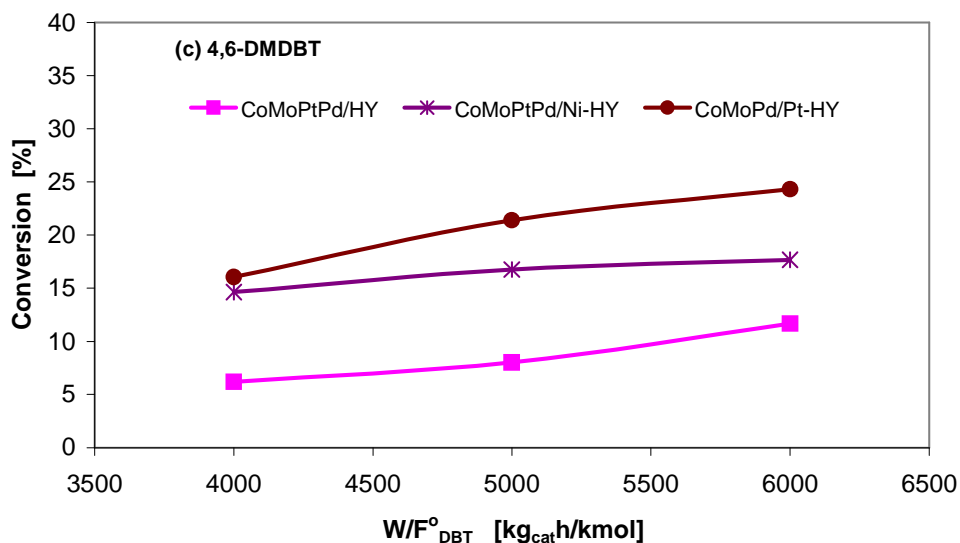


Figure 7.8 Hydrodesulfurization conversions of 4,6-dimethyldibenzothiophene (4,6-DMDBT) in heavy gas oil over CoMoPtPd/HY, CoMoPtPd/Ni-HY and CoMoPd/Pt-HY catalysts. (65 bar, 310 °C, 7.2 molar H₂/HGO ratio).

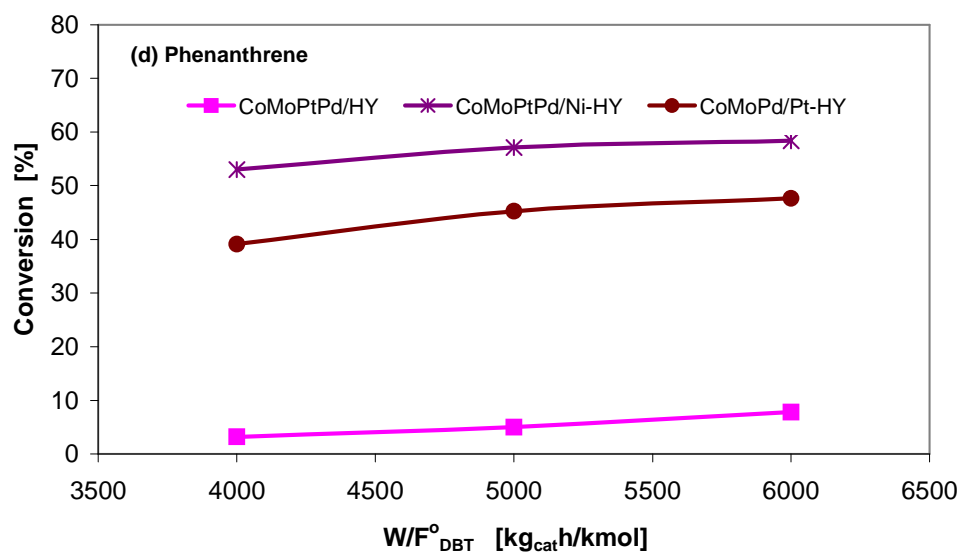


Figure 7.9 Hydrodesulfurization conversions of phenanthrene in heavy gas oil over CoMoPtPd/HY, CoMoPtPd/Ni-HY and CoMoPd/Pt-HY catalysts. (65 bar, 310 °C, 7.2 molar H₂/HGO ratio).

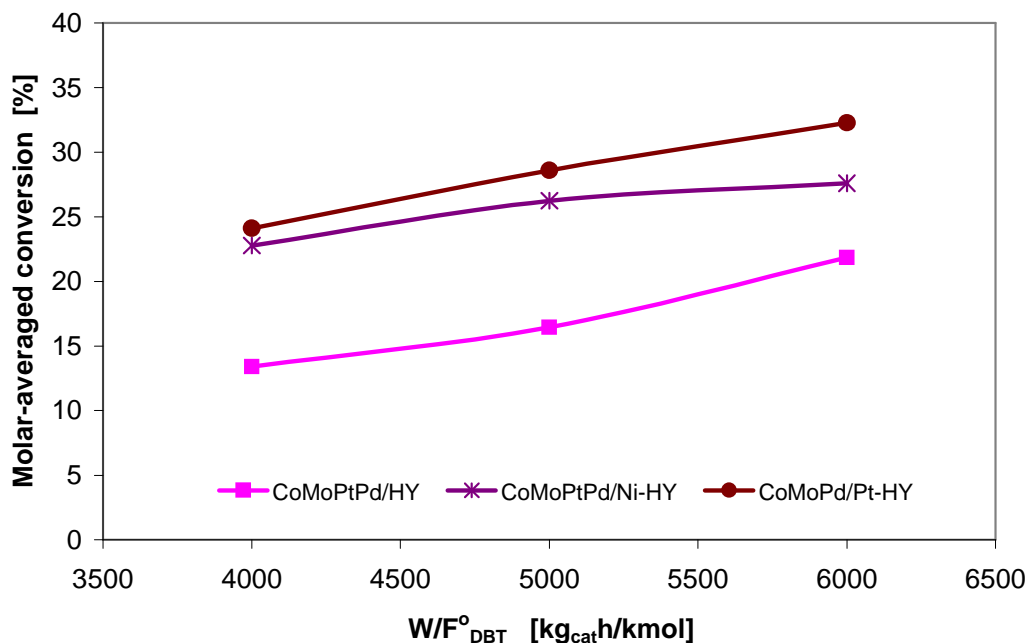


Figure 7.10 Molar-averaged conversions in heavy gas oil over CoMoPtPd/HY, CoMoPtPd/Ni-HY and CoMoPd/Pt-HY catalysts. (65 bar, 310 °C, 7.2 molar H₂/HGO ratio).

7.1.3 HDS of Heavy Gas Oil over CoMo/PdNiPt-HY, CoMoNi/PdPt-HY, and CoMoPtPd/Ni-HY Catalysts

Table 7.3 shows the molar-averaged conversions (X_{avg}), and conversions of DBT, 4-MDBT, 4,6-DMDBT and phenanthrene over CoMo/PdNiPt-HY and CoMoNi/PdPt-HY catalysts as well as CoMoPtPd/Ni-HY. CoMoNi/PdPt-HY exhibited the best activity for the HDS of DBT, 4-MDBT, 4,6-DMDBT but did not for the hydrogenation of phenanthrene among the catalyst examined giving conversions from 24.1-28.3%, 22.6-27.12%, 20.8-25.6%, and 33.9-39.6% respectively in the range of space time (W/F_{DBT}°) of 4000-6000 kg_{cat}h/kmol.

CoMo/PdNiPt-HY and CoMoPtPd/Ni-HY were certainly inferior to the former catalyst, providing the conversions showed in Table 7.2, except, CoMoPtPd/Ni-HY

which showed the highest activity for the hydrogenation of phenanthrene giving conversions from 53-58.4% in the same range of space time.

Figures 7.11-7.14 illustrate the conversion of alkyldibenzothiophenes in heavy gas oil as a function of space time. HDS reactivity evidently decreased in the order DBT, 4-MDBT, and 4,6-DMDBT over all catalysts.

HDS reactivities of DBT, 4-MDBT, and 4,6-DMDBT decrease certainly in the order of CoMo/PdNiPt-HY < CoMoPtPd/Ni-HY < CoMoNi/PdPt-HY in the interval space time of 4000-6000 Kg_{cat}h/Kmol, while hydrogenation reactivities of phenanthrene were in the order CoMo/PdNiPt-HY < CoMoNi/PdPt-HY < CoMoPtPd/Ni-HY for the same interval of space time. CoMo/PdNiPt-HY catalyst had better activity for the HDS reactions than CoMoPtPd/Ni-HY only at space time of 6000 kg_{cat}h/kmol, giving conversions of DBT, 4-MDBT, 4,6-DMDBT of 22.8, 20.4 and 18% vs 22.5, 18.7 and 17.7% correspondingly.

CoMoNi/PdPt-HY exhibited the highest molar-averaged conversions giving 27.1-32.5% in the interval of space time studied vs 17.44-30% over CoMo/PdNiPt-HY and 22.7-27.6% over CoMoPtPd/Ni-HY (Table 7.3 and Figure 7.15).

Table 7.3 Molar-averaged conversions and conversions of sulfur compounds and phenanthrene in the HDS and HDA of heavy gas oil over CoMo/PdNiPt-HY (HDS-8), CoMoNi/PdPt-HY (HDS-10), and CoMoPtPd/Ni-HY (HDS-3) catalysts

W/F ^o _{DBT} Kg _{cat} h/Kmol	Conversion [%]				Xavg ⁽¹⁾ [%]
	DBT	4-MDBT	4,6-DMDBT	Phenanthrene	
Catalyst: CoMo/PdNiPt-HY					
4000	10.8	9.3	7.4	4.6	17.4
5000	17.4	15.5	13.6	10.4	24.5
6000	22.8	20.4	18.0	14.3	30.0
Catalyst: CoMoNi/PdPt-HY					
4000	24.1	22.6	20.8	33.9	27.1
5000	25.8	24.4	23.0	36.8	30.1
6000	28.3	27.1	25.6	39.6	32.5
Catalyst: CoMoPtPd/Ni-HY					
4000	19.0	15.5	14.6	53.0	22.8
5000	20.9	17.9	16.8	57.1	26.2
6000	22.5	18.7	17.7	58.4	27.6

⁽¹⁾Molar-averaged conversion

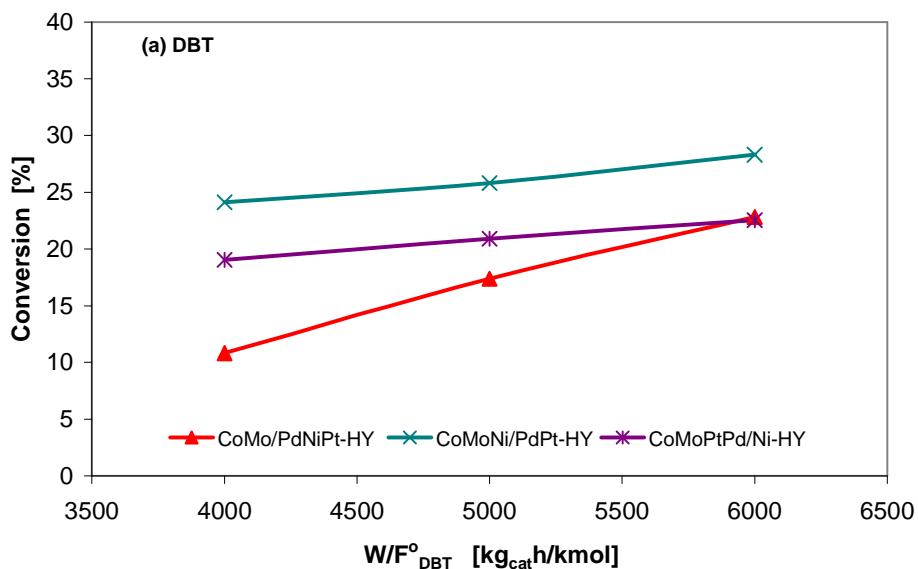


Figure 7.11 Hydrodesulfurization conversions of dibenzothiophene (DBT) in heavy gas oil over CoMo/PdNiPt-HY, CoMoNi/PdPt-HY and CoMoPtPd/Ni-HY catalysts. (65 bar, 310 °C, 7.2 molar H_2/HGO ratio).

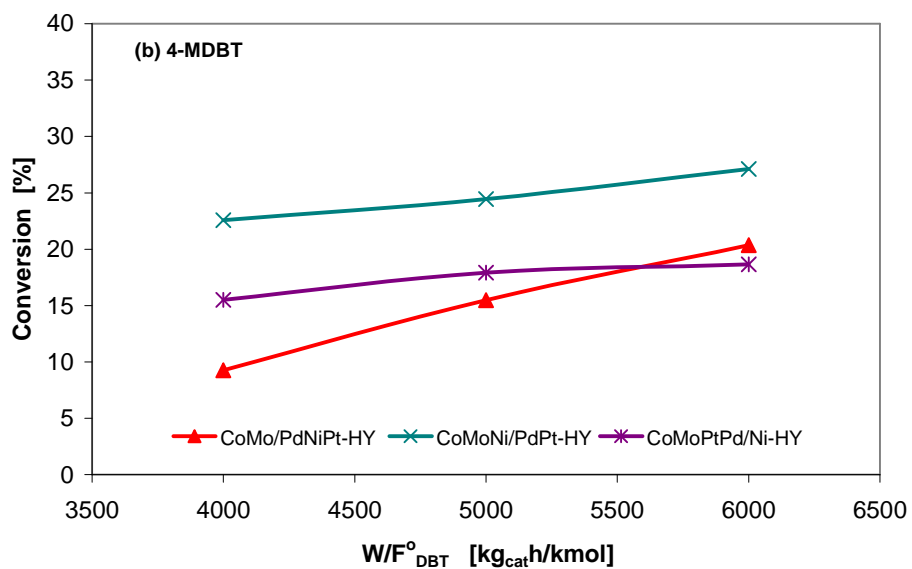


Figure 7.12 Hydrodesulfurization conversions of 4-methyldibenzothiophene (4-MDBT) in heavy gas oil over CoMo/PdNiPt-HY, CoMoNi/PdPt-HY and CoMoPtPd/Ni-HY catalysts. (65 bar, 310 °C, 7.2 molar H_2/HGO ratio).

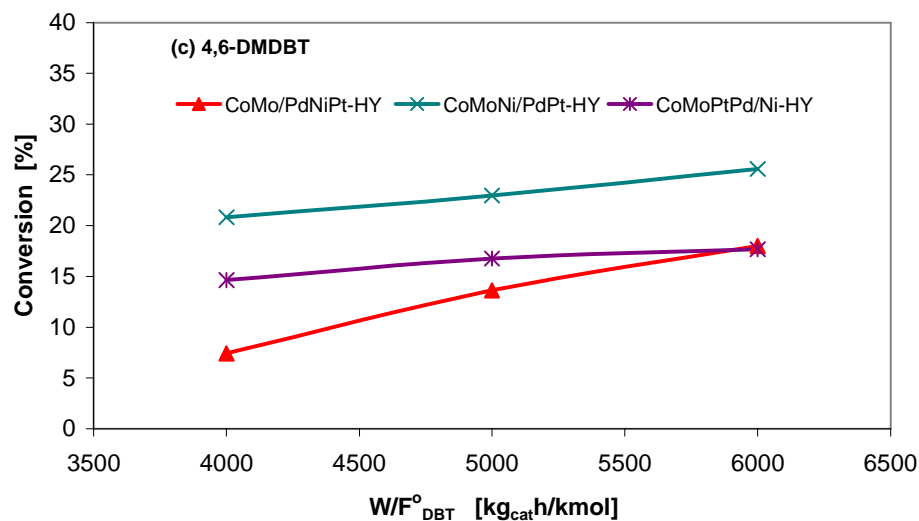


Figure 7.13 Hydrodesulfurization conversions of 4,6-dimethyldibenzothiophene (4,6-DMDBT) in heavy gas oil over CoMo/PdNiPt-HY, CoMoNi/PdPt-HY and CoMoPtPd/Ni-HY catalysts. (65 bar, 310 °C, 7.2 molar H₂/HGO ratio).

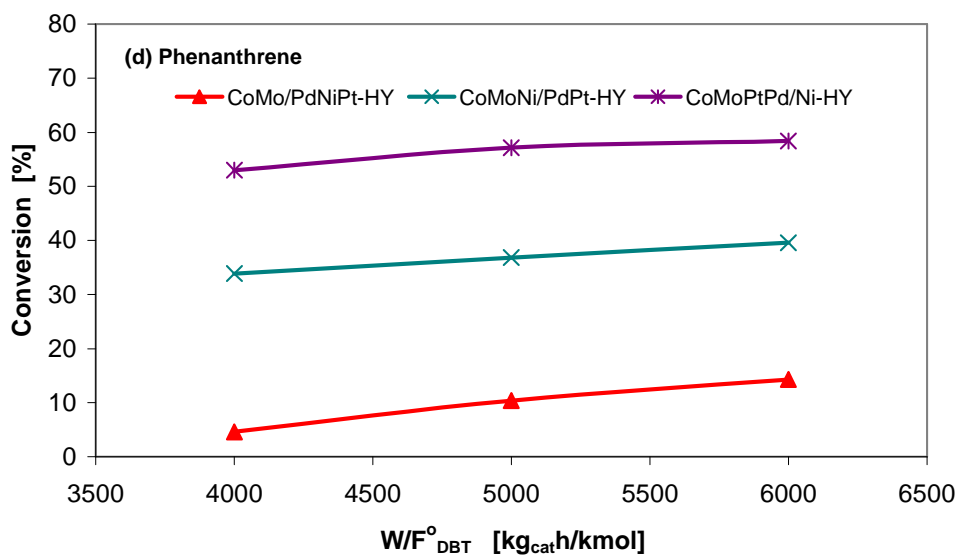


Figure 7.14 Hydrogenation conversions of phenanthrene in heavy gas oil over CoMo/PdNiPt-HY, CoMoNi/PdPt-HY and CoMoPtPd/Ni-HY catalysts. (65 bar, 310 °C, 7.2 molar H₂/HGO ratio).

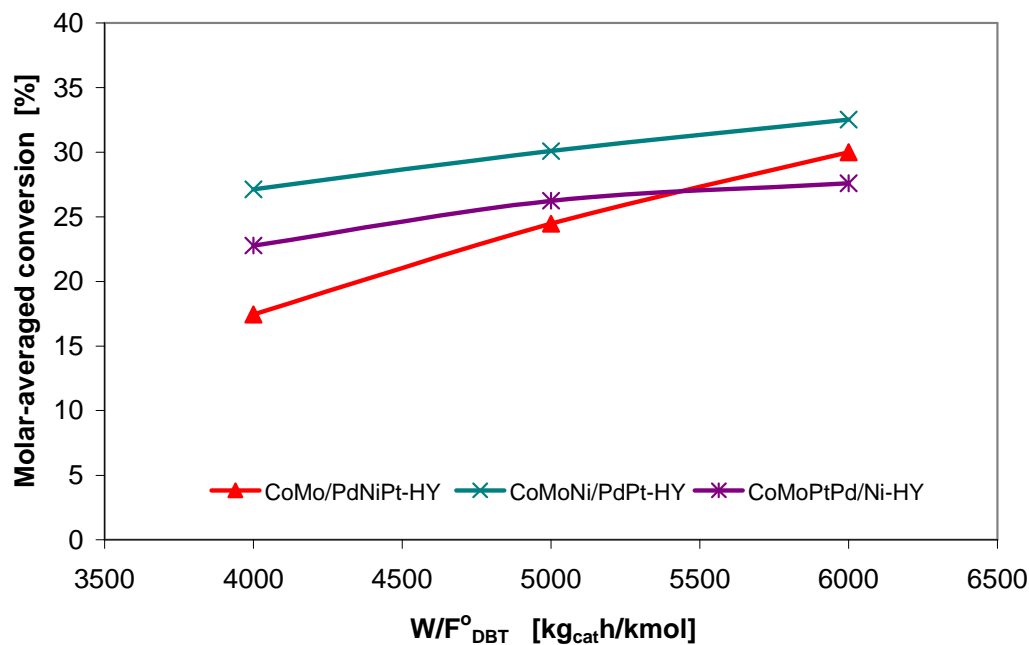


Figure 7.15 Molar-averaged conversions in heavy gas oil over CoMo/PdNiPt-HY, CoMoNi/PdPt-HY and CoMoPtPd/Ni-HY catalysts. (65 bar, 310 °C, 7.2 molar H₂/HGO ratio).

7.1.4 HDS of Heavy Gas Oil over CoMo/PdNiPt-HY, CoMoNi/PdPt-HY, and CoMoPd/Pt-HY Catalysts

Table 7.4 shows the molar-averaged conversions (X_{avg}), and conversions of DBT, 4-MDBT, 4,6-DMDBT and phenanthrene over CoMo/PdNiPt-HY and CoMoNi/PdPt-HY catalysts as well as CoMoPd/Pt-HY catalyst prepared in lab. CoMoNi/PdPt-HY exhibited an excellent activity for the HDS of DBT, 4-MDBT, 4,6-DMDBT, but did not for the hydrogenation of phenanthrene among the catalyst examined giving conversions from 24.1-28.3%, 22.6-27.12%, 20.8-25.6%, 33.9-39.6% respectively in the range of space time (W/F_{DBT}°) of 4000-6000 kg_{cat}h/kmol. CoMo/PdNiPt-HY and CoMoPd/Pt-HY were certainly inferior to the former catalyst, providing the conversions showed in

Table 7.4. However, CoMoPd/Pt-HY shows the best hydrogenation for phenanthrene providing conversions from 39.11-47.7% in the same range of space time.

Figures 7.16-7.19 illustrate the conversion of alkyldibenzothiophenes in heavy gas oil as a function of space time. HDS reactivity evidently decreased in the order DBT, 4-MDBT, and 4,6-DMDBT over all catalysts. HDS reactivities of DBT, 4-MDBT, and 4,6-DMDBT decline certainly in the order of CoMo/PdNiPt-HY < CoMoPd/Pt-HY < CoMoNi/PdPt-HY in the range space time of 4000-6000 kg_{cat}/kmol, while hydrogenation reactivities of phenanthrene were in the order of CoMo/PdNiPt-HY < CoMoNi/PdPt-HY < CoMoPd/Pt-HY for the same range of space time.

CoMoNi/PdPt-HY exhibited the highest molar-averaged conversions (Figure 7.20) giving 27.1-30.1% in the interval of space time of 4000-5000 kg_{cat}/kmol. However, its conversion at 6000 kg_{cat}/kmol was quite close to CoMo/PdNiPt-HY (32.5 vs 30%) and similar to CoMoPd/Pt-HY catalyst (32.5 vs 32.3%).

Table 7.4 Molar-averaged conversions and conversions of sulfur compounds and phenanthrene in the HDS and HDA of heavy gas oil over CoMo/PdNiPt-HY (HDS-8), CoMoNi/PdPt-HY (HDS-10), and CoMoPd/Pt-HY (HDS-5) catalysts

W/F ^o _{DBT} Kg _{cat} /Kmol	Conversion [%]				X _{avg} ⁽¹⁾ [%]
	DBT	4-MDBT	4,6-DMDBT	Phenanthrene	
Catalyst: CoMo/PdNiPt-HY					
4000	10.8	9.3	7.4	4.6	17.4
5000	17.4	15.5	13.6	10.4	24.5
6000	22.8	20.4	18.0	14.3	30.0
Catalyst: CoMoNi/PdPt-HY					
4000	24.1	22.6	20.8	33.9	27.1
5000	25.8	24.4	23.0	36.8	30.1
6000	28.3	27.1	25.6	39.6	32.5
Catalyst: CoMoPd/Pt-HY					
4000	19.6	17.8	16.1	39.1	24.1
5000	24.4	22.9	21.4	45.3	28.6
6000	26.9	25.6	24.3	47.7	32.3

⁽¹⁾Molar-averaged conversion

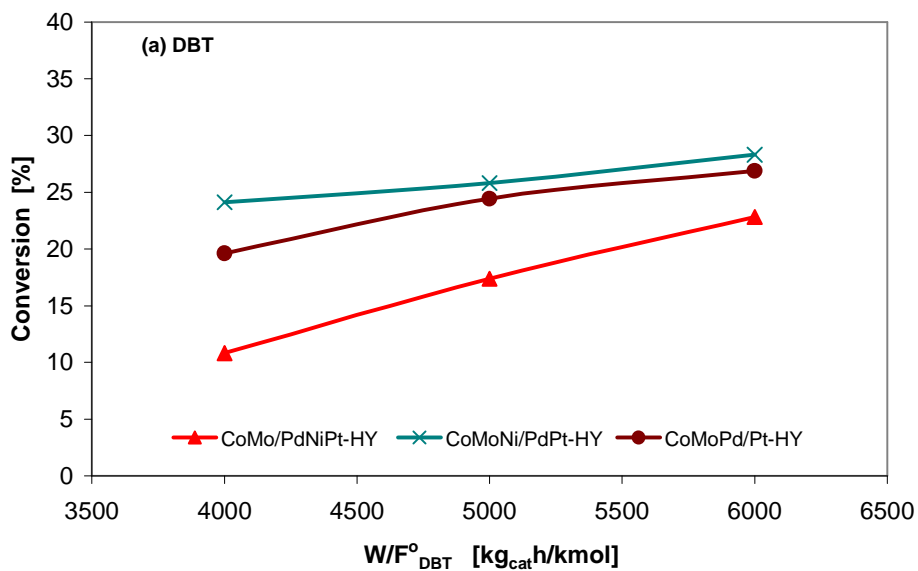


Figure 7.16 Hydrodesulfurization conversions of dibenzothiophene (DBT) in heavy gas oil over CoMo/PdNiPt-HY, CoMoNi/PdPt-HY and CoMoPd/Pt-HY catalysts. (65 bar, 310 °C, 7.2 molar H₂/HGO ratio).

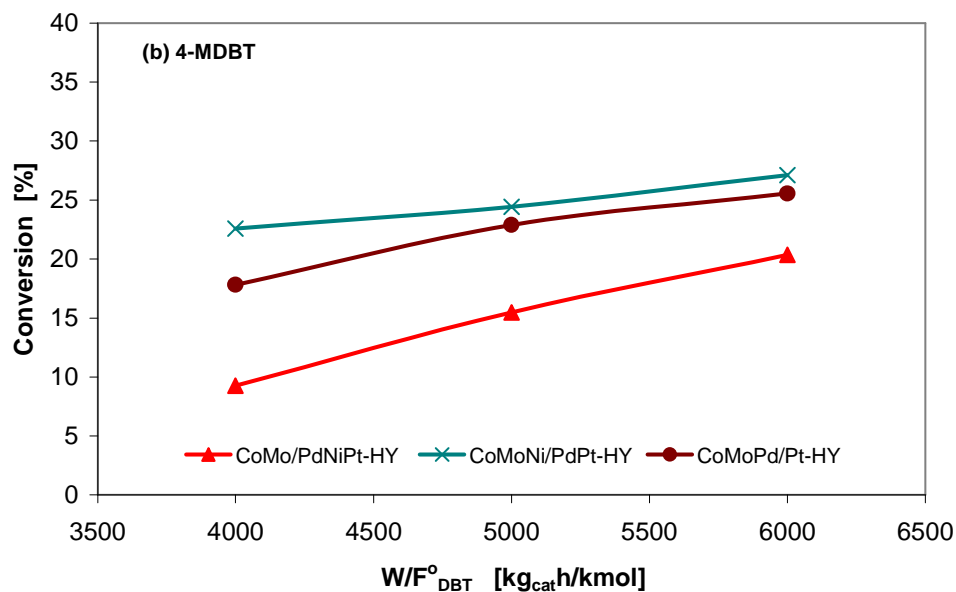


Figure 7.17 Hydrodesulfurization conversions of 4-methyldibenzothiophene (4-MDBT) in heavy gas oil over CoMo/PdNiPt-HY, CoMoNi/PdPt-HY and CoMoPd/Pt-HY catalysts. (65 bar, 310 °C, 7.2 molar H₂/HGO ratio).

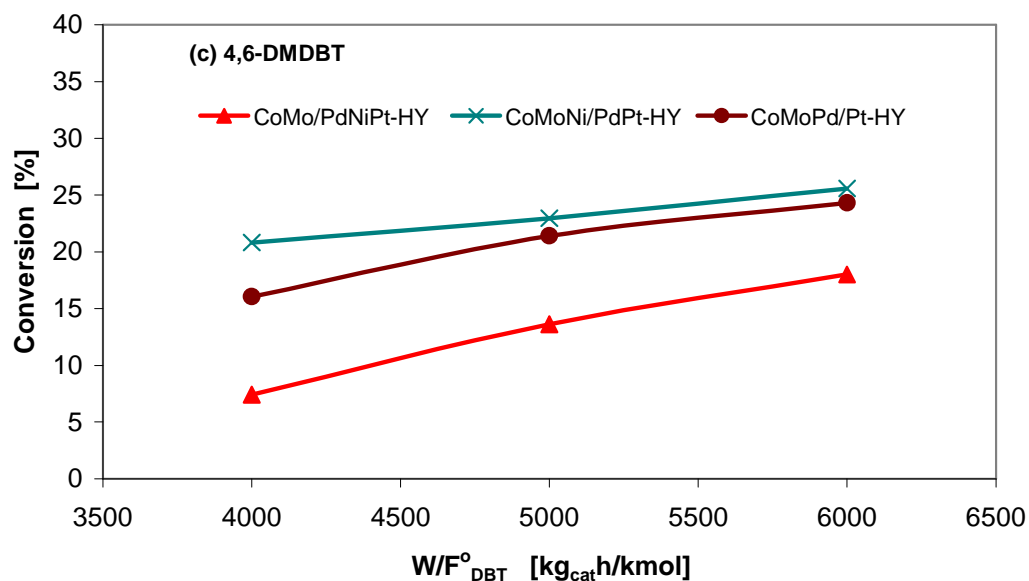


Figure 7.18 Hydrodesulfurization conversions of 4,6-dimethyldibenzothiophene (4,6-DMDBT) in heavy gas oil over CoMo/PdNiPt-HY, CoMoNi/PdPt-HY and CoMoPd/Pt-HY catalysts. (65 bar, 310 °C, 7.2 molar H₂/HGO ratio).

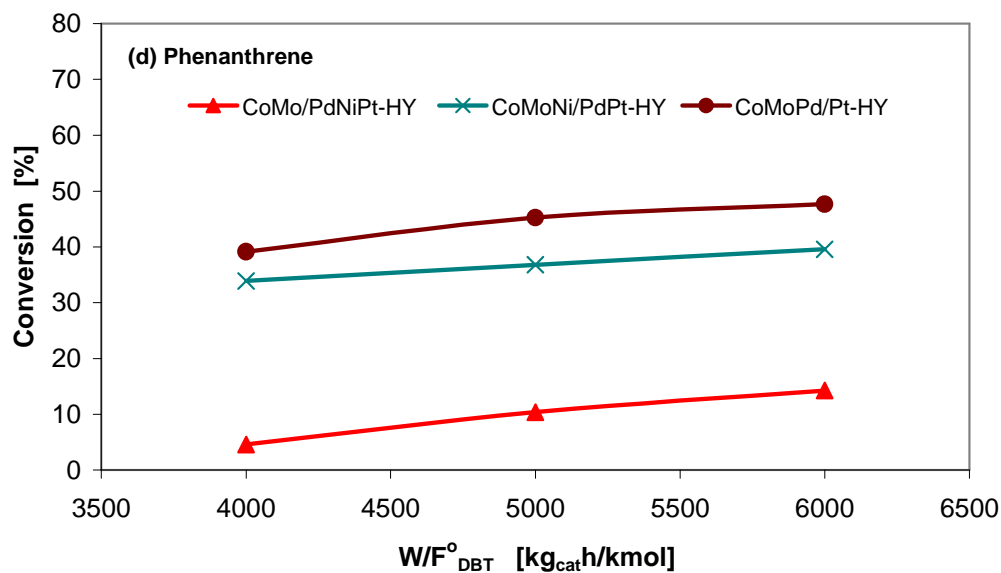


Figure 7.19 Hydrodesulfurization conversions of phenanthrene in heavy gas oil over CoMo/PdNiPt-HY, CoMoNi/PdPt-HY and CoMoPd/Pt-HY catalysts. (65 bar, 310 °C, 7.2 molar H₂/HGO ratio).

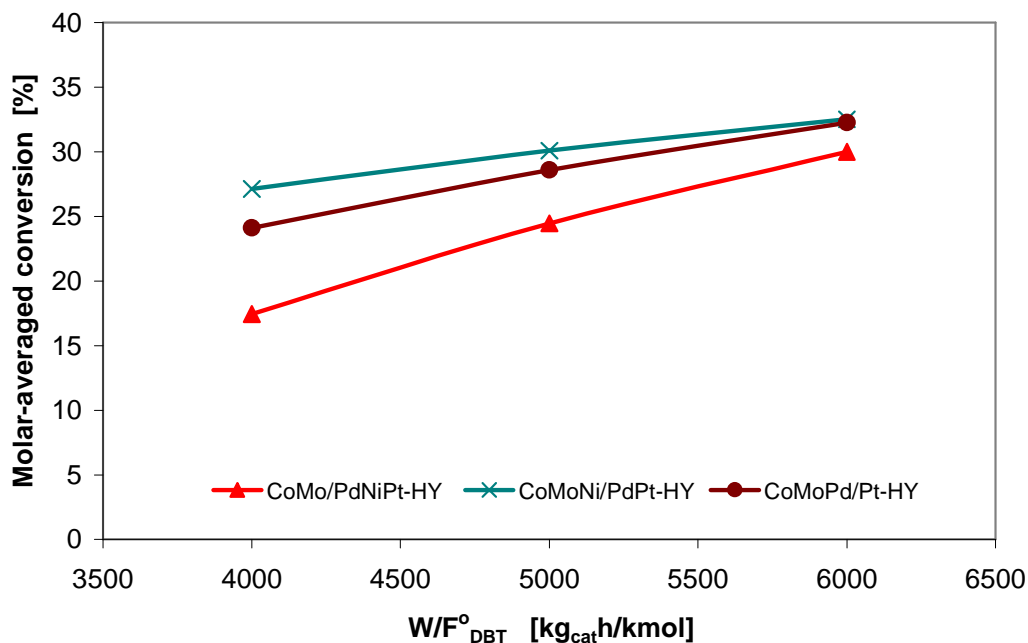


Figure 7.20 Molar-averaged conversions in heavy gas oil over CoMo/PdNiPt-HY, CoMoNi/PdPt-HY and CoMoPd/Pt-HY catalysts. (65 bar, 310 °C, 7.2 molar H₂/HGO ratio).

7.2 Effect of the Molar H₂/HC Ratio at Space Time of 6000 kg_{cat}h/kmol

This part shows the results of the effect of molar H₂/HC ratio on the HDS and HDA reactions in heavy gas oil at space time (W/F°_{DBT}) of 6000 kg_{cat}h/kmol. The three sets of catalyst mentioned below were defined to compare their activities.

Set	Catalysts
1	CoMoPtPd/HY, CoMoPtPd/Ni-HY and CoMoPd/Pt-HY catalysts.
2	CoMo/PdNiPt-HY, CoMoNi/PdPt-HY, and CoMoPtPd/Ni-HY.
3	CoMo/PdNiPt-HY, CoMoNi/PdPt-HY, and CoMoPd/Pt-HY.

Tables from pages 179-187 and Figures from pages 179-189 show the hydrodesulfurization conversions of sulfur compounds, hydrogenation conversion of phenanthrene and molar-averaged conversion in heavy gas oil as a function of the H₂/HC

ratio over basic and noble metals containing zeolite catalysts at the experimental conditions of 65 bar, 310 °C, and space time (W/F_{DBT}^0) of 6000 kg_{cat}/h/kmol.

7.2.1 HDS of Heavy Gas Oil over CoMoPtPd/HY, CoMoPtPd/Ni-HY, and CoMoPd/Pt-HY Catalysts

Table 7.5 shows the molar-averaged conversions (X_{avg}), and conversions of DBT, 4-MDBT, 4,6-DMDBT and phenanthrene over CoMoPtPd/Ni-HY and CoMoPd/Pt-HY catalysts as well as CoMoPtPd/HY. All catalysts showed their best HDS and HDA performance at molar H₂/HC ratio of 11.2.

CoMoPd/Pt-HY exhibited an excellent activity for the HDS of DBT, 4-MDBT, 4,6-DMDBT but did not for the hydrogenation of phenanthrene among the catalyst examined giving conversions from 26.8-34.7%, 25.6-33.2%, 24.31-32%, and 47.65-56.45% respectively in the range of the molar-averaged conversion of 7.2-11.2. CoMoPtPd/HY and CoMoPtPd/Ni-HY were certainly inferior to the former catalyst in HDS, providing the conversions showed in Table 7.5. However, for the hydrogenation of phenanthrene CoMoPtPd/Ni-HY showed the highest activity, giving conversions from 58.4-66.1% in the same range of space time.

Figures 7.21-7.24 illustrate the conversion of alkyldibenzothiophenes and phenanthrene in heavy gas oil as a function of the molar H₂/HC ratio. HDS reactivity clearly decreased in the order DBT, 4-MDBT, and 4,6-DMDBT over all catalysts.

The results of the space time study show that HDS reactivities of DBT, 4-MDBT, and 4,6-DMDBT decrease certainly in the order of CoMoPtPd/HY < CoMoPtPd/Ni-HY < CoMoPd/Pt-HY, while hydrogenation reactivities of phenanthrene was CoMoPtPd/HY < CoMoPd/Pt-HY < CoMoPtPd/Ni-HY

CoMoPd/Pt-HY also exhibited the highest molar-averaged conversions giving 32.3-39.1% in the interval of H₂/HC studied vs 21.9-25.1% over CoMoPtPd/HY and 27.6-35.7% over CoMoPtPd/Ni-HY (Table 7.5 and Figure 7.25).

Table 7.5 Molar-averaged conversion and conversions of sulfur compounds and phenanthrene in the HDS and HDA of heavy gas oil over CoMoPtPd/HY (HDS-1), CoMoPtPd/Ni-HY (HDS-3), and CoMoPd/Pt-HY (HDS-5) catalysts

H ₂ /HGO mol ratio	Conversion [%]				X _{avg} ⁽¹⁾ [%]
	DBT	4-MDBT	4,6-DMDBT	Phenanthrene	
Catalyst: CoMoPtPd/HY					
7.2	15.0	14.2	11.7	7.8	21.9
9.2	16.0	14.9	13.8	10.1	24.3
11.2	16.3	15.5	14.4	11.7	25.1
Catalyst: CoMoPtPd/Ni-HY					
7.2	22.5	18.7	17.7	58.4	27.6
9.2	28.5	23.8	23.0	62.5	35.4
11.2	33.0	28.7	27.5	66.1	35.7
Catalyst: CoMoPd/Pt-HY					
7.2	26.9	25.6	24.3	47.7	32.3
9.2	32.9	31.0	29.31	53.4	37.1
11.2	34.7	33.2	32.0	56.5	39.1

⁽¹⁾Molar-averaged conversion

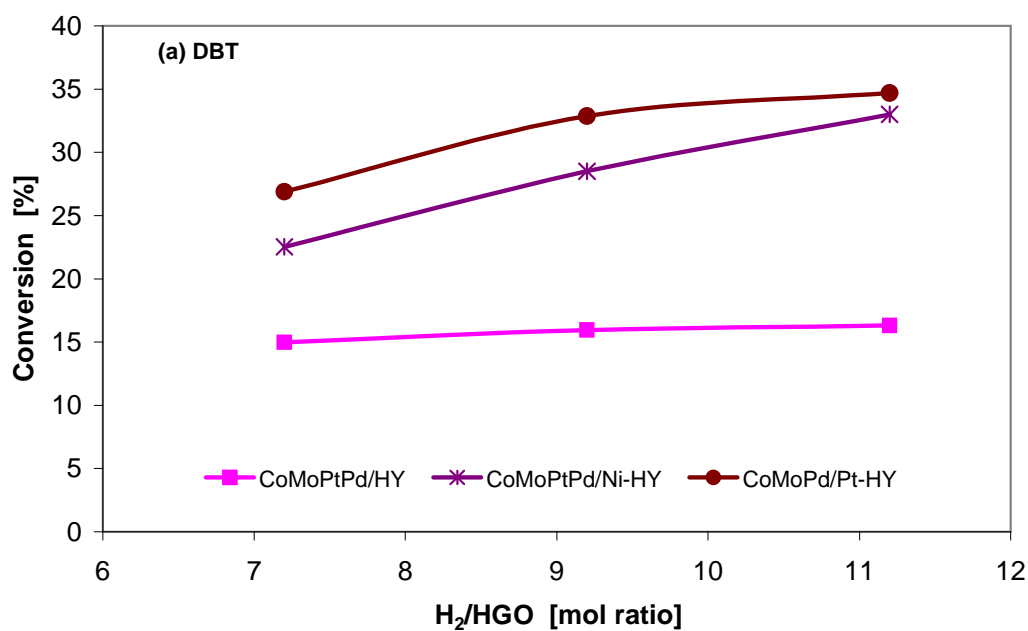


Figure 7.21 Hydrodesulfurization conversions of dibenzothiophene (DBT) in heavy gas oil over CoMoPtPd/HY, CoMoPtPd/Ni-HY and CoMoPd/Pt-HY catalysts. (65 bar, 310 °C, and space time of 6000 kg_{cat}h/kmol).

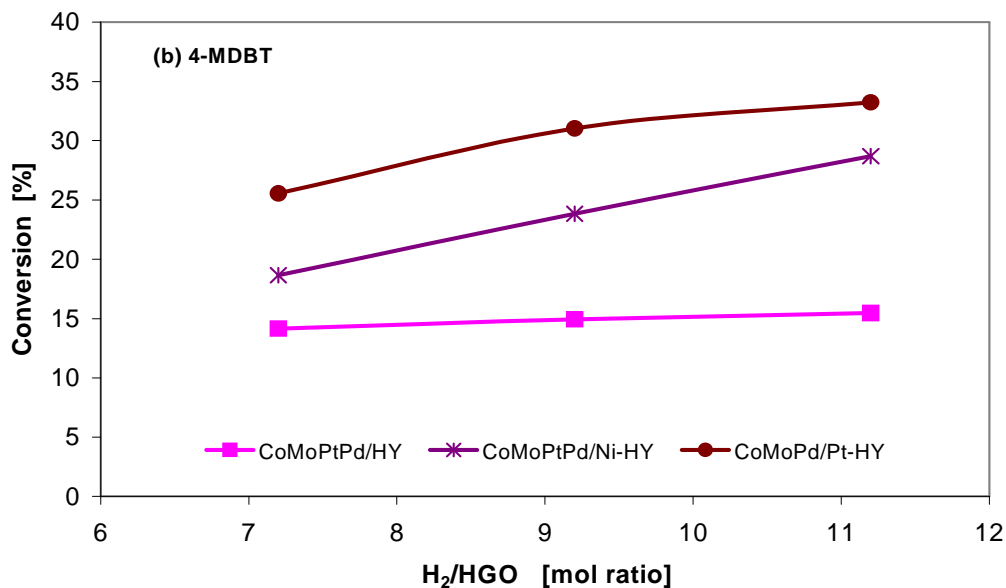


Figure 7.22 Hydrodesulfurization conversions of 4-methyldibenzothiophene (4-MDBT) in heavy gas oil over CoMoPtPd/HY, CoMoPtPd/Ni-HY and CoMoPd/Pt-HY catalysts. (65 bar, 310 °C, and space time of 6000 kg_{cat}h/kmol).

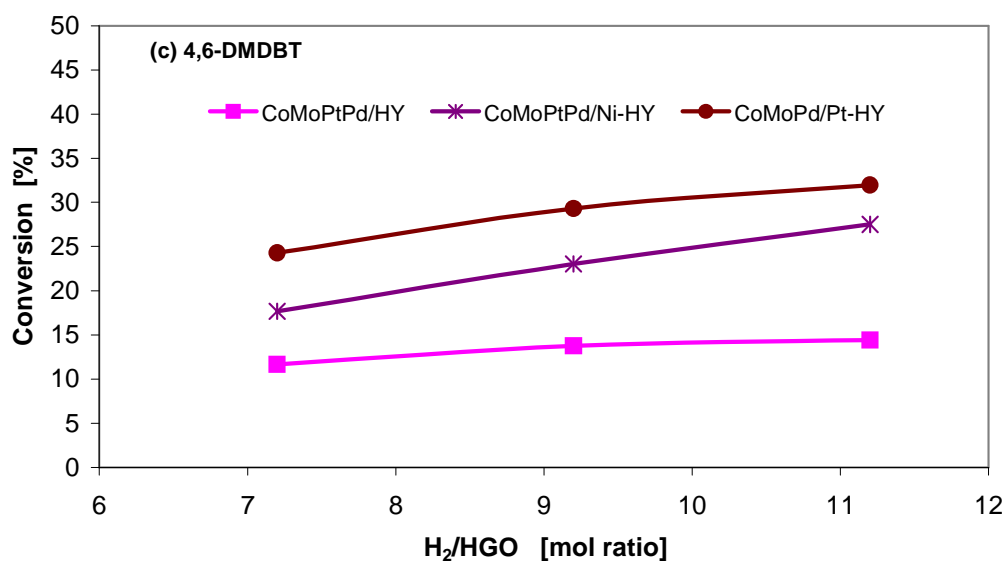


Figure 7.23 Hydrodesulfurization conversions of 4,6-dimethyldibenzothiophene (4,6-DMDBT) in heavy gas oil over CoMoPtPd/HY, CoMoPtPd/Ni-HY and CoMoPd/Pt-HY catalysts. (65 bar, 310 °C, and space time of 6000 kg_{cat}h/kmol).

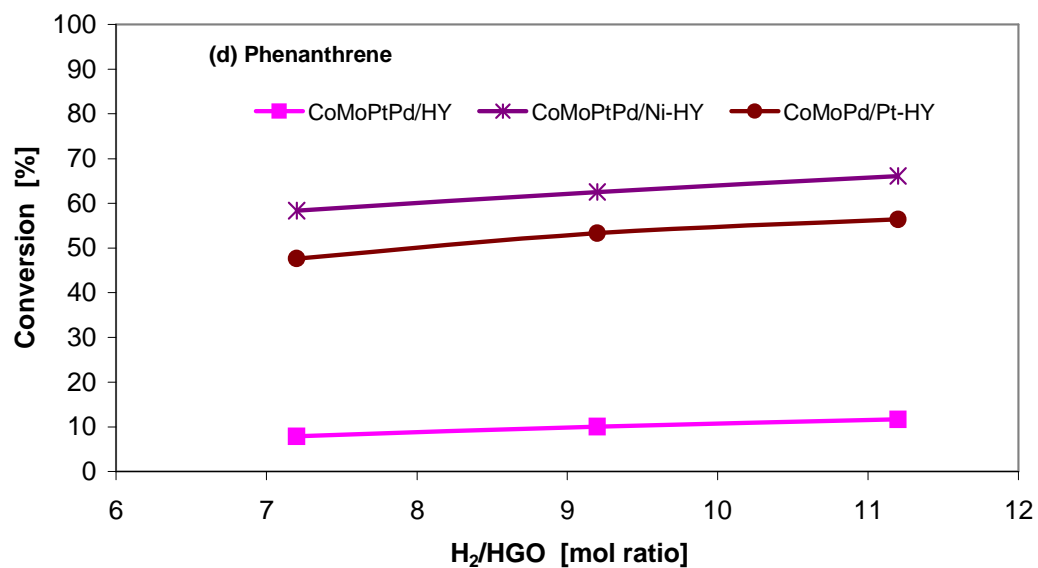


Figure 7.24 Hydrodesulfurization conversions of phenanthrene in heavy gas oil over CoMoPtPd/HY, CoMoPtPd/Ni-HY and CoMoPd/Pt-HY catalysts. (65 bar, 310 °C, and space time of 6000 kg_{cat}/h/kmol).

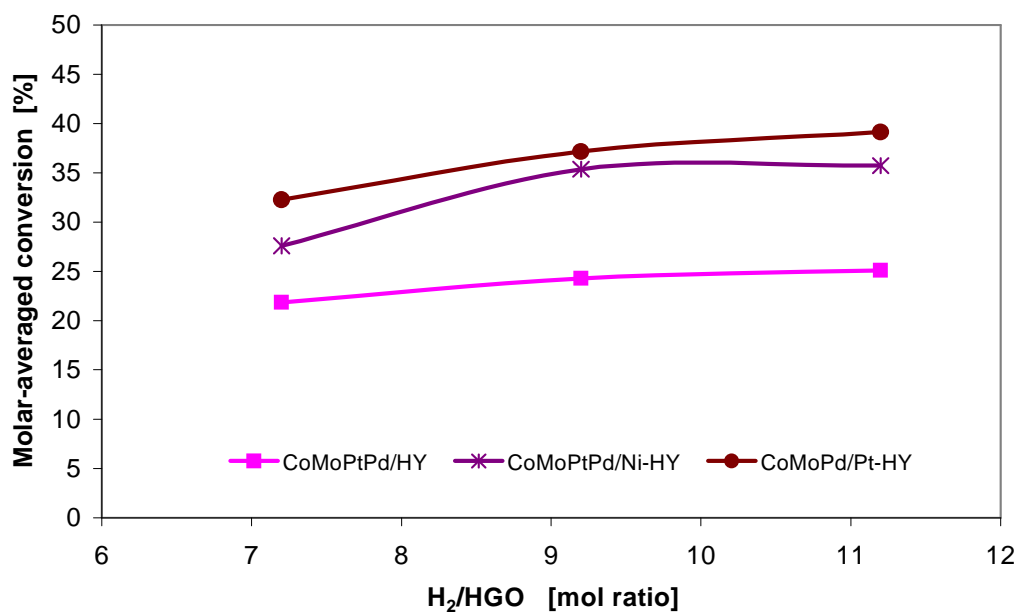


Figure 7.25 Molar-averaged conversions in heavy gas oil over CoMoPtPd/HY, CoMoPtPd/Ni-HY and CoMoPd/Pt-HY catalysts. (65 bar, 310 °C, and space time of 6000 kg_{cat}/h/kmol).

7.2.2 HDS of Heavy Gas Oil over CoMo/PdNiPt-HY, CoMoNi/PdPt-HY, and CoMoPtPd/Ni-HY Catalysts

Table 7.6 shows the molar-averaged conversions (X_{avg}), and conversions of DBT, 4-MDBT, 4,6-DMDBT and phenanthrene over CoMo/PdNiPt-HY and CoMoNi/PdPt-HY catalysts as well as CoMoPtPd/Ni-HY. Also all catalysts showed their best HDS and HDA performance at molar H_2/HC ratio of 11.2.

CoMoNi/PdPt-HY exhibited the best activity for the HDS of DBT, 4-MDBT, 4,6-DMDBT but did not for the hydrogenation of phenanthrene among the catalyst examined giving conversions from 28.3-32.2%, 27.12-31.3%, 25.6-30.1%, and 39.6-43.2% respectively in the range of H_2/HC of 7.2-11.2. CoMo/PdNiPt-HY and CoMoPtPd/Ni-HY were certainly inferior to the former catalyst, providing the conversions showed in Table 7.6, except, CoMoPtPd/Ni-HY showed the highest activity for the hydrogenation of phenanthrene giving conversions from 58.4-66.1% in the same range of H_2/HC ratio.

Figures 7.26-7.29 illustrate the conversion of alkyldibenzothiophenes and phenanthrene in heavy gas oil as a function of the molar H_2/HC ratio. HDS reactivity evidently decreased in the order DBT, 4-MDBT, and 4,6-DMDBT over all catalysts.

Even though the HDS reactivity of DBT, 4-MDBT, and 4,6-DMDBT over CoMo/PdNiPt-HY and CoMoPtPd/Ni-HY were quite close, CoMoNi/PdPt-HY shows the best performance in the range space time of 4000-6000 $kg_{cat}h/kmol$. The HDA reactivity of phenanthrene decrease certainly in the order of CoMo/PdNiPt-HY < CoMoNi/PdPt-HY < CoMoPtPd/Ni-HY at the same range of space time.

CoMoNi/PdPt-HY exhibited the highest molar-averaged conversions giving 32.5-43.2% in the interval of H_2/HC studied vs 30-37.2% over CoMo/PdNiPt-HY and 27.6-35.7% over CoMoPtPd/Ni-HY (Table 7.6 and Figure 7.30).

Table 7.6 Molar-averaged conversion and conversions of sulfur compounds and phenanthrene in the HDS and HDA of heavy gas oil over CoMo/PdNiPt-HY (HDS-8), CoMoNi/PdPt-HY (HDS-10), and CoMoPtPd/Ni-HY (HDS-3) catalysts

H ₂ /HGO mol ratio	Conversion [%]				X _{avg} ⁽¹⁾ [%]
	DBT	4-MDBT	4,6-DMDBT	Phenanthrene	
Catalyst: CoMo/PdNiPt-HY					
7.2	22.8	20.4	18.0	14.3	30.0
9.2	26.9	24.5	21.9	18.2	33.6
11.2	31.3	28.5	25.7	21.7	37.2
Catalyst: CoMoNi/PdPt-HY					
7.2	28.3	27.1	25.6	39.6	32.5
9.2	29.9	29.0	27.5	41.6	39.5
11.2	32.2	31.3	30.1	43.2	43.2
Catalyst: CoMoPtPd/Ni-HY					
7.2	22.5	18.7	17.7	58.4	27.6
9.2	28.5	23.8	23.0	62.5	35.4
11.2	33.0	28.7	27.5	66.1	35.7

⁽¹⁾Molar-averaged conversion

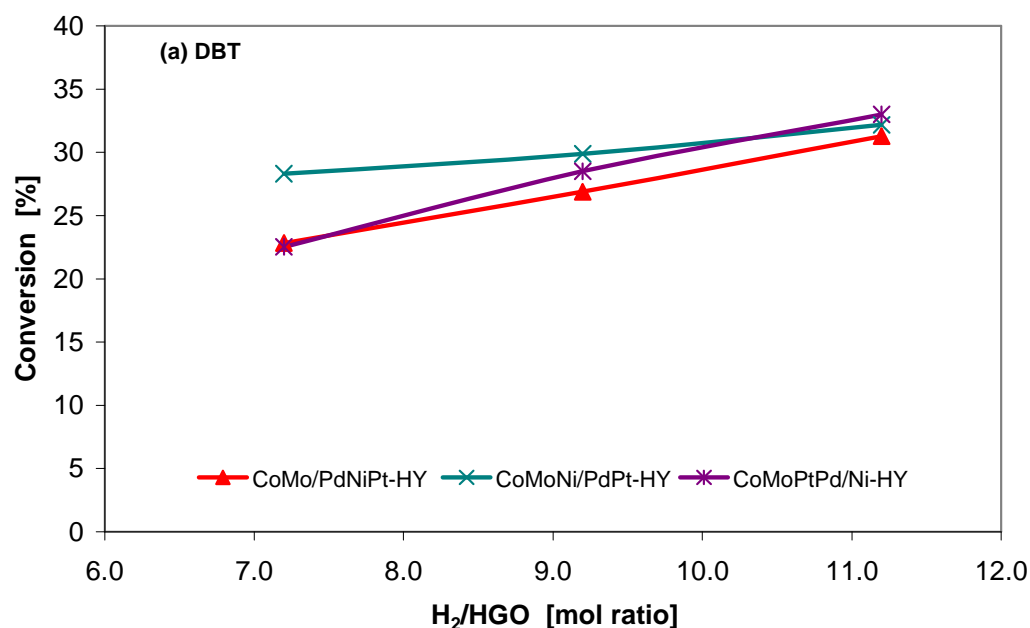


Figure 7.26 Hydrodesulfurization conversions of dibenzothiophene (DBT) in heavy gas oil over CoMo/PdNiPt-HY, CoMoNi/PdPt-HY and CoMoPtPd/Ni-HY catalysts. (65 bar, 310 °C, and space time of 6000 kg_{cat}/h/kmol).

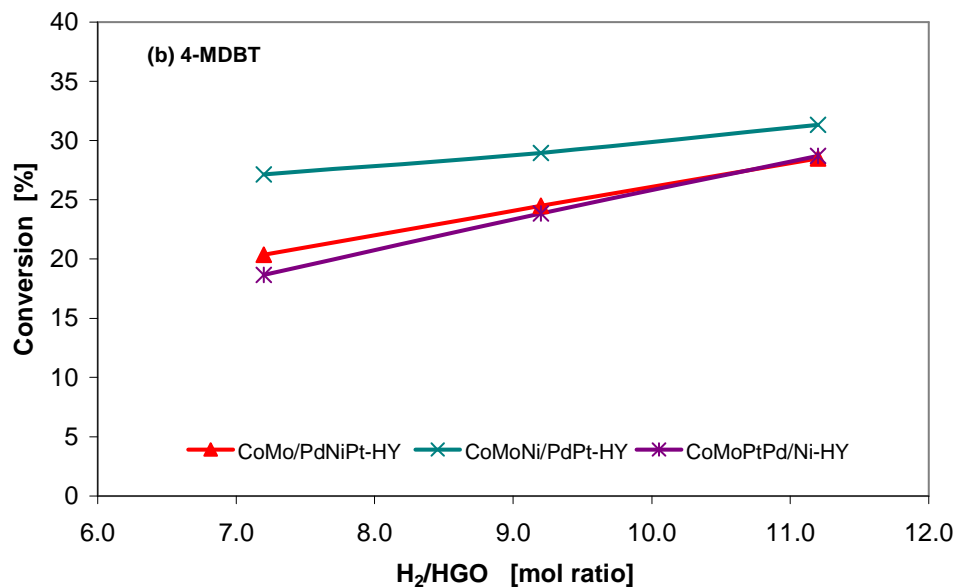


Figure 7.27 Hydrodesulfurization conversions of 4-methyldibenzothiophene (4-MDBT) in heavy gas oil over CoMo/PdNiPt-HY, CoMoNi/PdPt-HY and CoMoPtPd/Ni-HY catalysts. (65 bar, 310 °C, and space time of 6000 kg_{cat}h/kmol).

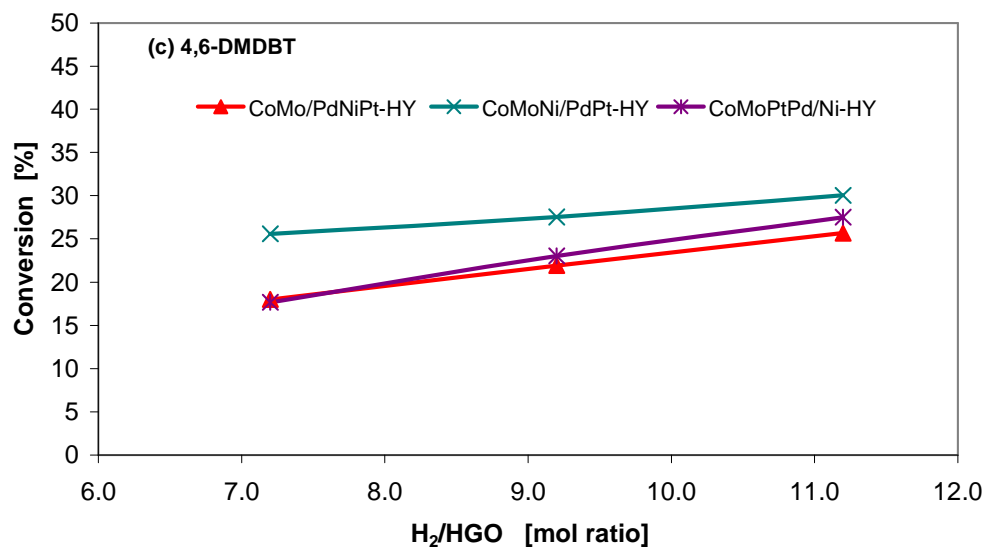


Figure 7.28 Hydrodesulfurization conversions of 4,6-dimethyldibenzothiophene (4,6-DMDBT) in heavy gas oil over CoMo/PdNiPt-HY, CoMoNi/PdPt-HY and CoMoPtPd/Ni-HY catalysts. (65 bar, 310 °C, and space time of 6000 kg_{cat}h/kmol).

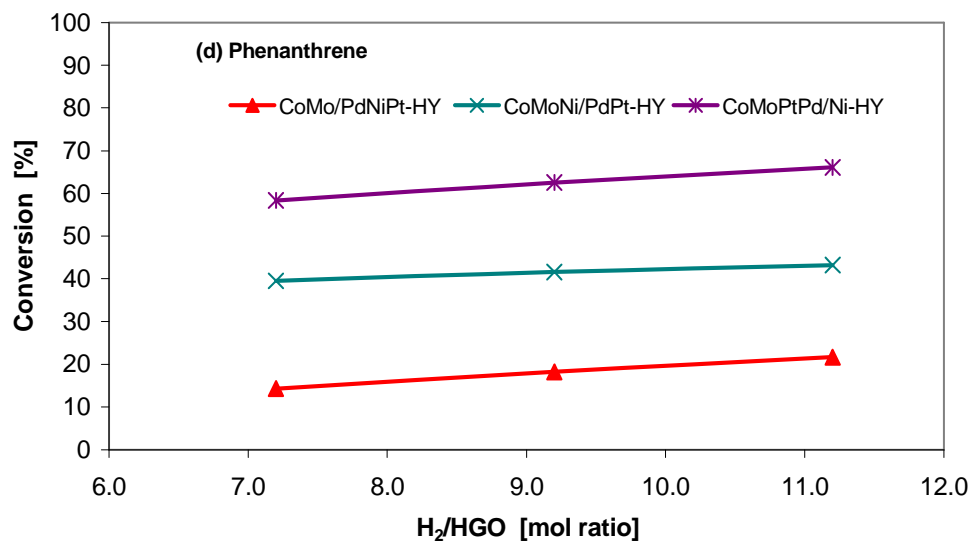


Figure 7.29 Hydrogenation conversions of phenanthrene in heavy gas oil over CoMo/PdNiPt-HY, CoMoNi/PdPt-HY and CoMoPtPd/Ni-HY catalysts. (65 bar, 310 °C, and space time of 6000 kg_{cat}h/kmol).

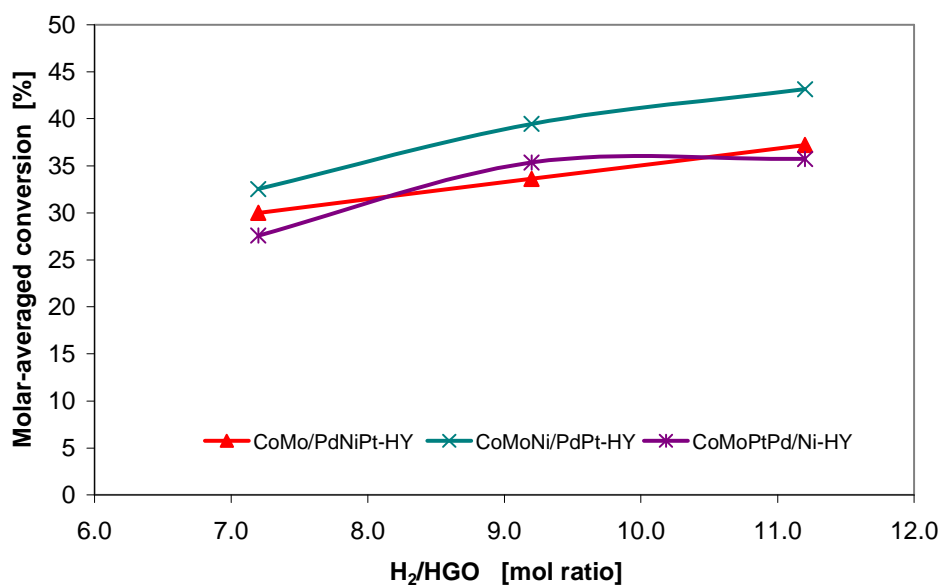


Figure 7.30 Molar-averaged conversions in heavy gas oil over CoMo/PdNiPt-HY, CoMoNi/PdPt-HY and CoMoPtPd/Ni-HY catalysts. (65 bar, 310 °C, and space time of 6000 kg_{cat}h/kmol).

7.2.3 HDS of Heavy Gas Oil over CoMo/PdNiPt-HY, CoMoNi/PdPt-HY, and CoMoPd/Pt-HY Catalysts

Table 7.7 shows the molar-averaged conversions (X_{avg}), and conversions of DBT, 4-MDBT, 4,6-DMDBT and phenanthrene over CoMo/PdNiPt-HY and CoMoNi/PdPt-HY catalysts as well as CoMoPd/Pt-HY catalyst prepared in lab.

CoMoNi/PdPt-HY exhibited the best activity for the HDS of DBT, 4-MDBT, 4,6-DMDBT at the molar H_2/HC ratio of 7.2 among the catalyst examined, giving conversions of 28.3%, 27.1%, and 25.6%, respectively. CoMoPd/Pt-HY shows the best activity for the same refractory sulfur compounds in the interval of 9.2-11.2 H_2/HC , providing conversions from 32.9-34.7 for DBT, 31-33.2% for 4-MDBT and 29.3-32% for 4,6-DMDBT. For the hydrogenation of phenanthrene CoMoPd/Pt-HY exhibited the best performance providing conversions from 47.7-56.5% in the interval of 7.2-11.2 molar H_2/HC ratio.

Figures 7.31-7.34 illustrate the conversion of alkyldibenzothiophenes and phenanthrene in heavy gas oil as a function of the molar H_2/HC ratio. HDS reactivity evidently decreased in the order DBT > 4-MDBT > 4,6-DMDBT over all catalysts. HDS reactivities of DBT, 4-MDBT, and 4,6-DMDBT decline certainly in the order of CoMo/PdNiPt-HY < CoMoNi/PdPt-HY < CoMoPd/Pt-HY in the range 9.2-11.2 H_2/HC mol ratio. While for the hydrogenation reactivities of phenanthrene the order was CoMo/PdNiPt-HY < CoMoPd/Pt-HY < CoMoNi/PdPt-HY from 7.2 to 11.2 H_2/HGO mol ratio.

CoMoNi/PdPt-HY exhibited the highest molar-averaged conversions giving 39.5-43.2% in the interval of 9.2-11.2 H_2/HC mol ratio. However, its conversion at 7.2 was quite close to CoMo/PdNiPt-HY (32.5 vs 30%) and similar to CoMoPd/Pt-HY catalyst (32.5 vs 32.3%) (Table 7.7 and Figure 7.35).

Table 7.7 Molar-averaged conversion and conversions of sulfur compounds and phenanthrene in the HDS and HDA of heavy gas oil over CoMo/PdNiPt-HY (HDS-8), CoMoNi/PdPt-HY (HDS-10), and CoMoPd/Pt-HY (HDS-5) catalysts

H ₂ /HGO mol ratio	Conversion [%]				X _{avg} ⁽¹⁾ [%]
	DBT	4-MDBT	4,6-DMDBT	Phenanthrene	
Catalyst: CoMo/PdNiPt-HY					
7.2	22.8	20.4	18.0	14.3	30.0
9.2	26.9	24.5	21.9	18.2	33.6
11.2	31.3	28.5	25.7	21.7	37.2
Catalyst: CoMoNi/PdPt-HY					
7.2	28.3	27.1	25.6	39.6	32.5
9.2	29.9	29.0	27.5	41.6	39.5
11.2	32.2	31.3	30.1	43.2	43.2
Catalyst: CoMoPd/Pt-HY					
7.2	26.9	25.6	24.3	47.7	32.3
9.2	32.9	31.0	29.31	53.4	37.1
11.2	34.7	33.2	32.0	56.5	39.1

⁽¹⁾Molar-averaged conversion

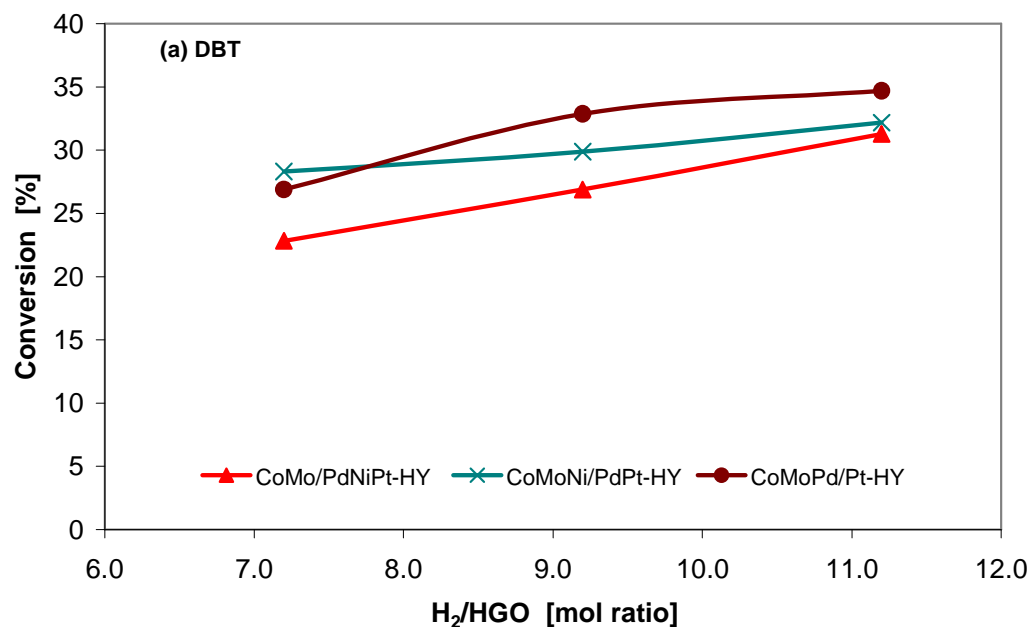


Figure 7.31 Hydrodesulfurization conversions of dibenzothiophene (DBT) in heavy gas oil over CoMo/PdNiPt-HY, CoMoNi/PdPt-HY and CoMoPd/Pt-HY catalysts. (65 bar, 310 °C, and space time of 6000 kg_{cat}/h/kmol).

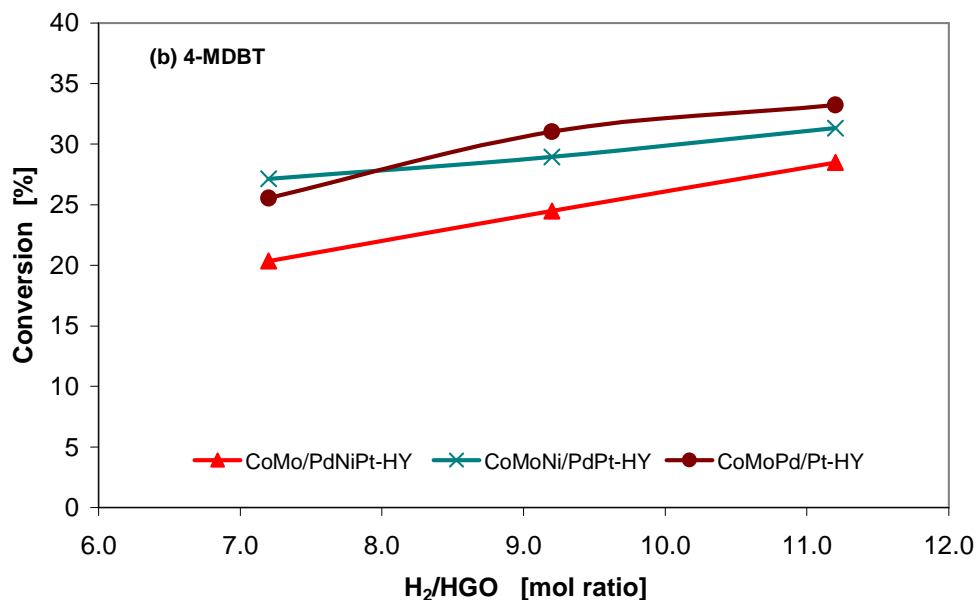


Figure 7.32 Hydrodesulfurization conversions of 4-methyldibenzothiophene (4-MDBT) in heavy gas oil over CoMo/PdNiPt-HY, CoMoNi/PdPt-HY and CoMoPd/Pt-HY catalysts. (65 bar, 310 °C, and space time of 6000 kg_{cat}h/kmol).

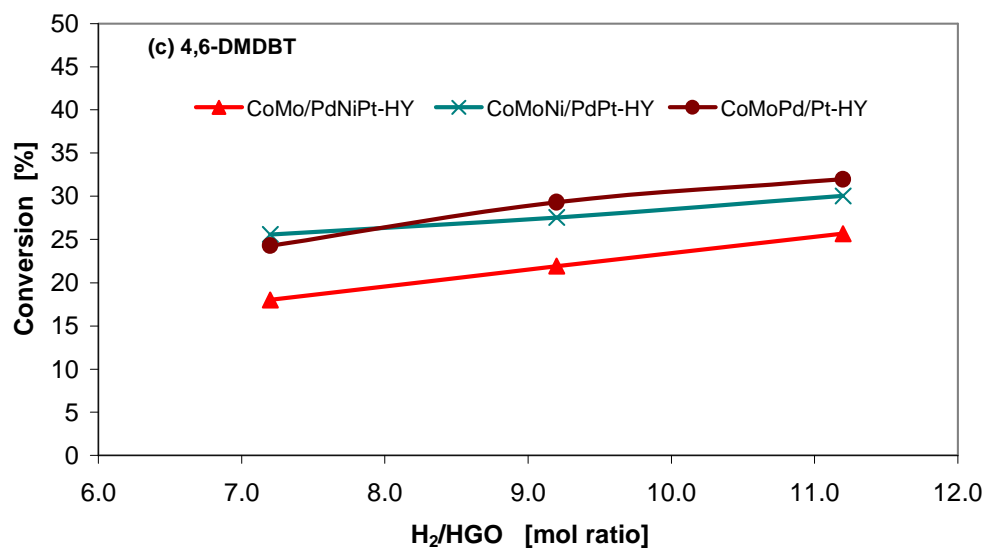


Figure 7.33 Hydrodesulfurization conversions of 4,6-dimethyldibenzothiophene (4,6-DMDBT) in heavy gas oil over CoMo/PdNiPt-HY, CoMoNi/PdPt-HY and CoMoPd/Pt-HY catalysts. (65 bar, 310 °C, and space time of 6000 kg_{cat}h/kmol).

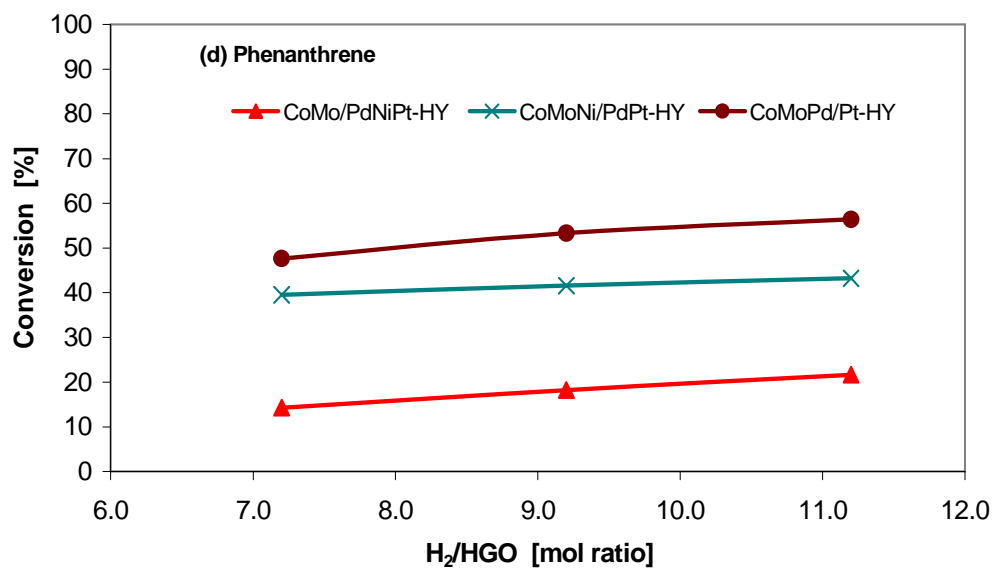


Figure 7.34 Hydrodesulfurization conversions of phenanthrene in heavy gas oil over CoMo/PdNiPt-HY, CoMoNi/PdPt-HY and CoMoPd/Pt-HY catalysts. (65 bar, 310 °C, and space time of 6000 kg_{cat}h/kmol).

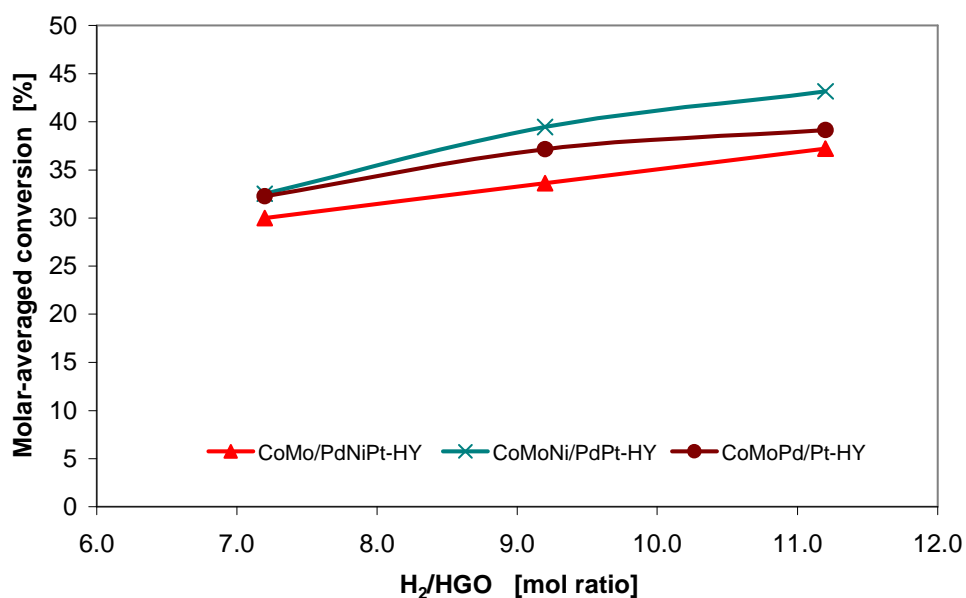


Figure 7.35 Molar-averaged conversions in heavy gas oil over CoMo/PdNiPt-HY, CoMoNi/PdPt-HY and CoMoPd/Pt-HY catalysts. (65 bar, 310 °C, and space time of 6000 kg_{cat}h/kmol).

7.3 Concluding Remarks

In noble-metal-catalyzed HDS and HDA reactions in heavy gas oil (HGO), the activity of the catalysts strongly depends on the type of support and metal. For hydrogenation of phenanthrene in HGO at 310 °C, 65 bar, 7.2 H₂/HC and 4000 kg_{cat}h/kmol, the CoMoPtPd/Ni-HY (HDS-3) catalyst is substantially more active than CoMoPd/Pt-HY (HDS-5) and CoMoNi/PdPt-HY (HDS-10), even when the two latter are used at higher H₂/HC ratio and space time.

Trimetallic CoMoPd supported on Pt-modified USY zeolite, i.e., CoMoPd/Pt-HY (HDS-5) catalyst, showed higher HDS and HDA than the conventional CoMo/Al₂O₃. Because the trimetallic CoMoNi supported on PdPt-modified US, i.e., CoMoNi/PdPt-HY (HDS-10) showed better HDS than trimetallic CoMoPd supported on Pt-modified USY zeolite, it can be concluded that metal or multimetal-modified USY zeolite, i.e., Pt-HY, Ni-HY, PdNiPt-HY and PdPt-HY supporting two or more metals, such as Co, Mo, Ni, Pt and Pd, show higher activity for HDS and HDA than the conventional CoMo/Al₂O₃

CHAPTER VIII

COMPARISON OF ACTIVITY IN TERMS OF CONVERSION OF DBT AND 4,6-DMDBT INTO THEIR REACTION PRODUCTS

The Hydrodesulfurization (HDS) of Heavy gas oil containing 0.453 mass% was performed at total pressure of 65 bar, temperature of 310 °C, space time (W/F_{DBT}^0) varied from 4000 to 6000 $kg_{cat}h/kmol$ and molar hydrogen to hydrocarbon ratio of 7.2 over a commercial CoMo/Al₂O₃ catalysts as well as experimental zeolite catalysts prepared in lab, CoMoPtPd/HY (HDS-1), CoMoPd/Pt-HY (HDS-5), CoMoPtPd/Ni-HY (HDS-3), CoMo/PdNiPt-HY (HDS-8), and CoMoNi/PdPt-HY (HDS-10) catalysts to examine the HDS reactivities of DBT and 4,6-DMDBT which exist in the Heavy gas oil. Among these catalysts, HDS-10 exhibited the highest HDS reactivity. Isomerization reaction of 4-6-DMDBT into 3,6-DMDBT, and then desulfurization into 3,4-DMBPH seems to be evident over the zeolites catalysts. The reaction products of the HDS of DBT were biphenyl (BPH), cyclohexylbenzene (CHB), bicyclohexyl (BCH), and H₂S. Tetra-(THDBT) and hexahydrodibenzothiophene (HHDBT) were not detected.

8.1 Effect of Space Time at 310 °C and Molar H₂/HC Ratio of 7.2

8.1.1 Commercial CoMo/Al₂O₃ (HDS-0) Catalyst

The catalyst used here was supplied by IMP. It contains 13.1-16.1 wt% MoO₃, 3.2-3.8 wt% CoO; total pore volume of 0.5 cm³/g and BET surface area mol of 215 m²/g. All catalysts were crushed at 850-1000 μ to avoid diffusional limitations.

8.1.1.1 Conversion of DBT in HDS of Heavy Gas Oil

Table 8.1 and Figure 8.1 show the total conversions of DBT (X_{DBT}), conversions of DBT into BPH (X_{BPH}), conversions of DBT into CHB (X_{CHB}) and conversions of DBT

into BCH (X_{BCH}). The DBT total conversion varied from 16.6 to 23.7% with space time. As expected, the conversions X_{DBT} , X_{BPH} , X_{CHB} and X_{BCH} increased with space time. DBT was mainly desulfurized into BPH and H_2S . DBT probably also hydrogenated into THDBT and or HHDBT. However, they were not detected since they are highly reactive intermediates that are instantaneously converted into CHB and H_2S . BPH was further hydrogenated into CHB. Partial hydrogenation of BPH occurred at the operating conditions which were applied, and leads to moderate amounts of BCH. The conversions of DBT into CHB and BCH varied from 8.3 to 10.3% and from 6.8 to 8.4% with space time respectively.

Table 8.1 Conversions of DBT into its reaction products as a function of space time (W/F_{DBT}^0) over CoMo/ Al_2O_3 catalyst

W/F_{DBT}^0		Conversion [%]			
$\text{Kg}_{\text{cat}}\text{h}/\text{Kmol}$	X_{DBT}	X_{BPH}	X_{CHB}	X_{BCH}	
4000	16.6	11.8	8.3	6.8	
5000	20.2	14.0	10.6	8.2	
6000	23.7	16.0	10.3	8.4	

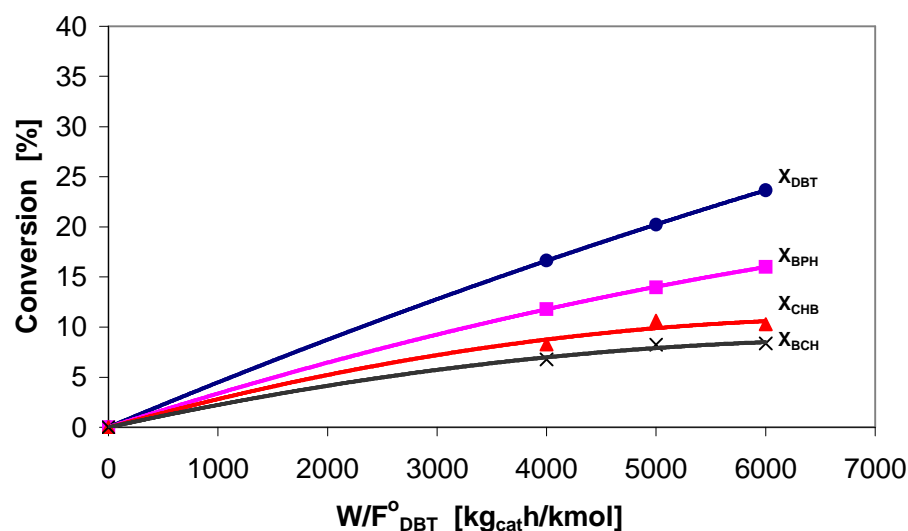


Figure 8.1 Conversions as a function of W/F_{DBT}^0 over CoMo/ Al_2O_3 catalyst. (X_{DBT}) total conversion of DBT, (X_{BPH}) conversion of DBT into BPH, (X_{CHB}) conversion of DBT into CHB, (X_{BCH}) conversion of DBT into BCH. Experimental conditions: $T = 310$ °C, $p_t = 65$ bar, $\text{H}_2/\text{HGO} = 7.2$, Feed: Heavy Gas Oil.

8.1.1.2 Conversion of 4,6-DMDBT in HDS of Heavy Gas Oil

The 3,4-dimethylbiphenyl was followed as a final reaction product of the HDS of 4,6-DMDBT. A route of the HDS reaction of 4,6-DMDBT is to isomerize 4,6-DMDBT into 3,6-DMDBT and then desulfurize into 3,4-DMBPH. According to Isoda et al., (1996) acid-catalyzed reactions take place certainly over CoMo/Al₂O₃-zeolite. However, conversions of 4,6-DMDBT into 3,4-DMBPH were traced since the commercial CoMo/Al₂O₃ catalyst was used as reference of the zeolite catalysts. The 4,6-DMDBT total conversion over CoMo/Al₂O₃ catalyst varied from 12.3 to 21.1% with space time (Table 8.2). As expected, the conversions $X_{4,6\text{-DMDBT}}$ and $X_{3,4\text{-DMBPH}}$, increased with space time. The desulfurization of 4,6-DMDBT by isomerization route led to very small amounts of 3,4-DMBPH, 3.3 to 3.9% in the range of space time of 4000 to 6000 kg_{cat}h/kmol. A Typical set of conversions vs space time plot is shown in Figure 8.2.

Table 8.2 Total Conversions of 4,6-DMDBT and conversions into 3,4-dimethylbiphenyl as a function of space time (W/F_{DBT}^0) over CoMo/Al₂O₃ catalyst

W/F_{DBT}^0 Kg _{cat} h/Kmol	Conversion [%]	
	$X_{4,6\text{-DMDBT}}$	$X_{3,4\text{-DMBPH}}$
4000	12.3	3.3
5000	16.3	3.5
6000	21.1	3.9

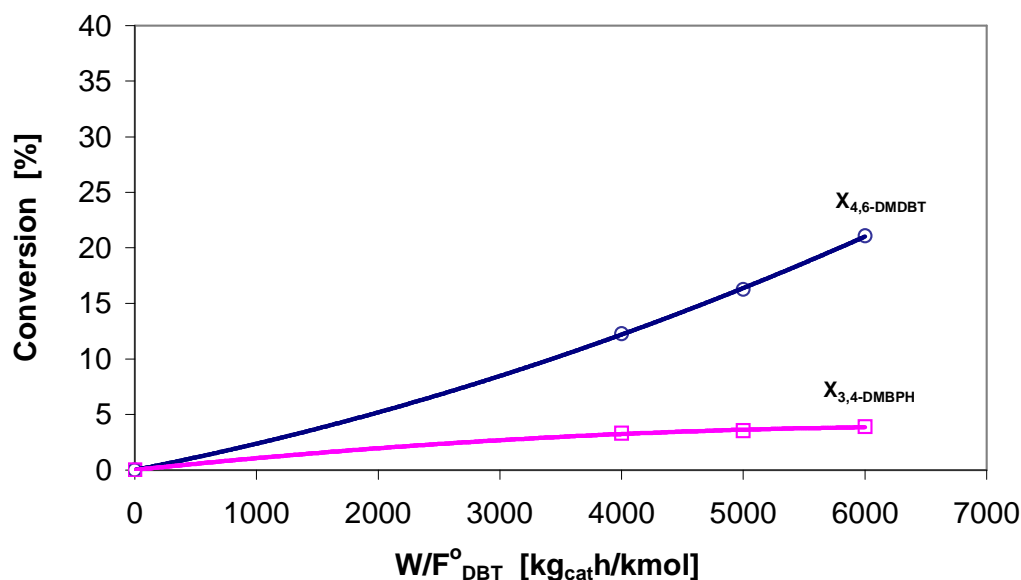


Figure 8.2 Conversions as a function of W/F°_{DBT} over CoMo/Al₂O₃ catalyst. ($X_{4,6-DMDBT}$) total conversion of 4,6-DMDBT, ($X_{3,4-DMBPH}$) conversion of 4,6-DMDBT into 3,4-DMBPH. Experimental conditions: $T = 310$ °C, $p_t = 65$ bar, $H_2/HGO = 7.2$, Feed: Heavy Gas Oil.

A set of five catalysts were prepared using incipient wetness impregnation and ion exchange procedures, which were described in the preparation of the catalyst section. The experiments with the heavy gas oil were carried out at a total pressure of 65 bars, temperature of 310 °C and molar hydrogen to hydrocarbon ratio of 7.2. The catalysts were dried at 120 °C for 1h and sulfided at 330 °C for 3.5 hr by flowing H₂S (8.5%) in H₂ under atmospheric pressure just before its use.

8.1.2 CoMoPtPd/HY (HDS-1) Catalyst

CoMoPtPd/HY as a test catalyst was prepared by the wet impregnation procedure of Co, Mo, Pt and Pd salt solutions into the support which consisted of Y-zeolite. The pellets show a BET surface area of 379 m²/g and a total pore volume of 0.104 cc/g. Others properties are summarized in the catalysts characterization section.

8.1.2.1 Conversion of DBT in HDS of Heavy Gas Oil

Table 8.3 and Figure 8.3 illustrate the reaction products of the HDS of DBT which were biphenyl (BPH), cyclohexylbenzene (CHB), bicyclohexyl (BCH), and H₂S. Tetra- (THDBT) and hexahydrodibenzothiophene (HHDBT) were not analyzed.

CoMoPtPd/HY exhibited less activity for the HDS of heavy gas oil among the catalysts examined, giving total conversion of DBT from 8.5 to 15 % in the range of space time of 4000 to 6000 kg_{cat}h/kmol.

As expected, the conversions X_{DBT} , X_{BPH} , X_{CHB} and X_{BCH} increased with space time. DBT was mainly desulfurized and hydrogenated into CHB and BCH and H₂S at the operating conditions used. The conversions of DBT into CHB and BCH varied from 5.7 to 8.3% and from 7.7 to 12.1% with space time respectively.

Table 8.3 Conversions of DBT into their reaction products as a function of space time (W/F_{DBT}^0) over CoMoPtPd/HY catalyst

W/F_{DBT}^0 Kg _{cat} h/Kmol	Conversion [%]			
	X_{DBT}	X_{BPH}	X_{CHB}	X_{BCH}
4000	8.5	3.6	5.7	7.7
5000	11.9	4.8	7.5	10.0
6000	15.0	5.1	8.3	12.1

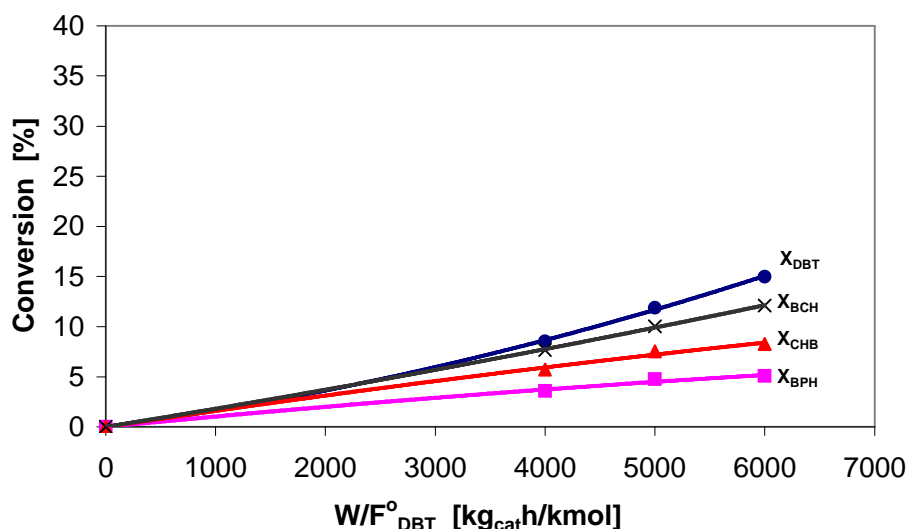


Figure 8.3 Conversions as a function of W/F°_{DBT} over CoMoPtPd/HY catalyst. (X_{DBT}) total conversion of DBT, (X_{BPH}) conversion of DBT into BPH, (X_{CHB}) conversion of DBT into CHB, (X_{BCH}) conversion of DBT into BCH. Experimental conditions: $T= 310$ °C, $p_t = 65$ bar, $H_2/HGO=7.2$. Feed: Heavy Gas Oil.

8.1.2.2 Conversion of 4,6-DMDBT in HDS of Heavy Gas Oil

Table 8.4 and Figure 8.4 show the conversions of the 4,6-DMDBT in the heavy gas oil as a function of space time. As previously mentioned 3,4- dimethylbiphenyl was followed as a final reaction product of the HDS of 4,6-DMDBT by the Isomerization route. CoMoPtPd/HY catalysts show better activity in terms of the conversion of 4,6-DMDBT into 3,4-dimethylbiphenyl than CoMo/Al₂O₃ catalyst, giving conversions from 5.23 to 8.84% vs 3.3 to 3.9% respectively (Table 8.2.)

Table 8.4 Total Conversions of 4,6-DMDBT and conversions into 3,4-dimethylbiphenyl as a function of space time (W/F°_{DBT}) over CoMoPtPd/HY catalyst

W/F°_{DBT} Kg _{cat} h/Kmol	Conversion [%]	
	$X_{4,6-DMDBT}$	$X_{3,4-DMBPH}$
4000	6.2	5.2
5000	8.0	7.3
6000	11.7	8.8

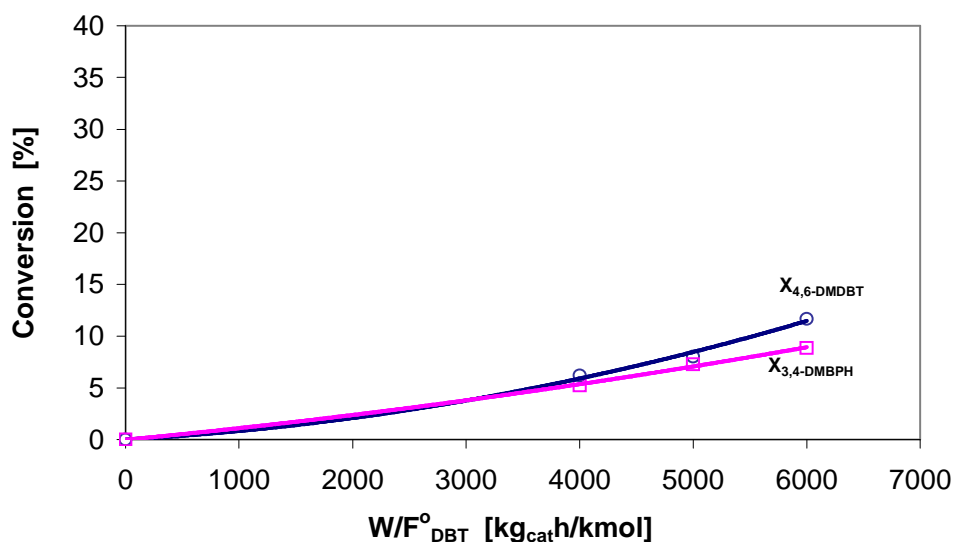


Figure 8.4 Conversions as a function of W/F_{DBT}^0 over CoMoPtPd/HY catalyst. ($X_{4,6-DMDBT}$) total conversion of 4,6-DMDBT, ($X_{3,4-DMBPH}$) conversion of 4,6-DMDBT into 3,4-DMBPH. Experimental conditions: $T = 310$ °C, $p_t = 65$ bar, $H_2/HGO = 7.2$. Feed: Heavy Gas Oil.

8.1.3 CoMoPd/Pt-HY (HDS-5) Catalyst

Platinum-containing zeolite (Pt-HY) was prepared by ion exchange procedure. Catalyst CoMoPd was prepared by wet impregnation of Pt-HY with Co, Mo, Pd salt solutions. The pellets show a BET surface area of $366 \text{ m}^2/\text{g}$ and a total pore volume of 0.114 cc/g .

8.1.3.1 Conversion of DBT in HDS of Heavy Gas Oil

The reaction products of the HDS of DBT at 310 °C over this noble metal catalyst studied is shown in Table 8.5 and Figure 8.5. The reaction products were biphenyl (BPH), cyclohexylbenzene (CHB), bicyclohexyl (BCH), and H_2S . Tetra-(THDBT) and hexahydrodibenzothiophene (HHDBT) were not analyzed. As expected, the conversions X_{DBT} , X_{BPH} , X_{CHB} and X_{BCH} increased with space time. DBT was also mainly

desulfurized and hydrogenated into CHB and BCH and H₂S at the operating conditions used.

Among the CoMo/Al₂O₃, CoMoPtPd/HY and CoMoPd/Pt-HY, the last catalyst shows better activity for the HDS and HDA. The total conversion of DBT over CoMoPd/Pt-HY is above of 19% in the range of W/F_{DBT}° from 4000 to 6000 kg_{cat}h/kmol (Table 8.5), compared to 8% conversion over CoMoPtPd/HY (Table 8.3.) and 16% conversion over CoMo/Al₂O₃ (Table 8.1.). The conversions of DBT into CHB and BCH over CoMoPd/Pt-HY varied from 8.1 to 11.5% and from 15.8 to 23.0% with space time respectively. Over CoMo/Al₂O₃ the variations of CHB and BCH were 8.3 to 10.3% and 6.8 to 8.4% (Table 8.1) correspondingly and over CoMoPtPd/HY was 5.7 to 8.3% and 7.7 to 12.1 (Table 8.1) in the same order.

Table 8.5 Conversions of DBT into their reaction products as a function of space time (W/F_{DBT}°) over CoMoPd/Pt-HY catalyst

W/F_{DBT}°		Conversion [%]		
Kg _{cat} h/Kmol	X_{DBT}	X_{BPH}	X_{CHB}	X_{BCH}
4000	19.6	6.1	8.1	15.8
5000	24.4	8.7	11.3	20.1
6000	26.9	9.4	11.5	23.0

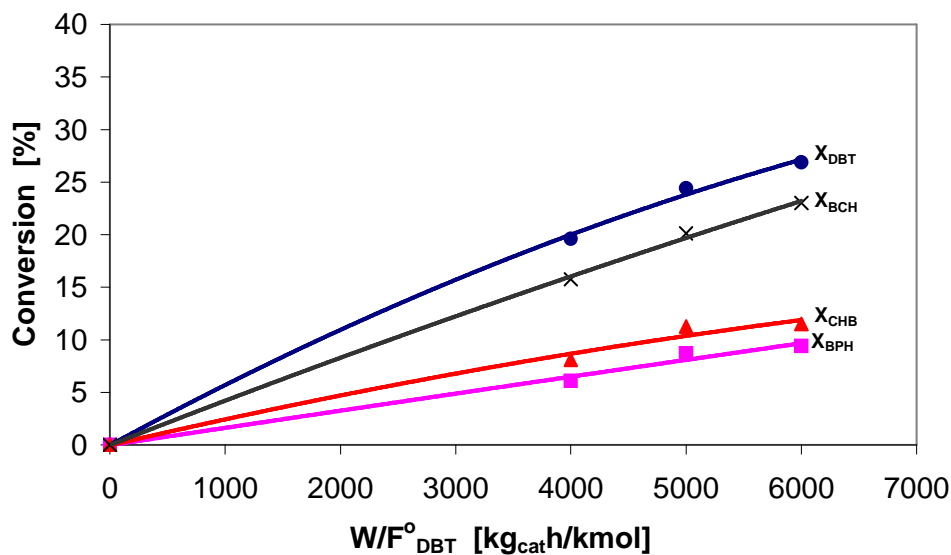


Figure 8.5 Conversions as a function of W/F°_{DBT} over CoMoPd/Pt-HY catalyst. (X_{DBT}) total conversion of DBT, (X_{BPH}) conversion of DBT into BPH, (X_{CHB}) conversion of DBT into CHB, (X_{BCH}) conversion of DBT into BCH. Experimental conditions: $T = 310$ °C, $p_t = 65$ bar, $H_2/HGO = 7.2$. Feed: Heavy Gas Oil.

8.1.3.2 Conversion of 4,6-DMDBT in HDS of Heavy Gas Oil

The 3,4-dimethylbiphenyl was followed as a final reaction product of the HDS of 4,6-DMDBT by the isomerization route. The conversions of 4,6-DMDBT and its reaction product are shown in Table 8.6 and Figure 8.6.

Among the CoMo/Al₂O₃, CoMoPtPd/HY and CoMoPd/Pt-HY, the last catalyst shows also better activity of 4,6-DMDBT and conversion into its product. The total conversion of 4,6-DMDBT over CoMoPd/Pt-HY is above of 16% in the range of W/F°_{DBT} from 4000 to 6000 kg_{cat}/h/kmol, compared to 6% conversion over CoMoPtPd/HY (Table 8.4.) and 12% conversion over CoMo/Al₂O₃ (Table 8.2.).

The CoMoPtPd/HY and CoMoPd/Pt-HY catalysts exhibited a higher activity for the conversion of 4,6-DMDBT into 3,4-dimethylbiphenyl than the conventional CoMo/Al₂O₃. The former provides a conversion above 5% (Table 8.4), and the CoMoPd/Pt/HY provide a conversion of 11% (Table 8.6) in the range of W/F°_{DBT} from

4000 to 6000 $\text{kg}_{\text{cat}}\text{h}/\text{kmol}$ vs a conversion of 3% provided by the conventional CoMo/ Al_2O_3 catalyst (Table 8.2).

The CoMoPd/Pt-HY catalyst, which was prepared combining the ion exchange and incipient wetness impregnation methods exhibited an excellent activity for the conversion of 4,6-DMDBT into 3,4- dimethylbiphenyl. The conversions varied from 11.7 to 16.7% vs 5.2-8.8% of CoMoPtPd/HY prepared only by wet impregnation method (Table 8.4).

Table 8.6 Total conversions of 4,6-DMDBT and conversions into 3,4-dimethylbiphenyl as a function of space time (W/F_{DBT}^0) over CoMoPd/Pt-HY catalyst

W/F_{DBT}^0	Conversion [%]	
	$\text{Kg}_{\text{cat}}\text{h}/\text{Kmol}$	$X_{3,4\text{-DMBPH}}$
4000	16.1	11.7
5000	21.4	14.9
6000	24.3	16.7

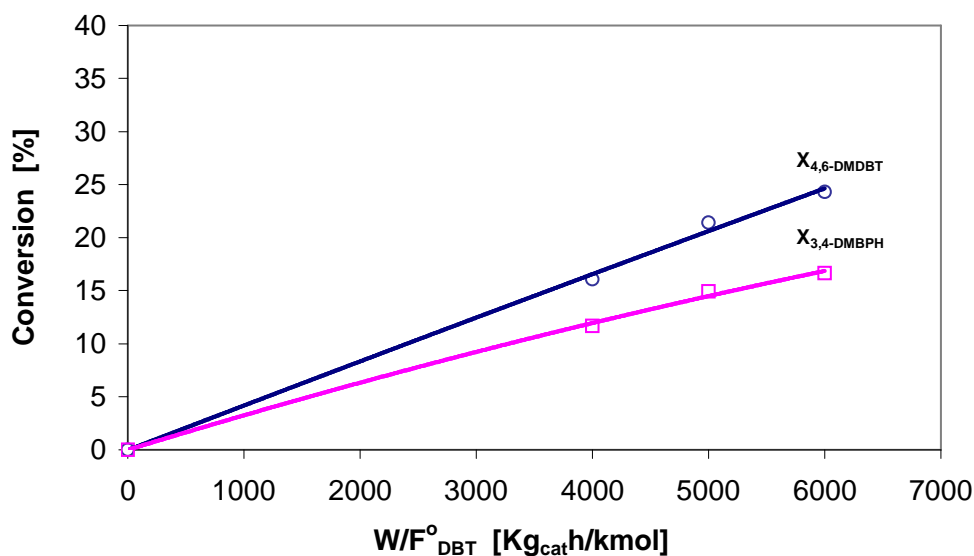


Figure 8.6 Conversions as a function of W/F_{DBT}^0 over CoMoPd/Pt-HY catalyst. ($X_{4,6\text{-DMDBT}}$) total conversion of 4,6-DMDBT, ($X_{3,4\text{-DMBPH}}$) conversion of 4,6-DMDBT into 3,4-DMBPH. Experimental conditions: $T = 310\text{ }^\circ\text{C}$, $p_t = 65\text{ bar}$, $\text{H}_2/\text{HGO} = 7.2$. Feed: Heavy Gas Oil.

8.1.4 CoMoPtPd/Ni-HY (HDS-3) Catalyst

Nickel-containing zeolite (Ni-HY) was prepared by the ion exchange procedure. Catalyst CoMoPtPd was prepared by incipient wetness method of Ni-HY using Co, Mo, Pt and Pd salt solutions. The pellets show a BET surface area of 332 m²/g and a total pore volume of 0.096 cc/g.

8.1.4.1 Conversion of DBT in HDS of Heavy Gas Oil

Table 8.7 and Figure 8.7 show the reaction products of the HDS of DBT at 310 °C over this noble metal catalyst. The reaction products were biphenyl (BPH), cyclohexylbenzene (CHB), bicyclohexyl (BCH), and H₂S. Tetra-(THDBT) and hexahydrodibenzothiophene (HHDBT) were not detected. As expected, the conversions X_{DBT} , X_{BPH} , X_{CHB} and X_{BCH} increased with space time. DBT was also desulfurized and hydrogenated into CHB and BCH and H₂S at the operating conditions used.

Between the CoMoPd/Pt-HY and CoMoPtPd/Ni-HY, the former catalyst shows better activity for the HDS and HDA. The total conversion of DBT over CoMoPd/Pt-HY is from 19.6 to 26.9% in the range of W/F_{DBT}^o from 4000 to 6000 kg_{cat}h/kmol (Table 8.5.), vs 19 to 22.5% over CoMoPtPd/Ni-HY (Table 8.7.).

Even though the conversions of DBT into BPH are quite similar for both catalysts, the conversions of DBT into CHB and BCH was higher over CoMoPd/Pt-HY which varied from 8.1 to 11.5% and from 15.8 to 23.0% as space time increased from 4000 to 6000 kg_{cat}h/kmol respectively. Over CoMoPtPd/Ni-HY the variations of CHB and BCH were 5.2 to 8.6% and 15.2 to 19.7% correspondingly.

Table 8.7 Conversions of DBT into their reaction products as a function of space time (W/F_{DBT}^0) over CoMoPtPd/Ni-HY catalyst

W/F_{DBT}^0		Conversion [%]			
$Kg_{cat}h/Kmol$	X_{DBT}	X_{BPH}	X_{CHB}	X_{BCH}	
4000	19.0	7.0	5.2	15.2	
5000	20.9	10.1	7.7	18.7	
6000	22.5	10.8	8.6	19.7	

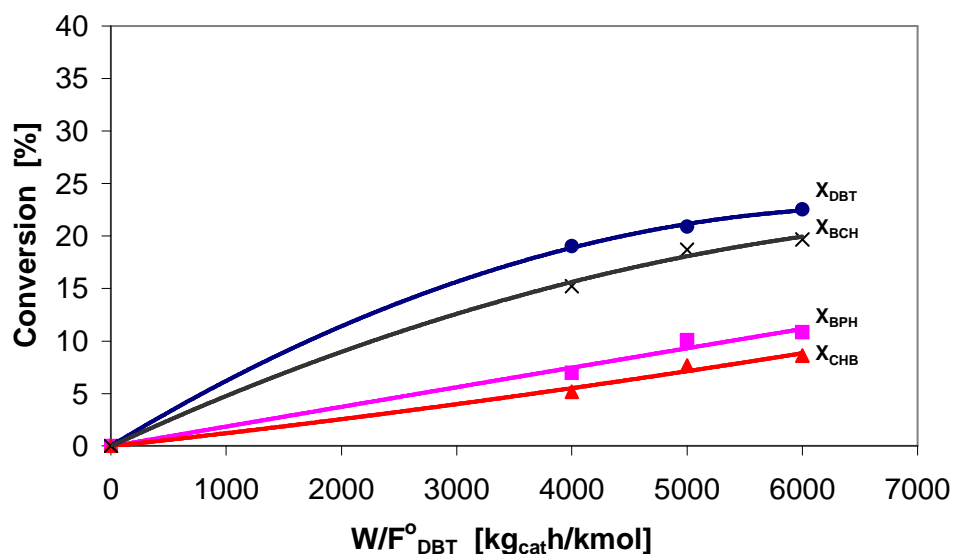


Figure 8.7 Conversions as a function of W/F_{DBT}^0 over CoMoPtPd/Ni-HY catalyst. (X_{DBT}) total conversion of DBT, (X_{BPH}) conversion of DBT into BPH, (X_{CHB}) conversion of DBT into CHB, (X_{BCH}) conversion of DBT into BCH. Experimental conditions: $T = 310$ °C, $p_t = 65$ bar, $H_2/HGO = 7.2$. Feed: Heavy Gas Oil.

8.1.4.2 Conversion of 4,6-DMDBT in HDS of Heavy Gas Oil

Again 3,4-dimethylbiphenyl was observed as a final reaction product of the HDS of 4,6-DMDBT by the isomerization route. The conversions of 4,6-DMDBT and its reaction product are shown in Table 8.8 and Figure 8.8.

Comparing the CoMoPd/Pt-HY with CoMoPtPd/Ni-HY, the last catalyst shows lower activity of 4,6-DMDBT and inferior conversion into its product. The total

conversion of 4,6-DMDBT over CoMoPd/Pt-HY as mentioned is above of 16 wt% in the range of W/F_{DBT}° from 4000 to 6000 $\text{kg}_{\text{cat}}\text{h}/\text{kmol}$ (Table 8.6), compared to 14% conversion over CoMoPtPd/Ni-HY (Table 8.8.).

CoMoPtPd/Ni-HY catalyst exhibited also a lower activity for the conversion of 4,6-DMDBT into 3,4- dimethylbiphenyl than the CoMoPd/Pt-HY, giving above 7% in the range of W/F_{DBT}° from 4000 to 6000 $\text{kg}_{\text{cat}}\text{h}/\text{kmol}$ vs above 11% over CoMoPd/Pt-HY catalyst.

Among the CoMoPtPd/HY, CoMoPtPd/Ni-HY and CoMoPd/Pt-HY the activity of HDS and HDA increased in that order. That means that CoMoPd/Pt-HY catalyst has shown the best activity for the hydrodesulfurization of heavy gas oil so far.

Table 8.8 Total conversions of 4,6-DMDBT and conversions into 3,4-dimethylbiphenyl as a function of space time (W/F_{DBT}°) over CoMoPtPd/Ni-HY catalyst

W/F_{DBT}° $\text{Kg}_{\text{cat}}\text{h}/\text{Kmol}$	Conversion [%]	
	$X_{4,6\text{-DMDBT}}$	$X_{3,4\text{-DMBPH}}$
4000	14.6	7.4
5000	16.8	9.7
6000	17.7	11.2

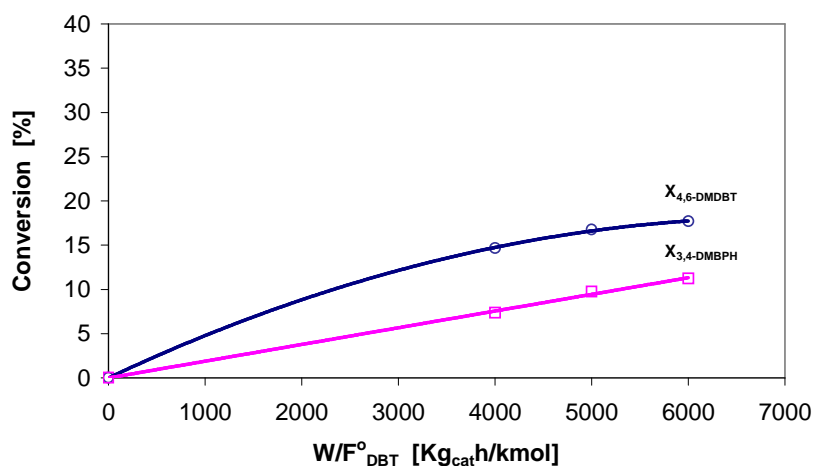


Figure 8.8 Conversions as a function of W/F_{DBT}° over CoMoPtPd/Ni-HY catalyst. ($X_{4,6\text{-DMDBT}}$) total conversion of 4,6-DMDBT, ($X_{3,4\text{-DMBPH}}$) conversion of 4,6-DMDBT into 3,4-DMBPH. Experimental conditions: $T = 310\text{ }^{\circ}\text{C}$, $p_t = 65\text{ bar}$, $\text{H}_2/\text{HGO} = 7.2$. Feed: Heavy Gas Oil.

8.1.5 CoMo/PdNiPt-HY (HDS-8) Catalyst

Pd, Ni and Pt containing zeolite was prepared using ion exchange method in three stages. PdNiPt-Zeolite supported CoMo catalyst was prepared by incipient wetness method. The pellets had the lowest BET surface area than the before catalyst presented. CoMoPtPd/Ni-HY had 298 m²/g and a total pore volume of 0.096 cc/g while CoMoPtPd/Ni was of 332 m²/g with similar total pore volume.

8.1.5.1 Conversion of DBT in HDS of Heavy Gas Oil

The reaction products of the HDS of DBT at 310 °C over this noble metal catalyst studied is shown in Table 8.9 and Figure 8.9. The reaction products were biphenyl (BPH), cyclohexylbenzene (CHB), bicyclohexyl (BCH), and H₂S. Tetra-(THDBT) and hexahydrodibenzothiophene (HHDBT) were not analyzed. As expected, the conversions X_{DBT} , X_{BPH} , X_{CHB} and X_{BCH} increased with space time. DBT was also mainly desulfurized and hydrogenated into CHB and BCH and H₂S at the operating conditions used.

The DBT and 4,6-DMDBT HDS activities of PdNiPt-Zeolite supported CoMo catalyst showed considerably lower activities at low space time (4000 kg_{cat}h/kmol) than CoMoPtPd/Ni-HY, but did not a high values (6000 kg_{cat}h/kmol) since DBT conversions were the same. The total conversion of DBT over CoMo/PdNiPt-HY is above of 10.8% in the range of W/F_{DBT}° from 4000 to 6000 kg_{cat}h/kmol, compared to 19% conversion over CoMoPtPd/Ni-HY (Table 8.7.). The conversions of DBT into CHB and BCH over CoMo/PdNiPt-HY varied from 5.1 to 14.4% and from 7.9 to 18.9% with space time respectively. Over CoMoPtPd/Ni-HY the variations of CHB and BCH were 5.2 to 8.6% and 15.2 to 19.7% correspondingly (Table 8.7).

Table 8.9 Conversions of DBT into reaction products as a function of space time (W/F_{DBT}^0) over CoMo/PdNiPt-HY catalyst

W/F_{DBT}^0	Conversion [%]			
$Kg_{cat}h/Kmol$	X_{DBT}	X_{BPH}	X_{CHB}	X_{BCH}
4000	10.8	4.0	5.1	7.9
5000	17.4	8.6	10.5	14.0
6000	22.8	12.3	14.4	19.9

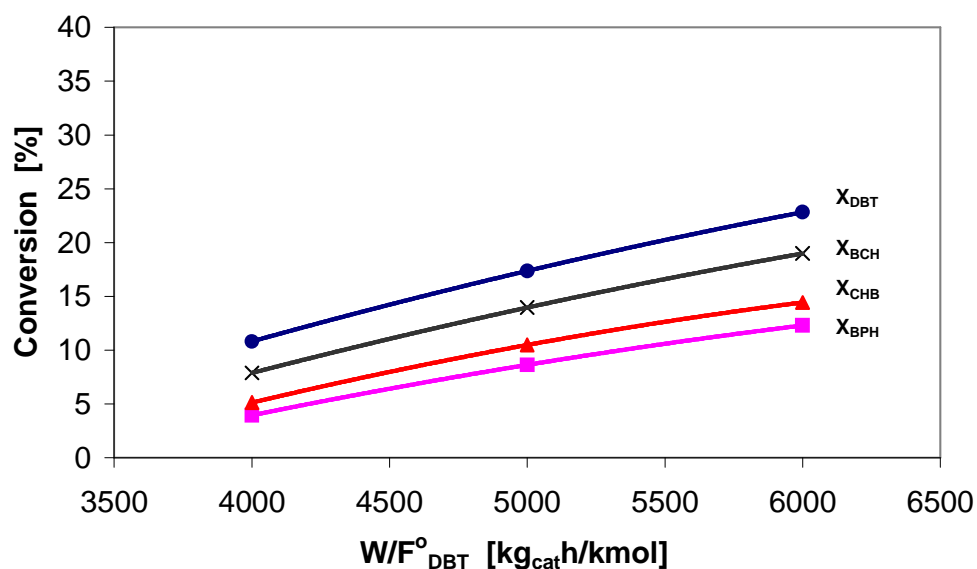


Figure 8.9 Conversions as a function of W/F_{DBT}^0 CoMo/PdNiPt-HY catalyst. (X_{DBT}) total conversion of DBT, (X_{BPH}) conversion of DBT into BPH, (X_{CHB}) conversion of DBT into CHB, (X_{BCH}) conversion of DBT into BCH. Experimental conditions: $T=310$ °C, $p_t=65$ bar, $H_2/HGO=7.2$. Feed: Heavy Gas Oil.

8.1.5.2 Conversion of 4,6-DMDBT in HDS of Heavy Gas Oil

For the other catalysts, 3,4-dimethylbiphenyl was observed as a final reaction product of the HDS of 4,6-DMDBT by the isomerization route. The conversions of 4,6-DMDBT and its reaction product are shown in Table 8.10 and Figure 8.10. CoMo/PdNiPt-HY showed also considerably lower activity for the HDS of 4,6-DMDBT

and inferior conversion into its product at 4000 $\text{kg}_{\text{cat}}\text{h}/\text{kmol}$ than CoMoPtPd/Ni-HY catalyst.

The total conversion of 4,6-DMDBT over CoMo/PdNiPt-HY is above of 7% in the range of W/F_{DBT}° from 4000 to 6000 $\text{kg}_{\text{cat}}\text{h}/\text{kmol}$ (Table 8.10), compared to above 14% conversion over CoMoPtPd/Ni-HY (Table 8.8). CoMo/PdNiPt-HY catalyst exhibited also a lower activity for the conversion of 4,6-DMDBT into 3,4- dimethylbiphenyl (5.9%) than the CoMoPtPd/Ni-HY (7.4%) at 4000 $\text{kg}_{\text{cat}}\text{h}/\text{kmol}$, but not in the interval of 5000-6000 $\text{kg}_{\text{cat}}\text{h}/\text{kmol}$ where the values ranked from 12.2-16.4% vs 9.7-11.2% respectively.

Table 8.10 Total conversions of 4,6-DMDBT and conversions into 3,4-dimethylbiphenyl as a function of space time (W/F_{DBT}°) over CoMo/PdNiPt-HY catalyst

W/F_{DBT}° $\text{Kg}_{\text{cat}}\text{h}/\text{Kmol}$	Conversion [%]	
	$X_{4,6\text{-DMDBT}}$	$X_{3,4\text{-DMBPH}}$
4000	7.4	5.9
5000	13.6	12.2
6000	18.0	16.4

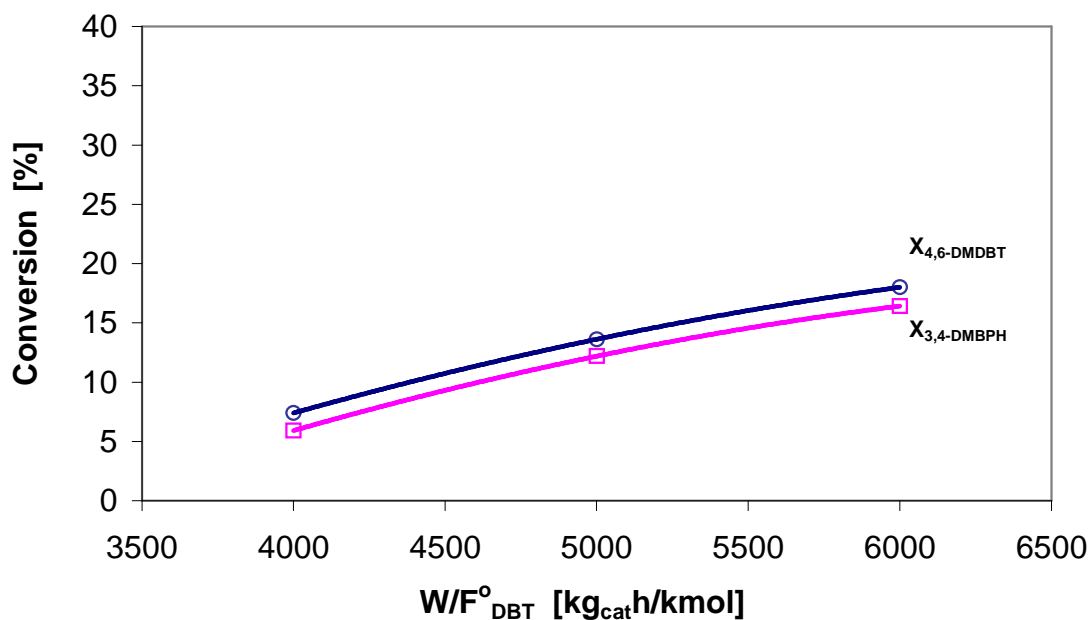


Figure 8.10 Conversions as a function of W/F_{DBT}^o over CoMo/PdNiPt-HY catalyst. ($X_{4,6-DMDBT}$) total conversion of 4,6-DMDBT, ($X_{3,4-DMBPH}$) conversion of 4,6-DMDBT into 3,4-DMBPH. Experimental conditions: $T=310\text{ }^\circ\text{C}$, $p_t=65\text{ bar}$, $H_2/HGO=7.2$. Feed: Heavy Gas Oil.

8.1.6 CoMoNi/PdPt-HY (HDS-10) Catalyst

Zeolite-supported Pt, Pd, Co, Mo and Ni catalyst was prepared combining ion exchange and incipient wetness impregnation methods. First of all, Pd and Pt were exchange ionally into zeolite in two stages to prepare PdPt-zeolite. Then incipient wetness impregnation with NiMo and CoMo solutions in two stages was used on PdPt-zeolite to get the final CoMoNi/PdPt-HY catalyst.

8.1.6.1 Conversion of DBT in HDS of Heavy Gas Oil

The reaction products of the HDS of DBT at $310\text{ }^\circ\text{C}$ over this noble metal catalyst studied is shown in Table 8.11 and Figure 8.11. The reaction products were biphenyl

(BPH), cyclohexylbenzene (CHB), bicyclohexyl (BCH), and H₂S. Tetra-(THDBT) and hexahydrodibenzothiophene (HHDBT) were not analyzed. As expected, the conversions X_{DBT} , X_{BPH} , X_{CHB} and X_{BCH} increased with space time.

DBT was also mainly desulfurized and hydrogenated into CHB and BCH and H₂S at the operating conditions used. Even though CoMoNi/PdPt-HY had a BET surface area of 129.6 m²/g and total pore volume of 0.083 cc/g was the best of all catalysts studied. The catalyst shows an excellent activity for HDS and HDA of DBT and 4,6-DMDBT. The high performance is attributed at its higher molybdenum concentration and its final metal composition (Co 2.37 wt%, Mo 17.6 wt%, Ni 1.49 wt , Pt 0.39 wt%, and Pd 0.24wt%)

CoMoNi/PdPt-HY compared with the CoMoPd/Pt-HY catalyst, which had been the best catalysts, shows better activity for the HDS. The DBT total conversion over CoMoNi/PdPt-HY varied from 24.1 to 28.3% with space time vs from 19.6 to 26.9% over CoMoPd/Pt-HY is (Table 8.5.)

The conversions of DBT into BPH, CHB and BCH varied from 3.2 to 4.7%, from 7.6 to 9.9% and from 9.7 to 13.8% with space time respectively.

Table 8.11 Conversions of DBT into their reaction products as a function of space time (W/F_{DBT}^o) over CoMoNi/PdPt-HY catalyst

W/F_{DBT}^o		Conversion [%]		
$Kg_{cat}h/Kmol$	X_{DBT}	X_{BPH}	X_{CHB}	X_{BCH}
4000	24.1	3.2	7.6	9.7
5000	25.8	4.4	8.7	12.5
6000	28.3	4.7	9.9	13.8

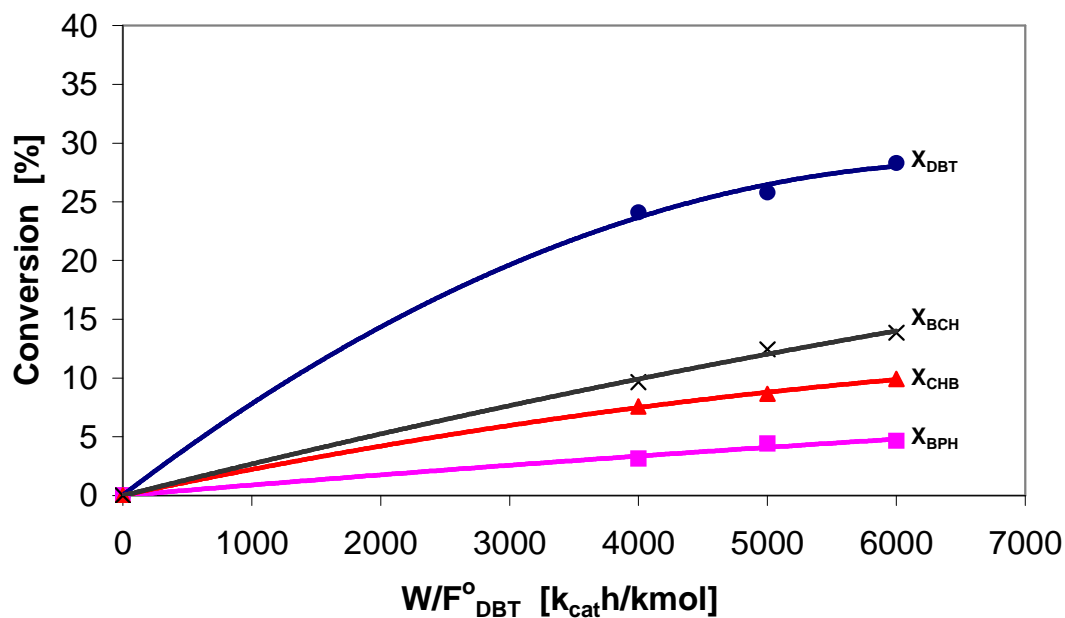


Figure 8.11 Conversions as a function of W/F°_{DBT} over CoMoNi/PdPt-HY catalyst. (X_{DBT}) total conversion of DBT, (X_{BPH}) conversion of DBT into BPH, (X_{CHB}) conversion of DBT into CHB, (X_{BCH}) conversion of DBT into BCH. Experimental conditions: $T=310$ °C, $p_t=65$ bar, $H_2/HGO=7.2$. Feed: Heavy Gas Oil.

8.1.6.2 Conversion of 4,6-DMDBT in HDS of Heavy Gas Oil

Like others catalysts, 3,4-dimethylbiphenyl was observed as a final reaction product of the HDS of 4,6-DMDBT by the isomerization route. The conversions of 4,6-DMDBT and its reaction product are shown in Table 8.12 and Figure 8.12. CoMoNi/PdPt-HY showed considerably higher activity for the HDS of 4,6-DMDBT at 4000 kg_{cat}h/kmol than CoMoPd/Pt-HY catalyst.

The total conversion of 4,6-DMDBT over CoMoNi/PdPt-HY is above of 20.8% in the range of W/F°_{DBT} from 4000 to 6000 kg_{cat}h/kmol (Table 8.12), compared to 16 % conversion over CoMoPd/Pt-HY (Table 8.6).

The CoMoNi/PdPt-HY catalyst exhibited an activity for the conversion of 4,6-DMDBT into 3,4-dimethylbiphenyl very close to that of the CoMoPd/Pt-HY catalyst. The former catalyst provided conversions from 10.9 to 16.1% vs conversions from 11.7 to 16.7 % provided by the CoMoPd/Pt-HY catalysts in the interval of 4000-6000 $\text{kg}_{\text{cat}}\text{h}/\text{kmol}$ (Table 8.6).

Table 8.12 Total conversions of 4,6-DMDBT and conversions into 3,4-dimethylbiphenyl as a function of space time (W/F°_{DBT}) over CoMoNi/PdPt-HY catalyst

W/F°_{DBT} $\text{Kg}_{\text{cat}}\text{h}/\text{Kmol}$	Conversion [%]	
	$X_{4,6\text{-DMDBT}}$	$X_{3,4\text{-DMBPH}}$
4000	20.8	10.9
5000	23.0	13.8
6000	25.6	16.7

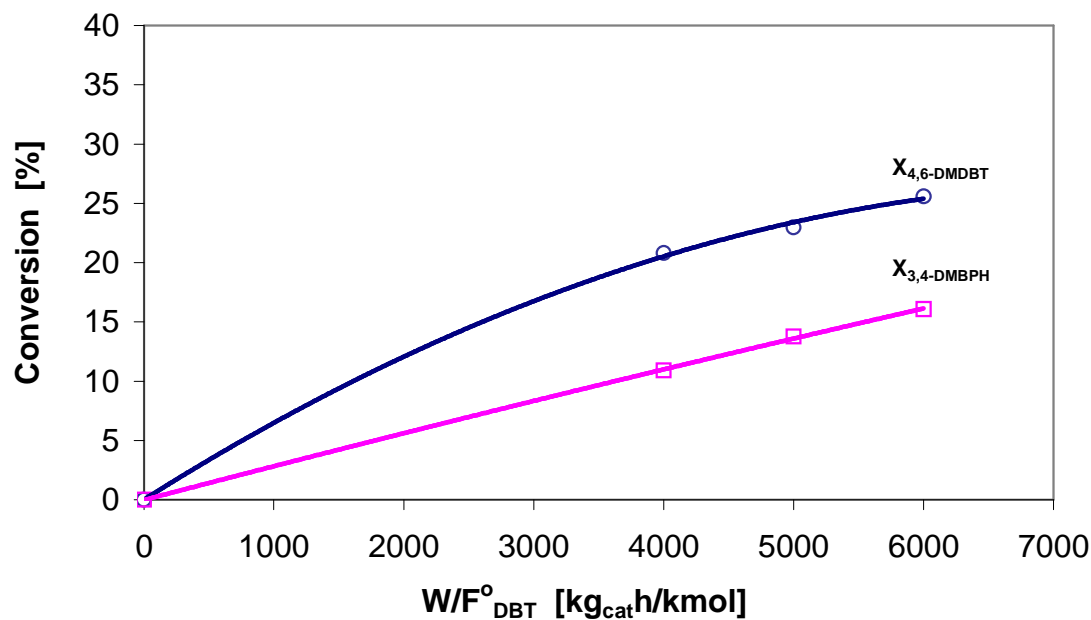


Figure 8.12 Conversions as a function of W/F°_{DBT} over CoMoNi/PdPt-HY catalyst. ($X_{4,6\text{-DMDBT}}$) total conversion of 4,6-DMDBT, ($X_{3,4\text{-DMBPH}}$) conversion of 4,6-DMDBT into 3,4-DMBPH. Experimental conditions: $T = 310^{\circ}\text{C}$, $p_t = 65$ bar, $\text{H}_2/\text{HGO} = 7.2$. Feed: Heavy Gas Oil.

8.2 Concluding Remarks

Among the catalysts examined, catalysts containing metal-zeolite exhibited the best activity for HDS conversions of alkyldibenzothiophenes in the heavy gas oil.

The trimetallic CoMoNi supported on PdPt-modified USY zeolite, i.e., CoMoNi/PdPt-HY (HDS-10) catalyst and trimetallic CoMoPd supported on Pt-modified USY zeolite, i.e., CoMoPd/Pt-HY (HDS-5) catalyst, showed excellent HDS and HDA activity. These catalysts could be used in one-stage hydrotreating, in which deep HDS reaction of fractions oil containing $S < 500$ ppm are used; however, some studies of the performance over a long period of operating time should be addressed to confirm the sulfur tolerance.

Hydrodesulfurization of 4,6-DMDBT into 3,4-dimethylbiphenyl certainly was observed. The results suggest isomerization of 4,6-DMDBT prior to HDS. This agrees with Isoda et al., (1996), since methyl migrations could occur over zeolite catalysts.

More characterizations of these catalysts are still needed to fully understand how the chemistry of the supports is related to the activity.

The optimization of the activation conditions could be essential to fully define the potential of these catalysts.

CHAPTER IX

CONCLUSIONS

Co, Mo, Ni, Pd, Pt-promoted zeolites were synthesized to enhance the removal of sulfur containing compounds through the hydrogenation route. The synthesis of the catalysts was carried out by two different methods, namely the incipient wetness impregnation and combining impregnation and ion exchange. Metal contents and texture of the metal zeolite catalysts were analyzed and compared. Hydrodesulfurization of heavy gas oil is used as probe reactions to examine the activity of the zeolite catalysts as well as the activity of a commercial CoMo/Al₂O₃ catalyst. From the results, the following conclusions can be drawn.

In the dibenzothiophene family dibenzothiophene exhibits the highest HDS reactivity, whereas alkyl-DBTs exhibit very different reactivities, strongly depending on the positions of the alkyl substituents. Alkyl substituents at the 4 and/or 6 positions appeared to have the lowest reactivity as observed in diesel fuel (Ma et al., 1994).

Three routes of HDS of 4,6-DMDBT are proposed: One is the hydrogenolysis route where the sulfur atom is directly eliminated without hydrogenation of the aromatic ring, the other is the hydrogenation route where the hydrogenation of an olefinic bond or an aromatic ring takes place prior to the hydrogenolysis of the C-S bond and finally the isomerization route where the migration of the substituted methyl groups of 4,6-DMDBT occur prior to the hydrogenolysis of the C-S bond.

Since the conversions of sulfur containing compounds depend strongly on the reactions conditions, such as temperature, H₂/HC ratio and space time, and HGO contains a lot of light and heavy aromatic compounds in the boiling range of 151-406 °C which are easily cracked at high temperature and low H₂ concentration, it is recommended that the hydrodesulfurization of heavy gas oil be carried out at temperature of 310 °C, higher H₂/HC ratio than 7.2 and higher space time than 6000 kg_{cat}h/kmol.

The study has examined the use of zeolite catalysts for hydrodesulfurization of heavy gas oil. The CoMoPd/Pt-HY (HDS-5) and CoMoNi/PdPt-HY (HDS-10) catalysts belong to a new class of hydrotreating catalysts with distinct properties, such as potential to tolerate sulphur compounds due to its palladium content. Those catalysts are candidates for deep HDS ($S < 50$ ppm) of heavy gas oil with good hydrogenation of aromatic compounds.

LITERATURE CITED

- Anderson, J.R.; Pratt, K.C. *Introduction to Characterization and Testing of Catalysts*; Academic Press: Sydney, Australia, 1985.
- Anderson J.R.; Boudart M. *Catalysis: Science and Technology*; Springer-Verlag: New York, 1996.
- Albermale Catalysts. Effect of H₂S on Hydroprocessing Reactions. From the web. : http://www.albemarlecatalysts.com/navigation/hydroprocessing/A_home.htm, accessed on July 2003.
- Bekkim V.H.; Flanigen E.M.; Jansen E.M., J.C. (Eds). *Introduction into Zeolite Science and Practice*; Elsevier: Amsterdam, 1991.
- Buteyn, J. L.; Kosman, J. J. Multielement Simulated Distillation by Capillary GC-MED. *Journal of Chromatographic Science*. **1990**, 28(1), 19-23.
- Chen, J.; Te, M.; Yang, H., and Ring, Z. Hydrodesulfurization of Dibenzothiophenic Compounds in a Light Cycle Oil. *Petroleum Science and Technology*. **2003**, 21 (5&6), 911-935.
- Chianelli, R. R.; Pecoraro, T. A.; Halbert, T. R.; Pan, W. H.; Stiefel, E. I. Transition Metal Sulfide Catalysis: Relation of the Synergic Systems to the Periodic Trends in Hydrodesulfurization. *Journal of Catalysis*. **1984**, 86(1), 226-30.
- Cid, R.; Neira, J.; Godoy, J.; Palacios, J.M.; López, A. A. Thiophene Hydrodesulfurization on Sulfided Nickel-exchanged USY Zeolites. Effect of the pH of the Catalyst Preparation, *Appl. Catal. A. General*. **1995**, 125, 169–183.
- Cid, R.; Atanasova, P.; López, C. R.; Palacios, J. M.; López, A. A. Gas Oil Hydrodesulfurization and Pyridine Hydrodenitrogenation over NaY-Supported Nickel Sulfide Catalysts: Effect of Ni Loading and Preparation Method, *J. Catal.* **1999**, 182, 328–338.
- Criterion Catalysts & Technologies. Centinel DC-2118 for Ultra Deep Desulphurisation. *Product Bulletin Centinel DC-2118*, **2003**
- DePauw, G. A.; Froment, G. F. Molecular Analysis of the Sulphur Components in a Light Cycle Oil of a Catalytic Cracking Unit by GC-MS and GC-AED. *J. Chromatog. A*, **1997**, 761 (1-2), 231.

- Farragher, A.L. *Symposium on the Role of Solid State Chemistry in Catalysis*. ACS Meeting, New Orleans, LA, 1977.
- Farragher, A. L.; Cossee, P. Catalytic Chemistry of Molybdenum and Tungsten Sulfides and Related Ternary Compounds. *Catal., Proc. Int. Congr.*, 5th. 1973, Meeting Date 1972, 2 1301-18.
- Froment, G. F. Modeling in the Development of Hydrotreatment Processes. *Catalysis Today*. **2004**, 98(1-2), 43-54
- Froment G.F.; Depauw G.; Vanrysselberghe V. Kinetic Modeling and Reactor Simulation in Hydrodesulfurization of Oil Fractions, *Ind. Eng. Chem. Res.* **1994**, 33, 2975.
- Fujikawa, T.; Chiyoda, O.; Tsukagoshi, M.; Idei, K; Takehara, S. Development of a High Activity HDS Catalyst for Diesel Fuel: From Basic Research to Commercial Experience, *Cat. Today*. **1998**, 45, 307–312.
- Gates, B. C.; Katzer, J. R.; Schuit, G. C. A. *Chemistry of Catalytic Processes*; McGraw-Hill: New York, 1979.
- Girgis, M.J.; Gates, B. C. Reactivities, Reaction Networks, and Kinetics in High-Pressure Catalytic Hydroprocessing. *Ind. Eng. Chem. Res.* **1991**, 30, 2021.
- Honna, K.; Sato, K. ; Araki, Y.; Miki, Y.; Matsubayashi, N.; Shimada, H. HY Zeolite-Based Catalysts for Hydrocracking Heavy Oils. In *Hydrotreatment and Hydrocracking of Oil Fractions*, *Stud. Surf. Sci. Cat. B.* 127, Delmon, G.F. Froment and P. Grange, Eds., *Elsevier Science*: Amsterdam, The Netherlands, 1999, 427–430.
- Houalla, M.; Broderick, D. H.; Sapre, A. V.; Nag, N. K.; De Beer, V. H. J.; Gates, B. C.; Kwart, H. Hydrodesulfurization of Methyl-Substituted Dibenzothiophenes Catalyzed by Sulfided Co-Mo/ γ -Al₂O₃. *J. Catal.* **1980**, 61, 523.
- Houalla, Marwan; Nag, N. K.; Sapre, A. V.; Broderick, D. H.; Gates, B. C. Hydrodesulfurization of Dibenzothiophene Catalyzed by Sulfided Cobalt Oxide-molybdenum trioxide/ γ -alumina: the reaction network. *AIChE Journal*, **1978**, 24(6), 1015-21.
- Isoda T.; Ma X.; Mochida I. Hydrodesulfurization Reactivities of Alkyldibenzothiophenes over Sulfided Molybdenum Based catalysts., 208th National Meeting, *Am. Chem. Soc.: Washington, D.C., August 21-26*, **1994**.

- Isoda T.; Nagao S.; Ma X.; Korai Y.; Mochida I. Hydrodesulfurization Pathway of 4,6-Dimethyldibenzothiophene through Isomerization over Y-Zeolite Containing CoMo/Al₂O₃ Catalyst. *Energy & Fuels*. **1996**, *10*, 1078.
- Isoda, T.; Takase, Y.; Kusakabe, K.; Morooka, S. Changes in Desulfurization Reactivity of 4,6-Dimethyldibenzothiophene by Skeletal Isomerization Using a Ni Supported Y-Type Zeolite, *Energy & Fuels*, **2000**, *14*, 585–590.
- Jan, C.; Lin, T.; Chang J. Aromatics Reduction over Supported Platinum Catalysts. 2. Effects of Catalyst Precursors and Pretreatment Conditions on the Performance of Palladium-Promoted Platinum Catalysts. *Ind. Eng. Chem. Res.* **1996**, *35*, 3893–3898.
- Kabe, T.; Ishihara, A.; Tajima, H. Hydrodesulfurization of Sulfur-Containing Polyaromatic Compounds in Light Oil. *Ind. Eng. Chem. Res.* **1992**, *31*, 1577.
- Kabe, Toshiaki; Ishihara, Atsushi; Zhang, Qing; Tsutsui, Hiroko; Tajima, Haruhiko. Deep desulfurization of light oil. (Part 1). Hydrodesulfurization of Methyl-Substituted Benzothiophenes and Dibenzothiophenes in Light Gas Oil. *Sekiyu Gakkaishi*, **1993**, *36*(6), 467-71.
- Kabe, T.; Ishihara, A.; Qian, W. *Hydrodesulfurization and Hydrodenitrogenation*; Kodansha Ltd.: Tokyo, 1999.
- Kerkhof, F. P. J. M.; Moulijn, J. A. Quantitative Analysis of XPS Intensities for Supported Catalysts. *Journal of Physical Chemistry*, **1979**, *83*(12), 1612-19.
- Kilanowski, D. R.; Teeuwen, H.; De Beer, V. H. J.; Gates, B. C.; Schuit, G. C. A.; Kwart, H. Hydrodesulfurization of Thiophene, Benzothiophene, Dibenzothiophene, and Related Compounds Catalyzed by Sulfided Cobalt Oxide-molybdenum trioxide/ γ -alumina: low-pressure reactivity studies. *Journal of Catalysis*, **1978**, *55*(2), 129-37.
- Landau, M.V.; Berger, D.; Herskowitz, M. Hydrodesulfurization of Methyl-Substituted Dibenzothiophenes: Fundamental Study of Routes to Deep Desulfurization. *J. Catal.*, **1996**, *159*, 236–245.
- Laniecki, M.; Zmierczak, W. Thiophene Hydrodesulfurization and Water-gas Shift Reaction over Molybdenum-loaded Y-zeolite Catalysts. *Zeolites*. **1991**, *11*(1), 18-26.
- Lapinas, Arunas T.; Klein, Michael T.; Gates, Bruce C.; Macris, Aris; Lyons, James E. Catalytic Hydrogenation and Hydrocracking of Fluorene: Reaction Pathways, Kinetics, and Mechanisms. *Industrial & Engineering Chemistry Research*. **1991**, *30*(1), 42-50.

- Li, D.; Nishijima, A.; Morris, D. E. Zeolite-supported Ni and Mo Catalysts for Hydrotreatments. I. Catalytic Activity and Spectroscopy, *J. Catal.* **1999a**, *182*, 339–348.
- Li, D.; Nishijima, A.; Morris, D. E.; Guthrie, G.D. Activity and Structure of Hydrotreating Ni, Mo, and Ni-Mo Sulfide Catalysts Supported on γ -Al₂O₃-USY Zeolite, *J. Catal.* **1999b**, *188*, 111–124.
- Li, D.; Xu, H.; Guthrie Jr, G. D. Zeolite-Supported Ni and Mo Catalysts for Hydrotreatments. II. HRTEM Observations, *J. Catal.* **2000**, *189*, 281–296.
- Ma, X.; Sakanishi, K.; Mochida, I. Hydrodesulfurization Reactivities of Various Compounds in Diesel Fuel. *Ind. Eng. Chem. Res.* **1994**, *33*, 218.
- Ma, X.; Sakanishi, K.; Isoda, T.; Mochida, I. Hydrodesulfurization Reactivities of Narrow-Cut fractions in a Gas Oil. *Ind. Eng. Chem. Res.* **1995**, *34*, 748.
- Ma, X.; Sakanishi, K.; Mochida, I. Hydrodesulfurization Reactivities of Various Compounds in Vacuum Gasoil. *Ind. Eng. Chem. Res.* **1996**, *35*, 2487.
- Marin C.; Murrieta F.; Galvan E. Technical Reports on Hydrodesulfurization of Diesel over Zeolite Catalysts. Instituto Mexicano del Petroleo, Mexico D.F., 2001.
- Meyers R.A. *Handbook of Petroleum Refining Processes*; McGraw-Hill Book Company: New York, 1986.
- Moraweck, B.; Bergeret, G.; Cattenot, M.; Kougionas, V.; Geantet, C.; Portefaix, J.; Zotin, J.; Breyse, M. The Nature of Ruthenium Sulfide Clusters Encaged in a Y Zeolite. *Journal of Catalysis.* **1997**, *165*(1), 45-56.
- Nag, N. K.; Sapre, A. V.; Broderick, D. H.; Gates, B. C. Hydrodesulfurization of Polycyclic Aromatics Catalyzed by Sulfided CoOMoO₃/ γ -Al₂O₃: The Relative Reactivities. *J. Catal.* **1979**, *57*, 509.
- Nishioka, M.; Bradshaw, J. S.; Lee, M. L.; Tominaga, Y.; Tedjamulia, M.; Castle, R. N. Capillary Column Gas Chromatography of Sulfur Heterocycles in Heavy Oils and Tars Using a Biphenyl Polysiloxane Stationary Phase. *Analytical Chemistry.* **1985**, *57*(1), 309-12.
- Okamoto, Y.; Preparation and Characterization of Zeolite-supported Molybdenum and Cobalt-molybdenum Sulfide Catalysts. *Catalysis Today.* **1997**, *39*(1-2), 45-60.

- Pawelec, B.; Fierro, J.L.G.; Cambra, J.F.; Arias, P.L.; Legarreta, J.A.; Vorbeck, G.; De Haan, J.W.; De Beer, V.H.J.; Van Santen, R.A. The Effect of Sulfidation on the Ni Distribution in Ni/USY Zeolites. *Zeolites*. **1997**, *18*(4), 250-259.
- Penchev, V.; Davidova, N.; Kanazirev, V.; Minchev, Kh.; Neinska, I. Catalytic Functions of Metal-zeolite Systems. *Advances in Chemistry Series*. **1973**, *121*, 461.
- Prins R. Catalytic Hydrodenitrogenation, *Adv. Catal.* **2001**, *46*, 399.
- Satterfield C.; Modell M.; Wilkens J. Simultaneous Catalytic Hydrodenitrogenation of Pyridine and Hydrodesulfurization of Thiophene. *Ind. Eng. And Chem. Proc. Design and Dev.* **1980**, *19*, 154.
- Schuit, G.C.A.; Gates, B.C. Chemistry and Engineering of Catalytic Hydrodesulfurization. *AIChE Journal*. **1973**, *19*(3), 417-38.
- Set Laboratories, Inc. Catalytic Hydrodesulfurization Process. From the web: <http://www.setlaboratories.com/cat2.htm#Hydrodesulfurization%20Process>, accessed on March 2006.
- Shimada, K.; Yoshimura, Y. Ultra- deep Hydrodesulfurization and Aromatics Hydrogenation of Diesel Fuel over a Pd-Pt Catalyst Supported on Yttrium-modified USY. *Journal of the Japan Petroleum Institute*. **2003**, *46*(6), 368-374.
- Song, C.; Schmitz, A. D. Zeolite-supported Pd and Pt Catalysts for Low-Temperature Hydrogenation of Naphthalene in the Absence and Presence of Benzothiophene. *Energy & Fuels*. **1997**, *11*(3), 656-661.
- Song C., Designing Sulfur-resistant, Noble-metal Hydrotreating Catalysts, *Chemtech*. **1999**, *29*(3), 26-30
- Song, C.; Hsu, C. S.; Mochida, I. *Chemistry of Diesel Fuels*; Taylor and Francis: New York, NY, 2000.
- Speight, J. G. *The Desulfurization of Heavy Oils and Residua*; Marcel Dekker: New York, 1981.
- Speight, J. G. *The Desulfurization of Heavy Oils and Residua*; Second edition, revised and expanded, Marcel Dekker: New York, 2000.
- Speight J.G., *Handbook of Petroleum Product Analysis*; John Wiley & Sons, Inc.: Hoboken, New Jersey, 2002.

- Sugioka, M.; Sado, F.; Matsumoto, Y.; Maesaki, N. New Hydrodesulfurization Catalysts: Noble Metals Supported on USY Zeolite. *Catalysis Today*, **1996**, 29(1-4), 255-259.
- Szostak, R. *Handbook of Molecular Sieves*; Van Nostrand Reinhold: New York, 1992.
- Taniguchi, M.; Imamura, D.; Ishige, H.; Ishii, Y.; Murata, T.; Hidai, M.; Zanibelli, L.; Berti, D.; Ferrari, M.; Flego, C.; Riva, R. The Influence of Zeolite Introduction on the HDS Activity of CoMo Catalysts. In *Hydrotreatment and Hydrocracking of Oil Fractions*, Stud. Surf. Sci. Cat. 127, B. Delmon, G.F. Froment and P. Grange, Eds., Elsevier Science, Amsterdam, The Netherlands, 1999, 219–226.
- Thomas J. M. Thomas W.J., *Principles and Practice of Heterogeneous Catalysis*; VCH: Weinheim, Germany, 1997.
- Topsoe, H.; Clausen, B.; Topsoe, N.Y.; Hyldtoft, J. Experimental and Theoretical Studies of Periodic Trends and Promotional Behavior of Hydrotreating Catalysts. *Preprints - American Chemical Society, Division of Petroleum Chemistry*. **1993**, 38(3), 638-41.
- Topsoe H.; Clausen B.S.; Massoth F.E. *Hydrotreating Catalysis: Science and Technology*; Springer-Verlag: Berlin, 1996.
- Velu S.; Song C.; Engelhard M.; Chin Y. Adsorptive Removal of Organic Sulfur Compounds from Jet Fuel over K-Exchanged NiY Zeolites Prepared by Impregnation and Ion Exchange, *Ind. Eng. Chem. Res.* **2005**, 44, 5740.
- Vanrysselberghe, V.; Froment, G. F. Hydrodesulfurization of Dibenzothiophene on a CoMo/Al₂O₃ Catalyst: Reaction Network and Kinetics. *Ind. Eng. Chem. Res.* **1996**, 35, 3311.
- Vanrysselberghe, V.; Le Gall, R.; Froment, G. F. Hydrodesulfurization of 4-Methyldibenzothiophene and 4,6-Dimethyldibenzothiophene on a CoMo/Al₂O₃ Catalyst: Reaction Network and Kinetics. *Ind. Eng. Chem. Res.* **1998**, 37, 1235.
- Vanrysselberghe, V.; Froment, G. F. Kinetic Modeling of Hydrodesulfurization of Oil Fractions: Light Cycle Oil. *Ind. Eng. Chem. Res.* **1998**, 37, 4231.
- Vanrysselberghe V.; Froment G. F. *Hydrodesulfurization-Heterogeneous*. *Encyclopedia of Catalysis*, John Wiley & Sons, Inc., New York, 2003.
- Voorhoeve, R. J. H. Electron Spin Resonance Study of Active Centers in Nickel-tungsten Sulfide Hydrogenation Catalysts. *Journal of Catalysis*. **1971**, 23(2), 236-42.

- Voorhoeve, R. J. H.; Stuiiver, J. C. M. Kinetics of Hydrogenation on Supported and Bulk Nickel-tungsten Sulfide Catalysts. *Journal of Catalysis*. **1971**, 23(2), 228-35.
- Vrinat, M. L.; The Kinetics of the Hydrodesulfurization Process: A Review. *Appl. Catal.* **1983**, 6, 137-158.
- Weisser, O.; Landa, S. *Sulfided Catalysts, Their Properties and Applications*; Pergamon Press: Oxford, 1973.
- Yasuda, H.; Kameoka, T.; Sato, T.; Kijima, N.; Yoshimura, Y. Sulfur-tolerant Pd-Pt/Al₂O₃ Catalyst for Aromatic Hydrogenation. *Applied Catalysis, A: General*. **1999**, 185(2), L199-L201.
- Zanibelli, L.; Berti, D.; Ferrari, M.; Flego, C.; Riva, R. The Influence of Zeolite Introduction on the HDS Activity of CoMo Catalysts. *Studies in Surface Science and Catalysis*. **1999**, 127, 219-226.

APPENDIX A

TEXTURES OF HY AND BOUND ZEOLITE

In this section, textures of the powdered fresh zeolite (HY), nickel containing zeolite (Ni-HY) and platinum containing zeolite (Pt-HY) are reported.

The zeolite pores are represented by the internal pores. BET surface area, total volume in pores and pore size distribution are analyzed using a Micromeritics BET machine with nitrogen as adsorbate at 77.3 K. Porosity distribution is determined by Original Density Functional Theory with the slit pore geometry model. Table A.1 and Figure A.1 show the physical properties of the HY, Ni-HY and Pt-HY zeolites.

BET surface area and total area in pores of the Ni and Pt containing zeolite are less than the values of HY zeolite as expected probably due to the introduction of the metal into zeolite by ion exchange. Ni-HY shows lower surface area than Pt-HY possibly because the nickel content into zeolite is higher (11.3 wt%) than platinum into zeolite (0.73 wt %). Since total area in pores of the Ni-HY zeolite is lower than HY and Pt-HY is assumed that a portion of the nickel could be blocking the pores of zeolite due to its high content and as consequence BET surface area is reduced. The porosity distribution is also affected. Ni-HY shows the highest pore size distribution in the interval of pore size of 8-12 Å. But, a small pore distribution in the mesopores region of 26-685 Å is also observed (Figure A.2). Pt-HY and HY zeolite show the highest pore size distribution in the interval of 10-12 Å with a scarcely pore distribution in the mesopores region in the interval of 26-544 Å (Figures A.3 and A.4).

Table A.1 Physical properties of the powdered HY fresh zeolite, Pt containing zeolite and Ni containing zeolite

Physical Properties	HY	Pt-HY	Ni-HY
BET Surface Area, m²/g	652	638	564
Total Area in pores¹, m²/g	491	476	422
Total Volume in Pores¹, cc/g	0.38	0.44	0.60

(1) By Density Functional Theory

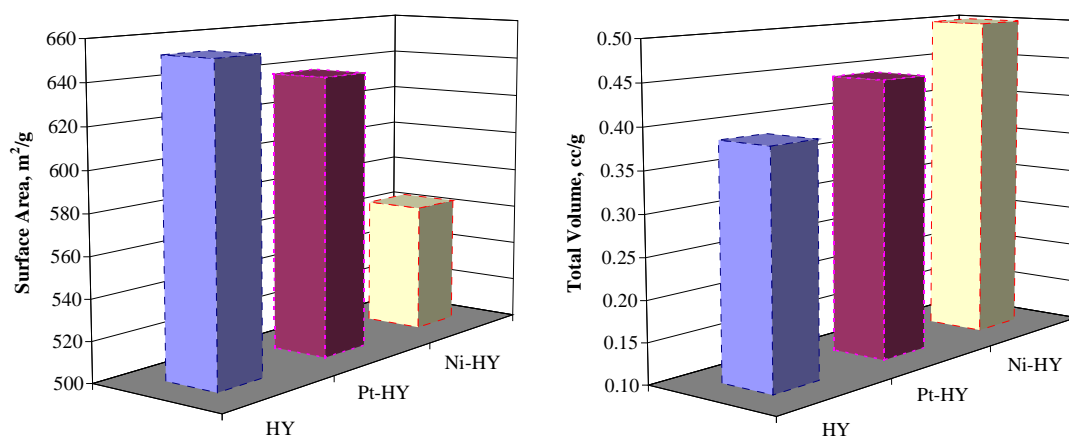


Figure A.1 BET surface area and total volume in pores of the powdered HY, Pt-HY and Ni-HY zeolites.

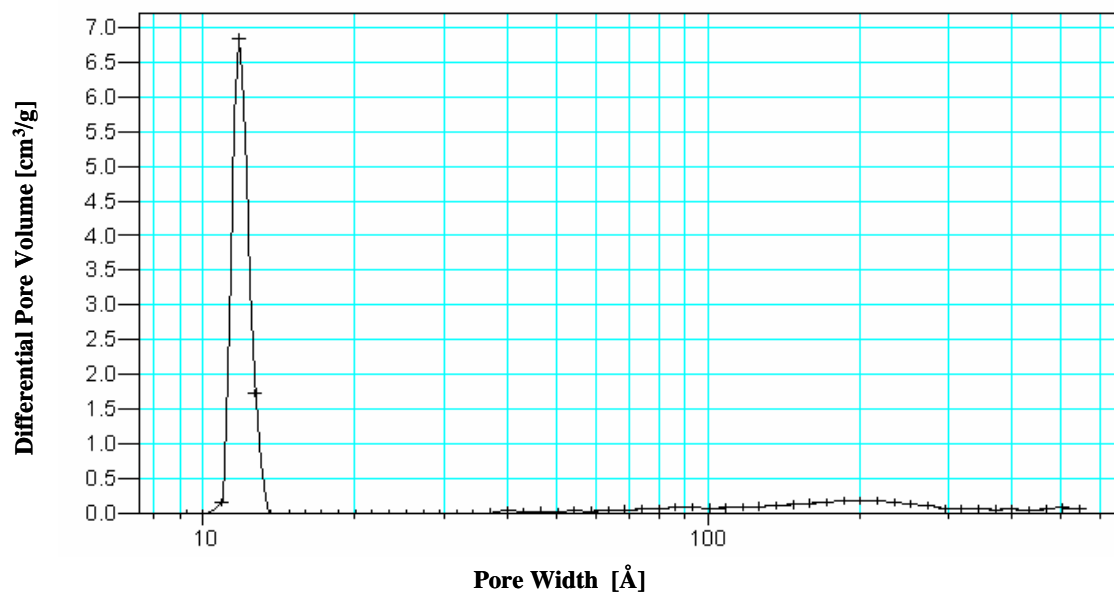


Figure A.2 Pore size distribution of the powdered and calcined HY as determined by Density Functional Theory.

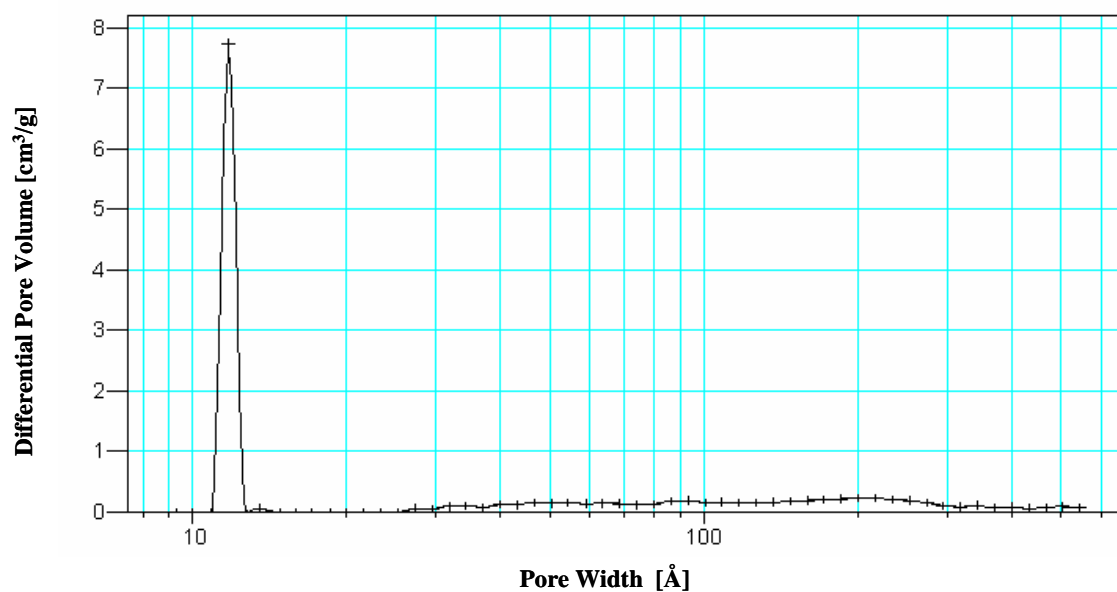


Figure A.3 Pore size distribution of the powdered and calcined Pt-HY as determined by Density Functional Theory.

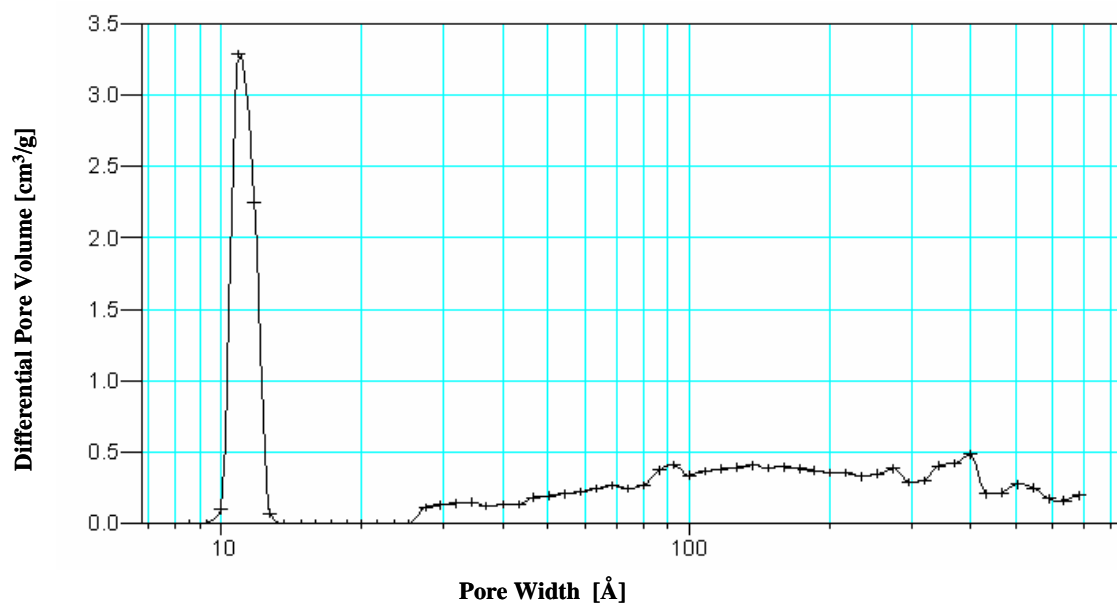


Figure A.4 Pore size distribution of the powdered and calcined Ni-HY as determined by Density Functional Theory.

Figures A.5, A.6 and A.7 show the corresponding adsorption and desorption isotherms. The isotherms were determined at or near the normal boiling point of the adsorbate. The Pt-HY and Ni-HY zeolites have larger hysteresis loops due to the mesopores size.

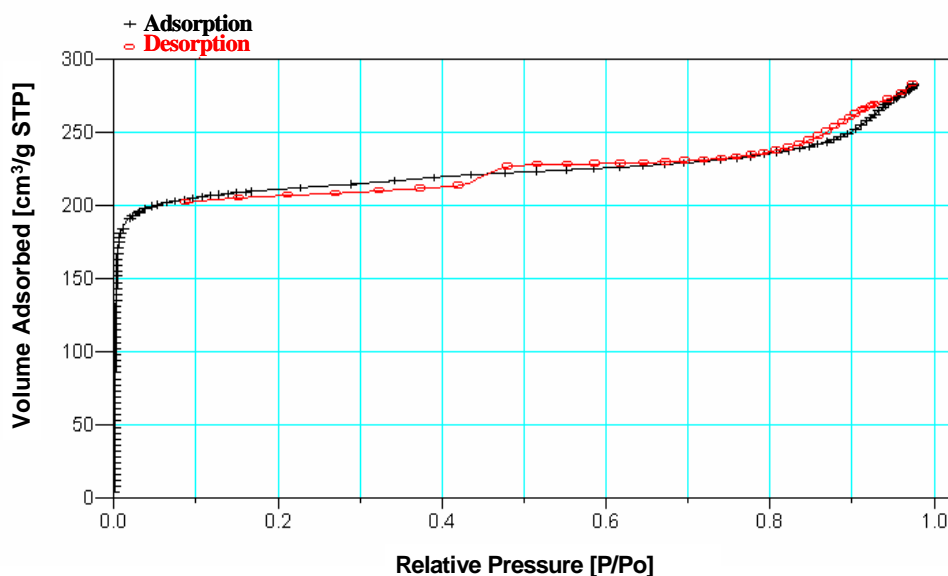


Figure A.5 Data for nitrogen sorption at 77.3 K on calcined HY

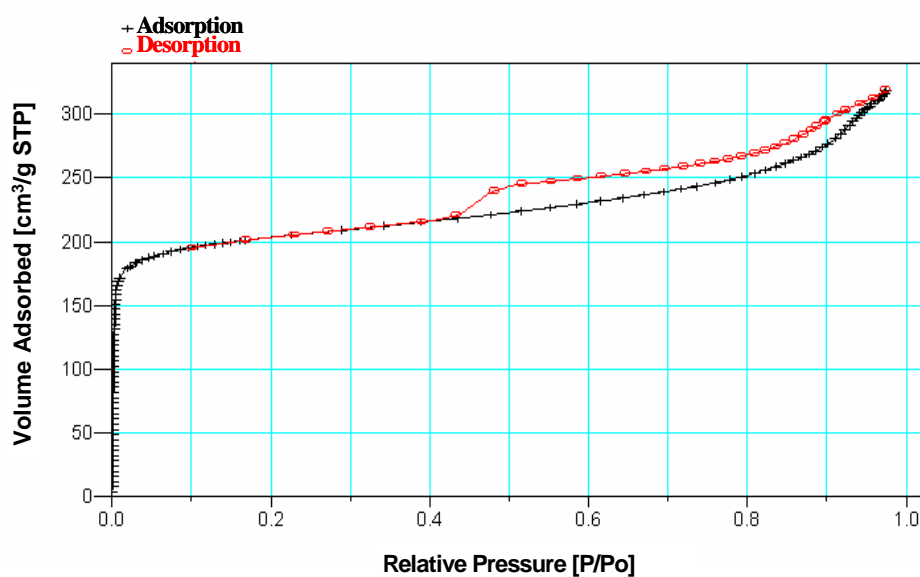


Figure A.6 Data for nitrogen sorption at 77.3 K on calcined Pt-HY.

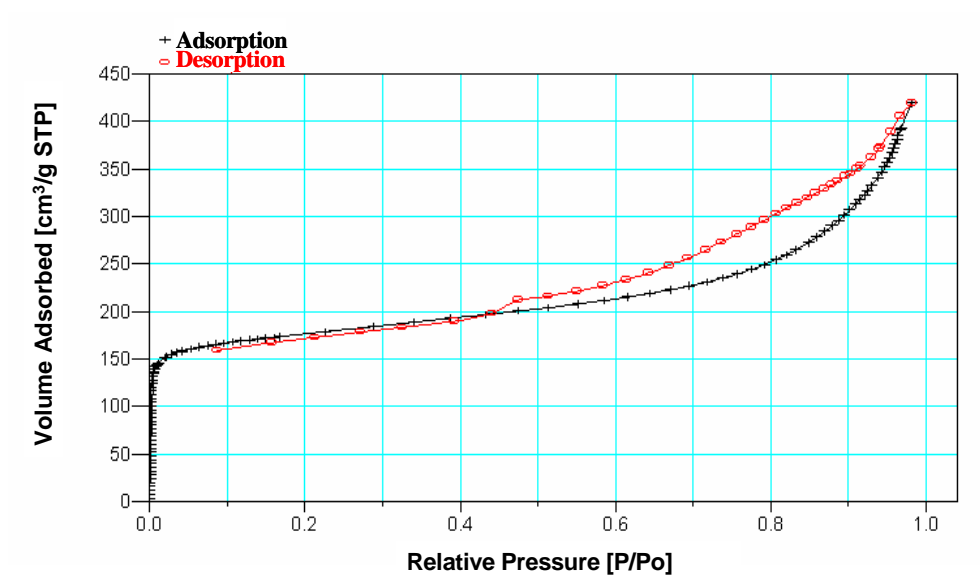


Figure A.7 Data for nitrogen sorption at 77.3 K on calcined Ni-HY.

VITA

Celia Marin-Rosas was born in D.F., Mexico, to Mr. Pablo Marin Cervantes and Mrs. Celia Rosas Blancas. In 1980, She attended the Universidad Nacional Autonoma de Mexico, Mexico, where she received a Bachelor of Science degree in chemical engineering in 1984. In this year, she began to work at Instituto Mexicano del Petroleo (IMP) as a researcher in the Department of Catalysis. While she was working at IMP, she attended the Instituto Politecnico Nacional, Mexico, for a master's degree in chemical engineering (1988-1990). She is author of several patents and papers of catalysts development for the Petrochemical and Refining Industries.

She received a scholarship from IMP to study in the USA for a Ph.D. in chemical engineering. Therefore, in 2002 she attended the Texas A&M University in College Station to begin her graduate study toward her Ph.D. in the Artie McFerrin Department of Chemical Engineering. Her future work place after graduation will be the Mexican Petroleum Institute in the Coordination of Research Programs and Technological Development of Reactors and Processes, Mexico.

She can be reached through the following address: Lazaro Cardenas Mz. 7, Lt. 17, Colonia Consejo Agrarista Mexicano, C.P. 09760, Mexico, D.F. Her permanent e-mail address in cmrosas14@hotmail.com.